General Motors LLC Final Project Report:
Improving Energy Efficiency by Developing Components for Distributed Cooling and Heating Based on Thermal Comfort Modeling

U.S. Department of Energy
Cooperative Agreement Award Number: DE-EE0000014

Date of report: December 9, 2014

Principal Investigators:
Jeffrey Bozeman – General Motors LLC
Kuo-Huey Chen – General Motors LLC

Team Members:
Delphi – Thermal Systems
Faurecia Automotive Seating
University of California – Berkeley
University of Nevada – Las Vegas
UT-Battelle LLC

This material is based upon work supported by the Department of Energy National Energy Technology Laboratory and the California Energy Commission under Award Number DE-EE0000014.

ACKNOWLEDGEMENTS

General Motors wishes to thank the U.S. Department of Energy (specifically, the EERE Vehicle Technologies Program and NETL Project Management Center) and the California Energy Commission for their support in developing these important energy-saving technologies.

TABLE OF CONTENTS

LIST OF FIGURES

LIST OF TABLES

EXECUTIVE SUMMARY

On November 3, 2009, General Motors (GM) accepted U.S. Department of Energy (DOE) Cooperative Agreement award number DE-EE0000014 from the National Energy Technology Laboratory (NETL). GM was selected to execute a three-year cost shared research and development project on Solid State Energy Conversion for Vehicular Heating, Ventilation & Air Conditioning (HVAC) and for Waste Heat Recovery. This area of interest from Funding Opportunity Announcement DE-PS26-08NT01045 supports the Office of Energy Efficiency and Renewable Energy's (EERE) Vehicle Technologies Program. In addition to funding from DOE EERE, this project is supported by funding from the California Energy Commission (CEC).

In the summer of 2010, the GM team proposed a substantial revision to the Statement of Project Objectives to perform additional activities that would specifically benefit electrified vehicles such as the Chevrolet Volt. DOE approved a corresponding increase in government funding for the proposed change in project scope, which included the delivery of a Volt demonstration vehicle initially planned for July 31, 2013. Subsequent delays in the project have resulted in a no-cost time extension for the project with the mainstream Buick Lacrosse demonstration vehicle scheduled to be available by September 30, 2013, and the Chevrolet Volt demonstration vehicle scheduled to be available by March 31, 2014.

GM Project Objectives

The primary objective of this project was to develop a distributed automotive HVAC system that provides thermal comfort equivalent to current state-of-the-art centralized systems while using significantly less energy. To satisfy this objective, the team identified the following goals:

- Reduce by at least 30% of the "billions of gallons" the fuel used in cooling mode to maintain occupant comfort through the localized use of thermoelectric (TE) technology while maintaining occupant comfort and safety.
- Develop TE HVAC components with a coefficient of performance (COP) greater than 1.3 for cooling and greater than 2.3 for heating, then integrate and test these components as part of a reliable distributed HVAC system in a conventional vehicle (an eAssist Buick Lacrosse) and an extended range electric vehicle (a Chevrolet Volt).
- Update the UCB Thermal Comfort model to predict the response of vehicle occupants to localized heating and cooling based on human subject testing, and develop associated computer-aided engineering (CAE) tools to support the integration of distributed HVAC components into future vehicle designs.

A secondary objective of the project was to improve the efficiency of thermoelectric generators for converting engine waste heat into electricity.

GM Methodology

GM's approach reduced the energy consumption of the vehicle's central HVAC system (producing a warmer than desired passenger cabin temperature for a cooling situation) while maintaining occupant comfort by using distributed HVAC components to delivering local spot

cooling to each occupant. While cooling individual occupant(s) instead of the entire passenger cabin is a basic method for producing energy savings, GM's approach was further optimized by applying scientific knowledge of human physiology and psychology regarding thermal comfort that recognizes local cooling of some key body segments significantly affects perceived comfort. The team's premise was that the energy consumption of the distributed HVAC system would still result in substantial net energy savings and corresponding reductions in fuel usage for air conditioning, while providing the vehicle occupants with equivalent thermal comfort.

The project team used human subject testing to develop a math-based thermal comfort model that characterized the sensation and comfort responses to the localized cooling and heating of body segments in a vehicle environment. The model identified optimal locations and operating parameters for energy-efficient distributed HVAC components that would deliver local spot cooling and heating. Based on an analysis that comprehended vehicle constraints, the team selected an optimal combination of locations for distributed HVAC components.

The project team developed an initial set of prototype HVAC components that featured thermoelectric modules for energy-efficient distributed cooling and heating. These functional components and the associated control strategies were integrated into a mule vehicle for testing and evaluation.

Based on the performance analysis of the initial prototype components, the project team developed a final set of prototype HVAC components to further optimize performance while considering production-intent requirements such as noise and packaging. These final prototype distributed cooling and heating components and their associated control strategies will be integrated into demonstration vehicles for final testing and evaluation.

The activities to achieve the primary objective were performed in four standard research and development phases described immediately below. The activities to achieve the secondary objective for improving engine waste heat recovery were performed in a fifth phase of the project that was concurrent with these first four phases.

GM Phase 1 – Applied Research

The focus of this phase was to develop a Thermal Comfort model of human responses to potential locations for distributed heating and cooling and to identify optimal locations.

GM Phase 2 – Exploratory Development

The focus of this phase was to develop the initial prototype distributed HVAC components and to evaluate them on both a test bench and a mule vehicle. At the conclusion of this phase, a Go / No-Go decision was made based on expectations of achieving the primary project objective.

GM Phase 3 – Advanced Development

The focus of this phase was to develop the final prototype distributed HVAC components while considering production-intent requirements such as noise and packaging.

GM Phase 4 – Engineering Development

The focus of this phase was to integrate the final prototype distributed HVAC components with the production central HVAC system and to optimize the performance of the demonstration

vehicles. A final analysis will be made to compare the expected efficiency and fuel economy improvements to the program targets.

GM Phase 5 – Thermoelectric Generator Development

The focus of this phase was to develop improvements in the TE materials for thermoelectric generators that could be used to produce electrical power for TE HVAC system loads.

GM Major Findings with Results

Energy saving demonstrated in our Buick eAssist LaCrosse was hampered by heat from the optionally equipped large sunroof that reduced the effectiveness of the prototype roof-mounted face and chest localized TEDs. On the warmest days, the face and chest TEDs were not able to drop the air temperature to even the human skin temperature of 33°C. This resulted in no improvement in the occupant breath temperature but did result in improved convective cooling. Experiments with the TEDs turned off, then turned on, showed improved comfort with the TED turned on despite limited temperature performance.

- The demonstration vehicle utilized a TED "blowing" seat for the driver and a lower cost ventilated seat (with "sucking" airflow but no TED) for the passenger. The comfort in the driver seat was often superior to the passenger seat, but both locations proved more comfortable than the baseline vehicle.
- Subjective comfort in the rear seat was significantly improved compared to the baseline vehicle primarily due to the improved climate measures. The proximity of the chest and face cooling TEDs in the front seat back proved to be very effective with improving comfort along with the low cost ventilated seat cushion and backrest.
- The combination of roof, lap, and seat climate measures were shown to improve system efficiency significantly. The TED climate control automatic set point was 24°C while the baseline used an automatic set point of 22°C. The TED system was superior in comfort early in a transient test as a result of the faster TED system response; steady-state comfort was equivalent while saving energy.
- The energy applied to the localized comfort features was about 40 watts per occupant yet was able to save about 36.5% of the 6 kW centralized climate energy.

The Chevrolet Volt heating localized measures included Face, Chest, Lap, Foot, and contact TE seating. Objective comfort data demonstrated equal comfort (EHT) with the baseline Volt at 23°C automatic climate setting compared to the localized setting of 21.5°C ECO mode climate setting.

Subjective transient comfort measured during road tests showed the TED configuration consistently was more comfortable, logging a 0.5 comfort point advantage, during steady operation.

Energy savings demonstrated in the Chevrolet Volt during Electric Vehicle operation met project targets despite several limitations with the demonstration property:

- Winter testing used the hot coolant loop to exchange heat with the cold side of the TEDs. An air-cooled TED cold side heat exchange would save the energy pulled from the hot coolant loop and improve system COP.
- The TED CHCM (coolant heater) was not employed in the demonstration property and the reduced energy of the device was not included in efficiency calculations. The cost and complexity of the TED CHCM was not commercially viable, and the energy gains could not offset the system cost limitation (~$10K per unit if commercialized).
- Winter testing dispelled the notion that the higher winter clothing level would reduce the effectiveness of localized climate control. The comfort rides and objective thermal manikin data shows effective warming using the face, lap, and seat localized measures despite winter clothing.

Annualized Energy reduction values for Electrical Vehicle operation during winter usage were shown to be 37.7% less than the baseline 2013 Chevrolet Volt. The production Chevrolet Volt has a reported 40-mile range in mild climate, but range can be reduced as much as 17 miles in winter usage due in part to climate control energy usage. Our demonstration property is expected to experience less range reduction during the winter, estimated at an 11-mile loss, or a range of 29 miles compared to the production estimate of 23 miles. These six miles in increased range represent a significant improvement.

Annualized Energy reduction values for Electrical Vehicle operation during summer were shown to be 36.6% less than the baseline 2013 Chevrolet Volt.

The Volt demonstration vehicle used many of the same comfort measures demonstrated on the 2012 Buick eAssist LaCrosse. The face, chest, and lap TEDs from the LaCrosse were adapted into the Volt as well. The Volt differed from the LaCrosse in the seat TED; the Volt used a more efficient contact TED fabric whereas the LaCrosse used a TED with an air distribution system for the driver and ventilation only for other seating locations. The peak summer range reduction due to Climate Control energy usage is 15 miles, netting a 25-mile summer range. Our demonstration property is expected to perform 36.6% better in term of range with only 9.5 miles of range reduction. The 30.5-mile peak summer range is a 5.5-mile improvement over the Volt with the baseline climate control system.

GM Conclusions and Recommendations

The GM team has successfully executed the HVAC energy savings project by installing prototype thermoelectric devices (TEDs) that provided distributed and localized climate measures on both an eAssist Buick LaCrosse and a Chevrolet Volt extended-range electric vehicle. For the Buick LaCrosse, annualized HVAC energy saving of 30.9% was achieved over the baseline vehicle. For the Chevrolet Volt, annualized HVAC energy saving of 36.6% for the summer operation and 37.7% for the winter operation were accomplished. Both vehicles met and exceeded the energy savings target of 30% set for the project. The COPs for the TE components varying between 1.26 to 1.89 (1.56 average value) for cooling and between 2.5 to 2.7 for heating; these values also met the COP targets set for the project to be greater than 1.3 for cooling and 2.3 for heating. While using much less energy, the distributed TED configuration for

both vehicles demonstrated that the occupant thermal comfort was not compromised. In fact, subjective transient comfort measured during road tests showed that the TED configuration consistently delivered greater comfort, with a 0.5 comfort point advantage during steady-state operation.

While the GM team was satisfied with the achievements to reach the target set for the project, future study was recommended to make the TE HVAC system more viable for future vehicles.

- To dissipate the TE waste heat in the summer operation and provide heat to the cold side of the TED during winter operation for the electrical vehicle, a liquid heat exchanger was chosen early in the project to conservatively meet the performance targets. The cooling system performed very well for the project and overall thermal comfort level was in general higher than baseline during steady-state operation. To reduce the complexity of the liquid system and to save cost, an air-cooling system might be reconsidered.
- The contact TED system used in the front seats of the Volt is very effective in comfort attainment. Further exploration of such contact TE seats that can provide energy savings while working together with the existing HVAC system while is recommended.

CHAPTER G1:
GM Introduction

G1.1 Project Overview

On November 3, 2009, General Motors (GM) accepted U.S. Department of Energy (DOE) Cooperative Agreement award number DE-EE0000014 from the National Energy Technology Laboratory (NETL). GM was selected to execute a three-year cost shared research and development project on Solid State Energy Conversion for Vehicular Heating, Ventilation & Air Conditioning (HVAC) and for Waste Heat Recovery. This area of interest from Funding Opportunity Announcement DE-PS26-08NT01045 supports the Office of Energy Efficiency and Renewable Energy's (EERE) Vehicle Technologies Program. In addition to funding from DOE EERE, this project is supported by funding from the California Energy Commission (CEC).

In the summer of 2010, the GM team proposed a substantial revision to the Statement of Project Objectives to perform additional activities that would specifically benefit electrified vehicles such as the Chevrolet Volt. DOE approved a corresponding increase in government funding for the proposed change in project scope, which included the delivery of a Volt demonstration vehicle initially planned for July 31, 2013. Subsequent delays in the project have resulted in a no-cost time extension for the project with the mainstream Buick Lacrosse demonstration vehicle scheduled to be available by September 30, 2013, and the Chevrolet Volt demonstration vehicle scheduled to be available by March 31, 2014.

G1.2 Project Objectives

The primary objective of this project was to develop a distributed automotive HVAC system that provides thermal comfort equivalent to current state-of-the-art centralized systems while using significantly less energy. To satisfy this objective, the team identified the following goals:

- Reduce by at least 30% of the "billions of gallons" the fuel used in cooling mode to maintain occupant comfort through the localized use of TE technology while maintaining occupant comfort and safety.
- Develop TE HVAC components with a coefficient of performance greater than 1.3 for cooling and greater than 2.3 for heating, then integrate and test these components as part of a reliable distributed HVAC system in a conventional vehicle (an eAssist Buick Lacrosse) and an extended range electric vehicle (a Chevrolet Volt).
- Update the UCB Thermal Comfort model to predict the response of vehicle occupants to localized heating and cooling based on human subject testing, and develop associated computer-aided engineering (CAE) tools to support the integration of distributed HVAC components into future vehicle designs.

A secondary objective of the project was to improve the efficiency of thermoelectric generators for converting engine waste heat into electricity.

G1.3 Methodology

GM's approach reduced the energy consumption of the vehicle's central HVAC system (producing a warmer than desired passenger cabin temperature for a cooling situation) while maintaining occupant comfort by using distributed HVAC components to delivering local spot cooling to each occupant. While cooling individual occupant(s) instead of the entire passenger cabin is a basic method for producing energy savings, GM's approach was further optimized by applying scientific knowledge of human physiology and psychology regarding thermal comfort that recognizes local cooling of some key body segments significantly affects perceived comfort. The team's premise was that the energy consumption of the distributed HVAC system would still result in substantial net energy savings and corresponding reductions in fuel usage for air conditioning, while providing the vehicle occupants with equivalent thermal comfort.

The project team used human subject testing to develop a math-based thermal comfort model that characterized the sensation and comfort responses to the localized cooling and heating of body segments in a vehicle environment. The model identified optimal locations and operating parameters for energy-efficient distributed HVAC components that would deliver local spot cooling and heating. Based on an analysis that comprehended vehicle constraints, the team selected an optimal combination of locations for distributed HVAC components.

The project team developed an initial set of prototype HVAC components that featured thermoelectric modules for energy-efficient distributed cooling and heating. These functional components and the associated control strategies were integrated into a mule vehicle for testing and evaluation.

Based on the performance analysis of the initial prototype components, the project team developed a final set of prototype HVAC components to further optimize performance while considering production-intent requirements such as noise and packaging. These final prototype distributed cooling and heating components and their associated control strategies will be integrated into demonstration vehicles for final testing and evaluation.

The activities to achieve the primary objective were performed in four standard research and development phases shown in the project timeline below. The activities to achieve the secondary objective for improving engine waste heat recovery were performed in a fifth phase of the project that was concurrent with these first four phases.

G1.4 Project Timeline and Milestones

The timeline of project phases, tasks, and milestones is shown in Figure G1. The detailed timing of the project milestones is documented in Table G1.

Figure G1: Project Phases, Tasks, and Milestones Timeline Chart

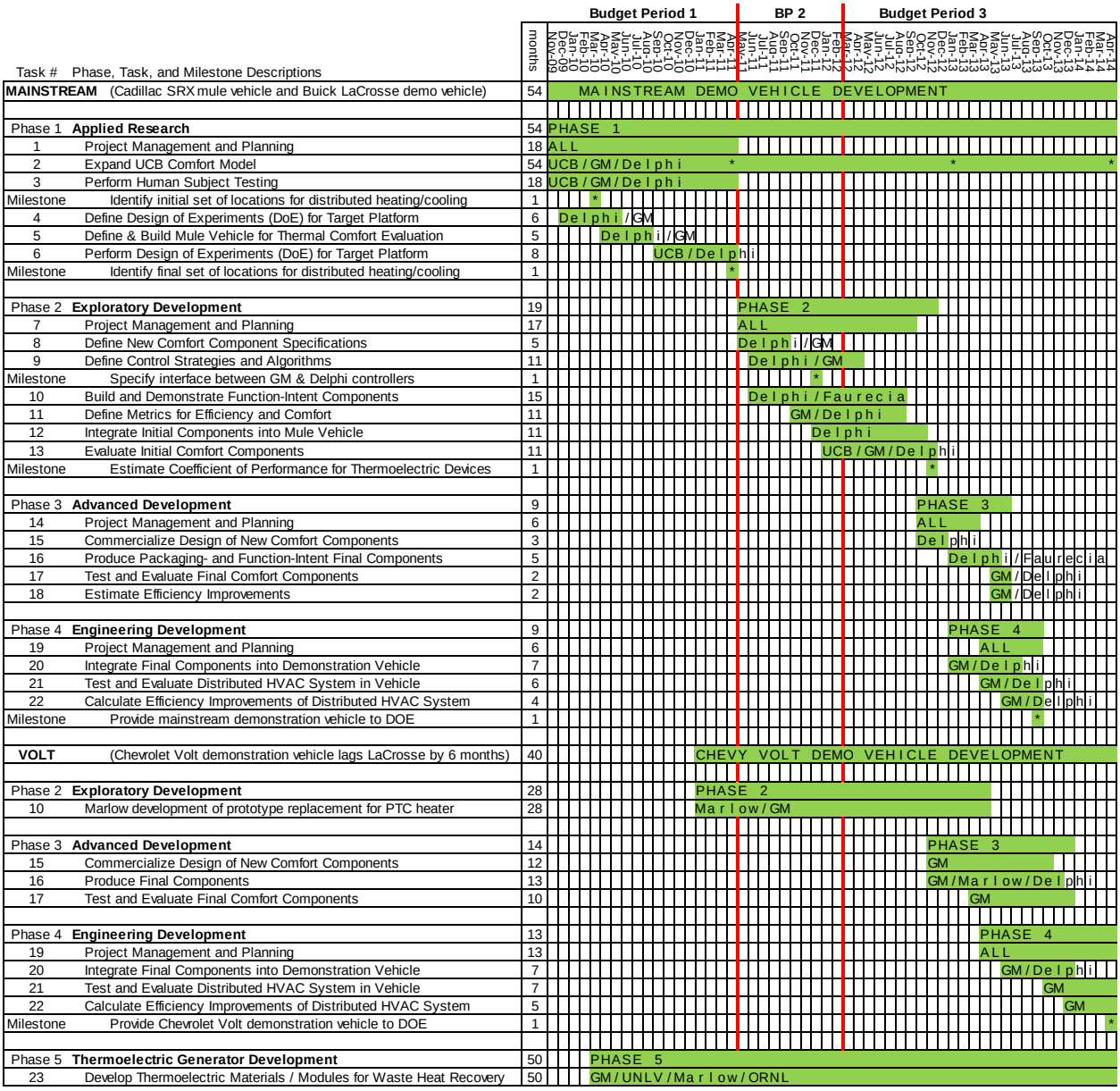

Task #	Phase, Task, and Milestone Descriptions	months
MAINSTREAM	(Cadillac SRX mule vehicle and Buick LaCrosse demo vehicle)	54
Phase 1	**Applied Research**	54
1	Project Management and Planning	18
2	Expand UCB Comfort Model	54
3	Perform Human Subject Testing	18
Milestone	Identify initial set of locations for distributed heating/cooling	1
4	Define Design of Experiments (DoE) for Target Platform	6
5	Define & Build Mule Vehicle for Thermal Comfort Evaluation	5
6	Perform Design of Experiments (DoE) for Target Platform	8
Milestone	Identify final set of locations for distributed heating/cooling	1
Phase 2	**Exploratory Development**	19
7	Project Management and Planning	17
8	Define New Comfort Component Specifications	5
9	Define Control Strategies and Algorithms	11
Milestone	Specify interface between GM & Delphi controllers	1
10	Build and Demonstrate Function-Intent Components	15
11	Define Metrics for Efficiency and Comfort	11
12	Integrate Initial Components into Mule Vehicle	11
13	Evaluate Initial Comfort Components	11
Milestone	Estimate Coefficient of Performance for Thermoelectric Devices	1
Phase 3	**Advanced Development**	9
14	Project Management and Planning	6
15	Commercialize Design of New Comfort Components	3
16	Produce Packaging- and Function-Intent Final Components	5
17	Test and Evaluate Final Comfort Components	2
18	Estimate Efficiency Improvements	2
Phase 4	**Engineering Development**	9
19	Project Management and Planning	6
20	Integrate Final Components into Demonstration Vehicle	7
21	Test and Evaluate Distributed HVAC System in Vehicle	6
22	Calculate Efficiency Improvements of Distributed HVAC System	4
Milestone	Provide mainstream demonstration vehicle to DOE	1
VOLT	(Chevrolet Volt demonstration vehicle lags LaCrosse by 6 months)	40
Phase 2	**Exploratory Development**	28
10	Marlow development of prototype replacement for PTC heater	28
Phase 3	**Advanced Development**	14
15	Commercialize Design of New Comfort Components	12
16	Produce Final Components	13
17	Test and Evaluate Final Comfort Components	10
Phase 4	**Engineering Development**	13
19	Project Management and Planning	13
20	Integrate Final Components into Demonstration Vehicle	7
21	Test and Evaluate Distributed HVAC System in Vehicle	7
22	Calculate Efficiency Improvements of Distributed HVAC System	5
Milestone	Provide Chevrolet Volt demonstration vehicle to DOE	1
Phase 5	**Thermoelectric Generator Development**	50
23	Develop Thermoelectric Materials / Modules for Waste Heat Recovery	50

Table G1: Project Milestone Timing

Completion Date	Phase	Milestone	Key Project Milestone Description
31-Mar-2010	1	1	Identify initial set of locations for distributed heating/cooling
28-May-2010	1	2	Definition of Design of Experiments (DoE) for Target Platform Completed
31-Aug-2010	1	3	Build Mule Vehicle for Thermal Comfort Evaluation Completed
26-Apr-2011	1	4	UCB Comfort Model initial update released
29-Apr-2011	1	5	Identify final set of locations for distributed heating/cooling
19-Dec-2011	2	6	Specify interface between GM & Delphi controllers completed
27-Nov-2012	2	7	Evaluate Initial Comfort Components Completed
27-Nov-2012	2	8	Estimate Final Coefficient of Performance for Thermoelectric Devices
16-Jan-2013	1	9	UCB Comfort Model second update released
16-Sep-2013	3	10	Evaluate Final Comfort Components Completed
16-Sep-2013	1	11	Mainstream demonstration vehicle (Buick LaCrosse) available for DOE
31-Oct-2013	4	12	Calculate Efficiency Improvements of Distributed HVAC System Completed
30-Apr-2014	4	13	Chevrolet Volt demonstration vehicle available for DOE
30-Apr-2014	4	14	UCB Comfort Model final update released

CHAPTER G2:
GM Phase 1 – Applied Research

The focus of this phase was to develop a Thermal Comfort model of human responses to potential locations for distributed heating and cooling and to identify optimal locations. For this phase of the project, GM worked with Delphi Thermal Systems and the University of California at Berkeley (UCB). UCB developed a vehicle mock-up in the Environmental Test Chamber for the first set of human subject testing. Delphi modified a Cadillac SRX for the second set of human subject testing that was performed in their climatic wind tunnel. Both test setups used highly configurable systems for delivering distributed spot cooling and heating.

G2.1 Task 1 – Project Management and Planning

The planning and coordination of the overall project began with the project kickoff meeting with the DOE program managers followed by the internal kickoff and initial working meeting of the project team. For this 18-month phase that was fully half of the original project timeline, the execution of the project closely followed the project plan and it was completed on schedule.

G2.2 Task 2 – Expand UCB Comfort Model

For Task 2, Expand UCB Comfort Model, the main activity was to enhance the existing UCB Thermal Comfort Model to consider the affect from the spot heating and cooling of 16 body segments on a person's overall thermal sensation and thermal comfort (see scale in Figure G37). In addition, other key parameters of the model were examined. For example, the model's existing assumptions about the impact of age and gender on perceived comfort were revisited. Another key activity was to implement computer-aided engineering (CAE) tools based on the enhanced version of the Thermal Comfort Model.

G2.2.1 Enhance the existing Thermal Comfort Model

Age and gender thermal sensation analysis:

The goal of the study was to analyze the differences among different age and gender. The results allowed the team to determine whether significant differences exist and whether the composition of the test group should be adjusted for age or gender. The differences found by this analysis are fundamentally due to:

- Thermal receptors of elderly people are less sensitive, so they might be less sensitive to thermal environments
- Blood circulation might be less effective in elderly than in young people, so they might be more sensitive to cool environments
- The metabolic level for elderly might be lower than young people; therefore, elderly may feel cooler than young in the same environments
- The body fat might be higher in elderly than in young people in general; that will result in higher insulation levels and higher metabolic levels if they are working (heavy weight

people need carry more body mass). This would results in greater sensitivity to warm environments in elderly.

- Elderly people normally dress well corresponding to seasons and ambient air temperatures, therefore, their thermal sensations are less influenced by the environment

Due to these somewhat conflicting differences, we were uncertain whether the elderly are more or less sensitive to the environment than young people. If a difference exists, we were also uncertain whether the difference was sufficiently significant to affect our test plans. Therefore, a detailed analysis was conducted, and the proprietary results were appropriately incorporated into the team's plans for the project.

Improvements in physiology modeling

Not many studies exist about sweat distribution coefficients because the measurements to obtain these values are difficult to conduct. Our previous sweat distribution coefficients in the physiology model were inherited from the Stolwijk's model in 1970s. Much of the information from Stolwijk's model was from an earlier study by Kuno in 1956.

These previous coefficients assigned large values to the trunk of the body, i.e., the chest, back, and pelvis (as shown by the values marked green in Figure G2). This weighting resulted in flat skin temperature predictions for these body parts in warm environments due to the severe sweating predicted by the distribution coefficients (see left portion on Figure G2).

Figure G2: Skin temperature predictions with old and new sweat distributions (resting nude body)

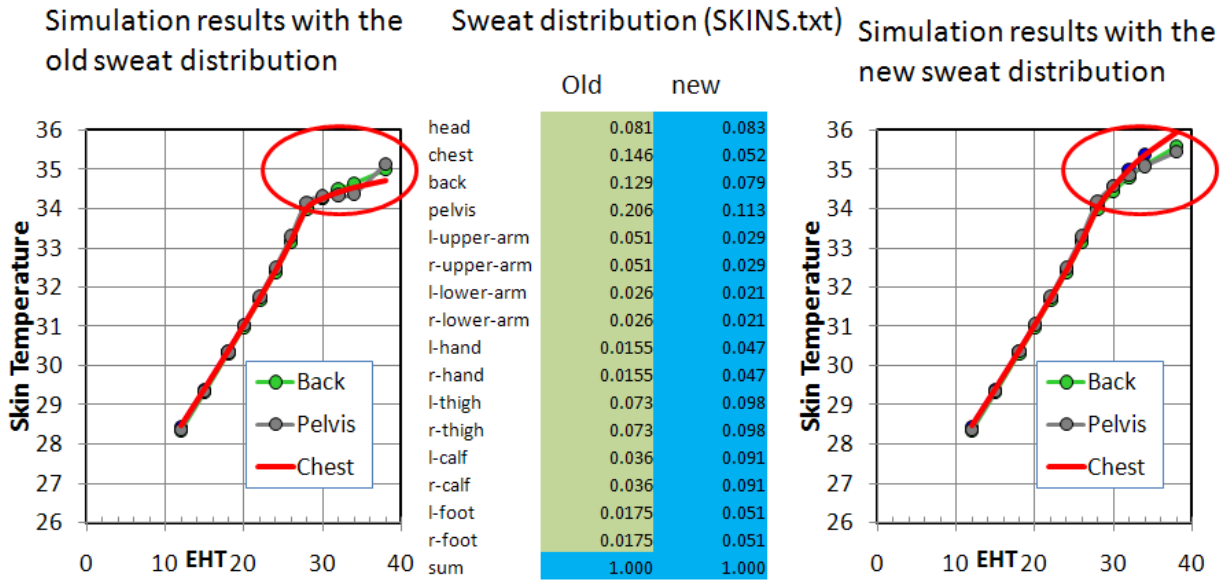

Park and Tamura (1992) measured the local skin temperature distributions for resting nude people under various ambient conditions from 25 – 28°C. The sweat distributions under ambient air temperature between 34°C and 38°C are similar, but they are different from the distributions at the lower ambient air temperatures. Because warm environments generally are

the cause of sweat, we decided to use the distributions under warm conditions. The values in Figure G2 (the column marked blue) are the calculated distributions based on the measured data under a 34°C environmental condition. The distributions for the trunk regions (chest, back, and pelvis) are much smaller than the old values, but they are much larger for the hands and feet.

The skin temperatures for the chest, back, and pelvis with the new sweat distributions from Park and Tamura are shown in the right portion of Figure G2. Indeed, the flat shape of the skin temperatures in warm environments as shown for the old distribution coefficients is gone; instead, the skin temperatures for these body parts increased significantly when the ambient air temperature increased from 30°C to 38°C.

The skin temperatures with both the old and new sweat distributions under air temperatures below 26°C are very similar (comparing the left and right portions of Figure G2), because the sweat distributions only affect skin temperatures under warm environments when the skin actually sweats.

We compared the simulated skin temperatures using the old and the new sweat distributions with measured data. Werner (1980) measured nude subjects' skin temperatures under supine resting conditions for air temperatures between 10 – 50°C. The skin temperature sensors were exposed to the ambient air without a layer of tape.

The comparisons were made for key body segments, including the chest, pelvis, hands, and feet, and some example results are shown for the chest in Figure G3 and for the hands in Figure G4. The solid lines are the simulated skin temperatures with both the new and the old sweat distributions, and the red dots represent the measured skin temperatures by Werner.

Figure G3: Comparison of measured and predicted skin temperatures for chest

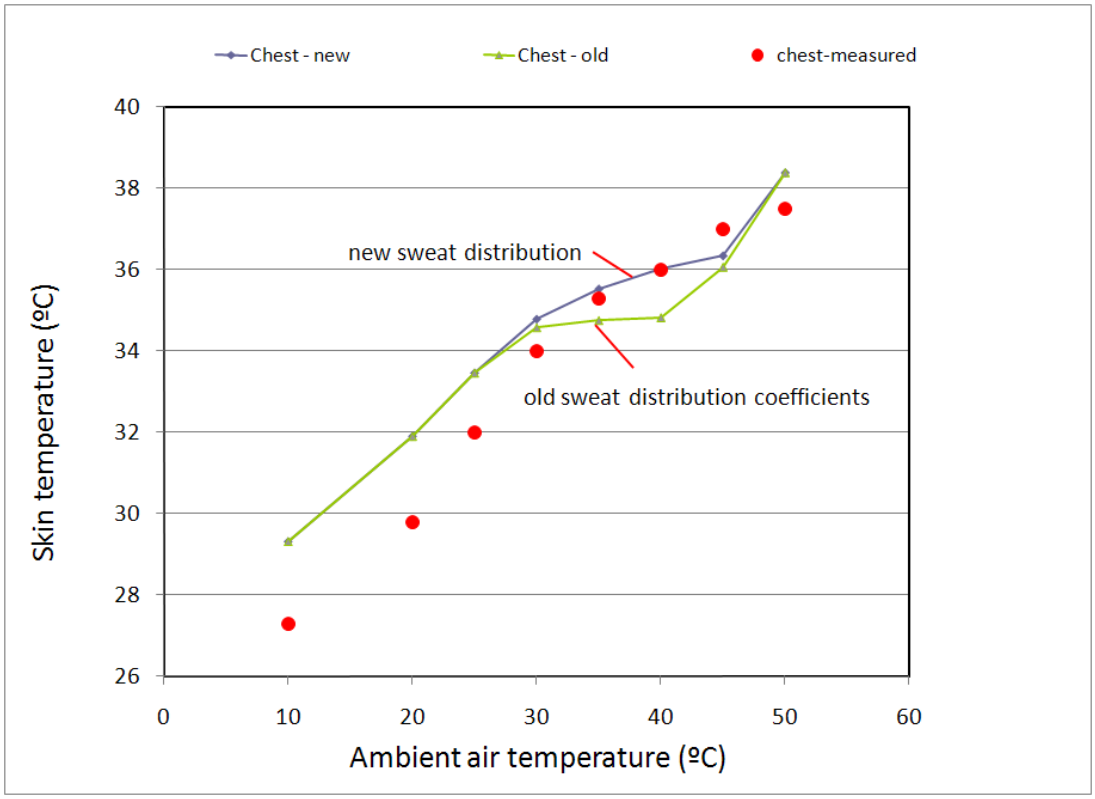

Figure G4: Comparison of measured and predicted skin temperatures for hands

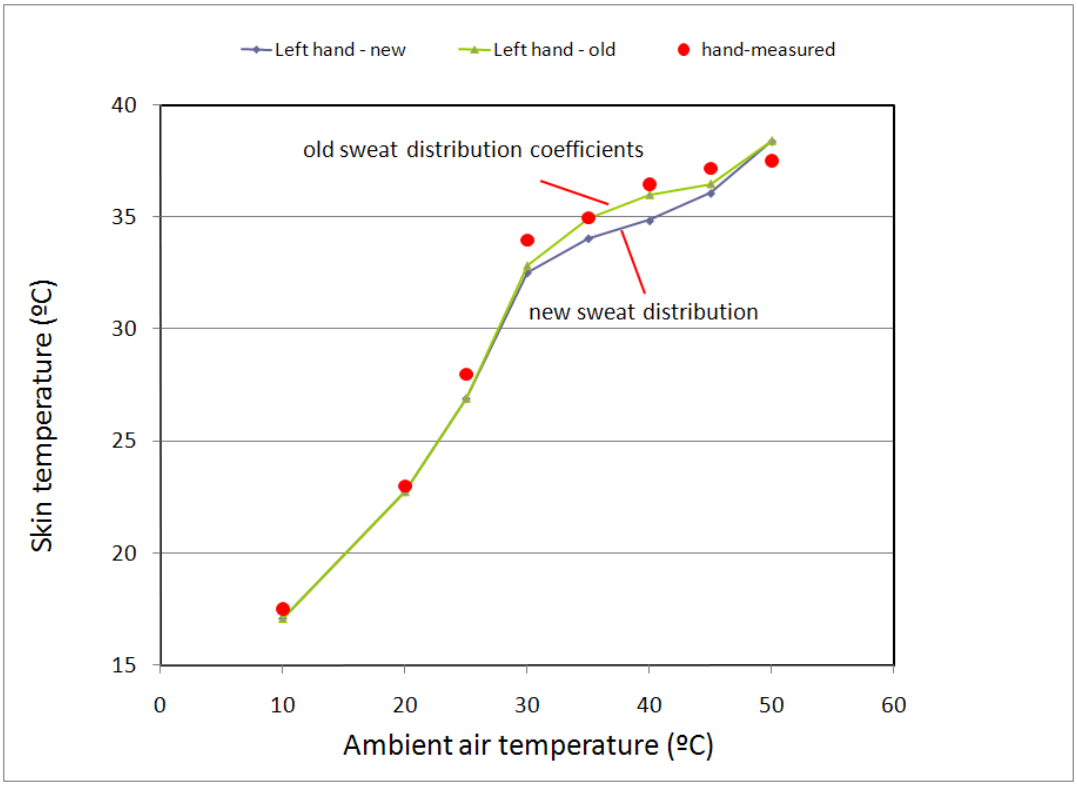

With the new sweat distributions, the simulated skin temperatures under warm conditions (between 30 – 50°C) for the chest and pelvis are much higher than the simulated results with the old sweat distributions, and they are much closer to the measured data. As expected, under air temperatures between 30 and 50°C, the simulated skin temperatures for hands and feet are lower with the new sweat distributions than with the old distributions. For feet, the simulated skin temperatures are closer with the new distributions than with the old distributions. For hands, however, the simulated skin temperatures with the old distributions are much closer to the measured data.

In cool environments (10 – 26°C), the simulated skin temperatures for the chest and pelvis are significantly higher than the measured skin temperatures. This difference didn't occur for the hands and feet, which matched very well between the simulated and the measured skin temperatures. In Werner's tests, they used skin temperature sensors that were exposed to the ambient air without a layer of tape. The sensors in fact partially measured the ambient air temperature, which would cause errors. For the chest and pelvis, when the differences between the skin and the ambient air temperature were large, the influences of the ambient air were larger; therefore, the measured skin temperatures were lower than the actual skin temperatures.

Whether the sweat distributions from Park and Tamura measured under resting conditions represent the distribution during exercise needs to be further analyzed. Cotter et al. (1995) and Smith and Havenith (2010) measured sweat distributions under different levels of exercise and different environmental conditions. Our next step is to compare the sweat distributions from Park and Tamura with the results from Cotter and Smith.

Clothing insulation testing and model updates

UCB completed clothing insulation testing for about 50 typical clothing ensembles using the thermal manikin (see Figure G5). Clothing provides insulation for the 16 body segments considered by the UCB Thermal Comfort model, as well as an insulation factor for the whole body. The objective data from the manikin was used for the UCB advanced Thermal Comfort model, which can evaluate the impact of insulation values for each body part. The UCB team developed a paper on this topic that has been accepted by Clima 2013. The next step for the program is to revise the Thermal Comfort model, so it will be linked to the new clothing database when calculating comfort.

Figure G5: Measuring insulation levels for 16 body parts in typical clothing ensembles

Comfort models for body-segment-specific sensation and comfort were put forward in 2010 in a three-part series in the Building and Environments journal. The models predict the subjective responses to the environment from thermo-physiological measurements or predictions of skin and core temperatures, and they apply to a range of environments, including uniform and non-uniform or transient and stable. The models are based on unique experimental data, and they are formulated in a rational (i.e., piecewise) structure that simplifies further validation and refinement. These models received significant critical attention, and this led to the identification of two issues that need improvement at the fundamental level.

- In the local sensation model, the neutral set points for segment skin temperatures are sensitive to metabolic rate and to the distribution of clothing insulation provided by different clothing ensembles. A calculation sequence that automatically creates segment set points for specific clothing and activity levels has been developed and programmed into the comfort model.
- In the overall sensation model, the piecewise model construction produced unrealistic jumps in output at the transitions. A smoothing technique using the model's key organizational variables was developed and incorporated into the original equations.

To resolve these issues, the team developed mathematical solutions in order to smooth the piece-wise model. A LabView program was subsequently developed to validate the smoothing functions. A paper has been drafted to describe these smoothing functions. The UCB team plans to submit the paper to the Building and Environments journal. The next step is to incorporate the smoothing functions into the existing UCB advanced comfort model.

G2.2.2 Human thermal comfort (HTC) analytical procedure

These research activities focus primarily on validating the newly developed numerical procedures for thermal comfort prediction. Continuing on from the earlier development, UC-Berkeley (UCB) test conditions were put into the GM-developed CFD procedure for simulation; the thermal comfort and sensation were calculated and compared to the human test subject data gathered by UCB. During the study, all airflows and temperatures were obtained for various combinations of localized spot cooling configurations. A few selected transient simulations were also conducted.

Passenger Compartment Model

The proposed HTC analytical procedure begins with identifying and modeling all the interior surfaces that comprise the passenger compartment, including seats and appropriately segmented manikins, in the CAD system. In this study, we created both the Fluent and the Radtherm models of a Cadillac SRX passenger compartment as shown in Figure G6. The model has all the key design parameters for thermal comfort modeling, such as the AC outlet location and size, windshield angle, body vent locations, and many other parameters that influence the performance of the HVAC system. Figure G6 shows the corresponding CFD model in Fluent with a manikin representing a 50-percentile male in the driver's seat. ANSA modeling software was used to mesh the SRX passenger compartment. In this report, only the driver-side manikin,

segmented into 21 body parts, was modeled. A separate 2D surface mesh model of the identical passenger cabin for analysis in Radtherm is also shown in Figure G6.

Figure G6: Fluent and Radtherm surface mesh representations of the passenger compartment

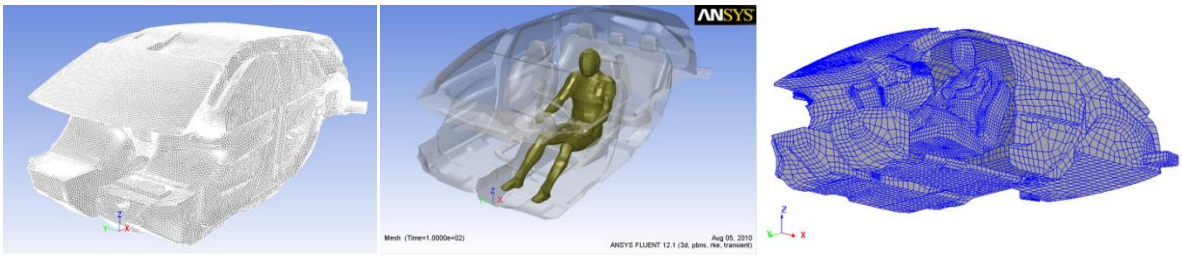

Passenger Compartment CFD Airflow Analysis in Fluent

Prior to predicting human thermal comfort and sensation levels using UCB's HTC model, it is first required to compute both the core and the skin temperatures of all body segments. These are computed in Radtherm through the solution of energy balance equations at the surface of these body segments. However, since Radtherm relies on a CFD solution for convective boundary conditions, Fluent was used in this study to provide this information. Around 3,000,000 tetrahedral elements were required to capture the geometric and the flow details of the passenger compartment with Fluent. A converged steady-state flow solution in Fluent was used to provide the convective heat transfer coefficients and film temperatures on the entire model to Radtherm. However, velocities close to the surface calculated in Fluent were used to compute the heat transfer coefficients for the manikin based on an empirical formulation available in Radtherm. The entire data transfer process between Fluent and Radtherm has been fully automated.

Passenger Compartment Thermal Analysis in Radtherm

As mentioned in the above sub-section, the convection heat transfer coefficient and the film temperature distribution on the entire passenger compartment (including the manikin) were imported from Fluent and mapped onto the much coarser Radtherm surface mesh model. However, the empirical formula relating velocity to heat transfer coefficients on the manikin was chosen instead of the Fluent convective coefficients. This was done primarily because of the limitation of the wall-function based formulation to provide accurate convective coefficients on the relatively low-velocity regions of the manikin. One can observe a checkerboard pattern of the heat transfer coefficient distribution on the manikin when plotted in Fluent. In this study, the standard procedure recommended by Radtherm for HTC was followed.

Prediction of occupant skin and core temperatures

The human physiology model in Radtherm can simulate an arbitrary number of body segments. Each of these segments consists of four body layers (core, muscle, fat, and skin tissues) and a clothing layer. A blood pool node and a series of conductors provide for convective heat transfer between arterial blood and the tissue nodes as well as for the countercurrent heat exchange between the arteries and the veins. The human body thermal regulation is mainly

achieved by regulating the blood flow, so a realistic blood flow model is important for any dynamic model of human thermal comfort. A vehicle occupant's body uses vasoconstriction and vasodilatation to regulate blood distribution in order to control the skin temperature through an increase or decrease of heat loss to the environment. Veins and arteries are paired, even down to very small vessels, and veins carry heat from the arteries back to the core. The model is able to predict both core and extremity skin temperatures with reasonable accuracy under a broad range of environmental conditions.

The current model includes clothing nodes to model the heat capacitance and resistance to the flow of both heat and moisture due to the clothing. The heat capacity of clothing is important when considering transient effects. Moisture resistance is important to correctly model the evaporative heat loss from the body through clothing. The human physiology varies significantly among individuals, and these differences can affect the perceptions of thermal comfort, e.g., a higher metabolic rate or increased body fat can cause people to feel warmer. The present model has a standard 50-percentile human physiology model with a metabolic rate of 2 MET (1 MET = 1 kcal/kg/hr). Clothing levels vary based on the body segment; we assumed a short sleeve shirt, trousers, socks, shoes, etc. for summer clothing during cool-down simulations.

In almost any environment, the body is in contact with solid surfaces, and this results in body heat gains or losses via heat conduction. In the vehicle passenger compartment, the seat contacts a considerable portion of the occupant's body; this must be considered to accurately model the thermal impact to the occupant. The current model includes a contact surface for each body segment. The thermal properties of the contact surface are used to simulate its surface temperature. Each body segment model includes the fractions of exposed skin and clothed skin that are in contact with vehicle surfaces.

Prediction of thermal sensation and thermal comfort from the skin and core temperatures

The human sense of thermal comfort is very complex; it involves both the physiological and the psychological states of a person under specific conditions. In uniform environments, sensation and comfort correlate well: a neutral sensation corresponds to the best comfort; warmer or cooler sensations correspond to reduced comfort. In non-uniform or transient environments, however, the relationship between sensation and comfort becomes more complex. For example, the same cool face sensation could be perceived as very pleasant if the whole body is warm or uncomfortable if the whole body is cold.

Over the past few years, UC Berkeley has worked on studies of local body part thermal comfort. UC Berkeley has carried out human subject tests, developed comfort predictive models, and gained valuable knowledge regarding human responses to local cooling and heating. The human subject test results and local comfort predictive models developed from those tests provide unique information for understanding and predicting human responses to their thermal environment. In both uniform and non-uniform environments, different parts of the body feel warmth and coolness to varying levels. The differences obviously depend on many factors, such as how the body’s thermoregulatory physiology responds to the body’s overall

thermal state, the asymmetric effect of clothing insulation and environmental conditions around the body, the rate of change in the body's skin and core temperatures, and the thermal sensitivity of the different body parts involved.

UC Berkeley proposed to develop a local sensation model of the form shown in Eq. (1). The local sensation model is a function of local skin temperature, mean skin (or core) temperature, and their rates of change. The local and mean skin temperatures represent the body's response to stable conditions; the derivatives of these skin and core temperatures represent the response to transients. The local skin temperature represents the local skin thermal conditions. Mean skin temperature represents the whole body thermal status in the static part of the model. There will be a distinct model for each body part, so that together they capture the asymmetrical features of their environments. Based on the overall whole body sensation, the local body sensations, and the comfort votes from the human subject tests, UC Berkeley performed regression analyses to arrive at the overall sensation and comfort models that are shown in Figure G7.

$$Local\ Sensation = f(T_{skin,i}, \frac{dT_{skin,i}}{dt}, \bar{T}_{skin}, \frac{dT_{core}}{dt}) \qquad \text{Eq. (1)}$$

where:

$T_{skin,i}$ = local skin temperature of one body part
t = time
$\bar{T}_{skin}$ = the mean skin temperature
$dT_{skin,I}/dt$ = the derivative of local skin temperature
dT_{core}/dt = the derivative of the core temperature

The term i in the model ranges from 1 to 19, corresponding to the body parts: head, face, neck, breathing zone, chest, back, pelvis, left and right upper arms, left and right lower arms, left and right hands, left and right thighs, left and right lower legs, plus left and right feet.

Figure G7: Flow chart to show models developed and their relationships

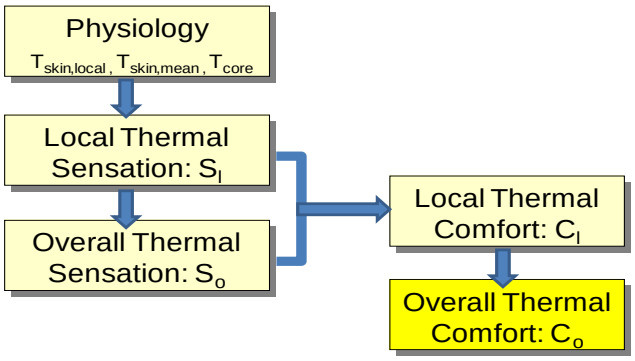

G2.2.3 Milestone 4 – UCB Comfort Model initial update released

The project's fourth major milestone, "UCB Comfort Model initial update released", was successfully completed slightly behind schedule on April 26, 2011. The project team decided to

allow this delay in order to significantly increase the scope of the model update. By incorporating a PC version of the model into this first update, the resulting delay of this milestone actually had a positive effect on the overall execution of the project.

G2.2.4 Implement the enhanced Thermal Comfort Model in a CAE tool

A computer-aided engineering (CAE) tool called the Virtual Thermal Comfort Engineering (VTCE) tool was implemented into commercial code called Radtherm from ThermoAnalytics, Inc. GM successfully completed testing of the procedure using the Cadillac SRX baseline CFD results (calculated with Fluent software) as inputs into Radtherm to generate a thermal comfort index. To evaluate the localized cooling configuration, GM has built a CFD model with exactly the same localized cooling setup as used at UC Berkeley.

Validation of Human Subject Testing Results from UC Berkeley

The GM developed VTCE (Virtual Thermal Comfort Engineering) tool implements the following procedure to obtain thermal comfort and thermal sensation:

1. Run the airflow and temperature solution from CFD tool (Fluent).
2. Export the airflow and temperature solution in the cabin and around the manikin to Radtherm.
3. Evaluate the thermal comfort and thermal sensation in Radtherm.

The team compared the thermal comfort and sensation for the four spot cooling configurations from the VTCE prediction and the UCB test data. The test thermal comfort and sensation values for this comparison were the average values from the 20 human subject test data at UCB. The thermal sensation index is ranging from -4 to +4 with -4 being very cold and +4 being very hot and 0 is neutral. The thermal comfort index is also ranging from -4 to +4 with -4 being very uncomfortable and +4 being very comfortable. Usually, we need thermal comfort index to be +2 and above to comfortably good.

The team also examined the standard deviation for the thermal sensation and comfort from the 20 human subject tests. Both standard deviations for the sensation and comfort are higher than 1 for the four spot cooling flow configurations. This is due to gender, body size, and metabolism variation for each individual. The VTCE predictions are comparing to the average values from the test. For the thermal sensation, which indicates whether you are feeling hot or cold during the spot cooling configuration in this hot ambient temperature condition, the VTCE predictions are correlated quite well with the test. The largest discrepancy shows a difference between test and prediction is 0.3; considering the sensation range being -4 and +4, this is still within the range for a very reasonable correlation. The other three cooling configurations are all comparing very close to the test values within 0.1. The predictions for all four configurations indicate results that are cooler than the actual test data.

The thermal comfort indexes from these analyses indicate the predictions for all four cooling configurations are in a more comfortable state than the test. The differences between predictions and test data for the comfort indexes are higher than the sensation indexes, ranging

from 0.142 to 0.64. For this higher ambient temperature environment, the predictions for the higher comfort values than the test data are consistent with the predictions in cooler thermal sensation for all configurations. Again, the comparison between the prediction and the test are deemed satisfactory for the comfort range between -4 and +4.

Further VTCE validation in a real vehicle environment

The success of the two validations for the VTCE tool with the ideal control test environment at UCB has prompted the project team to move to the next step with the test data from the Delphi wind tunnel test. In late September and early October 2010, the project team completed wind tunnel tests to evaluate various spot cooling concepts. The test data and engineering report were completed and available in December 2010. During the test, a limited number of human subjects were available to evaluate the thermal comfort and sensation for the baseline case without the localized spot cooling and with various spot cooling configurations. All test cases are with solar load. For this validation, Delphi conducted the flow simulation for the baseline case and at least two spot cooling cases. GM then applied the VTCE tool for thermal comfort and sensation validation based on Delphi's flow results.

During the test, the localized spot cooling conditions were implemented in the Cadillac SRX vehicle. For CFD VTCE tool validation, the following two conditions are selected for comparison:

1. Baseline (no spot cooling): $T_{ambient}$=30°C, solar load= 500 W/m2, RH=55%
2. Baseline + high flow combination spot cooling

For the baseline case, the volumetric flow rate is equally distributed across the four main registers. For the combined spot cooling, the tested volumetric flow rate was used for each nozzle. The Fluent simulation was conducted with about 7 million volume elements. Both driver and passenger manikins were included in the model. The Fluent calculations for flow and temperature were carried out by Delphi according to the above condition. The results were transferred to GM for thermal comfort and sensation processing with the VTCE tool.

Figure G8 shows the flow traces originally from the four main HVAC outlet registers for the baseline case. The color indicates the flow velocity in m/s. The flow direction of the main HVAC points to the chest and neck area of the manikins.

Figure G8: Particle trace for the baseline case

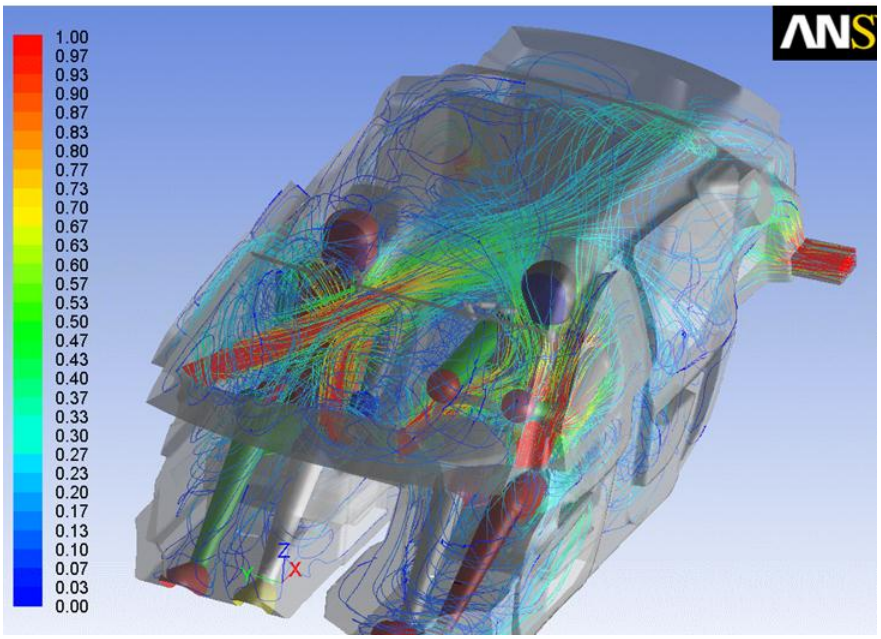

The team analyzed the flow velocity vectors and contours for both baseline and high flow spot cooling cases on the surfaces of both manikins. The convective heat transfer coefficients and film temperature for the baseline case are shown in Figure G9.

Figure G9: CFD convective heat transfer coefficient and film temperature for baseline case on manikin surfaces

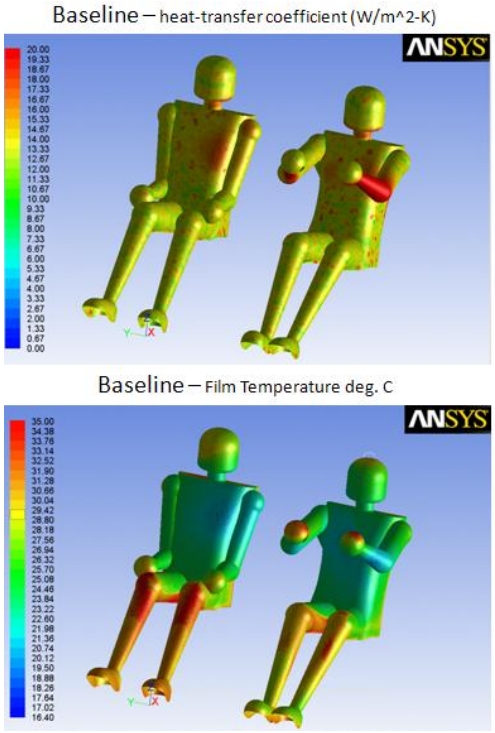

The VTCE tool at GM is used to process the thermal sensation (TS) and the thermal comfort (TC) levels. During the process, the average velocity and temperature values for each body segment 5 mm away from the manikin surfaces and the convective heat transfer coefficients for the entire vehicle surface panels are extracted from the CFD results and imported into Radtherm. Radtherm uses these CFD data coupled with the specified solar load to invoke a human physiological model to calculate body skin and core temperature and sweating level with a specified clothing type. The overall and local thermal comfort and sensation levels are then predicted based on the correlations between TS and TC levels and physiological outputs. The technology involved here is evolving dynamically since it is still in its infancy, and more test data are needed to better understand the insight of this modeling technology.

The overall sensation compares quite reasonably between the test and the simulation. The local sensation levels of some spot cooling locations are in the same trend as the test data and their levels are in the reasonable agreements. However, the sensations for two locations are totally in the opposite direction from the test data. It is clear that the model did not predict the trend and absolute level. GM has been in frequent contact and worked with TAI, Inc. (vendor of the Radtherm software) and UC Berkeley to at least figure out the cause of such inconsistency and then to improve the modeling capability. The thermal comfort prediction for the same comparison is similar to the sensation level prediction, the overall comfort level is reasonably good, but the comfort levels for two locations are in the wrong trend.

With the comparison issue in mind for the baseline case, we feel strongly that finding ways to improve the predictive capability of the VTCE tool for the baseline case should be the current focus, and we have been doing that with the UC Berkeley team and TAI, Inc. So far, the predicted TS and TC levels for the spot cooling case have been obtained, but the comparison with the test data is currently on hold until the accuracy and trend issue for the baseline case has been resolved.

PC version development of the VTCE tool

The PC version development started in January 2011 between GM and UC Berkeley with the focus on developing a quick vehicle architecture level thermal comfort evaluation. This tool is intended to be used in GM's AVDC (Advanced Vehicle Development Center). The idea is to choose some representative vehicles from a broad range of categories, such as small sedan, large sedan, compact SUV, full size SUV and pick-up truck, and so on to build a CFD flow database around each representative vehicle with various predefined HVAC operation modes, fan levels, and air velocity and temperature around the manikin. This CFD database will be implemented into a PC-based thermal comfort predictor so that an HVAC engineer can specify HVAC operation mode, fan speed, discharge temperature, solar load, and desired vehicle type from the database to understand the impact on human thermal comfort and sensation. This PC thermal comfort tool runs very quickly on a PC, since it does not require detailed CFD meshing and calculations. The flow and temperature around the manikin are purely done based on the pre-calculated CFD results for each representative vehicle. Data interpolation is needed for HVAC user input of outlet velocity and temperature that are different from the database. The solar radiation, convection, and face-to-face radiation does enter into the energy balance on the surface

of the manikin when the human physiology model is used to calculate the skin and core temperature under the vehicle thermal environment.

The UCB team incorporated the SRX geometry into the comfort model. Preliminary tests were finished to check the results. Currently, the number of polygons used to represent the car is 3000, which is relatively low in order to maintain the fast speed of the model simulation.

One of the input features of the PC tool is that it provides a user interface to bring in the air velocity and temperature around the manikin and the vehicle panel temperature from an external CFD flow simulation. The graphic user interface (GUI) of the PC version is shown in Figure G10. We are taking advantage of this feature to enable the VTCE validation process. During the course of the past few months, Delphi has tested and obtained valuable thermal sensation and comfort data for various spot cooling and heating configurations, and GM has been using CFD to compute the flow and temperature according to the test conditions. Although this effort is still early in the validation stage due to the complexity and uncertainty. Of the specific conditions of the thermal environment on the human subject test, we have managed to obtain favorable correlations between the prediction and the test for the baseline case. We have made continued progress in validating more cases with various cooling/heating combinations. Two additional validation cases have been attempted. In summary, we believe that the tool's thermal comfort prediction for the vehicle in the real world environment is very encouraging, and that these test successfully demonstrate the capabilities of the VTCE tool.

Figure G10: SRX geometry in the PC Comfort model

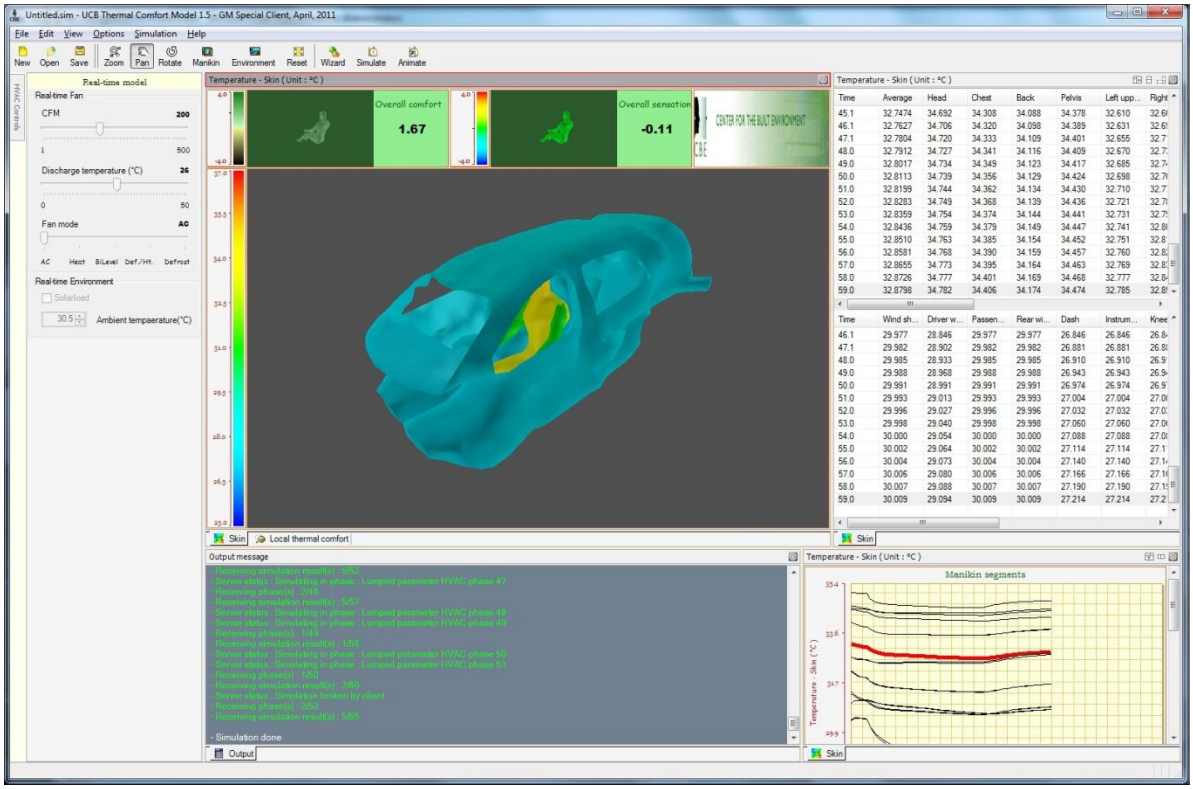

In addition to the standard Thermal Comfort model predictions of sensation and comfort, the PC tool added new features for GM engineers designing advanced HVAC systems for future vehicles. One very useful feature developed for the initial release of the PC tool was automatic set point temperature calculation for body parts. The set point temperatures for all body parts are generated and saved in a single pre-defined file before the comfort simulation based on either "summer" or "winter" condition and also manikin clothing level and metabolic rate. For various environmental and manikin's conditions, the set point temperature file is used in the model to calculate the local sensation and comfort values. It requires a deeper understanding of the model in order to generate this file and usually this task doesn't belong to the users. As a result, UC Berkeley made the set point temperature calculation as a dynamic process based on the simulation condition. This implementation in the final release makes the PC tool flexible and user-friendly.

Vehicle library in the PC version

A total of six vehicles have been chosen to be included in the PC tool. The vehicles are grouped into the following three categories:

- Sedan: Chevrolet Volt (Extended-Range Electric Vehicle, mid-size), Buick Lacrosse (mid-full size), Chevrolet mini (compact size)
- Sport Utility Vehicle: Cadillac SRX (compact size), Chevrolet Tahoe (full size)
- Pick-up Truck: Chevrolet Silverado (full size)

Each vehicle represents a typical type in each category in terms of size and function. The noticeable exceptions are the Chevrolet Volt and the Buick Lacrosse. They are in a similar size category, although the Volt is an E-REV and the Lacrosse is a traditional gas-powered vehicle. Because these two were selected as demonstration vehicles, we want to have detailed data for future analysis under this project. Other than these exceptions, each vehicle chosen should have distinct features in HVAC distribution and the thermal comfort characteristics in the category it represents.

For each vehicle, we carefully model all AC outlets into the cabin. These includes four main AC panel outlets, two side window outlets, defrost outlet, heater outlets in the driver and front passenger foot well area, floor outlets under the driver and front passenger seats and finally outlets on the center console toward to the rear seat if any. Keeping track of airflow in all the outlets is essential later to apply flow measurement data from the proving ground in order to generate CFD database for each vehicle.

The surface mesh usually built for CFD applications is in the order of hundreds of thousand elements to ensure enough resolution for the vehicle feature lines. However, in the PC tool application, no such detailed refine mesh is necessary due to the following two reasons. First, it does not solve complicated flow equations (Navier-Stokes) to obtain solution. Instead, simple discharge coefficient (to be explained later) is needed to relate HVAC discharge velocity and temperature to the air speed and temperature around the manikin. Also lumped parameter thermal analysis is used to account for the energy balance between solar load gain, heat

loss/gain through cabin walls and heat from human subjects in the cabin and to speed-up the view factor calculation in thermal radiation analysis. Usually for the later reason, the total surface element numbers including the manikin and vehicle panels has to be limited fewer than 7,000. Because of this, the fine mesh vehicle model used for CFD calculation has to be further coarsened to be included into PC tool. Figure G11 shows the six coarsened vehicle models implemented in the VTCE tool.

Figure G11: The six vehicles implemented in the VTCE PC tool

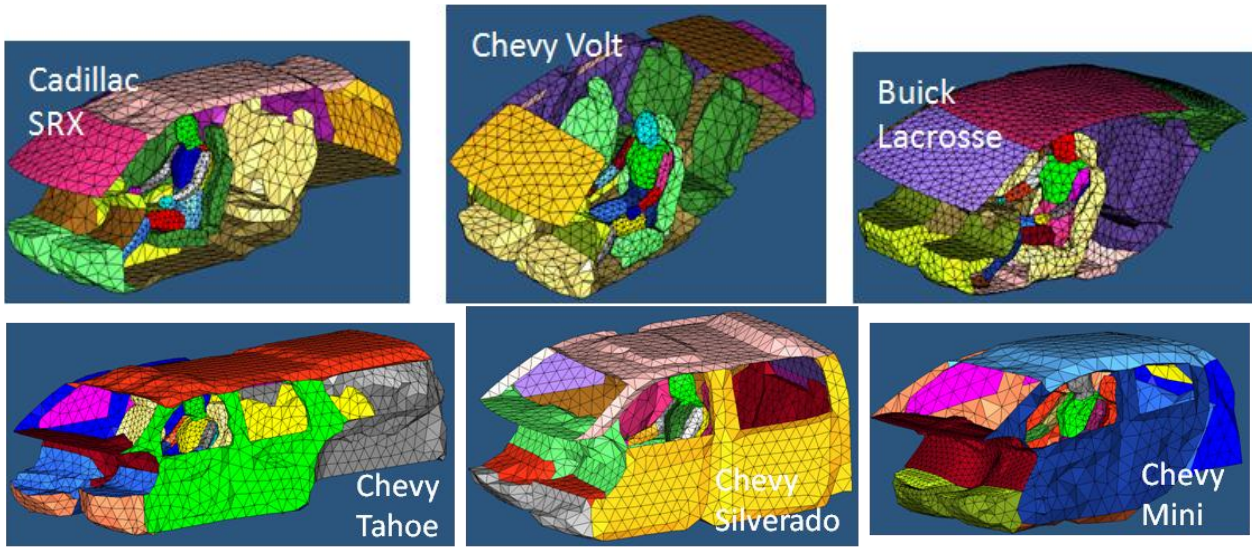

CFD flow database corresponding to the Vehicles in the library

The routines in the PC version to evaluate the human thermal comfort for the occupant are based on the following energy balance between environmental factors and heat generation/loss controlled by the human physiology. For vehicle, the environmental factors include: (1) HVAC airflow rate and temperature around the manikin surface, (2) air relative humidity, (3) location of the HVAC outlet registers, (4) solar load, and (5) vehicle body panel temperature and ambient air temperature. For the physiology model used in PC version, the following parameters are needed: (1) occupant metabolic rate, (2) body build (there are various body builder option in the tool), and (3) clothing level. The parameters related to human physiology calculation have been implemented in the tool already. For the environmental factors, the existing PC tool from UC Berkeley has everything to calculate the energy balance on the manikin skin surface and to evaluate the thermal comfort. The only data missing to enable the thermal comfort prediction for each built-in vehicle is the airflow distribution around the surface of the manikin. The airflow around the surface of the manikin depends on the HVAC operating mode and fan blower speed. We have pre-selected 5 HVAC operating modes and 4 fan blower speeds to cover all possible cooling and heating HVAC scenarios for each vehicle. This is the task that the computational fluid dynamics (CFD) tool can be used effectively to generate a complete airflow map around the manikin. Table G2 shows the five different HVAC operating modes used with four fan blower speeds, which are 100%, 75%, 50%, and 25%.

Table G2: Five HVAC operating modes

AC mode	Non-AC mode			
	Bi-level	Heater	Defrost	Defrost/heater

To conduct the CFD simulation to map the airflow around the manikin surface, the exact air velocity (flow rate) at the exit of each HVAC register has to be specified. The airflow data at the register location can only be determined by tedious measurement in the flow measurement Lab. The following steps are required to complete the CFD HVAC flow database in the PC tool for each vehicle:

2 Flow measurement at the GM Proving Ground test facilities to obtain the airflow distribution at each HVAC outlet register at four blower speeds and five operational modes. The four blower speeds are set at 100%, 75%, 50%, and 25% and the HVAC operational modes are AC, Bi-Level, Heater, Defrost and Defog modes.

3 Based on the airflow rate distribution from measurement, CFD simulations with 20 cases (4 blower speeds x 5 operational modes) are conducted by specifying the exact discharge mass flow rate from each HVAC outlet.

4 The air velocities at 3 cm away from the manikin surface for 16 body segments are recorded.

5 The correlations between the discharge velocity and the velocity at each body segment for the manikin are calculated for all HVAC operational modes.

With this database, the tool is used to obtain thermal comfort by specifying any desired discharge velocity and temperature, HVAC operational mode, solar load for the chosen vehicle platform. Using the relationship between the HVAC discharge airflow rate and the average discharge velocity, the user selects a discharge flow rate to run the HVAC system in the selected vehicle. The CFD calculated discharge coefficients for each individual HVAC operation mode is used to calculate the air velocity at each body segment: Based on this simulation, the PC tool can estimate the thermal sensation and comfort for each vehicle occupant.

PC Tool Thermal Comfort validation

One of the input features of the PC tool is that it provides a user interface to bring in the air velocity and temperature around manikin and the vehicle panel temperature from an external CFD flow simulation. We are taking advantage of this feature to the VTCE (Virtual Thermal Comfort Engineering) validation process. During the course of the past few months, when Delphi has tested and obtained valuable thermal sensation and comfort data for various spot cooling and heating configurations, we have been using CFD to compute the flow and temperature according to the test condition. Although this is still early in the validation stage, due to the complexity and uncertainty of the test condition of the thermal environment on the human subject test, we have managed to obtain favorable correlations between the prediction and the test for the baseline case. We are still working hard to inch closer to both the spot cooling and heating condition. Figure G12 shows the baseline case for the SRX condition we are

using for this validation. The baseline localized spot cooling test case specified the wind speed, ambient temperature, relative humidity (RH), and solar load as indicated in Figure G12.

Figure G12: Thermal comfort validation setup for the baseline spot cooling case

Spot cooling simulation equipment in the rear hatch

Chest, face nozzle

Lap nozzle

UCB thermal manikin and human subject testing for evaluation of spot cooling

- Wind speed 30 mph (48.3 km/h)
- T = 29°C
- RH = 55%
- Solar load = 500 W/m²

Vehicle

1) Baseline SRX
2) Modified with distributed cooling

All the spot cooling nozzle flows are off, and the discharge airflow from the main front panels is 95 CFM and the discharge temperature is 18 C. The CFD simulation was set up as closely to the tunnel test environment as possible. The air velocity and temperature 3 cm away from the surface of the manikin were extracted from the results and used as input to the PC version. The body panel temperatures were also recorded and used as input. Figure G13 and Figure G14 show the comparison between predictions and tunnel test data for thermal sensation and comfort respectively. We are quite satisfied with the comparison results since this is the first validation against the real asymmetric harsh thermal environment.

Figure G13: Thermal sensation comparison between prediction and test for the baseline case for Delphi's SRX tunnel test

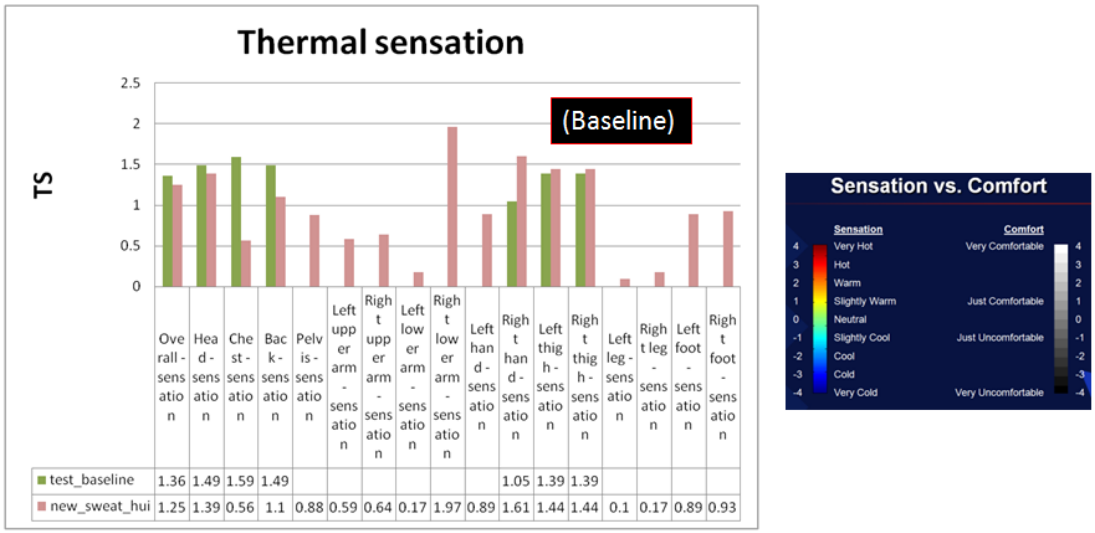

Figure G14: Thermal comfort comparison between prediction and test for the baseline case for Delphi's SRX tunnel test

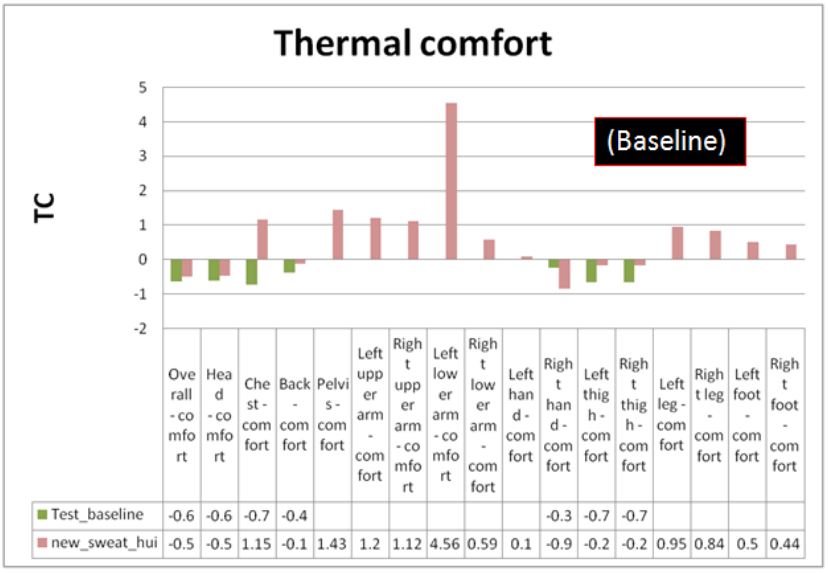

Development updates to the PC-based VTCE tool

UC Berkeley released two updated versions of the tool to GM. The latest version includes the following bug fixes and modeling enhancements: (1) calling to the correct fan data when one of the GM's built-in vehicles is used, (2) correcting the code freeze issue when the solar load is activated in the 64-bit version, (3) fixing the bug for using the winter clothing, and (4) sweat distribution enhancement. Using this new enhanced version, the previous spot-cooling configuration cases are redone to check the new version's consistency with the old version of these two cases. In addition, the validations are done with two new cases for the spot-heating

configuration. These four cases are examples of the analysis performed to validate these cases. Figure G15 shows the velocity vectors cutting through the manikin. Figure G16 and Figure G17 show the temperature and velocity contours at the manikin surface and air temperature and velocity at 3cm off the manikin surface. Figure G18 shows the temperature contours on the vehicle panels. These are some of the methods employed to perform the tool validation.

Figure G15: Velocity vectors (left) and streamlines (right) for the spot-heating baseline case.

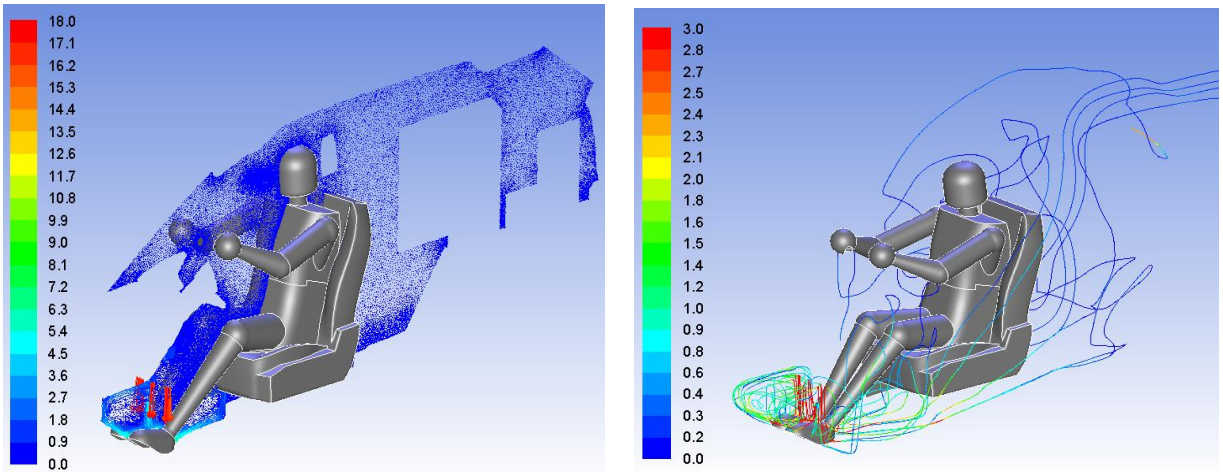

Figure G16: Manikin skin temperature (^{0}C) (left) and velocity (m/s) (right) for the spot-heating baseline case.

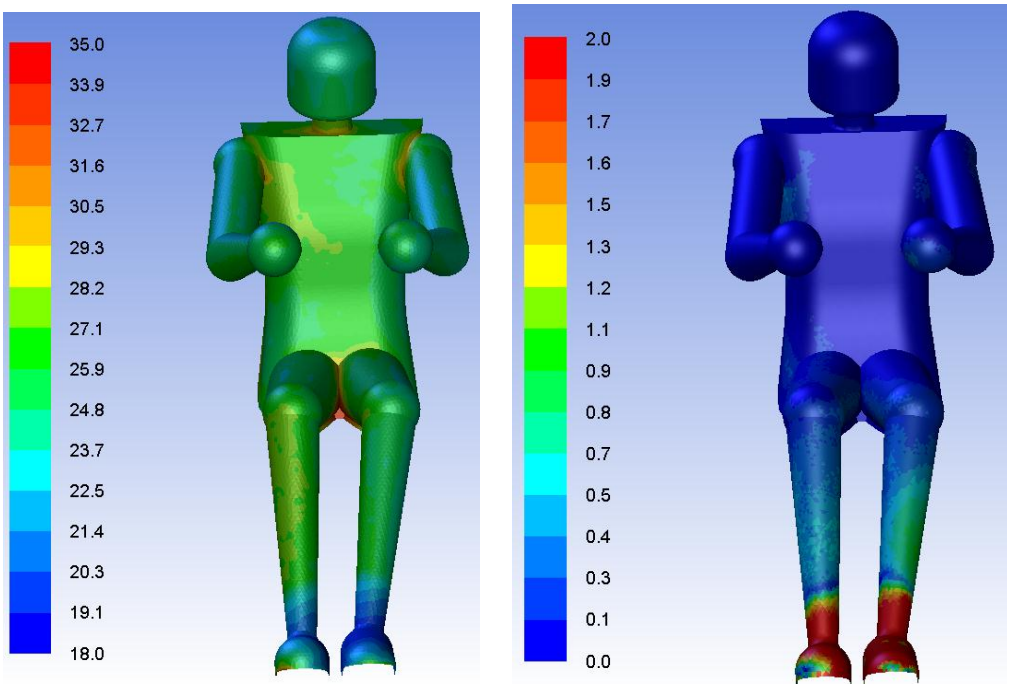

Figure G17: Airflow temperature (^{0}C) (left) and velocity (m/s), 3 cm off manikin skin surface for the spot-heating baseline case.

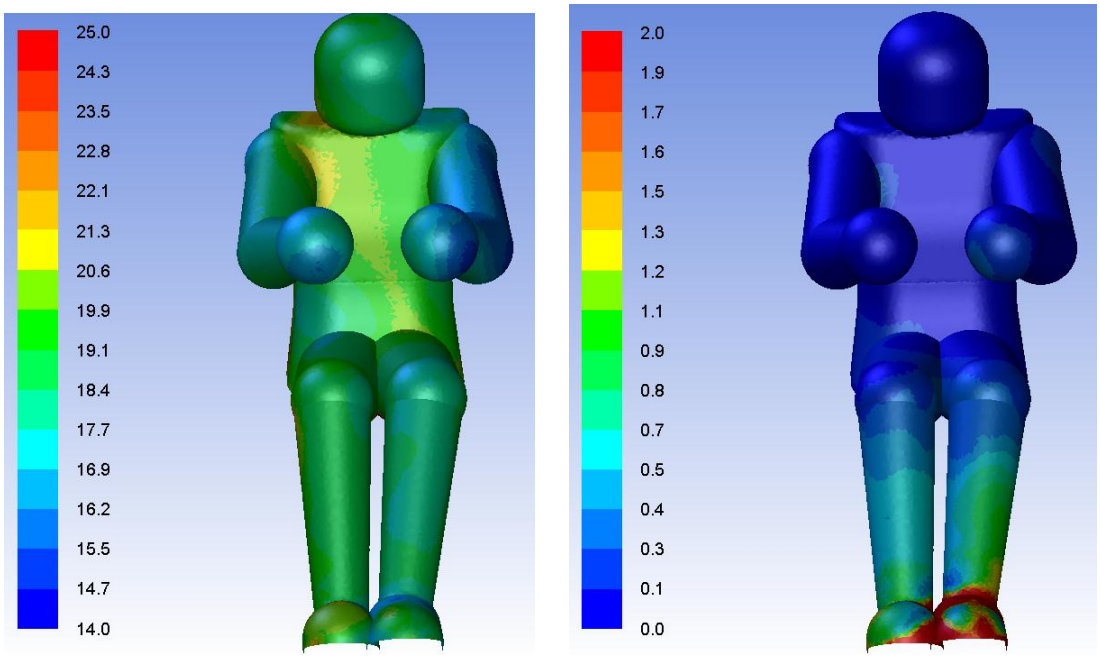

Figure G18: Vehicle body panel temperature contours.

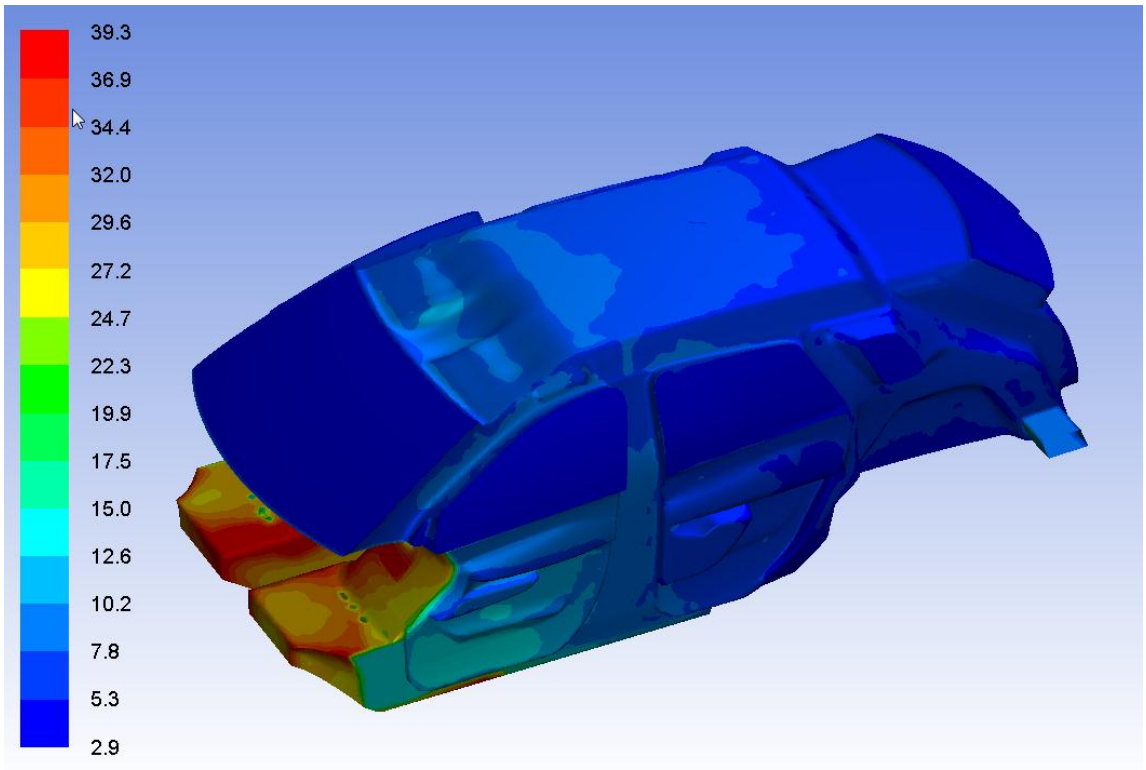

Development of a new stand-alone Thermal Comfort Control Tool

This activity developed a "stand-alone" thermal comfort module (tool) that will interact with GM's HVAC control software such that the thermal comfort index can be used as part of the HVAC automatic climate control (ACC) strategy. Traditionally, HVAC control loop either uses the in-car breath level temperature as a feedback to adjust the air discharge flow rate and temperature to reach comfort. Or in some other cases, it completely relies on mathematical model to provide HVAC air discharge flow rate and temperature based on some other indicators such as solar load sensor, outside air temperature and humidity level. None of the above methods directly address the need of the occupant for thermal comfort, which indeed is the purpose of the HVAC climate control. The current project will be using the existing PC comfort tool but to modify it from the current GUI based operation to a batch tool operation. The new comfort module will maintain the core thermal comfort capability but move some of the inputs from the GUI to be part of the interface between the new comfort module and the control software SIMULINK. Figure G19 shows the conceptual operation of this control software. The SIMULINK is the control software that GM is currently using for the vehicle HVAC ACC system. This developing module is to be interacted with the SIMULINK with a new clear defined interface that facilitates the data exchange between the comfort output and the instructional inputs from the main controller – SIMULINK. The SIMULINK GUI is shown in Figure G20. For the control operation:

- Users can provide their own routine in C into SIMULINK environment (called S function) to perform the required task.
- The comfort module will become a C code S function in Simulink.
- The data exchange between Simulink and comfort module can be done by the external ASCII files or clearly defined interface.

Figure G19: The schematic of the thermal comfort PC control tool operation

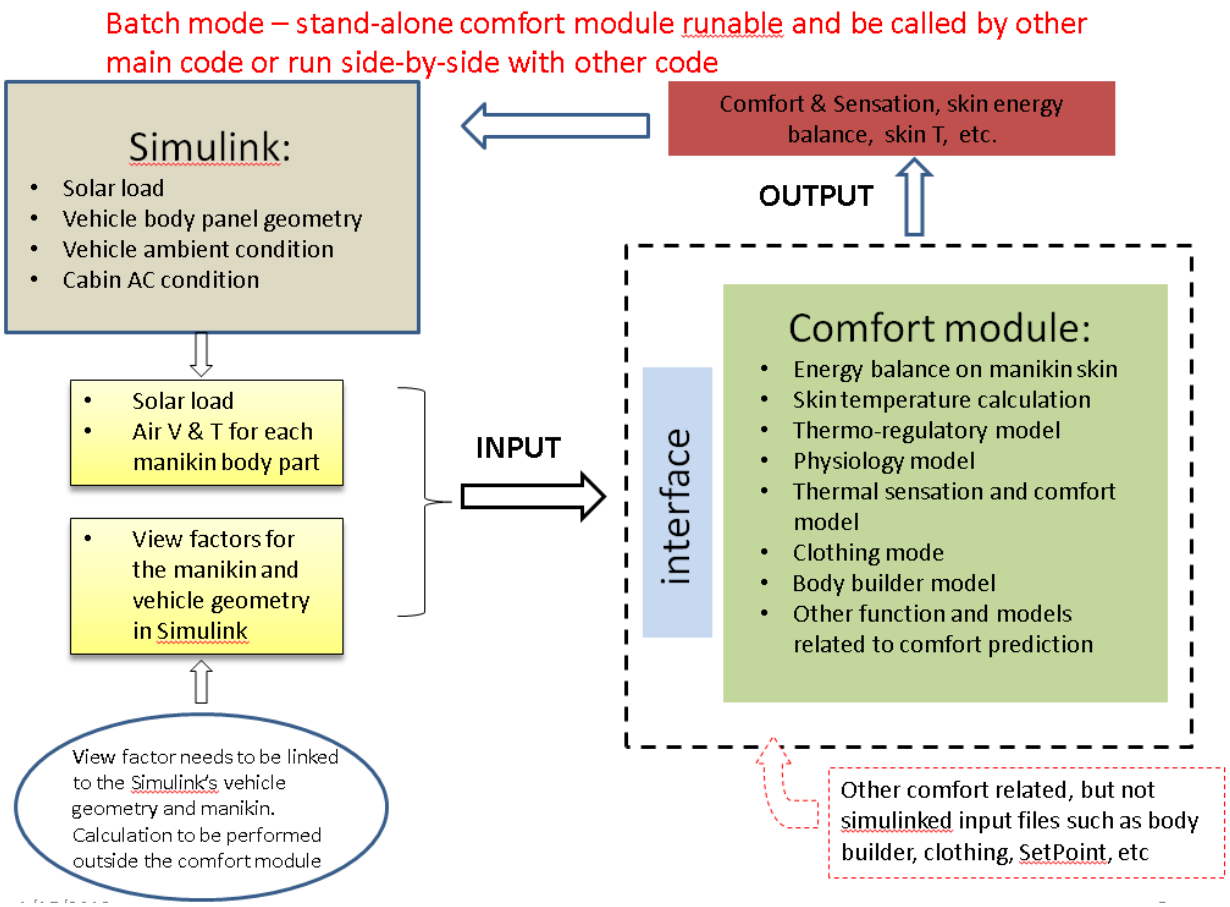

Figure G20: The SIMULINK GUI

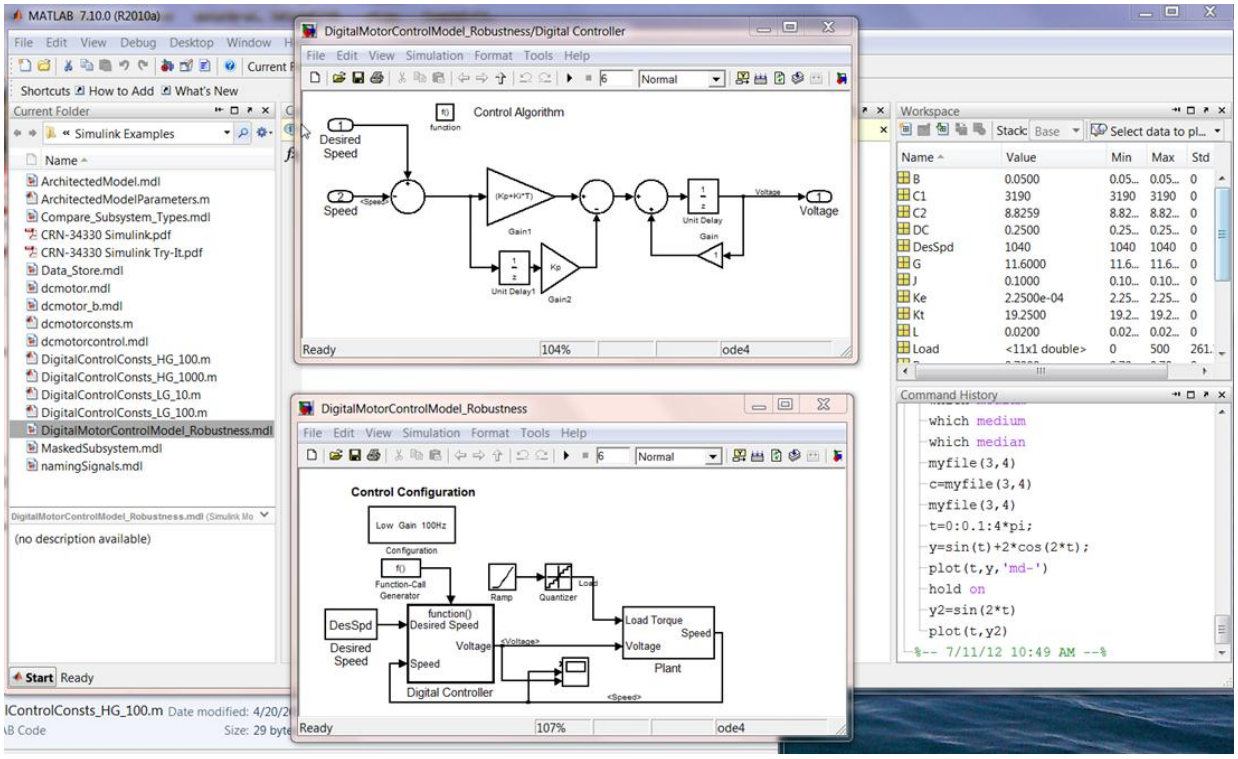

G2.2.5 Milestone 9 – UCB Comfort Model second update released

On January 16, 2013, the team released the UCB Comfort Model update to complete this project milestone, and the corresponding release of the CAE advanced comfort model supported the development and release of associated engineering tools. To integrate the UCB Comfort Model with other third-party applications and tools that provide environmental conditions, we developed the UCB Comfort C-API interface, which can be called in a tool supporting C-program extensions like Simulink. We successfully linked the CAE advanced comfort model into Simulink. The link is based on the C-mex S function in Simulink, where the UCB Comfort API dynamic link library (dll) was loaded and called. The primary demo code segments have been successfully executed. All of those code segments can be encapsulated in a self-defined block within Simulink, and other common blocks can be further designed based on the need to support further simulation.

G2.2.6 Milestone 11 – UCB Comfort Model third update released

This milestone is planned for completion by 3/31/2014. This third update of the UCB Comfort Model will incorporate the latest testing and analysis to create the final validated release.

G2.3 Task 3 – Perform Human Subject Testing

The main activity for this task was to perform the first set of human subject testing in a vehicle mock-up in the UCB Environmental Test Chamber for. Subsequent human subject testing was

performed in their climatic wind tunnel under other project tasks, but those results were also correlated and incorporated into updates of the UCB Comfort Model.

G2.3.1 Testing in the automotive mockup at the UCB environmental test chamber

The automotive mockup for the UCB environmental test chamber was designed (see Figure G21) and built.

Figure G21: Automotive mockup in the UCB environmental test chamber

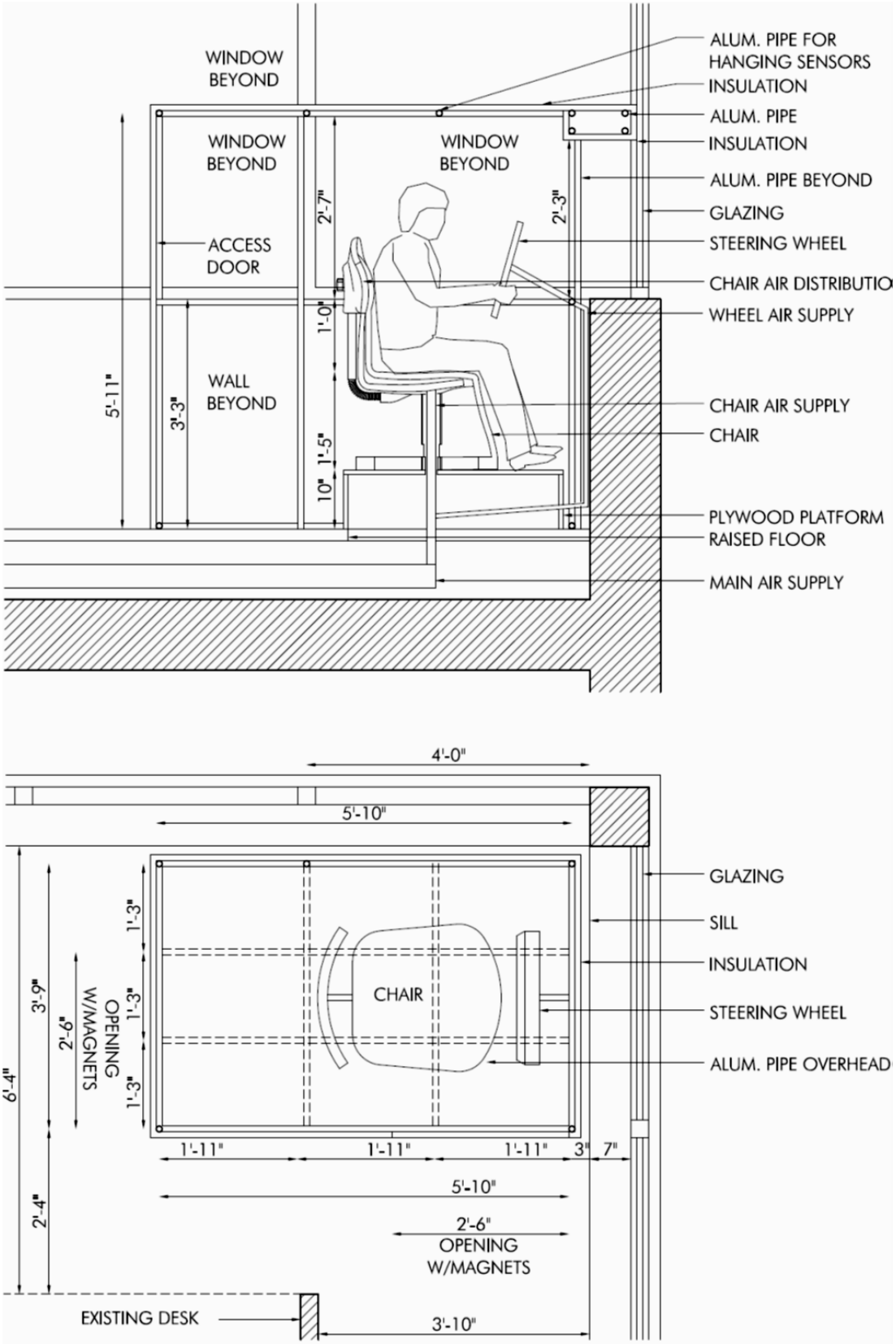

Experiment set up:

The test setup for the vehicle mockup car in the UC Berkeley Environment Chamber is show in Figure G22. The chamber has two areas, a car space for human subject measurements and an anteroom; the anteroom is where subjects stay between test conditions and do step exercises during recovery periods. There are windows on three sides of the car space, similar to the space in an actual car. The window between the car and the anteroom provides light to the anteroom. There is a curved skylight installed in the anteroom to provide additional light, and it also provides additional height for tall people performing the step exercises.

Figure G22: The mockup "car" in the chamber. It has two spaces, the car space, and the anteroom space. A skylight is installed in the anteroom

Mock up car in the chamber | Car space | Anteroom | Skylight in the anteroom

All the local cooling/heating strategies are mocked up and installed. They include ventilated seat, seat belt, air supplied from A-pillar, B-pillar, headliner, around neck towards the breathing zone, and behind the driving wheel towards hands. The driving wheel is heated. The three images in Figure G23 show the ventilated seat (including the seat side and the back side). The duct in the picture provides cooled air to the back of the seat. There is a radiation heater installed in front of driver's seat to simulate solar radiation.

Figure G23: Ventilated seat

The local cooling/heating control is carried out through a program in a computer. The interface controlling the local fan speeds is presented in Figure G24. The fan speeds can be individually adjusted from high to low by moving the sliders up and down. The computer program also records the settings of the speed for each fan.

The manifold controlling the fans is also shown in Figure G24. There are five fans installed in the manifold to provide air to the local cooling/heating devices (such as the ventilated seat). The air supply to the manifold comes from a spot cooling supply from the chamber HVAC system, which can control the supply air temperature to various levels.

Figure G24: Local fan speed control software interface and the manifold hosting fans

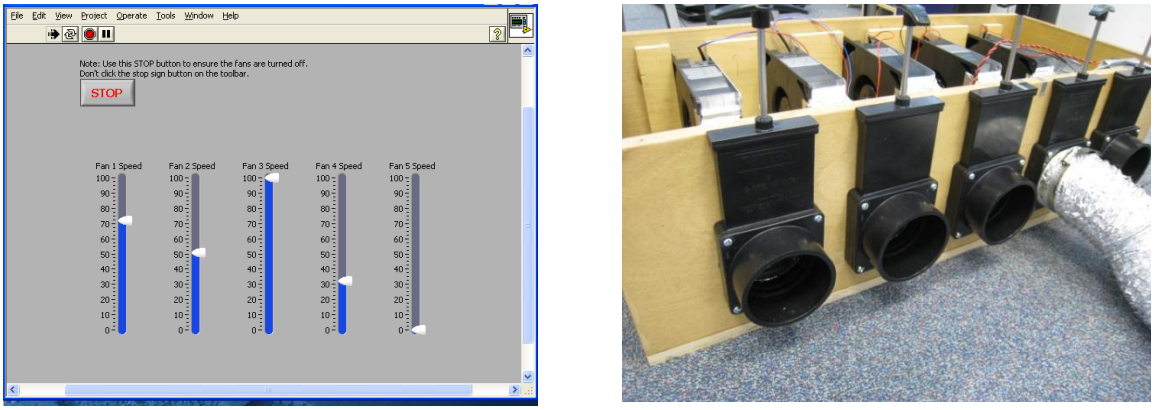

a. interface controlling local fan speed b. manifold

Pilot tests:

First, we used a thermal manikin to measure the heat loss for each of 16 body parts (see Figure G25). The manikin tests at this stage were preliminary and used to help identify the effectiveness of local cooling/heating strategies. Following the human subject tests and after the manikin had been upgraded and repaired, more complete manikin tests were conducted.

Figure G25: A thermal manikin is used to measure the heat loss of various local cooling/heating devices

We conducted pilot tests with human subjects to provide an initial evaluation of different local cooling/heating strategies (as shown in three images in Figure G26).

Figure G26: Pilot tests

The goal of the pilot testing was to identify the most effective local strategies. Based on pilot human subject tests and heat loss measurement from the thermal manikin, UCB provided initial recommended effective local cooling/heating strategies and their supply temperatures and flow rates to the rest of the team. After combining the pilot test results and the feedback from the project team discussion, the chamber test conditions were finalized for the UCB human subject testing.

Conducting human subject tests:

One test procedure covered six local conditions, and each local condition continued for 15 minutes. Two subjects participated simultaneously during the 3.5-hour test period. When one subject was inside the mockup car undergoing a local test condition, the second person waited in the anteroom. They alternated positions every 15 minutes. In the anteroom, the person climbed 12-steps every 5 minutes in order to simulate the metabolic rate of walking outdoors (see Figure G27). The test procedure also specified consistent clothing insulation levels, where summer clothes were a short-sleeved shirt, pants, thin socks, and shoes while the winter clothes were a long-sleeved shirt, T-shirt, pants, thick socks, and shoes.

Figure G27: Seasonal clothing and the 12-steps exercise in the anteroom during tests

	
Summer clothing	Winter clothing

We measured skin temperature at 10 locations, allowing us to calculate mean skin temperature using standard procedures. The locations include key locations for our purposes of this study, e.g. gluteal region and face (see Figure G28). We used thermistors for locations where the skin temperatures do not change quickly, and thermocouples for cheek and gluteal locations where the skin temperatures changes rapidly due to impinging supply airflows.

Figure G28: Skin temperature measurement sites

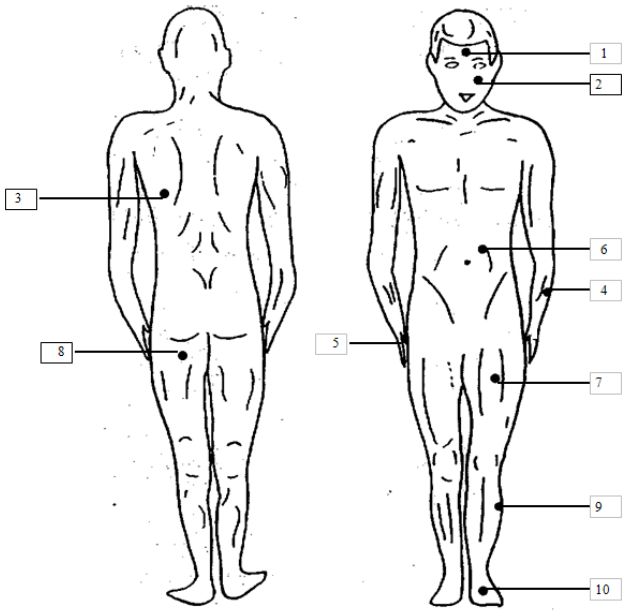

The thermal sensation and comfort scales were presented to the subjects on a computer screen. They appeared right after the subjects get into the car, then at 2, 5, and 8 minutes later during the 15 minutes of test. They apply to the different body parts (such as chest, whole body). The major questions are shown in Figure G29. We conducted four 2-hour training sessions for all 30 subjects to explain the test procedures, behavioral requirements, and survey questions, and to conduct a pilot test for each subject.

Figure G29: Thermal comfort survey questions

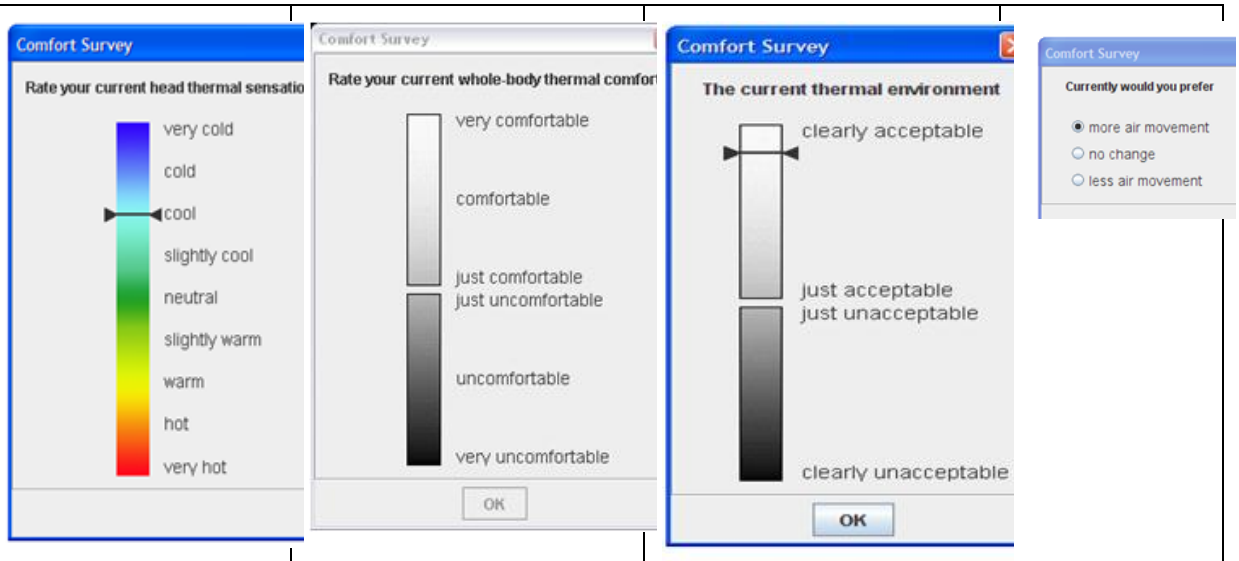

Thermal sensation scale	Comfort scale	Acceptability scale	Air movement preference

The human subject testing resulted in the following conclusions about the effectiveness of the distributed HVAC approach: 1) comfort is maintained with local cooling at the tested temperatures; and 2) with a high solar radiation load, comfort is still well maintained when all localized cooling components are applied.

.3.2 Milestone 1 – Identify initial set of locations for distributed heating/cooling

The project's first major milestone, Identify initial set of locations for distributed heating and cooling, was successfully completed as scheduled on March 31, 2010. UCB was responsible for completing this initial evaluation of potential distributed HVAC components. UCB based their recommendation on their pilot human subject testing, which began in early March. UCB's findings for this milestone allowed the team to proceed with the subsequent steps of the project.

G2.4 Task 4 – Define Design of Experiments (DoE) for Target Platform

For Task 4, Define Design of Experiments for Target Platform, the team developed vehicle selection criteria to choose the target platform. The team selected the Cadillac SRX from GM's portfolio as the vehicle that best satisfied the project's requirements. This vehicle selection allowed CFD modeling and other activities to be performed as scheduled.

G2.4.1 Develop and Define the Design of Experiments

The team created a baseline CFD model for Cadillac SRX and successfully simulated the baseline thermal comfort cases as described below. The team prepared the geometry model from a CAD file for airflow and thermal analysis. The surface mesh using ANSYS' TGRID is shown in Figure G30, where the roof has been removed to show the interior meshing. The baseline model is used to check that the basic setup is correct and running without any numerical issues. This baseline SRX model is then used to analyze many AC cooling flow conditions with solar radiation. For the solar load simulation, the PPG green glass is used for all the windows. Its solar properties are listed in Table G3: Glass solar properties. The α value is the absorptivity, ϱ is the reflectivity, and τ is the transmissivity. These properties are specified for visible and infrared portions of the spectrum. The solar radiation is calculated by the solar calculator in Fluent. The location is at Phoenix, Arizona, and the time 1 p.m. on June 21. The solar load distribution on the windows into the cabin is listed in Figure G31.

Figure G30: Cadillac SRX surface mesh: shown here with one manikin and the roof removed to show the interior

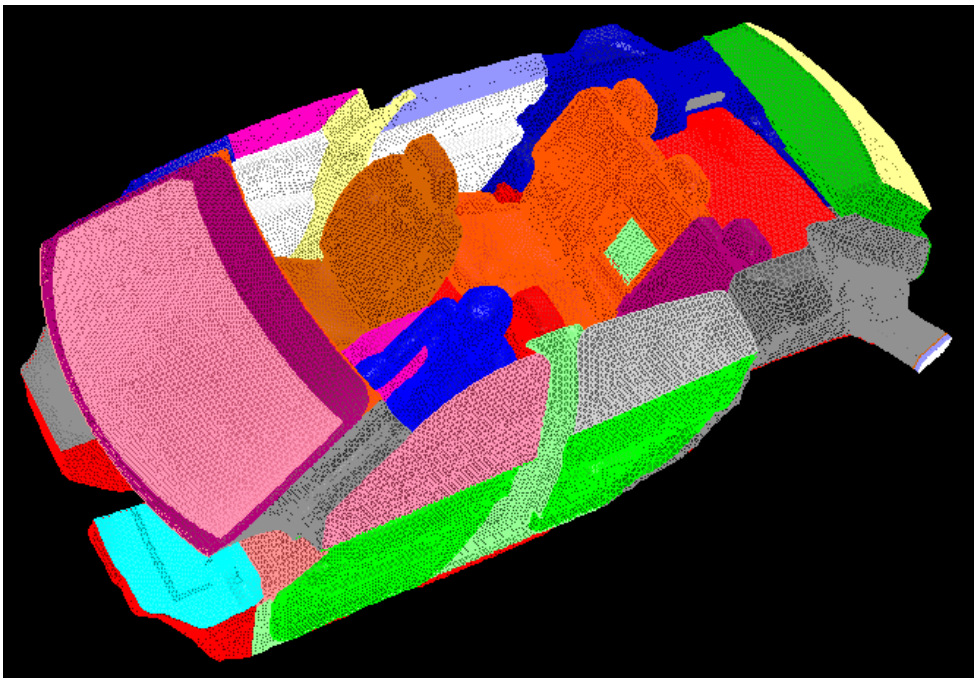

Table G3: Glass solar properties

Glass solar properties	A	ϱ	τ
Direct visible	0.22	0.06	0.72
IR	0.72	0.06	0.22

Figure G31: Solar load distributions through the windows of the SRX

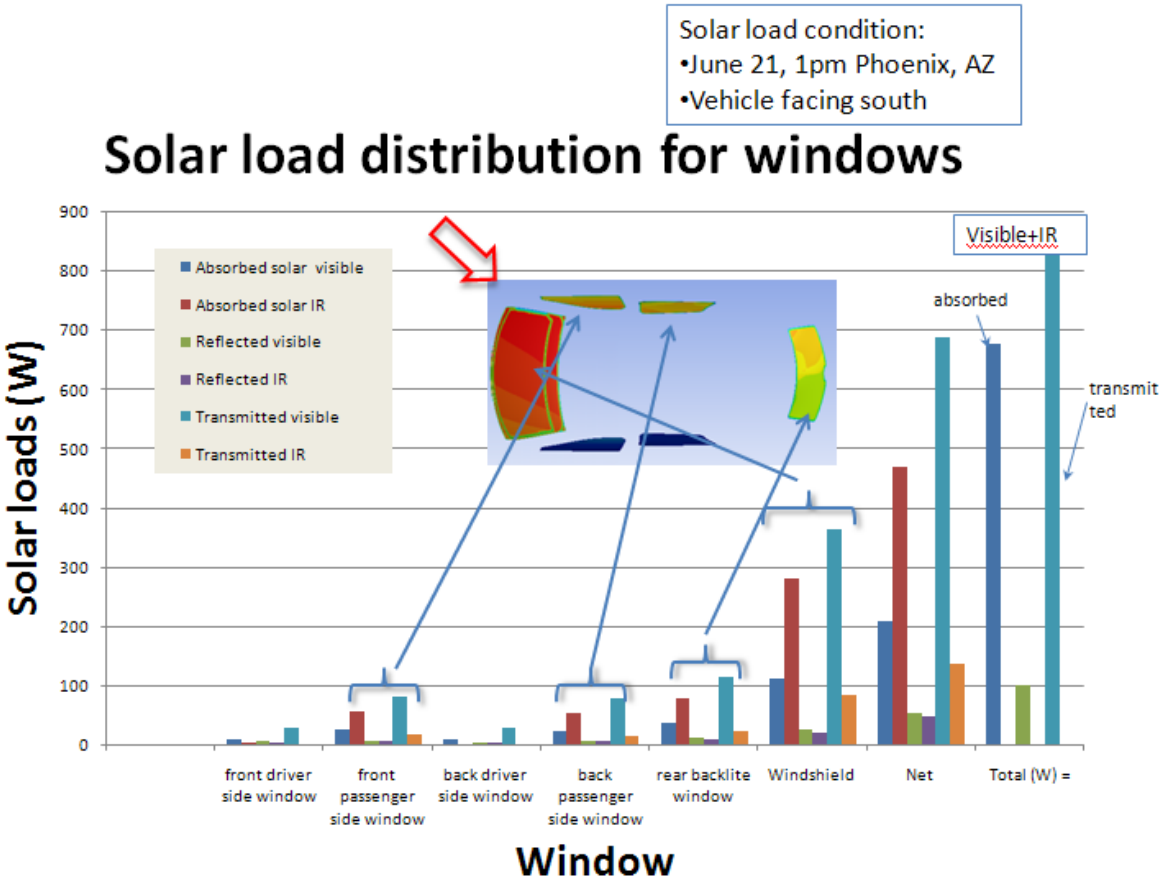

For the baseline SRX calculation, the team analyzed seven cases for various AC exit flow rates including one with no AC flow. Figure G32 shows the temperature contours for the solar soaking condition only (no AC flow). From the temperature contours on the seats, the direction of the solar load at 1 p.m. in Phoenix, Arizona, is quite clear – from the passenger side angled at above A-pillar direction.

Figure G32: Temperature contours for solar soak – no AC flow

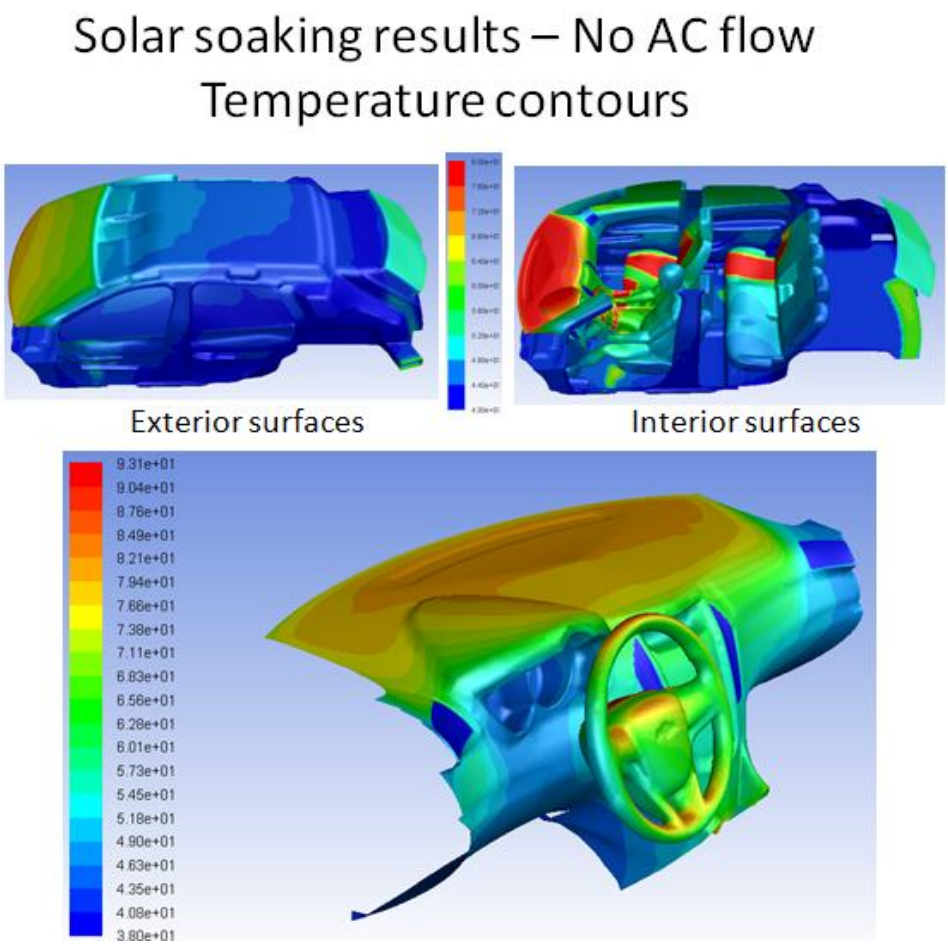

G2.4.2 Milestone 2 – Definition of Design of Experiments for Target Platform Completed

The project's second major milestone, Definition of Design of Experiments (DoE) for Target Platform, was successfully completed as scheduled on May 28, 2010. Delphi had lead responsibility for completing this activity. Delphi constructed a test matrix and conducted a DoE to study the different spot cooling locations to determine their effectiveness in providing passenger comfort. UCB and GM reviewed the initial test matrix and provided feedback to Delphi. After some final revisions, GM reviewed the developed testing parameters and approved the final DoE.

G2.5 Task 5 – Define & Build Mule Vehicle for Thermal Comfort Evaluation

For Task 5, Define & Build Mule Vehicle for Thermal Comfort Evaluation, the team ordered a 2010 Cadillac SRX with the options required to serve as the mule vehicle for the project. The SRX was airflow tested to determine the appropriate inputs for CFD modeling and correlation data for tunnel testing. The airflow data was collected using the zero body method, where air is removed by a measuring device from the vehicle interior at the same rate the HVAC system is flowing, allowing the team to determine the flow from the HVAC system into the vehicle

interior. Airflow was also collected at each outlet in each mode to determine the percentage of airflow leaving each duct. This information was input into the CFD model to determine the HVAC's contribution to cooling and heating vs. the spot cooling that will be supplied by thermoelectrics. Additionally, the airflow data was collected versus a pressure drop in the module, which allows one to determine instantly in the tunnel the airflow quantity through the vehicle HVAC. This allowed the team to determine what the actual airflows are during our testing process without having to install the airflow device. A Solar Load simulation was performed for Arizona at 1pm in June with ~1500 W of solar load entering the cabin and an outside ambient of 37°C. HVAC airflow in vent (outside air) mode was let into the cabin through all 4 front outlets. The outside ambient was assumed to be 37°C. The basic simulation with HVAC airflow in vent (outside air) mode ran quite well with good heat balance shown in the CFD run.

For the Cadillac SRX mule vehicle, the team designed and built a method to simulate thermoelectric device (TED) cooling that uses mini-heaters, tubes, nozzles, fans, and all the necessary electronic controls needed to set temperatures and airflow rates. The design of the simulated TED required extensive CFD analysis in order to quantify the range for the control parameters properly.

G2.5.1 Computational Fluid Dynamics (CFD) Analysis of Mule Vehicle

CFD analysis was performed to locate the nozzles for cooling each targeted body part. Simple conical nozzles were used for the analysis. The nozzle diameters were dictated by air exit velocity considerations. The nozzle location (i.e., distance from the passenger) was dictated by the physics of airflow entrainment and airflow spread and impingement velocities on the targeted body part. CFD analysis was very useful in optimizing the nozzle location and evaluating the sensitivity of nozzle directivity to cooling. Nozzles for each passenger were investigated in the CFD analysis and recommendations were incorporated for cooling the targeted body parts.

Based on the airflow results of single spot cooling strategies, combination spot cooling strategies were developed. The goal of combination cooling CFD analysis was to arrive at maximum airflow coverage without substantial velocity and temperature gradients with the minimum number of nozzles. In identifying the best cooling combinations, it was important not having adverse interaction between the airflows from the different nozzles. Based on CFD analysis, the team identified the best airflow coverage at minimal overall airflow and minimum number of nozzles to implement two proprietary design strategies.

G2.5.2 Instrumentation & Final Build of Mule Vehicle

The vehicle instrumentation and final build included the refrigeration system, HVAC air handling system, and cabin temperature monitoring. The vehicle build also included the TED simulation system and controls to provide airflows to the spot cooling nozzles. Figure G33 shows the completed vehicle in the climatic wind tunnel for spot cooling testing.

Figure G33: Instrumented Mule Vehicle in Climatic Wind Tunnel

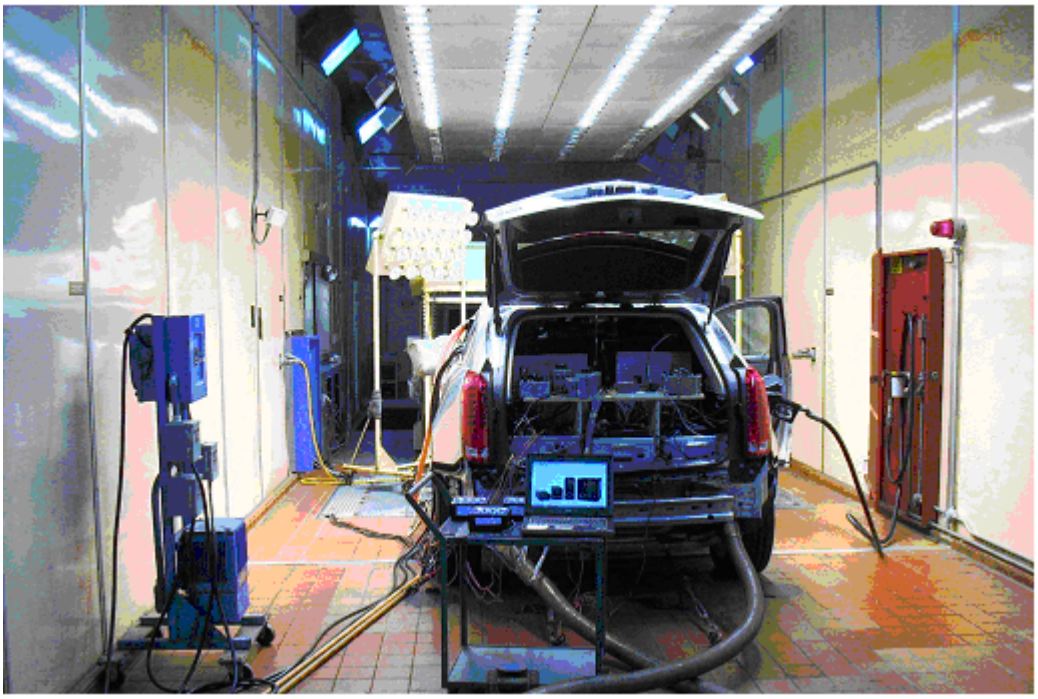

The spot cooling nozzles were fed by a thermoelectric device (TED) simulation system as illustrated in Figure G34. The TED simulation system (aka the Central Chamber System) had a built-in chiller to provide cold air that was sent through six hoses leading to the spot cooling nozzles. At the connection point for each hose, an electrical heater was installed to re-heat the air to a specified discharge temperature. The discharge temperature was controlled to a thermocouple reading at the exit of the nozzle to ensure that the desired discharge temperature was achieved. Within each hose, a small fan was installed to propel the air through the discharging nozzle. Behind the chiller, an air balance fan was installed to ensure that the air pressure downstream of the chiller was balanced to the air pressure outside the central chamber and within the car cabin. The purpose for this is to allow airflow measurement by using the spot cooling fan PWM control signal, which was correlated to an airflow rate prior to the tunnel testing in the Airflow Lab. Two of these TED simulation systems were built, one for the driver and one for the passenger.

Figure G34: TED Simulation System Design

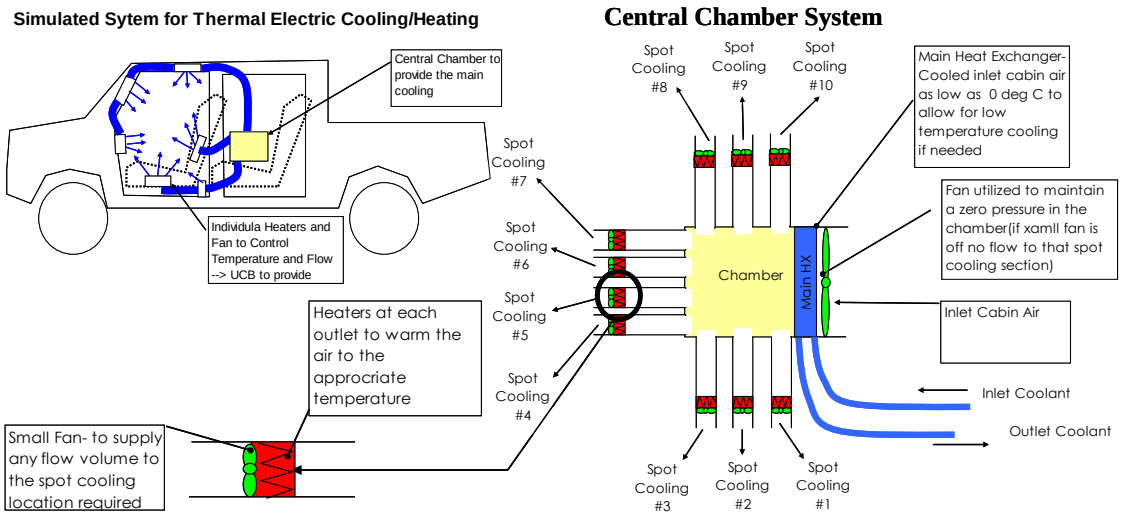

Figure G35 shows a view of the two TED simulation systems from the back of the vehicle with the trunk lift-gate open. Partially hidden behind various instruments in the foreground are the two TED simulation system units in square box shapes. The aluminum grille allows air to be drawn into the chiller to be cooled down. The semi-visible fan behind the grille provides air pressure balance needed for airflow measurement. On top of the "boxes" are low temperature coolant flow connections feeding the chiller inside of the "box".

Figure G35: The TED Simulation System Hosted in the SRX Trunk

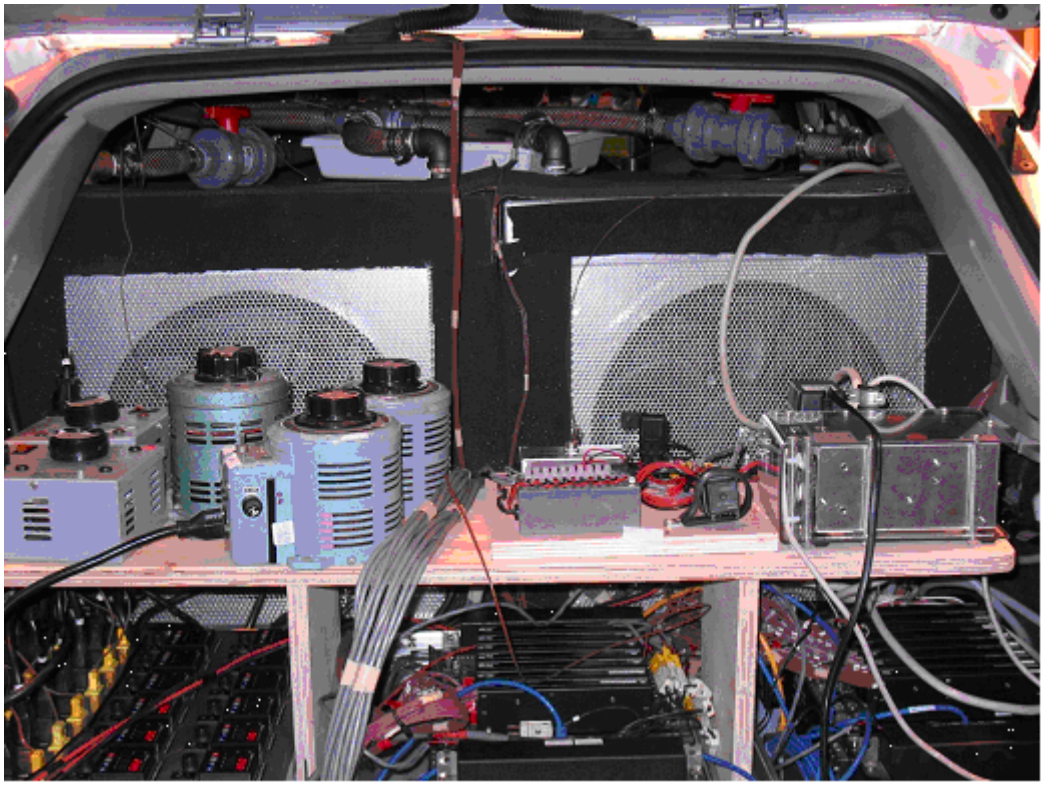

Figure G36 shows two rows of hose connections out of the TED simulation system for a total of 12 hoses connected to the two TED simulation system units. The straight portions out of the units that are wrapped in insulation tape are the electrical heaters used to control the discharge air temperature from the spot cooling nozzles. Imbedded within the hoses are small electrical PWM-controlled fans to meter airflow to each spot cooling nozzle.

Figure G36: Front Side of the TED Simulation System

Two data loggers were used to record the refrigerant temperatures and pressures and the air temperatures in various parts of the vehicle. Other signals such as the HVAC blower voltage and current, engine cooling fan voltage and current, and spot cooling nozzle temperatures were also logged. The two Campbell Scientific CR9000 data loggers are connected through an Ethernet switch to a logging/monitoring laptop computer to provide real-time feedback.

The simulated TED system was airflow was measured to determine the flow volume versus the PWM frequency input to the blower motors. There were six blowers each for the passenger and the driver. Each blower was operator via a PWM voltage frequency to vary the airflow rate. To determine the amount of flow delivered to the passenger, a calibrated orifice was used to deliver the same airflow that was supplied by the fan to both the passenger and the driver.

G2.5.3 Milestone 3 – Build Mule Vehicle for Thermal Comfort Evaluation Completed

The project's third major milestone, Build Mule Vehicle for Thermal Comfort Evaluation, was successfully completed as scheduled by August 31, 2010. Delphi had lead responsibility for completing this activity. Delphi designed and constructed a thermoelectric device simulation system for the mule vehicle. The simulation system and test instrumentation were installed into the mule vehicle to enable thermal comfort evaluation testing.

G2.6 Task 6 – Perform Design of Experiments (DoE) for Target Platform

The main activity for this task was to perform the second set of human subject testing in a modified mule vehicle inside Delphi's climatic wind tunnel. During the weeks of September 20 through October 7, 2010, the Cadillac SRX with spot cooling was evaluated in the climatic wind tunnel chambers at Lockport, NY. The test matrix included the following studies:

- Solar Calibration
- Automatic Climate Control (ACC) Setting and EHT Relationship Study
- Spot Cooling Steady-State Evaluations
    - Individual Spot Cooling Development
    - Combination Spot Cooling Evaluation and Development
    - Spot Cooling Delivery Per Comfort Group Classification
    - Baseline Comfort Study (No Spot Cooling)
    - Automatic AC Set Point Comfort Under Three Given Ambient Conditions
- Spot Cooling Transient Evaluation
- Miscellaneous Development: Cabin Surface Temperature Distribution Measurement

The first evaluation, Solar Calibration, involved placing the vehicle in Delphi Tunnel #2 where the vehicle was calibrated with breath temperatures using the "Full Solar Simulation, Full Spectrum Lighting" to determine the appropriate lighting in Tunnel #5. The calibration included soaking the vehicle at 300 W/m^2, 500 W/m^2, and 1000 W/m^2 to determine the steady-state breath temperatures. In Tunnel #5, the lights were added or subtracted to achieve the same breath temperatures as in Tunnel #2 to ensure that the correct solar radiation was being applied.

The second evaluation used the manikin from UCB to determine the Equivalent Homogeneous Temperature (EHT) for different ambient and different set points on the automatic climate control system. The following combination of ambient, ACC set points, and vehicle conditions was run to determine the EHT for the occupant with no spot cooling.

Thirdly, the vehicle was evaluated to determine the effectiveness of spot cooling at steady-state conditions under various test conditions.

- Spot cooling flow rate based on CFD and UCB recommendations
- Each spot cooling test condition is repeated once
- Each test has passenger and driver riding to provide comfort ratings
- Each test condition is re-run with manikin

This testing was used to determine the most effective spot cooling locations and conditions. Once these locations were identified along with the most effective temperature and airflow, the combination cooling evaluations began. The combination cooling evaluation included the following conditions and criteria. Baseline testing was also conducted at the same conditions above to understand the comfort without spot cooling. This provided a good comparison. Lastly, the effect of spot cooling on transient comfort was evaluated for a hot soak condition.

G2.6.1 Spot Cooling Test Results and Analysis

The spot cooling development was accomplished in two stages. Stage I development studied the working of individual spot cooling nozzles to determine their effectiveness. Stage II development evaluated and optimized the combination of the selected individual cooling nozzles to ensure that they work together coherently to provide optimal passenger comfort in a passenger compartment with elevated Equivalent Homogeneous Temperature (EHT). In addition to the two major stages of studies, a set of baseline comfort rides were conducted for 29°C EHT under the tunnel ambient of 29.4°C x 55% RH x 500W/m2 solar load. These baseline tests were done to gauge passenger discomfort when spot cooling was not instituted.

Baseline Comfort at 29°C EHT

During the subjective comfort rides, the UCB comfort evaluation software was used to log the riders' evaluation of their comfort. The software employs two indices: thermal sensation and thermal comfort. The rider's thermal sensation was an indication of the environmental temperature that he or she is experiencing. The rider may feel cold if the temperature is low and he may feel hot if the temperature is high. From cold to hot, there are nine gradations from -4 through 0 to +4, with -4 being the coldest and +4 the hottest (see Figure G37).

Figure G37: Scale for Thermal Sensation and Thermal Comfort

Similar to the thermal sensation scale, the thermal comfort scale also runs from -4 to +4, with -4 being most uncomfortable and +4 most comfortable (see Figure G37). Under steady-state conditions, it was expected that a thermal comfort index of +2 is the upper limit. Ratings beyond +2 can only be achieved during transient thermal process, such as when a cold-soaked passenger is exposed to a warm environment. Not fully aware of this limit for the thermal comfort index, some wind tunnel test riders occasionally rated comfort greater than +2.

Figure G38 shows the thermal sensation rating during the 29˚C EHT rides without spot cooling. There are five body parts rated during the rides: Face, Back, Gluteal, Right Hand, and Chest. Additionally, the whole body thermal sensation was also rated. The chart shows consistently warm ratings for the in-car environment among all riders. Each of the body parts registered warm to hot sensation, as did the whole body. The "whole-body" thermal sensation on average was rated at +1.4.

Figure G38: Baseline Thermal Sensation at 29˚C EHT without Spot Cooling

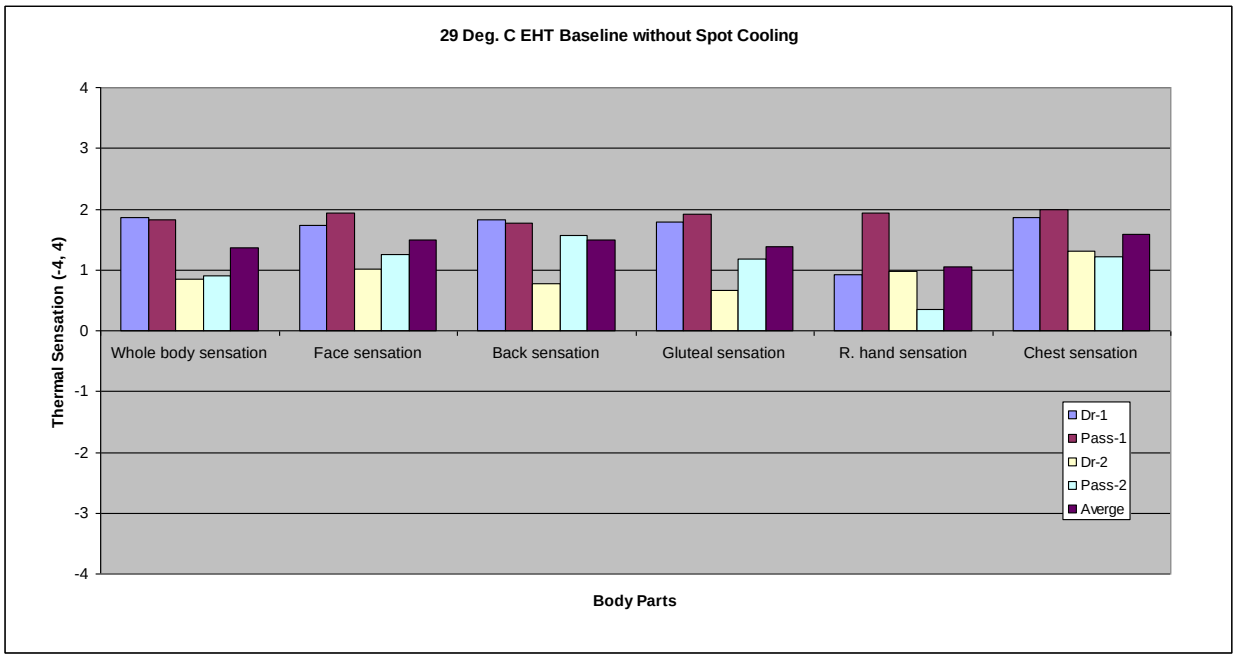

Figure G39 shows the corresponding thermal comfort rating for the 29˚C EHT rides without spot cooling. Most riders rated the riding experience uncomfortable with the average "whole-body" thermal comfort at -0.6. For steady-state comfort, a thermal comfort rating approaching +2 is desired.

Figure G39: Baseline Thermal Comfort at 29˚C EHT without Spot Cooling

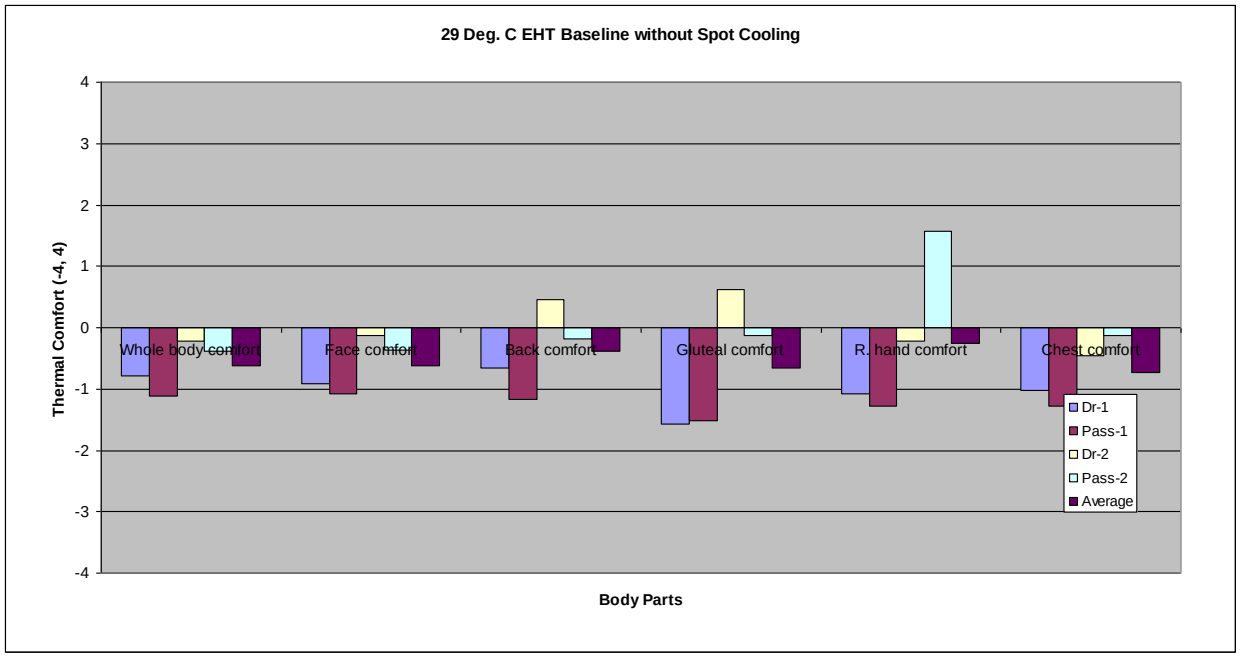

Individual Spot Cooling Studies

For individual spot cooling strategy studies, each of the spot cooling locations was examined under two airflows and two discharge temperatures. The in-car condition was controlled by the Automatic Climate Control system to either 29˚C or 31˚C EHT. The ambient condition used for the most part was 29.4˚C x 55% RH x 500W/m2 solar load. Comfort riders and a manikin were employed to assess the effectiveness of the spot cooling and to optimize the discharge temperature and the delivery of spot cooling airflow.

The impact on the whole body EHT by the five major cooling locations was evaluated. The EHT whole body impact was not the sole criteria used to select individual cooling locations for further development in cooling combinations; however, the rankings for whole body EHT does coincide with the final selected locations. The rankings were quantified as "recommended", "marginal", and "not recommended".

Combination Cooling Strategy Studies

Based on the individual spot cooling results of the Stage I studies, nozzle locations were selected for the Stage II studies to provide a combination strategy for comfort maintenance. The combination strategy was subjected to optimization development so the most effective comfort cooling delivery could be achieved.

The initial combination strategy was composed of the three spot cooling nozzle locations. The airflow rates used for these nozzles are the lower of the two airflow rates used during the individual spot cooling studies. In comparison with the previously shown baseline case (see Figure G39) where most riders rated the in-car conditions as being too warm, the combination of the three-spot-cooling strategies at the same in-car EHT of 29˚C significantly improved the passenger comfort. As a result, the thermal sensation in general is cooler than neutral. The same initial combination strategy was re-evaluated at the in-car temperature of 31˚C EHT. The results of this test show that the degree of over-cooling is reduced by this hotter in-car environment. However, the whole body thermal comfort rating showed a similar drop to +1.4, which still indicates a reasonably comfortable environment.

After the initial combination strategy was tested and evaluated, improvement to the airflow delivery and discharge temperature was made to fine-tune the cooling. The improved delivery settings were tested with another round of vehicle rides. The thermal sensation did move toward neutral for every body part. On average, the whole body thermal sensation is exactly at neutral, but some specific and important body part complaints persisted. Interestingly, the whole body thermal comfort rating did not improve from the previous testing. The average whole body comfort rating was rated at +1.6. This may indicate that the initial combination strategy with the original airflow delivery is harsh and some spot temperatures were too cold, but the whole body thermal comfort is actually better, whereas with the improved airflow delivery and discharge temperature, the objectionable harshness and overcooling were removed, but the overall whole body thermal comfort actually declined. Thus, the improved delivery may be a compromise solution.

During the development rides, it became clear that at least one additional specific body part complaint should be addressed. It had been a consistent detractor from the overall thermal comfort. However, by providing spot cooling to address this "warmth" complaint, a new issue arose from this additional airflow. The team discovered in the quad-combination study that it requires a delicate balance to make the flow acceptable to the riders in order to eliminate the "warmth", while not creating a new complaint. This study indicated a "whole body comfort" rating of +2.4; there also seemed to be less variation in comfort perception than with the tri-combination configuration. However, more people raised at least minor complaints about the secondary issue with the additional spot cooling location. Subsequently, the airflow for the additional nozzle was further reduced by using a higher resistance grid at the outlet of the nozzle. The quad combination with low face airflow was further evaluated through comfort rides at the 31°C EHT. The overall comfort was acceptable and the higher resistance grid seemed to provide a consistent improvement over the original nozzle.

Evaluating the comfort data, the project team concluded that individuals have differing comfort requirements due to age, gender, body fat ratio, bio-cycles, day-to-day health condition variation, weather preconditioning, etc. The subjective data from the comfort rides reflect all this variations. It was further recognized at this point that a single combination strategy would not be able to provide satisfactory comfort to everyone, just as in the case of Automatic Climate Control, where a set point temperature dial is provided to address comfort requirement variations. Subsequently, a multi-tiered combination strategy was devised and tested. The new combination strategies offered four levels of cooling capacity: Extra-High, High, Medium, and Low. The four strategies provided variations in some of the nozzle discharge temperatures for the quad-combination configuration, plus the original tri-combination configuration. With these multi-tiered capacity spot cooling, most people found their comfort satisfied with one of the four discharge levels.

The project team collected the thermal sensation and thermal comfort ratings for the multi-tiered spot cooling delivery during repeat rides at the 37.8°C x 40% RH x 1000W/m2 solar load and 29.4°C x 55% RH x500W/m2 solar load. Even though the comfort rating was in general improved and more uniform than before, the comfort rating was not perfect. Therefore, we asked the following question, "Given the baseline Automatic Climate Control System, what kind of comfort rating should we expect to see from the riders if they are allowed to make adjustment to the ACC set temperature to satisfy their individual comfort requirement?" The answer to this question is actually quite surprising! The test data indicates that quad spot cooling with multi-tiered capacity delivery is a good system, even in comparison with the traditional Automatic Climate Control systems.

Thermal Manikin Objective Data Analysis for the Combination Cooling Strategies

Manikin data were taken during the combination cooling development. The manikin skin temperature and heat flux were converted into Equivalent Homogeneous Temperature to indicate the comfort of the body part and whole body. The comfort impact of the multi-tiered combination strategies were evaluated for two standard EHT environments. The comfort rating by the manikin at 29°C EHT without spot cooling was similar to the subjective thermal

sensation and thermal comfort ratings of human riders who were warm and uncomfortable. The comfort level when the in-car control is set at 24°C EHT is acceptable for most people. However, the hands, forearm, and upper arm are overcooled.

The multi-tiered spot cooling strategies were tested under the elevated in-car environment of 29°C EHT. The ambient condition was 29.4°C x 55% RH x 500W/m2 solar load. With the general in-car environment at 29°C EHT and with the combination spot cooling turned on at various levels of cooling capacity, the in-car comfort was significantly improved without the side effect of hand/arm overcooling. The team also studied the impact of the ambient condition on the in-car comfort. For both of the ambient conditions (75°F x 65% RH x 300W/m2 solar load and 85°F x 55% RH x 500W/m2 solar load), it can be seen that the capacity level of the spot cooling made a difference in the body part comfort, but the ambient temperature change did not have any impact on the in-car comfort.

CFD Analysis of Spot Cooling

After all the tunnel tests were completed, the CAD model of the SRX cabin was updated with all the nozzle locations built into the SRX vehicle. CFD analysis was run post-factum to understand the airflow around the occupants for the final optimized combination cooling tested in the tunnel. In general, the airflow distribution was about the same as the CFD results predicted before the tunnel, but the body surface air velocity was slightly higher. The higher body surface velocities were attributed to the nozzles being closer to the passengers than originally planned due to the large diameter tubes supplying airflow to the nozzles in the vehicle. For the quad combination spot cooling when conventional HVAC was turned off, the CFD analysis identified the velocity contour around the passengers at 7.5mm above the passenger's skin. It is clearly evident that the airflow velocities in both their magnitude and distribution were quite uniform over the entire upper body in cooling mode.

Based on the tunnel configuration, the CAD of the SRX cabin was updated to mimic the test conditions. The changes that were made to the CAD included removing the rear seat and replacing it with two large TE simulations boxes in the rear of the car along with the instrument boxes in the trunk. The nozzles locations were same as tested in the tunnel. The CAD of the dummies was a 50-percentile male in the CFD model, as opposed to varied range of individuals of both gender for tests. The more accurate, but computationally intensive, Discrete Ordinates (DO) Radiation model was applied for Solar Load simulation.

The primary objective of enhancing the CFD model after the tunnel tests was to improve the accuracy of prediction so that good correlation could be obtained with test data in terms of airflow distribution and comfort prediction. The model was run at the tunnel conditions. The inputs to the CFD model were: a) Solar load into the cabin, b) AC vent airflow, and c) AC vent temperatures were obtained from test data at specific ambient conditions. A simplified version of the Sunroof model was added to the CFD simulation to better mimic the roof's thermal condition. Mostly, the two front passenger breath temperatures were used to correlate the CFD model with test data for the baseline case when spot cooling was turned off.

Quite a few pre-runs were conducted to evaluate the sensitivity of HVAC vent directivity towards the passenger on front breath temperature. From the CFD analysis, it was found that the front breath temperatures could vary by as much as 4°C due to different airflow directions from the A/C vents towards the passengers. The AC vent airflow into the cabin was not directly measured during the tunnel tests, so the airflow at a particular in-car set point was estimated from indirect HVAC module pressure drop and fan power data. 105 CFM airflow was estimated for 88°F / 55 RH under solar load test condition to obtain a 29°C in-car condition. The A/C vent outlet air temperatures were measured in the car.

Figure G40 shows the airflow path lines for the baseline case when spot cooling was off. From test data, 103 CFM airflow at 17°C was forced into the cabin by the automatic climate control system at 88°F x 55% RH x 500 w/m^2 solar load with the automatic climate control set to outside air / partial recirculation mode. These conditions were imposed as the boundary conditions for the CFD model. Figure G41 shows the velocity vectors in the mid-plane of the driver dummy. A number of complex circulatory cells are visible from the velocity vector plot. Figure G42 shows how the high velocity air hits the upper body of the driver in the facial region contributing to cooler breath temperature. Even though the in-car condition was around 29-30°C, the breath level temperature was around 25-27°C in the front of the vehicle for baseline case when no spot cooling was employed.

Figure G40: Airflow path lines originating from front HVAC AC vents

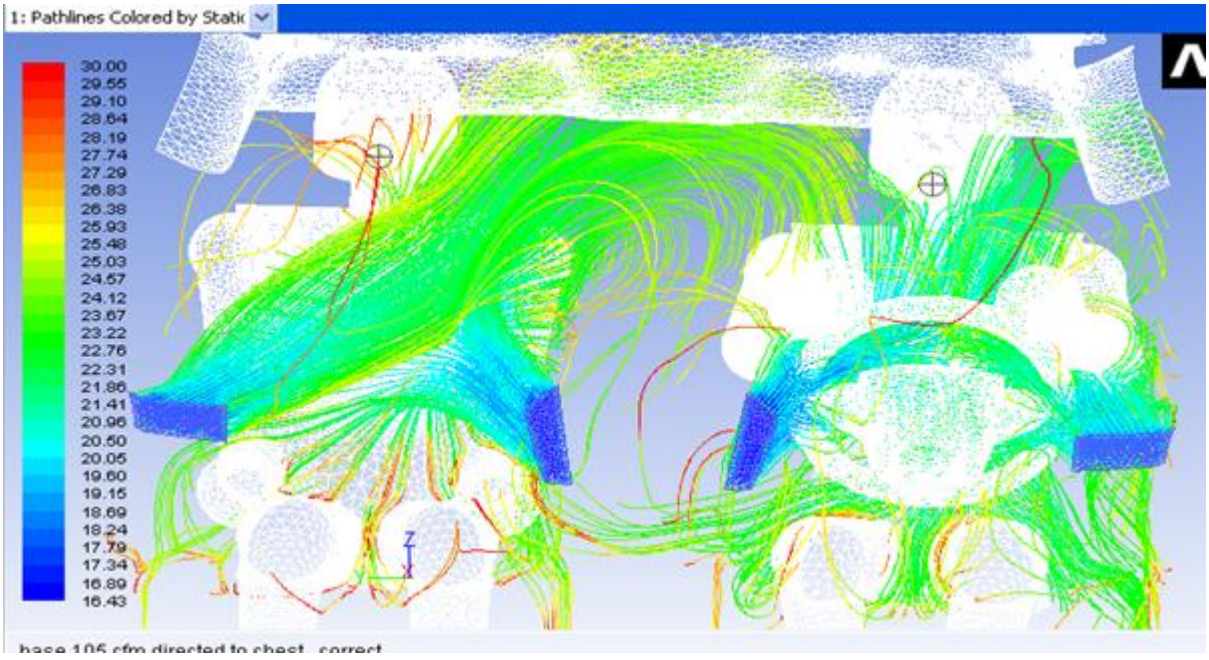

Figure G41: Air Velocity Vectors at mid-plane of the driver for Baseline case (Box model)

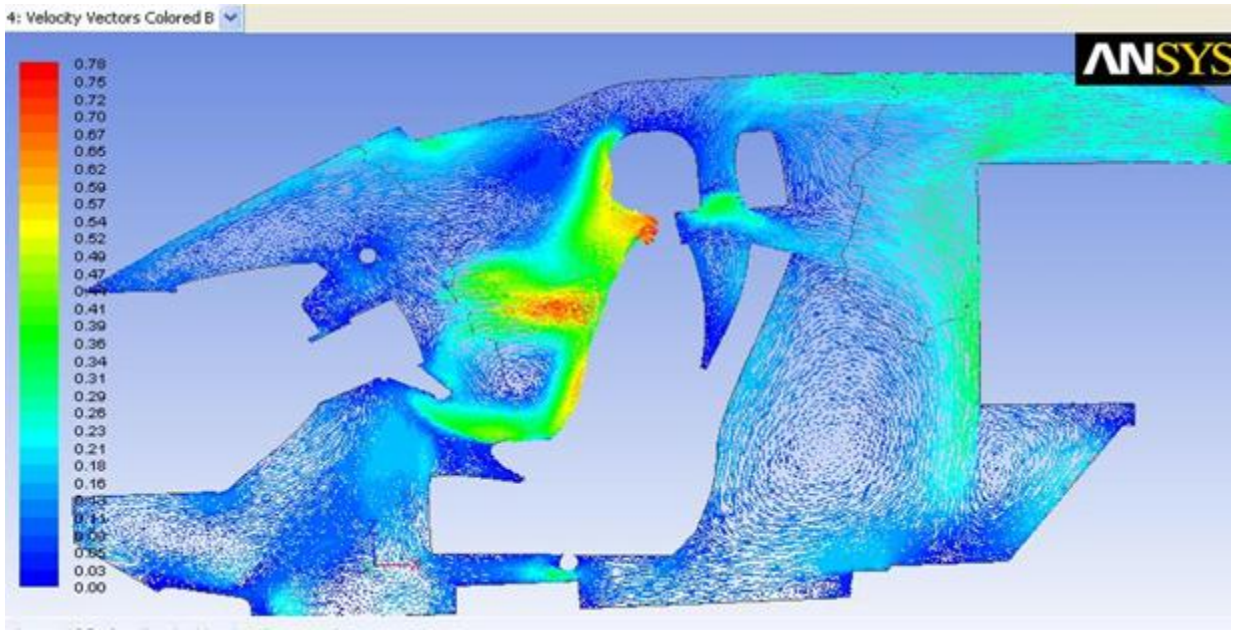

Figure G42: Velocity contours around the face due to front HVAC AC vent airflow for Baseline

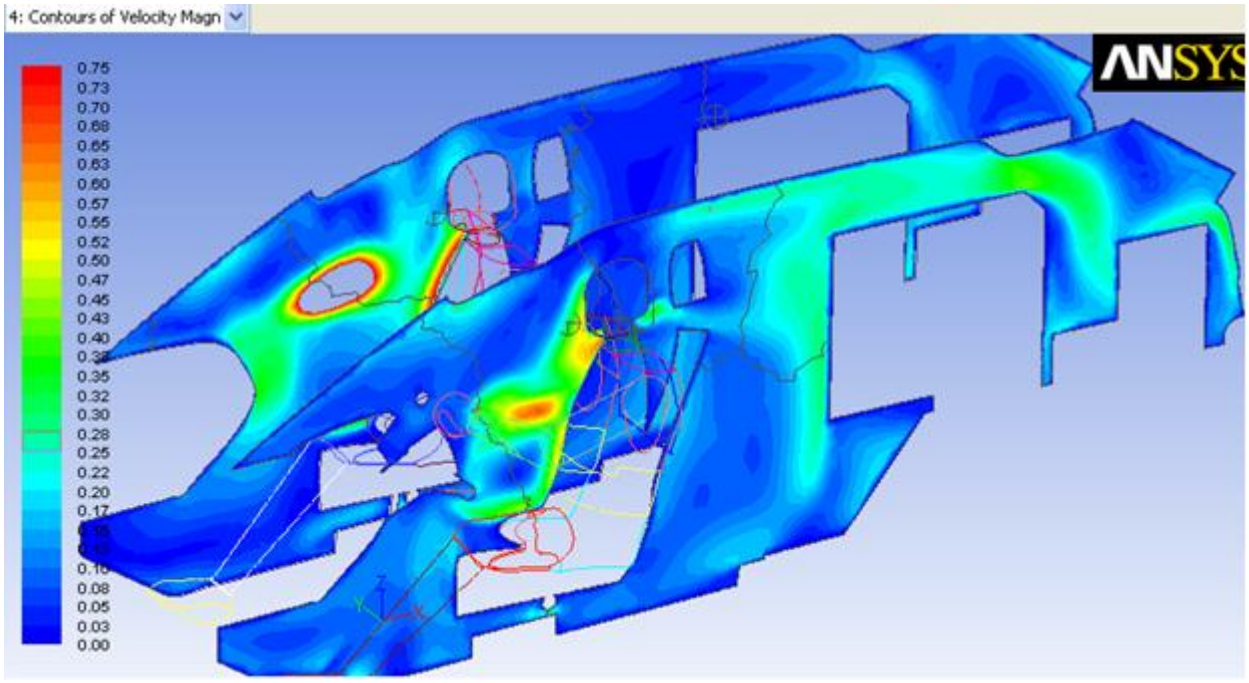

The CFD analysis showed the path-lines when spot cooling was turned on in conjunction with conventional HVAC air. The analysis also showed the temperature and velocity around the occupant when spot cooling was turned on. From this CFD run, it was observed that the front breath temperatures were lower by 1-3°C than the baseline case when spot cooling was off. As expected, the air temperatures around the occupant were much closer to the nozzle air temperature of 24°C.

The primary metric of significance that was used to compare the accuracy of the CFD model with test data was the front driver and passenger breath level temperatures. In the CFD model, the dummies were 50-percentile males. For the test data, thermocouples were hung a little higher and in front of the location specified for a 50-percentile male. The team performed a comparison of all the glass temperatures and the breath level temperatures from the CFD analysis with test data. Overall, the correlation was found to be quite good. The breath level temperature variations with test data were within < 2°C. The correlation for all the windows, i.e., the glass and roof temperatures, were much better for the full cabin model.

There can be many factors contributing to variation between test data and CFD predictions. Uncertainty in HVAC airflow, directivity of the HVAC vents, uncertainty in material properties, and variance of the tunnel lights radiation intensity and spectra from the actual diffuse solar radiation found outside the car are thought to be the primary variables. For design purposes of multi-physics complex real life in-situ automotive HVAC systems with spot cooling, the accuracy of CFD prediction was quite good. Therefore, this approach was followed to rank order designs in AC and Heater mode in the later stages of the project.

G2.6.2 Spot Heating Test Results and Analysis

The team conducted spot heating tests in the climatic wind tunnel during the period of March 21 through April 11, 2011. Figure G43 shows the cabin EHT curve as a function of the in-car set temperature for the automatic climate control system. Different temperature scales are used for the vertical and horizontal axis in the chart as a matter of convenience. The temperature in the vehicle was set in degrees Fahrenheit for higher accuracy, while normal analysis was done in degrees Celsius.

Figure G43: Cabin EHT vs. HVAC Automatic Set Point

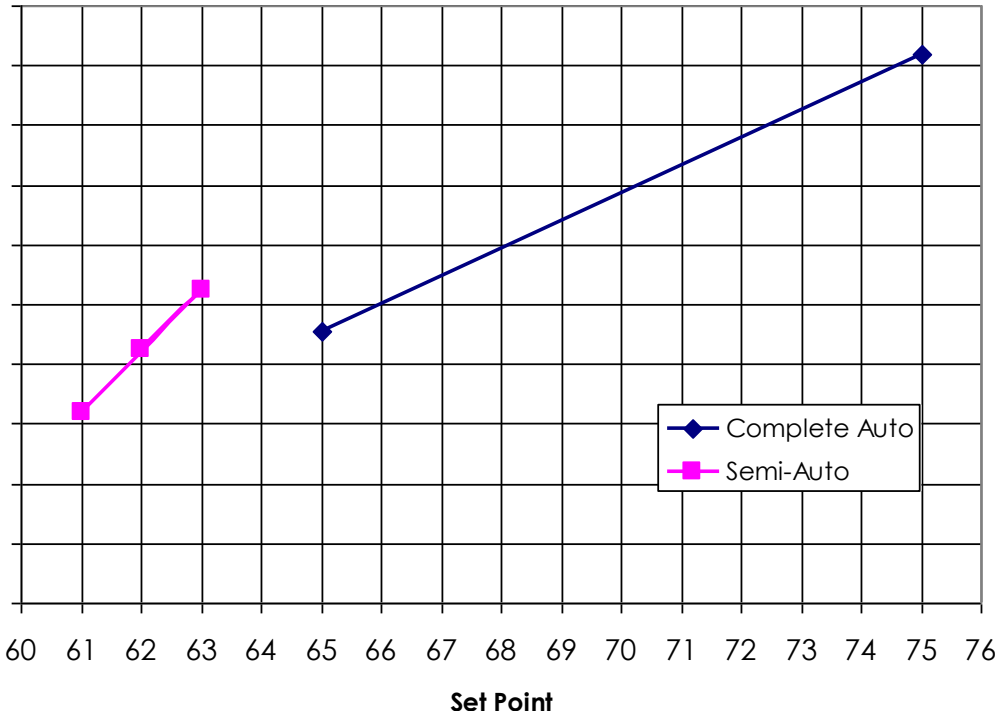

The manual HVAC settings were used to study the impact of the discharge temperature on body part EHT temperatures. In the manual settings, the blower voltage was overridden to 3 volts, and the discharge temperature was at the target level. The discharge mode was overridden to heater. These manual settings were determined to provide approximately the same amount of air discharge enthalpy from the HVAC system heater outlets as that when the HVAC system was in semi-auto mode. The subjective comfort rating from car riders was measured for the baseline EHT cabin. It was observed that most people indicated low thermal sensation and low thermal comfort.

CFD Analysis of Spot Heating

A CFD model was developed to simulate the vehicle in winter conditions. The challenges involved in developing the Heater Mode CFD model were the following.

1. The model had to comprehend convective & radiation heat loss from warm cabin to ambient accurately.
2. Since the vehicle potentially operated at low HVAC heater flows with spot heating, the vehicle thus operated in a weak convection regime. In weak convection regimes, radiation flux from within the vehicle, especially from the warm occupants, become very important.
3. Body heat from the occupants and clothing effects needed to be modeled.
4. Unlike spot cooling where temperature differential was small, the temperature differential in spot heating was significantly large and had to be taken into account.
5. Overall energy budget heat loss from the cabin (radiation + convection), body heat into & lost from the cabin, and energy expended (thermoelectrically or otherwise) to heat up the spot heating air had to be accounted for accurately in the CFD simulation and spot heating design.

In order to capture the radiation effects, the more accurate but computationally expensive DO (Discrete Ordinates) Radiation model was used in CFD analysis. The fine flow aligned mesh was developed to capture the entrainment dynamics accurately. Body heat was modeled through heat-source terms in the CFD model. Natural convection effects in the cabin were captured through density dependent air properties.

Design of the spot heating system was done for simulations run at 30 mph vehicle speed with no-solar load ambient condition. Initially for baseline CFD runs with no spot heating, heater discharge temperatures and airflow were varied to maintain in-car cabin conditions from cool to warm with a range of outside temperatures.

G2.6.3 Milestone 5 – Identify final set of locations for distributed heating/cooling

The project's fifth major milestone, Build Mule Vehicle for thermal comfort Evaluation, was successfully completed as scheduled by April 29, 2011. After examining the heating/cooling performance (both modeled and measured) for various nozzle positions, the team identified the final set of optimal locations for use in further developing the distributed TE HVAC system.

CHAPTER G3:
GM Phase 2 – Exploratory Development

The focus of this phase was to develop the initial prototype distributed HVAC components and to evaluate them on both a test bench and a mule vehicle. At the beginning of this phase, the team changed the mainstream demonstration vehicle to an eAssist Buick Lacrosse. At the conclusion of this phase, a Go / No-Go decision was successfully passed based on expectations of achieving the primary project objective. For this phase, GM utilized Delphi to develop most initial prototype HVAC components with the addition of Faurecia to develop prototype seats and Marlow Industries to develop a prototype TE-based heater for the Volt. UCB supported control strategies and tunnel tests while continuing their primary Phase 1 activities in parallel.

G3.1 Task 7 – Project Management and Planning

The planning and coordination for this phase primarily utilized weekly team meetings. The addition of an alternative set of prototype seats plus delays in securing support for prototype controls development resulted in several months delay for this phase and the overall project.

G3.2 Task 8 – Define New Comfort Component Specifications

A key goal of the project was to demonstrate thermoelectric devices (TEDs) with COPs of 1.3 for cooling and 2.3 for heating. The project team originally estimated air-based TED designs in August 2011. In September, a coolant-based TE HVAC system was selected as the best overall, where coolant would be used for the thermoelectric exhaust. Accordingly, the team updated its detailed analysis and component specifications. In summary, COPs of 1.3 and 2.3 for cooling and heating were the design targets; however, this level of performance drove larger packaging sizes and significantly higher costs than those associated with slightly lower COPs.

G3.3 Task 9 – Define Control Strategies and Algorithms

A strategy for the controls of the supplemental thermoelectric HVAC system and the coordination with the OEM automatic climate control system were developed. The automatic climate control algorithm used in production for the Buick Lacrosse was very complex, and it was deemed impractical for the project team to modify this source code for the demonstration vehicle. Ultimately, the team selected a control set point temperature offset that was indexed in real-time by the calculated HVAC power. The real time HVAC power was calculated from the discharge temperature and discharge airflow rate. The stability of this calculation for controls was unproven, but filters were applied to help stabilize this value.

G3.3.1 Initial Control Strategy Development

Mechanization of this control scheme with a coolant-based TE exhaust system was developed. H-bridges were used to drive PWM output for the TEDs. The team identified off the shelf control hardware with custom software that was obtained from Intrepid. Delphi designed and built custom interfacing hardware. The Intrepid controllers can communicate with the existing

Campbell data loggers to synchronize and record the system data. The system mechanization to implement the team's control strategy is shown below in Figure G44 through Figure G46.

Figure G44: Control system mechanization using Intrepid controllers

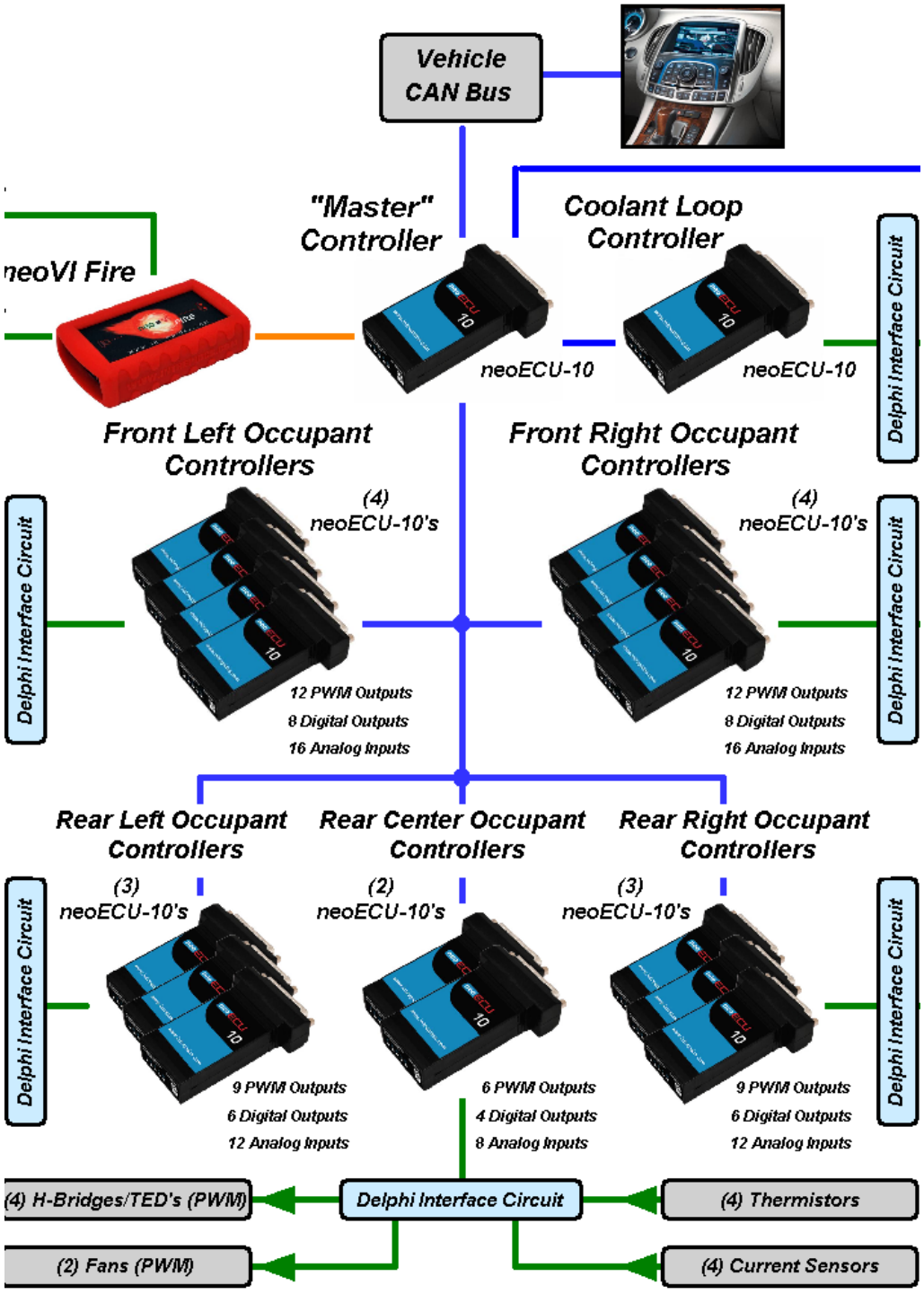

Figure G45: Control system mechanization using Intrepid controllers and remotes

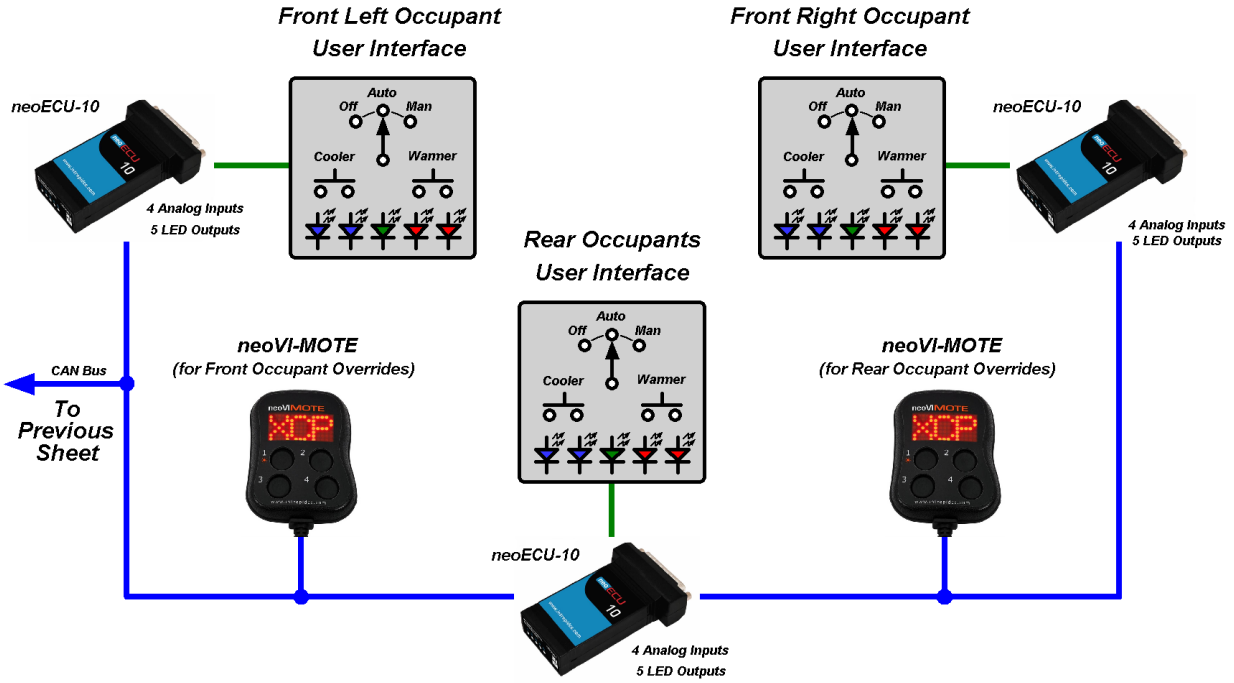

Figure G46: PWM H-Bridge, TED, and Fan Wiring Details

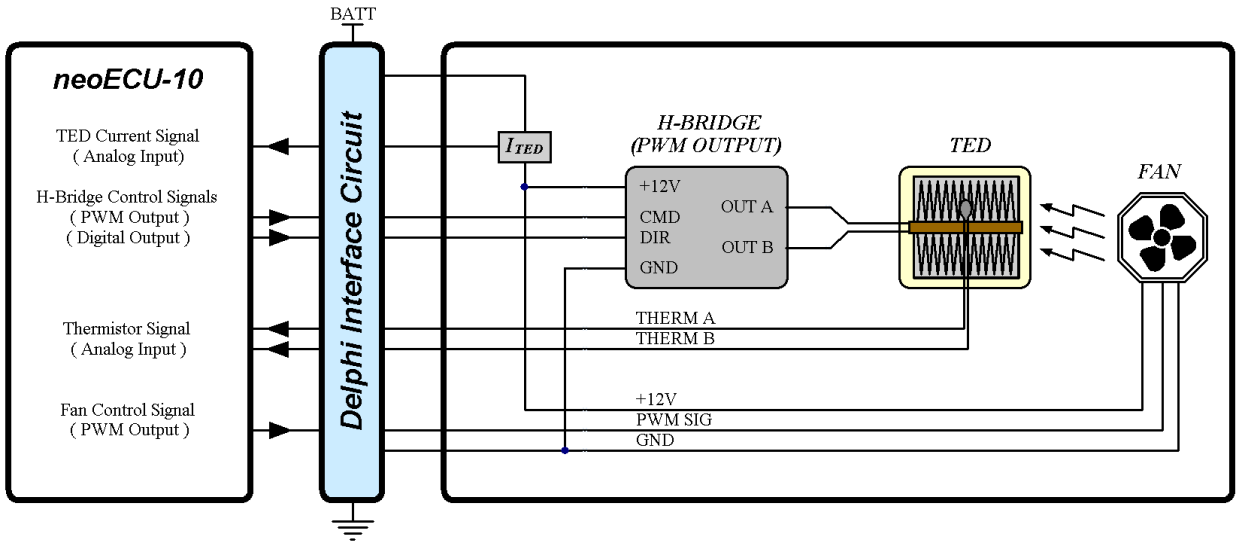

G3.3.2 Milestone 6 – Specify interface between GM & Delphi controllers completed

The project team completed the "Specify interface between GM & Delphi controllers" milestone on December 19, 2011. This milestone marked the project team's agreement on a control strategy for the interface and integration of the central HVAC system with the prototype distributed HVAC system. The system mechanization to implement this control strategy is shown above in Figure G44 through Figure G46

G3.3.3 Further Controls and Control Strategy Development

The control development activity spanned several fronts, each key to being able to test and develop the TED concept. These fronts included the development of control strategies, initial system calibrations, design & fabrication of support electronics, and configuration for data logging. The control strategy developed by the project team focused on the following areas:

- Partitioning control over a network of controllers.
- Providing the vehicle occupants with a method to bias or override the operation of their seat.
- Providing a control method for conditioning the coolant used with the TEDs.
- Providing a method to insure that the TEDs are operated within nominal conditions and only when sufficient cooling is being provided.
- Providing a "bypass" control method to allow individual control of each device to foster easier system checkout and development.
- Defining low-level drivers for interfacing with various system sensors and control devices.

Control Hardware

User control panels were developed and integrated into the vehicle. These can be seen in Figure G47 and Figure G48. These panels provided the occupants with a means to make adjustments to the TE HVAC system operation as desired. The front control panels were integrated into the center console of the Buick Lacrosse with labeling oriented for easy reading from the intended seating position. Each front seat had five inputs for setting automatic operation, manual operation, or to turn the system off. LEDs and switch ring lights provided user feedback on the state of operation. Similarly, the rear seat controls were mounted in the flip-down armrest located in the center of the rear seat. In addition to the functionality of the front control panel, the rear panel also was used to specify whether the rear seating positions were occupied by pressing the "Left On" or "Right On" switches.

Figure G47: Front seat system control panels

Figure G48: Rear seat system control panel close up

The software test bench consisted of several parts designed and built by Delphi. This resulted in a station that could simulate the entire coolant system, any seat of the system, and the control panels. Figure G49 shows the ECU10 mounting rack, bench wiring, and system simulator.

Figure G49: Software test / debug bench

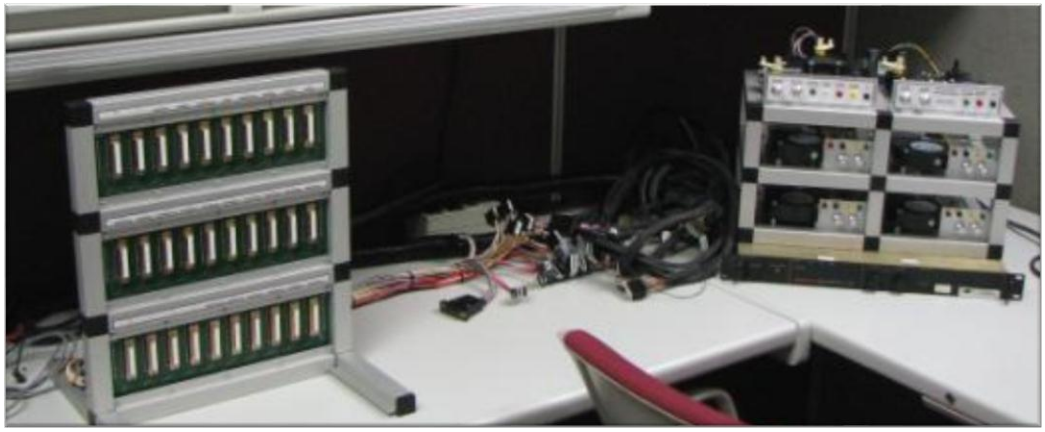

Control Software

The effort required to program and debug the software for the Intrepid vehicle development control system was substantially more than originally planned. Considerable time was spent in the testing and refinement of the control software to meet prototype HVAC system requirements. The complexity of the control system development was due to the large number of controllers, the number of devices that needed management, and bugs within the firmware of the Intrepid controllers that were discovered by this project. The unexpectedly high complexity has delayed the completion of this task, and this forced the delay of several key project activities including the climatic wind tunnel testing.

Campbell Data Logging

The project team configured the Intrepid vehicle development control system and software to interface with two Campbell data loggers. Both physical units can be accessed and their information logged with the rest of the system data into a common data file. There are approximately two hundred data channels wired from the car to the data loggers.

G3.4 Task 10 – Build and Demonstrate Function-Intent Components

G3.4.1 Development of initial prototype thermoelectric devices

TED Subassembly Packaging

Based on previous testing results, the plan were to have TED subassemblies in the seat bottom, seat back, knee bolster, and the roof. The available real estate in the roof area of any light-duty vehicle is generally quite limited. With sunroofs including oversized units being a reality for many vehicles, the packaging space for roof mounting of thermoelectrics is significantly constrained. The team focused on packaging in the roof with the expectation that packaging near the knee bolster and in the seat would not be so constrained. There was also a possibility to remote-mount the fan to gain packaging space. The team tentatively selected a dual fan design with one fan/motor assembly on each side of a person's head and located in the roof.

TED System Options

The team made formal trade-off assessments for the initial prototype designs to ensure that all relevant aspects were considered. Engineering Value Analysis (Pugh Analysis) was used to allow weighting for each of the selected parameters. These weighting were then multiplied by a numerical rating for each parameter and then sum totaled. The project team considered four possible system options:

- Cabin air-based TEDs
- HVAC module air-based TEDs
- Coolant-based exhaust air TEDs
- Hybrid-system consisting of a combination of HVAC module air and coolant based TEDs

The coolant based exhaust air TED system ranks the highest overall, but less than 10% better than the HVAC-air based TED system. The engineering estimated costs of all systems are relatively high. The cost is driven primarily by the significant number of fans, TEDs, and PWM controllers needed. As such, the team is presently working on ways to change the design and thereby reduce cost.

TED Development

The project team developed optimum solutions for cooling and heating with thermoelectrics based upon the initial requirements specified by the team for the distributed cooling and heating system. The initial design utilized air on the waste side to provide the heat rejection during cooling and heat utilization during heating. However, after several iterations, it was determined that air on the waste side was not satisfactory. Therefore, design concepts for air-to-water configurations were developed and completed. COP vs. cost plots were evaluated to understand the return on more couples. For seat heating in Figure G50, ~400 couples were required to achieve the 2.3 COP target. However, a 25% reduction in couples results in only an 8.5% reduction in the COP, indicating a high relative cost for that last increment of efficiency.

Figure G50: Seat Heating COP vs. # of Couples

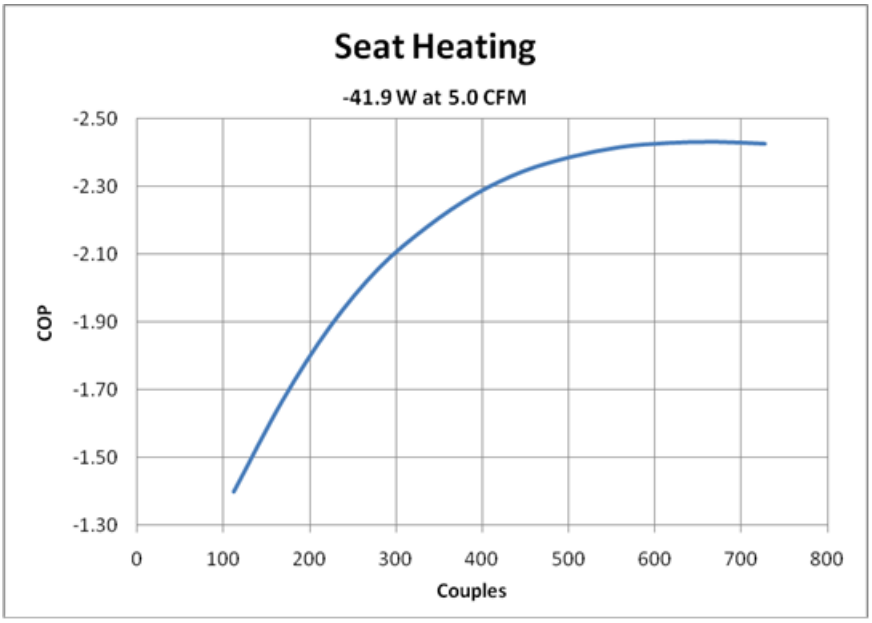

Based on these simulations, the team determined that the final set of recommended designs would feature two sizes, a small TED with 224 couples and a large TED with 336 couples. This approach gave the team flexibility to provide a wide range in the number of couples (from 224 with 1 small TED to 672 with 2 large TEDs). By using 1 or 2 TEDs at each position, these two TED sizes were able to supply an appropriate amount of TE material to meet the requirements of each location, e.g., seat, feet, lap, and chest. The TED designs required 20 large TEDs with 336 couples and 12 small TEDs with 224 couples to support the initial prototype components.

Fan & Blower Development

An initial fan and blower selection from EBM-PAPST was evaluated. Each blower was operated via a PWM voltage frequency to vary the airflow rate. To determine the amount of flow delivered to the passenger, a calibrated orifice was used to supply the same airflow that was delivered by the fan, and the pressure was recorded to understand the fan's performance. The initial fan and blower selected showed adequate flow, but its size was large, measuring 120mm x 120mm x 25mm. It was subsequently decided that a higher flow blower might be required for the thermoelectric designs. A Delta Fan was then identified that provided slightly more flow (as shown in Figure G51) at a higher delta P. However, the main benefit was in the package size, which was reduced from 120mm x 120mm x 25mm to 95mm x 95mm x 25mm. The increase in flow and significant reduction in size provides an optimum solution.

Figure G51: Delta Fan Flow and Delta P versus Resistance

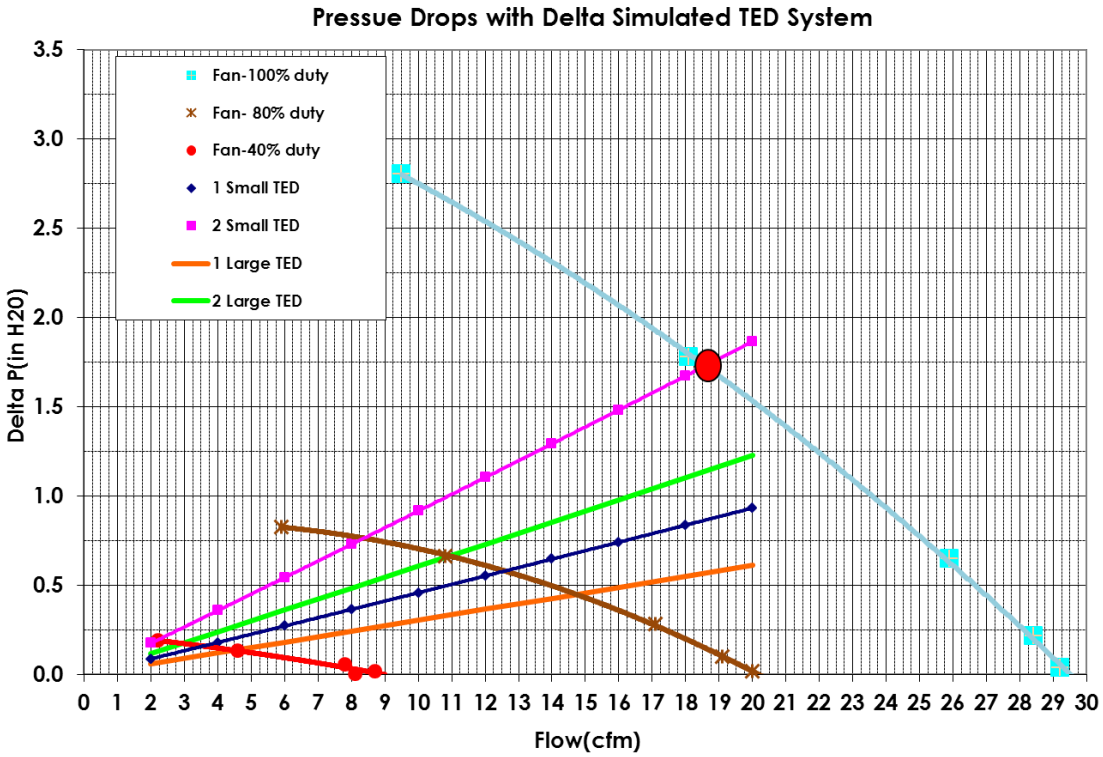

G3.4.2 Development of initial prototype TE-based cabin heater for Volt

The original project statement was amended to include the development of distributed HVAC components for electrified vehicles like the Chevrolet Volt. A key focus for this activity was to develop a TE-based alternative to the resistive cabin heater currently used in production for the Volt. During cold weather, electric vehicles must allocate a significant portion of the energy in their batteries to warm the cabin for the passengers, thereby reducing the effective electric-only range of the vehicle. This development effort used TE devices to provide improved heating efficiency beyond the existing electrical resistive heater. To accomplish this objective, a Plate and Frame heat exchanger concept was proposed that was designed specifically for use in conjunction with TE technology. This development activity is described below.

Initial Design Concept for TE modules - Plate and Frame Exchanger System

The goal of the design concept was to achieve a thermal system that integrated multiple TE modules and exchanger plates into a compact package while improving heat transfer across the active surfaces. The final thermal system is to operate within the outlined specifications regarding electrical input power, performance, volumetric flow rates, pressure drops, available pump power, and other various attributes. The initial Plate and Frame Exchanger concept is shown in Figure G52. This approach to the alternative heater design had the following characteristics:

- Segmented platform design that allows for expandability.
- Symmetrical design reduces number of parts.

- Parallel flow paths reduce pressure drop.
- TE modules are thermally in parallel. Can be electrically arranged is series, parallel or series/parallel circuit.
- Enhanced Plate and Frame exchanger design with improved heat transfer coefficient utilizing wire mesh screen.
- Compact size versus capacity.

Figure G52: Initial Plate and Frame Exchanger design concept

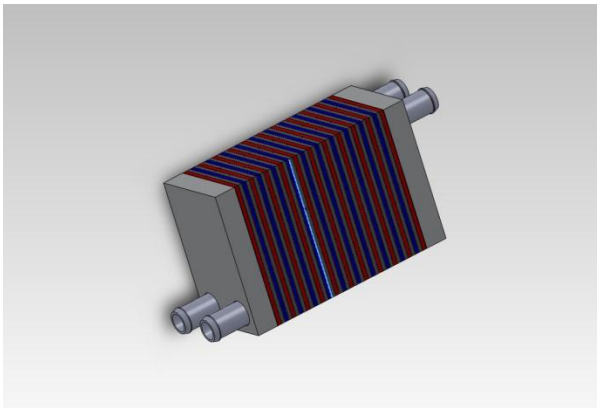

Initial Prototype Configuration and Performance Testing

The initial prototype for validating the enhanced plate and frame exchanger concept was constructed using two rectangular plates of Lexan material, which functioned as end plates and formed the "frame" part of the exchanger. Placed in between the plates were two wire mesh screens separated by a single, thin metal plate to define the two independent flow paths along with the appropriate gaskets. This allowed multiple wire mesh sizes to be quickly evaluated with the least test variability. The prototype exchanger was instrumented to measure flow rates, pressure drops, and temperatures of both inlet and outlet sides along with power into and rejected from each flow stream. The data was used to calculate the heat transfer and effective heat transfer coefficient for the different wire mesh screens tested. Based on the test data, the 8x8x063 wire screen mesh size was determined to provide the best overall performance for the given flow rate and pressure drop. Additional testing was performed using a single SP2297 TE module with the 8x8x063 wire mesh screen in the prototype system. This test yielded a total Q of 379 watts rejected into the hot side fluid stream with an input power of 257 watts to the TE module. 122 watts were transferred via the cold side.

To further improve the heating efficiency of the initial design, an enhanced Plate and Frame concept was proposed. The technical challenges addressed with the beta concept include:

- Thermal interface optimization
- Gasket optimization
- Plate material optimization

- Mesh orientation optimization
- High voltage experimental setup
- Beta prototype design

By increasing the thermal contact area, the COP of the alpha prototype was increased from 1.37 to 1.59. This represents a 14% decrease in necessary power to the thermoelectric cooler (TEC). These results were also verified using the alpha prototype with two TED layers, showing heat flux to be additive with number of TECs while maintaining a constant COP.

Pressure paper tests were also performed on the Alpha prototype with 20 TEC layers to verify even pressure distribution throughout the system. However, there were several layers with "hot spots" indicating higher pressures (see Figure G53). These were the result of inconsistent mesh thickness. Proprietary methods were developed to overcome this "hot spot" issue.

Figure G53: Hot Spots on Grafoil and Pressure Paper

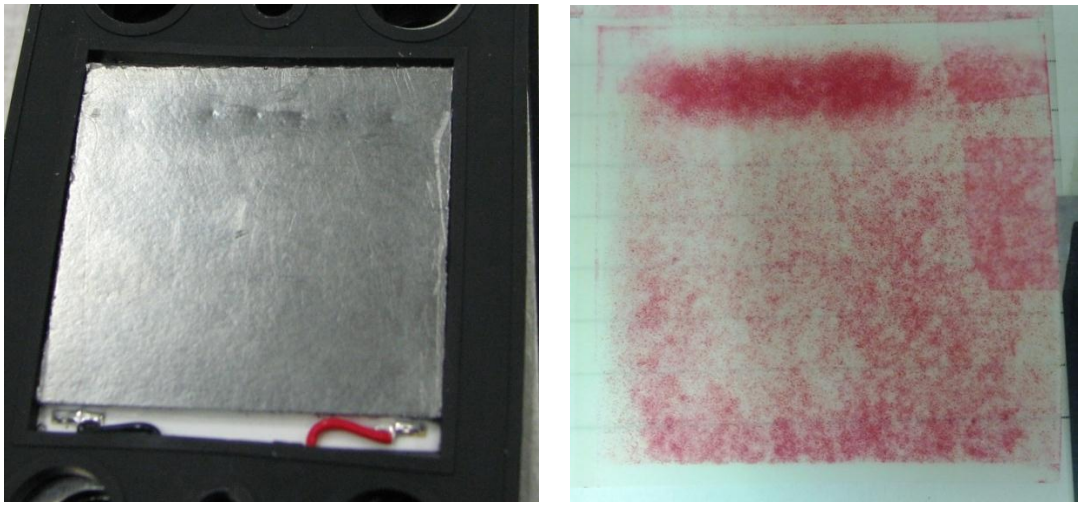

Prior to this point, the gaskets were in their original form. However, several design parameters were not believed to be optimized and, thus, changes were implemented. The new design accomplished two things: 1) increased U-value and 2) lowered pressure drop across the exchanger. The U-value increased approximately 26% using the new gasket design. The most obvious reason for this to occur would be due to a more efficient use of the heat transfer area. We hypothesized that the original design focused most of the water diagonally from one port to another. By opening up the entrance region, the water could more freely flow across the entire surface of the mesh. The ability to more freely flow across the entire mesh led to the second benefit: lower pressure drop. The water no longer had to fit through the small neck present in the original design, but could now spread out across the entire area. This led to a decrease in pressure drop of ~50% depending on the flow rate (see Figure G54).

Figure G54: Pressure Drop versus Flow Rate for the Two Gasket Designs

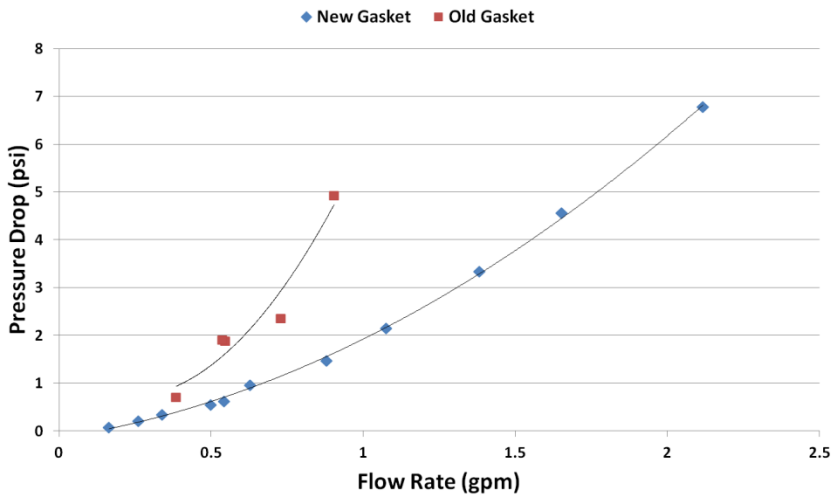

Beta Prototype Construction

A newly designed heat exchanger concept involving more TECs was needed in order to accomplish the desired coefficient of performance (COP) at the required heat load. Each TEC would be operating at a lower power and heat load. This beta prototype was designed and constructed as shown below (see Figure G55). The new prototype is 7.875″L x 7.45″H x 3.85″W.

Figure G55: Assembled Beta Prototype and Internal Components

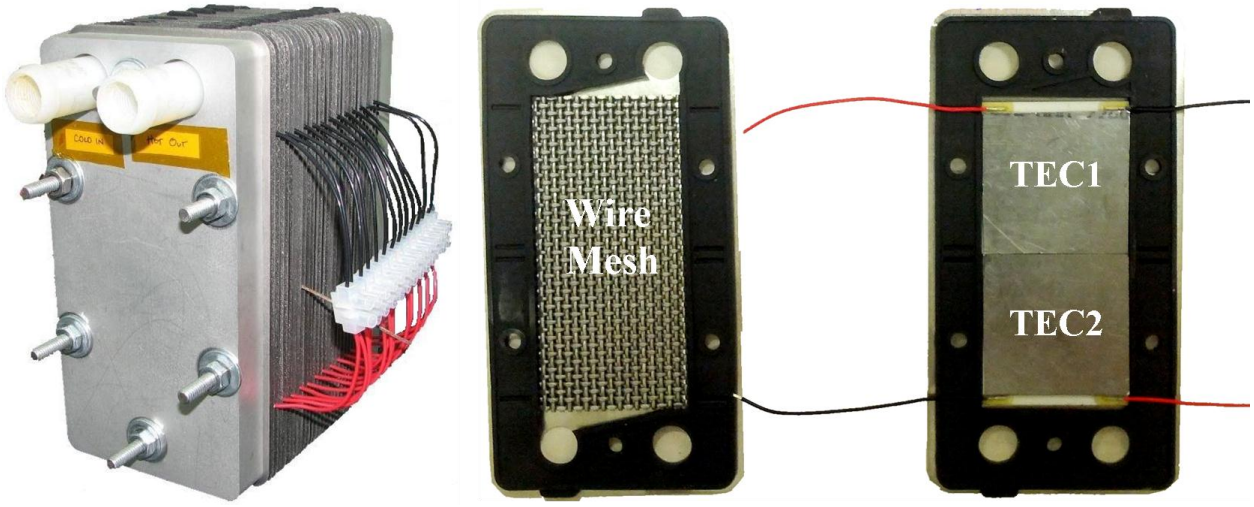

Beta Prototype Testing

Several tests were performed to evaluate the performance of the Beta prototype heat exchanger over a range of inlet temperatures and temperature differentials. Key to understanding the performance graph shown in Figure G56 is the definition of ΔT on the x-axis. In this test configuration, ΔT is defined as

$$\Delta T = T_{engine} - T_{heater}$$

where T_{engine} is defined as the engine cooling fluid loop temperature. T_{heater} is defined as the heater fluid loop.

Using this nomenclature, a negative temperature differential indicates heat would naturally flow from the heater fluid loop into the engine cooling loop. For positive temperature differentials, heat would naturally flow from the engine cooling loop into the heater fluid loop. The Beta prototype performed well at start up, achieving a COP of ~2.9 when both fluid streams were at equal temperatures. Likewise, it achieved the target COP of >2.3 at all temperature differentials greater than -5°C. However, using a power supply capable of 405V, the necessary heat load (Qh) of 5kW was achieved only at temperature differences greater than -13°C. Beyond that point, the heat exchanger lacks the power to continue to drive 5kW of heat against the temperature gradient and into the fluid stream. The fluid temperatures will continue to diverge but at a slower rate. Once the temperature differential reaches -40°C, the COP is approximately unity and ceases to outperform a typical resistive heater. At temperature differentials less than -40°C the COP is less than unity as heat naturally flows from a much hotter liquid to a much cooler, despite the efforts of the thermoelectric heat exchanger.

Figure G56: COP and Qh Performance

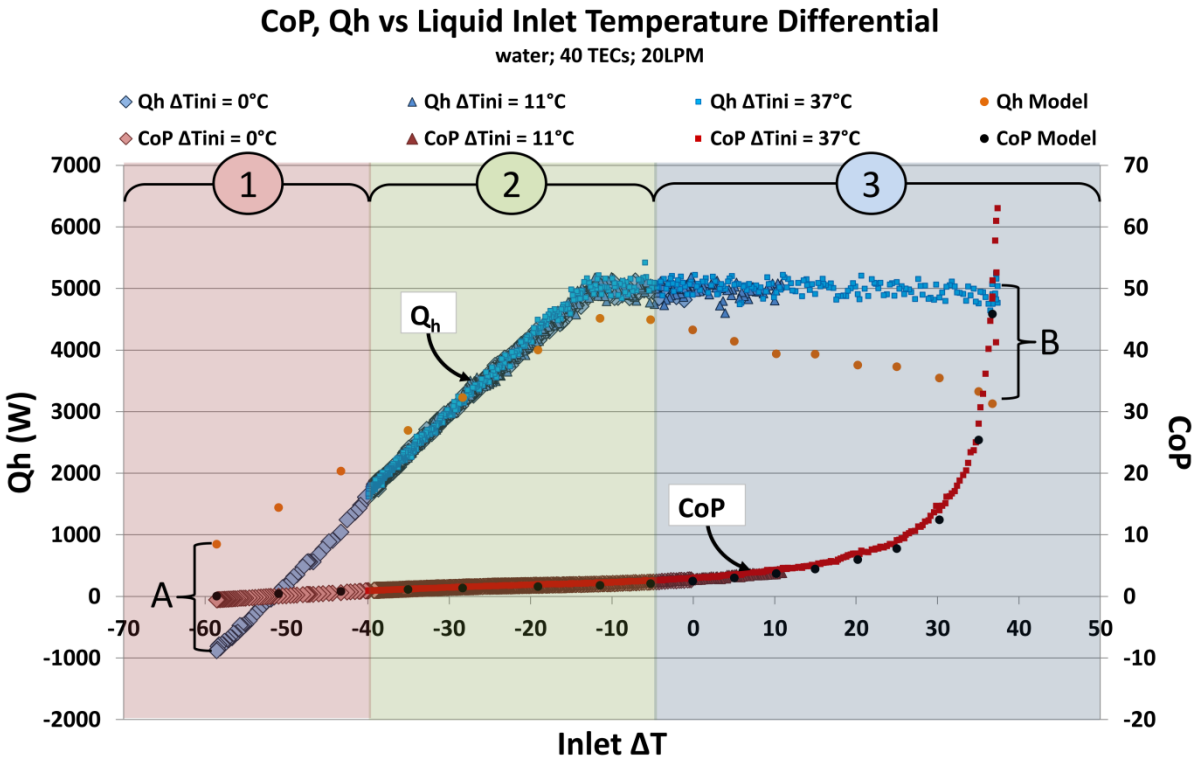

G3.5 Task 11 – Define Metrics for Efficiency and Comfort

The team's objective was to deliver equivalent comfort with the prototype distributed cooling and heating system while using significantly less energy than the production central HVAC system. The path for improving energy efficiency with distributed cooling and heating was through the reduction of A/C compressor work or electrical energy consumption by resistive

heating devices such as PTC heater in the vehicle. Within the scope of this project, the HVAC system power saving were achieved through elevation of the cabin temperature during cooling (or temperature reduction in the case of heating) to the threshold of discomfort, and then using the TE spot cooling or heating to regain the comfort. Under a constraint of equivalent comfort, a net energy reduction was expected after accounting for energy used by the TE HVAC system.

The team focused on the examination of the baseline comfort, which was expected to be maintained by the traditional HVAC system only, then reduced comfort when the ACC set point was raised for cooling and lowered for heating, and then restored comfort with the distributed TE HVAC system supplementing the reduced set point central HVAC system.

For spot cooling, the tunnel ambient condition of 85°Fx55%x500W/m^2 was the primary development condition, or standard ambient condition, for the TE HVAC system. Typically, steady-state evaluation of the distributed cooling and heating system, including the corresponding passenger comfort, was carried out under this tunnel ambient condition. Once the TE HVAC system met the operational requirements under the standard ambient condition, a higher tunnel ambient condition of 100°Fx40%x1000W/m^2 was used as a secondary test condition to assess the system performance under a more severe thermal load. For spot heating development, the standard ambient condition was 0°CxXX%x0W/m^2.

The measurement scales for thermal sensation and thermal comfort were previously defined under Task 3, Perform Human Subject Testing. The key metrics was to achieve an equivalent comfort and an equivalent homogeneous temperature with the prototype distributed system as the standard centralized HVAC system. Other metrics compared the actual thermoelectric device coefficient of performance (COP) in both heating and cooling modes to the established program targets. The COP measures the individual efficiency of each TE device.

G3.6 Task 12 – Integrate Initial Components into Mule Vehicle

Vehicle Build & Instrumentation

The vehicle build began with instrumentation and the critical parts to be incorporated for the cooling loop. The overall vehicle build was divided into three parts, and these include basic instrumentation, coolant loop design, and thermoelectric/duct installation.

The overall basic cooling loop was designed to allow for cooling of each thermoelectric to provide the necessary heat rejection required by each thermoelectric. The basic concept was to distribute the coolant to three zones, these being driver seat, front passenger seat, and the rear three seats. Two flow pumps were utilized, one for the front seats and one for the rear seats. Variable resistance valves were placed at each zone to control the total flow to these areas. To further control the flow to each thermoelectric, a rotometer flow meter with control was plumbed into the cooling circuit. The rotometers were used to enable the proper flow to each thermoelectric, that being one l/min to each thermoelectric. After the flow was delivered to each thermoelectric, the flow was collected in a manifold that delivered it to a reservoir prior to going to the waste heat exchanger, which removed or added the waste heat delivered by the thermoelectric.

Figure G57: Waste Heat Exchanger and Blower (left) and Reservoir (right)

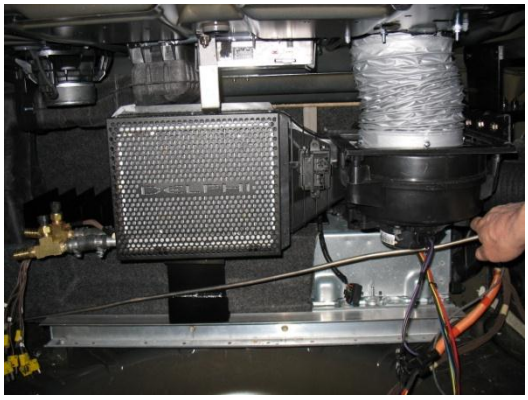

Figure G58: Rotometer Flow meter (left) and Liquid Pump (right)

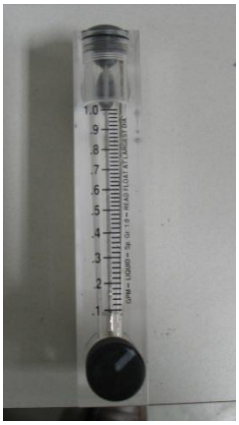

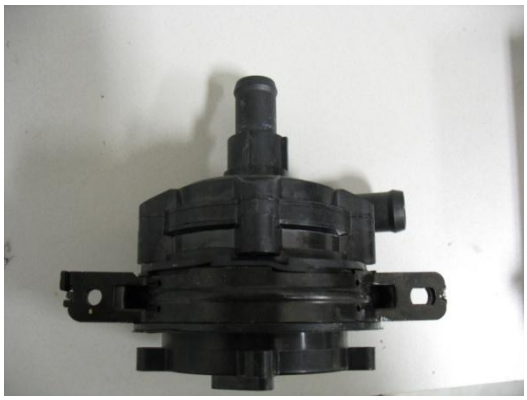

The vehicle instrumentation, coolant loop parts (see Figure G57 and Figure G58), thermoelectric devices, duct installation, and control system were installed in the Buick Lacrosse for testing.

G3.7 Task 13 – Evaluate Initial Comfort Components

G3.7.1 Perform testing and analysis of initial prototype HVAC components

ACC System Baseline Comfort for Spot Cooling

The baseline cabin comfort of the vehicle is dependent on the set point of the Automatic Climate Control (ACC) system. The ACC system is typically calibrated by the OEM to maintain cabin comfort at the generic set point of 72°F. The final calibration of the ACC system occurs on the road to ensure accurate control of comfort. It is generally known, however, that ACC system performance in the environmental tunnel differs some from the on-the-road performance, and the ACC set point needs to be adjusted to achieve comfort. One factor is that the solar sensor reads differently in the tunnel vs. on the road. The solar lamps in general do not have the exact spectrum as that of the sun. Additionally, the discharge nozzle area of the tunnel air is limited in comparison with the cross-flow area of the car, causing some disparity of flow distribution around the body of the car.

Another complication for the present ACC system in the Buick Lacrosse is that the control head calibration has been modified to provide an elevated in-car temperature to 29°C by offsetting

the control head set point input so as to save compressor power with the TE system making up for the lost comfort by using spot cooling. Therefore, at the standard set point of 72°F, comfort cannot be achieved with the ACC system alone. A further modification to the control head was the configuration of the blower curve to operate on a lowered blower curve, approximately 75% of the standard blower curve.

In order to achieve comfort with the modified control head so as to provide a basis of assessment for compressor power consumption, passenger comfort rides were used to search for the proper ACC set point. After going through a stabilization process with an estimated control head set point, a crew of three comfort riders entered the vehicle to evaluate the in-car comfort. The front passenger seat was occupied by a thermal manikin for objective data recording. The driver made adjustments to the control point until an acceptable comfort was attained for the cabin. It was recognized that there is substantial front-to-rear breath level air temperature variations in the cabin. In addition to the normal front-to-rear temperature variation of the vehicle, the eAssist battery in the trunk generated enough heat to exacerbate the comfort deficit for the rear passengers. As a result, the ACC set point was determined to a large extent by driver comfort with the rear passenger comfort serving as secondary input.

For the ambient of 85°Fx55%RHx500W/m^2, the final set point for the modified control head to achieve comfort was determined to be 66°F. The comfort rating and the compressor power consumption at this set point formed the basis of comparison for the TE-assisted HVAC system.

Figure G59: Baseline Thermal Sensation Rating at 66°F ACC Set Point

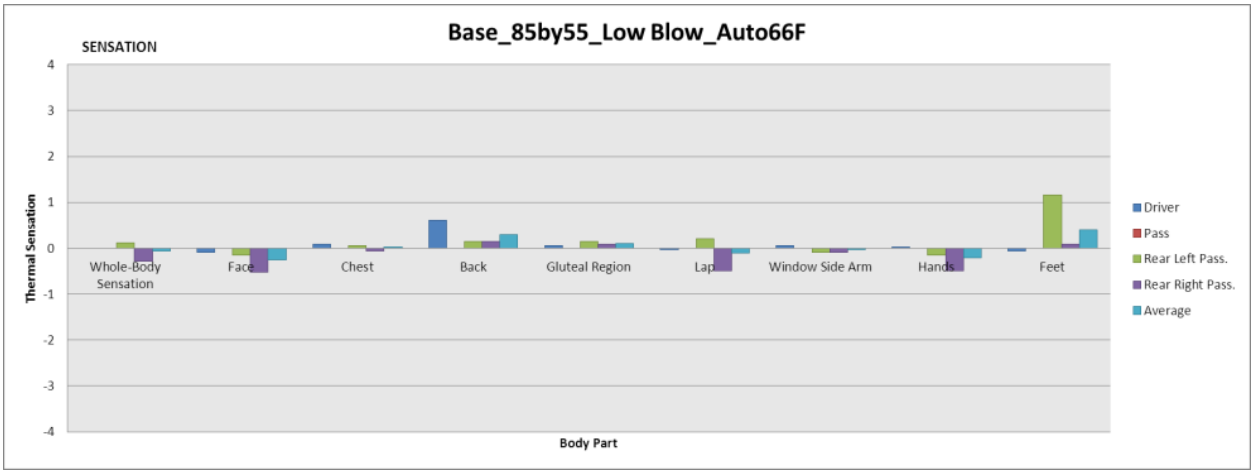

Figure G59 and Figure G60 show the baseline thermal sensation and baseline thermal comfort, respectively, for the Buick Lacrosse passenger compartment. It was seen that the cabin generally achieved thermal neutrality for the front and rear passengers. Thermal comfort ratings indicated that the driver and rear right passenger achieved better comfort than the rear left passenger. The average whole body thermal comfort was rated near the value of 1. It was recognized that, in additional to the normal temperature rise over the front passenger breath temperatures, there was also vertical temperature stratification for the rear seat. Toward the roof liner of the rear cabin, the temperature rose to a higher temperature. A tall passenger in

the rear seat would be impacted by the temperature stratification and perceive the associated discomfort while a shorter passenger in the rear seat would be less impacted.

Figure G60: Baseline Thermal Comfort at 66°F ACC Set Point

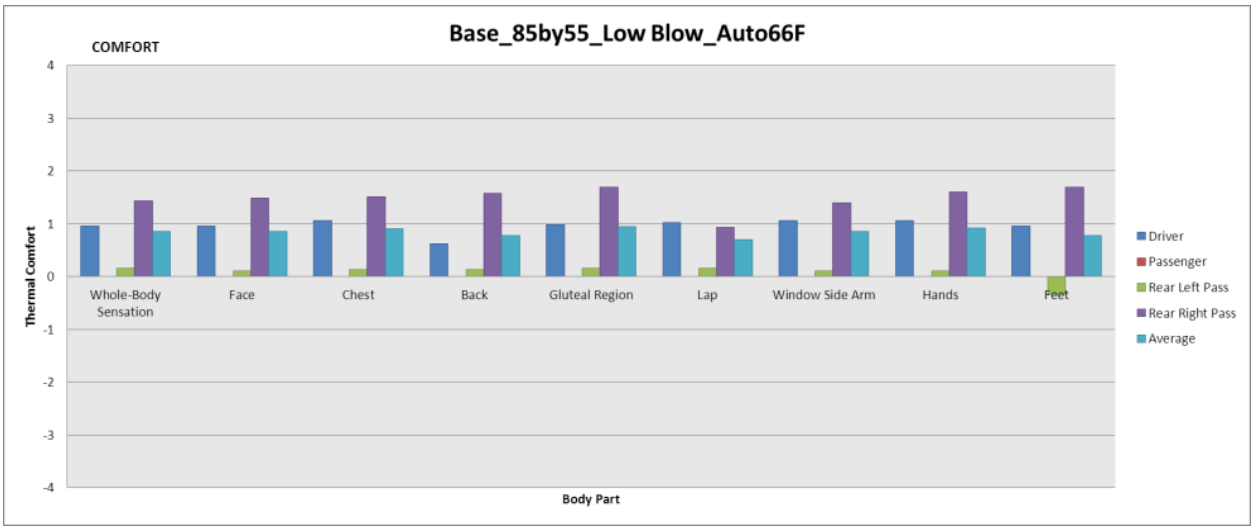

Distributed TE HVAC System Cooling Comfort

The TE HVAC System was composed of all the TE modules in proprietary locations for each seating position. The TE modules were calibrated and operated to provide comfort to the cabin occupants under an elevated cabin temperature. The standard elevated temperature planned for the cabin was 29°C EHT, as was recommended from the Phase I studies. The elevated in-car temperature was to be maintained by the ACC system with a higher set point than the baseline comfort set point. Vehicle testing showed that an ACC set point of 74°F provided the 29°C EHT cabin temperature. It was subsequently found that the 74°F set point introduced heating via the coolant heater in the HVAC module into the cabin, instead of the expected, elevated Evaporator Out Air Temperature (EOAT) setting for compressor power reduction, as is practiced in the Series Reheat Reduction technology for energy efficiency. At this set point, the EOAT set point for compressor reached it maximum temperature imposed for humidity control, and the mixed door (or temperature door) in the HVAC module opened up to introduce heater heat into the cabin. The portion of heat from the heater simply warmed up the cabin without allowing any compressor power reduction. In fact, additional electrical energy to the TE modules was required to reject the heat outside the cabin, leading to a deterioration of the overall energy efficiency.

It was therefore determined that the optimal set point when using the ACC system was 72°F. This control head set point allowed the in-car temperature to be raised to about 27°C EHT without any significant amount of coolant heat bleed. One does expect, however, that a more intelligent Series Reheat Reduction algorithm may be implemented with the support of an in-car humidity sensor to allow higher EOAT set point limit for the compressor when ambient conditions permitting. Such a smarter algorithm would allow higher energy efficiency to be achieved by the TE HVAC system.

Figure G61 shows the thermal sensation rating from comfort ride evaluation of the TE-assisted HVAC system under the ambient condition of 85°Fx55%RHx500W/m^2. Compared with the baseline thermal sensation rating of Figure G59, it can be seen that the TE HVAC system provided a comfort environment that is cooler than the baseline run. The whole body thermal sensation rating average is near zero for the baseline, whereas the whole body rating average for the TE HVAC system is -0.8, a fairly significant improvement over the baseline.

Figure G61: Passenger Thermal Sensation Rating with the TE HVAC System

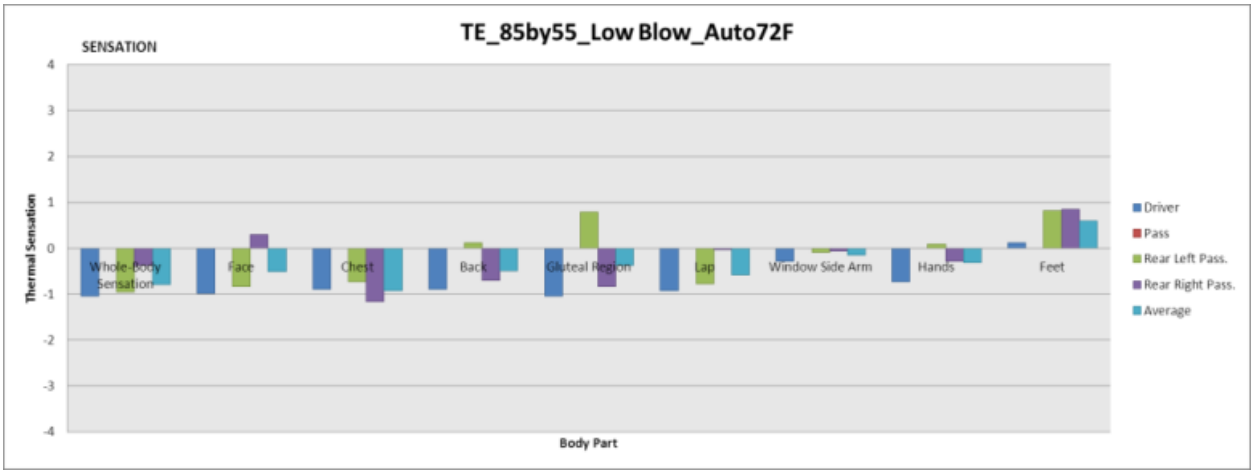

Figure G62 shows the thermal comfort rating from the same ride. Similarly, it can be seen that the thermal comfort rating for the TE HVAC system was more uniform across all the body parts and among the three riders. The whole body thermal comfort rating for the baseline system was about +0.9. For the TE-assisted HVAC System, the riders' whole body thermal comfort rating average was close to +1.5, confirming an improved riding comfort environment for the passengers.

Figure G62: Passenger Thermal Comfort Rating with TE HVAC System

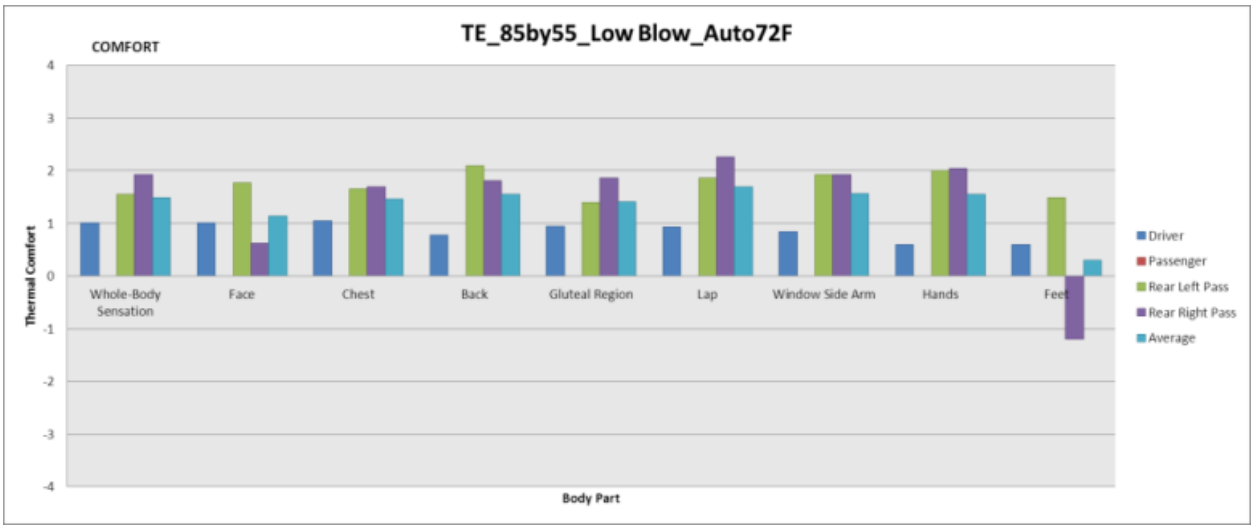

The slight edge for the TE HVAC system in maintaining comfort does not indicate that the TE HVAC system was more capable of maintaining comfort. In fact, the baseline system set point can be slightly reduced or the TE HVAC system operating point can be changed to bring about exactly equivalent comfort. However, it may still be concluded that comfort is achievable under a more elevated in-car temperature of 27°C EHT with the assistance of the TE HVAC system. And it may also be noted that any energy saving estimate for the TE HVAC system over that of the baseline system might be on the conservative side, since it is possible to further reduce the TE operating power to achieve a bit more energy efficiency.

Figure G63 shows the calculated EHT data as perceived by the different body parts and the whole body of the manikin for three different comfort evaluation runs: the baseline, TE HVAC system at a 72°F set point and at a 74°F set point with the manikin placed on the passenger seat during the comfort evaluations. The EHT curves indicate a general equivalency of comfort in the cabin for the three cases with slight variation for some body parts. The whole body EHT is within close proximity of each other.

Figure G63: Manikin Objective Comfort Comparison

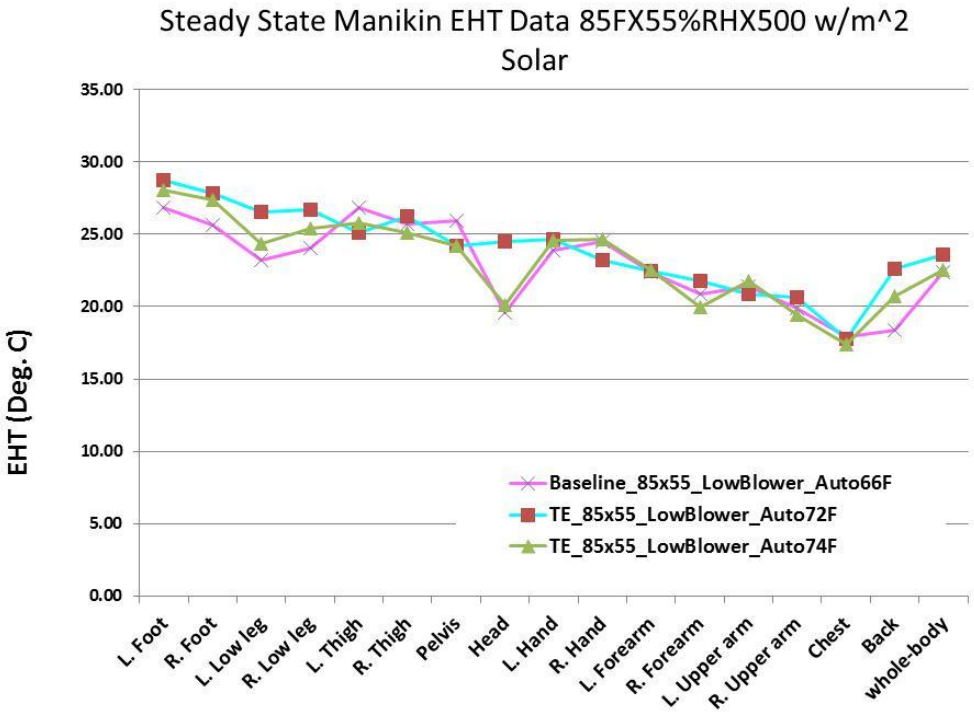

ACC System Baseline Comfort for Transient Cooling at High Ambient

As a starting point to evaluate the TE HVAC system for the higher ambient condition of 100°Fx40%x1000W/m^2, the baseline ACC system was evaluated for comfort using the 66°F as set point. The blower curve was still the 75% downscaled curve. Figure G64 shows the thermal sensation ratings for the baseline ACC system. The rear left passenger reported warm ratings, while the driver and the right rear passenger reported neutral to cool sensation. It appeared

that the driver was slightly overcooled and rear passengers perceived non-uniform thermal sensation ratings due to rider variation and in-car thermal stratifications.

Figure G64: Thermal Sensation for Baseline ACC System with Low Blower Curve and 66°F Set Point for 100°Fx40%x1000Watts Ambient Condition

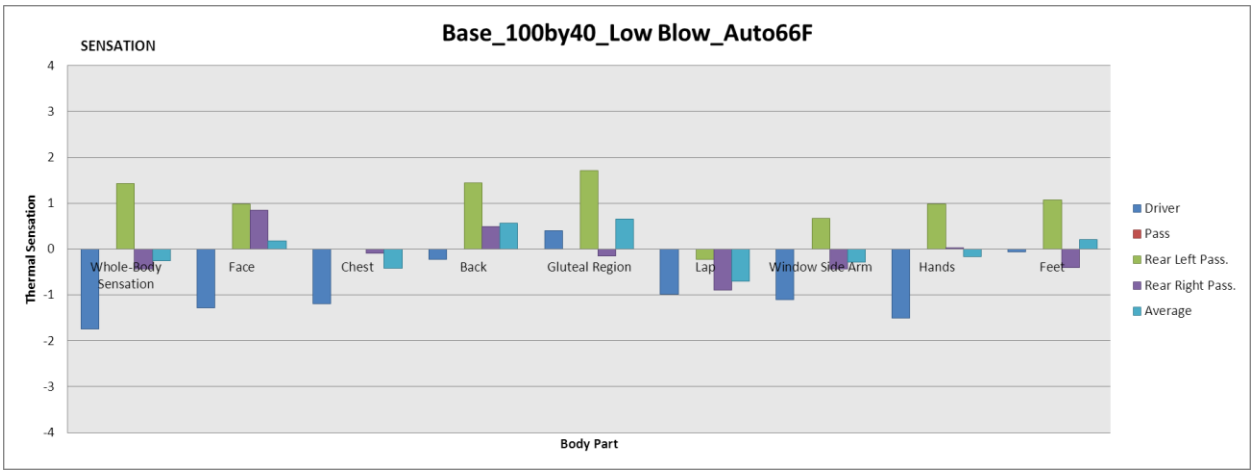

Figure G65 shows the thermal comfort ratings for the high ambient condition. The seating contact surface was marginal in comfort for the rear left passenger, but otherwise the riders were mostly comfortable. The average whole body thermal comfort rating for the riders was about +1.1. This evaluation basically established that the 66°F ACC set point was acceptable for the 100°Fx40%x1000W/m^2.

Figure G65: Thermal Comfort for Baseline ACC System with Low Blower Curve and 66°F Set Point for 100°Fx40%x1000Watts Ambient Condition

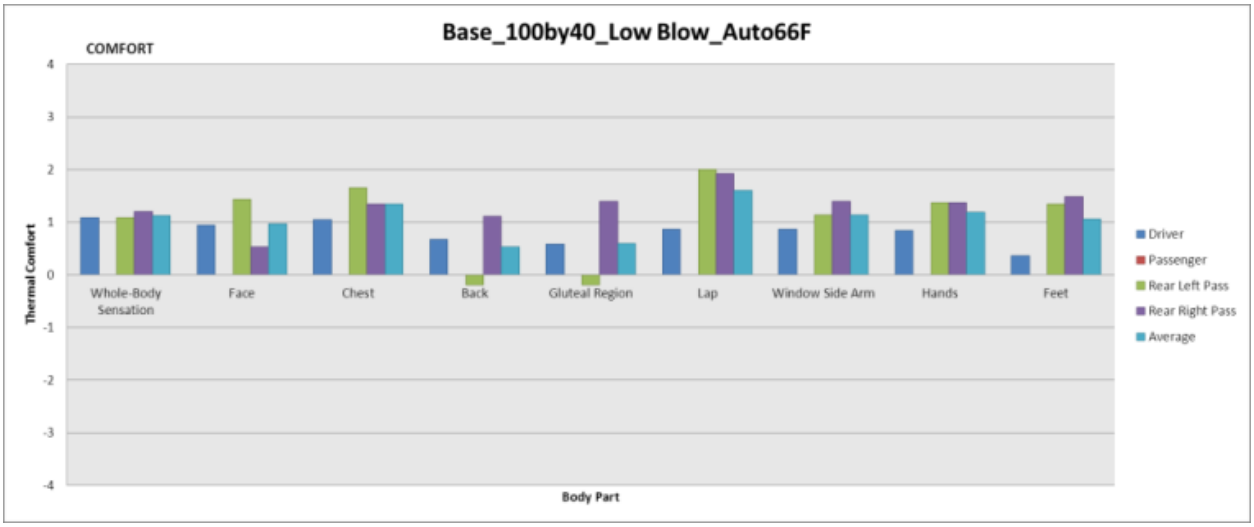

Distributed TE HVAC System Cooling Comfort for High Ambient

The TE HVAC system was first tested with the lower HVAC blower curve and an ACC set point of 72°F, similar settings used in the 85°Fx55%x500W/m^2 condition. Although the driver regarded the seating environment to be close to comfort, the rear passengers deemed it

unacceptable even when the TE modules operated at high settings. The main complaint was that there was insufficient airflow in the rear cabin from the HVAC rear console outlets.

To regain comfort, the ACC system was reset to run with the standard blower curve. Further, the operating point for the ACC system was lowered to a set point of 70°F. Under these new ACC operating settings, the TE HVAC system was able to provide in-car comfort when calibrated and optimized to run at near maximum settings. Figure G66 shows the improvement from the new ACC settings. The whole body EHT temperature decreased from about 26°C to about 24°C.

Figure G66: In-car EHT Improvement under Enhanced ACC Settings

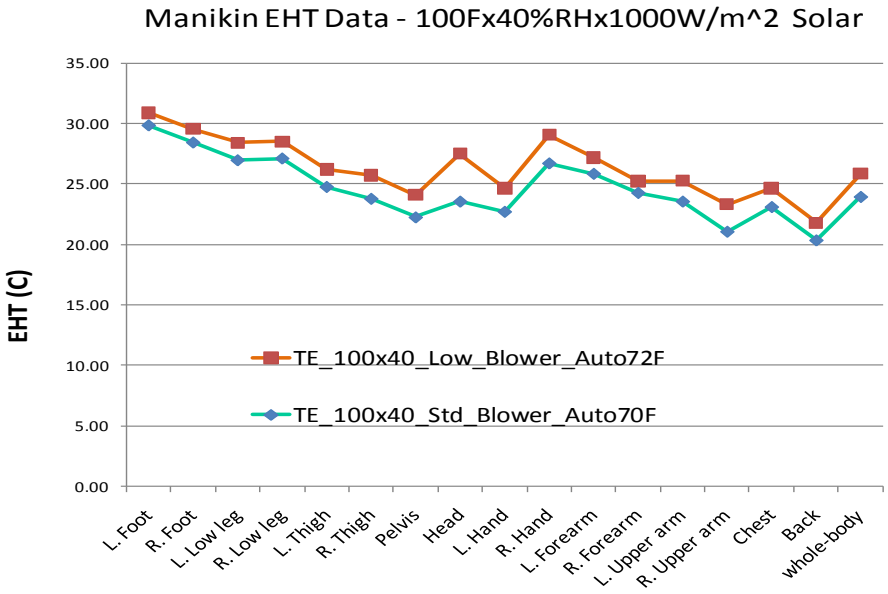

The thermal sensation ratings for the TE HVAC system under the new settings indicated that all riders gained neutral or cool thermal sensation ratings, except one or two body parts. Based on their thermal comfort ratings, the rear passengers achieved high comfort. It appears that the rear passengers were more comfortable than the driver was. This might be due to the sharp contrast in the improvement of the rear passenger thermal environment from the increased delivery of HVAC console airflow.

Spot Heating Comfort under Standard Ambient Condition

Spot heating evaluation was done under the ambient condition of 0°C without regard for humidity and with no solar. Spot heating was designed primarily for hybrid and electric vehicle applications where electric energy was used to provide heating under low ambient conditions. By reducing the cabin temperature maintained by the traditional HVAC system and using the TE HVAC system to provide localized heating, it is expected that overall energy saving may be achieved without sacrificing comfort.

On the Lacrosse test vehicle, due to the primary focus being on spot cooling and the obstacles of estimating energy saving on a vehicle with available engine waste heat, the spot heating development was focused mainly on functional development, i.e., to answer the question whether the TE HVAC system can be operated to provide spot heating and calibrated to supplement a down-powered HVAC system so as to provide equivalent comfort to the occupants.

Figure G67 shows the comfort ride thermal sensation evaluation under the 66°F ACC set point with the lower blower curve. The thermal sensation ratings are centered around neutral with the driver being on the cooler side. The average whole body thermal sensation rating from all riders was effectively zero. With the comfort ride evaluation, the 66°F ACC set point under the lower blower curve was established as the baseline condition for TE HVAC system development.

Figure G67: Baseline Thermal Sensation Ratings under 66F ACC Set Point

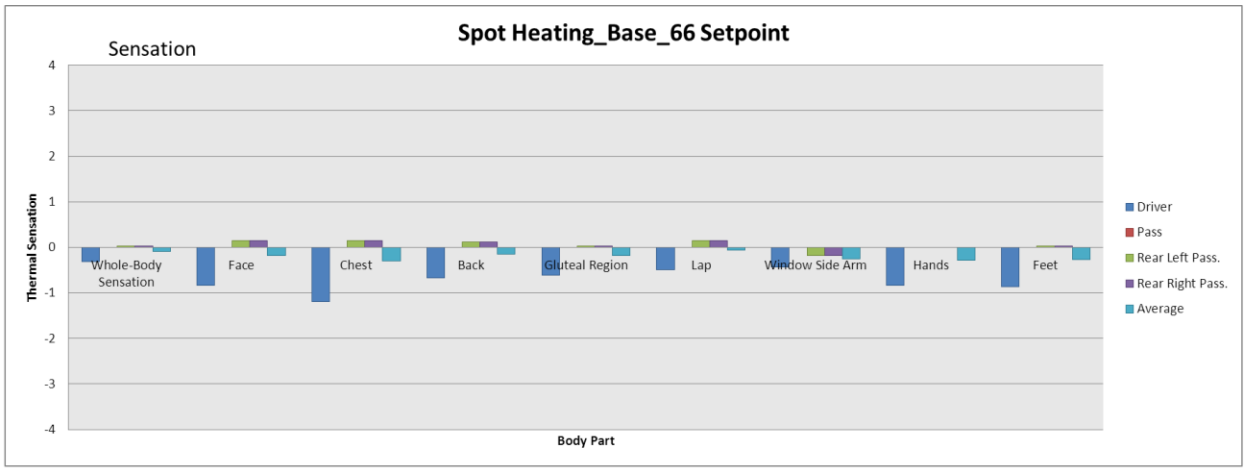

Figure G68 provides the thermal comfort ratings for the baseline ACC operation. The rear passengers indicated a high degree of thermal comfort satisfaction, whereas the driver gave a relatively low thermal comfort rating. The average whole body thermal comfort rating is at about +1.5, an acceptable level of comfort.

Figure G68: Baseline Thermal Comfort Ratings under 66F ACC Set Point

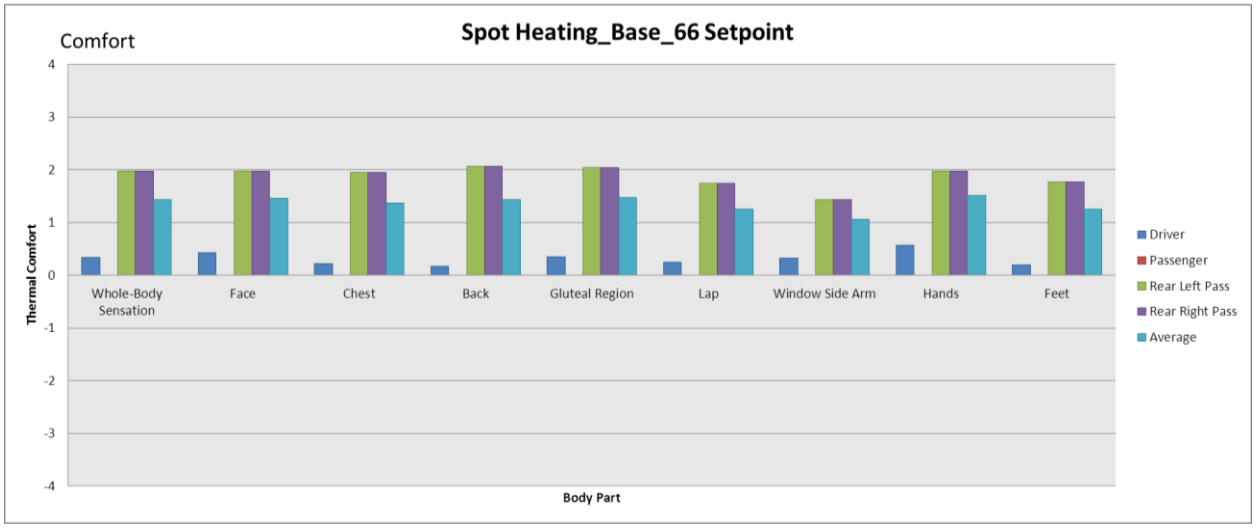

Figure G69 shows the deterioration of in-car condition when the ACC set point was reduced to 64°C while still under the lower blower curve. Under this operating condition, it was seen that all the comfort riders indicated discomfort. All the thermal sensation ratings were between "Cool" and "Cold".

Figure G69: Thermal Sensation Ratings for Reduced Set Point

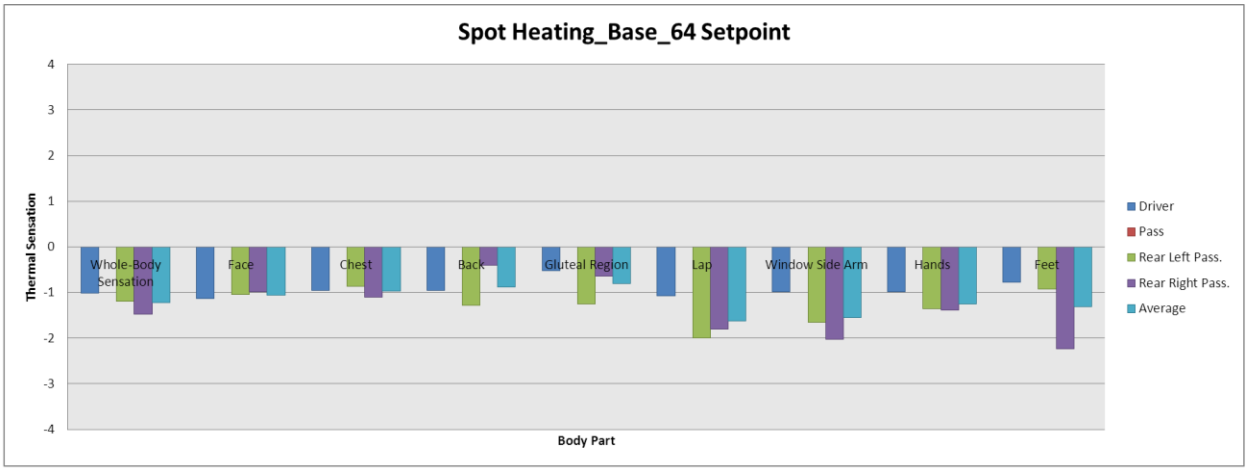

This was validated by the thermal comfort ratings in Figure G70. In general, the thermal comfort ratings were below zero, in the region of discomfort. As reminder, a thermal comfort rating in the range between +1 and +2 are required for comfort, preferable near +2.

Figure G70: Thermal Comfort Ratings for Reduced Set Point

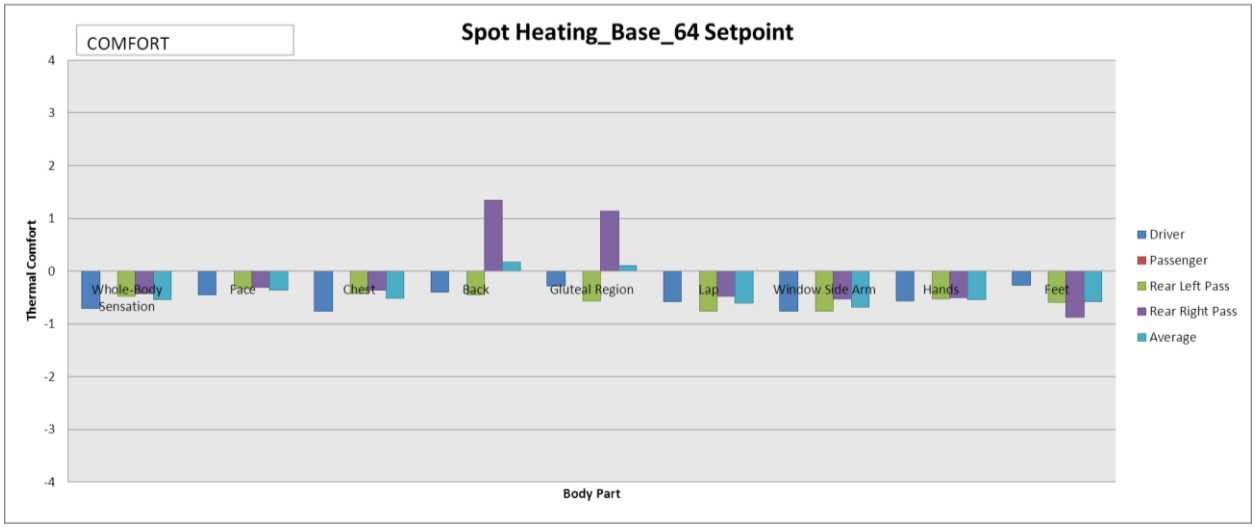

Subsequent to the establishment of the baseline operating point and comfort ratings, the TE HVAC system was turned on with the ACC system operating at 64°F set point to restore the thermal comfort deficit. In comparison with Figure G69, where the ratings were "Cool' or "Cold", Figure G71 shows that the thermal sensation ratings were restored to a range between "Neutral" and "Warm", making the in-car environment acceptable.

Figure G71: Thermal Sensation for TE HVAC System in Spot Heating

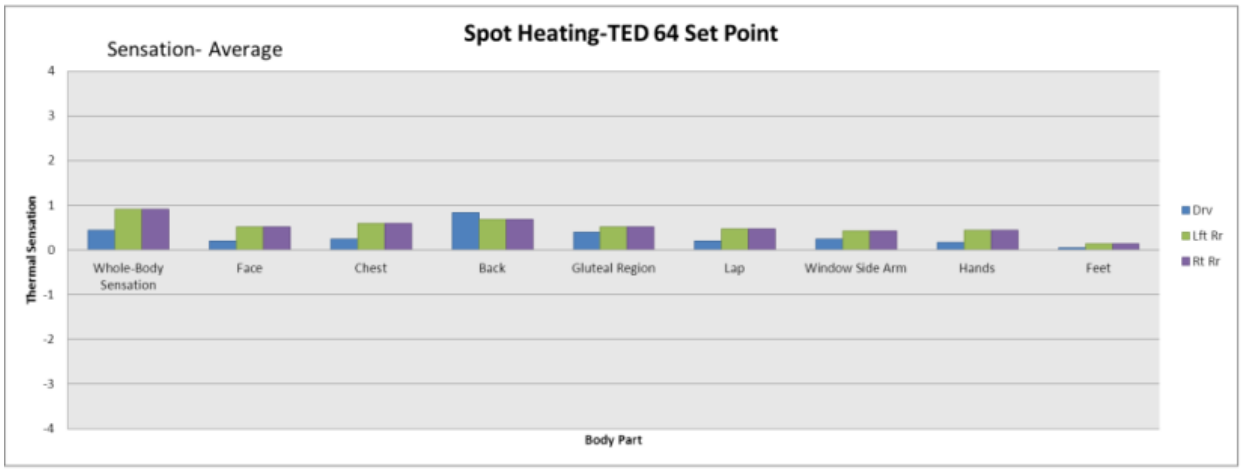

Figure G72 shows the corresponding thermal comfort ratings for the same car ride. It was seen that the thermal comfort ratings were comparable or better than that of the baseline ride in Figure G68. The driver's ratings were still relatively low compared with the rear passengers, but they showed a degree of improvement over the baseline case.

Figure G72: Thermal Comfort for TE HVAC System in Spot Heating

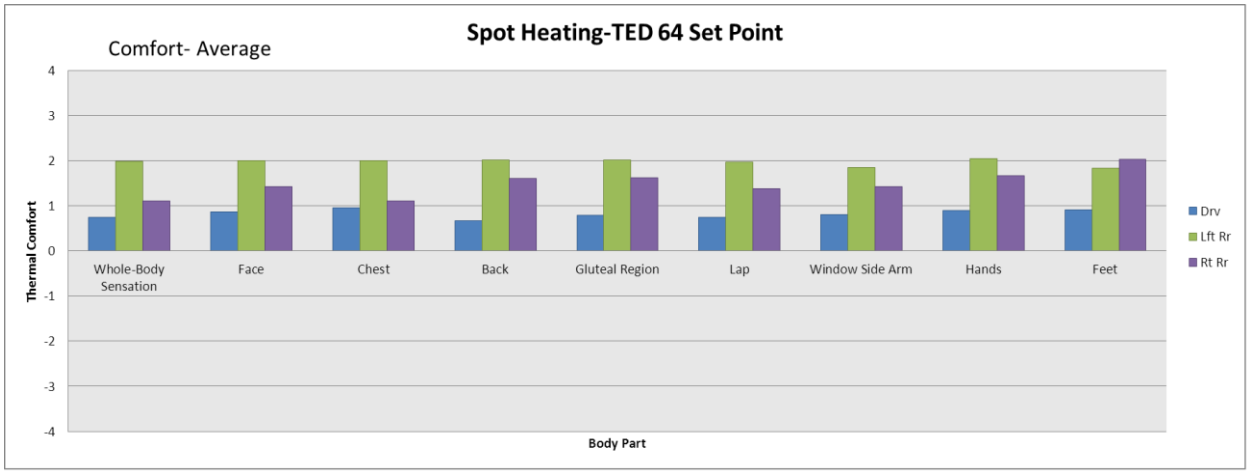

Figure G73 is the comparison of front passenger seat manikin EHT temperatures for the baseline ACC operating condition with 66°F set point and the reduced set point operation at 64°F supplemented by the TE HVAC system. The objective data demonstrates that better comfort was achieved with the TE HVAC system. In fact, the whole body EHT was at 24.3°C, while the baseline whole body EHT was at 21.4°C.

Figure G73: Manikin Objective Evaluation of Comfort

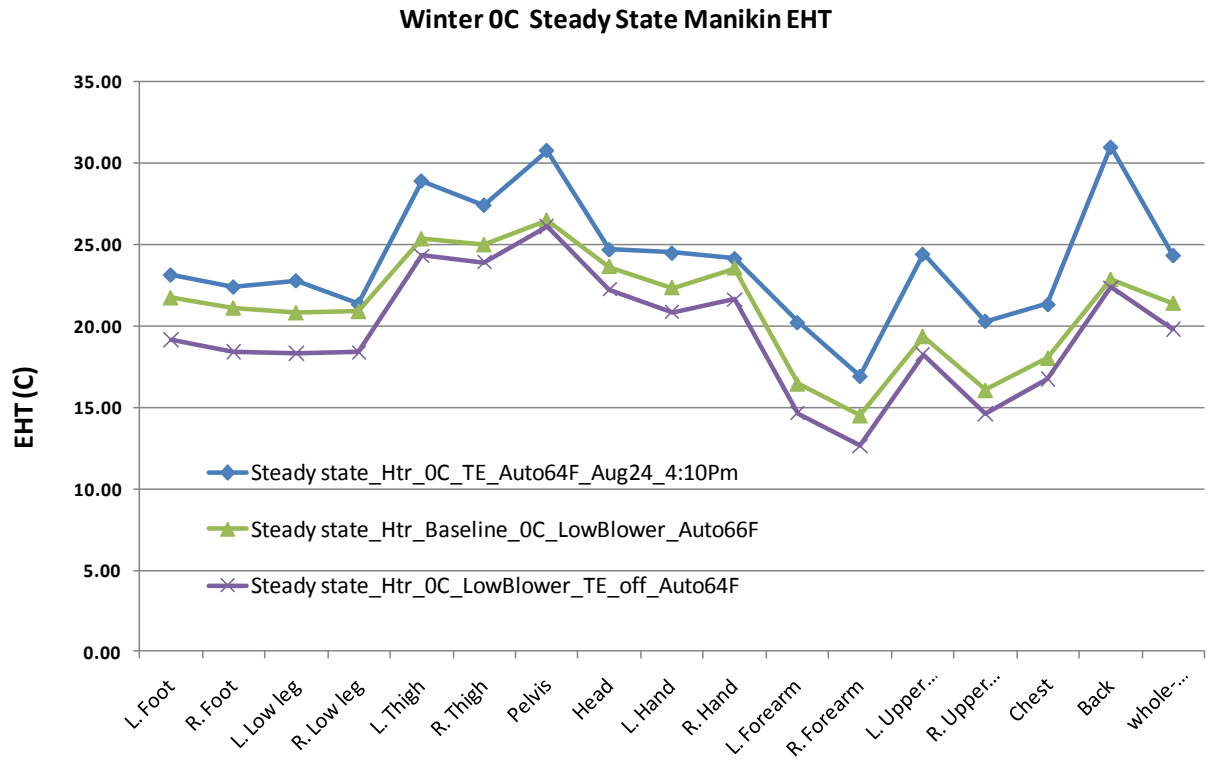

Due to the modified control head internal offset, the baseline comfort was established through comfort ride evaluation and not through manikin EHT mapping. It appeared that the baseline

set point of 66°F might be on the lower side in consideration of the driver ratings. On the other hand, the 64°F set point appeared to have established enough discomfort for the TE HVAC system to compensate and worked reasonably well. For future spot heating energy saving estimates, the baseline operating point needs to be increased, perhaps to 68°F with the modified control head, or to whatever setting that provides a baseline comfort close to 24°C EHT.

TE HVAC System Power Consumption Test and Analysis

A focused effort was made to provide the initial energy efficiency assessment of the TE HVAC system in comparison with the baseline eAssist Buick Lacrosse vehicle. The primary energy efficiency assessment of interest was in the area of compressor power saving.

Generally speaking, the energy efficiency assessment was based on the steady-state tunnel test data. It was understood that energy savings were available during the transient operations of the vehicle; however, due to the complexity of test protocols and concerns about repeatability, presently only the steady-state energy savings were examined. For the baseline vehicle steady-state energy consumption under each of the test ambient conditions, the compressor and HVAC blower power use were conglomerated to represent the HVAC system power use. For both the baseline and the TE HVAC system, miscellaneous power use by the Campbell data logger and the TE HVAC controller were not included.

The electrical power consumed by each passenger was then combined with the compressor and HVAC blower power to form three different occupancy scenarios: driver only, driver and passenger, and four passengers. There was no effort made to differentiate between one or two rear passengers. Even though the control mechanism may be designed into the vehicle's TE HVAC control system, the occupancy weighting for the rear passengers was very low when compared with the front passengers; therefore, four-passenger occupancy was considered an adequate representation of the power consumption by the rear passengers.

From the test point of view, no repeated tests were performed for each of the occupancy scenarios. For a given ambient condition, the vehicle was tested with all four TE seats switched on. The power consumption scenarios for one, two, and three/four occupants were based on the power allocated to each occupant. For the driver only case, the power allocated to the driver was added to the compressor and HVAC blower power used to achieve the total TE HVAC system power, while the power allocated to the other seats was ignored.

The Ambient Sweep test procedure was used to establish the power use for the baseline and the TE HVAC equipped Buick Lacrosse. Some complicating factors impacted the final test procedure. Typically, the Automatic Climate Control (ACC) system was road tested and calibrated before being launched into production. There was some difference in ACC performance when a vehicle was tested in the tunnel. The ACC system may not be able to maintain 100% comfort across the entire ambient sweep temperature range. The factors causing the performance variation from the road mainly are the airflow distribution around the vehicle and the solar sensor response to the actual sun versus the heating lamps in the climatic wind tunnel. The second complicating factor was that the control head for the Lacrosse was not a standard production control box. Modifications to the software were made in the effort to

automate the coordination of the TE module operation and the HVAC ACC system. The ACC set point was offset by certain amount according to the ambient temperature and solar sensor reading. Thus, there was a considerable uncertainty as to what comfort level the ACC system would offer at a particular set point.

The Ambient Sweep test procedure compensated for these ACC uncertainties by using actual passenger comfort rides. At any given ambient condition, the vehicle was run and stabilized with a preliminary control point. Once stabilized to a steady state, engineers were invited to sit in the car and make adjustment to the control point based on their comfort perception. This was done with a panel of three or four engineers based on consensus of the group. The same approach was followed for both the baseline vehicle and the TE HVAC equipped vehicle. Thus, the power usage data was collected on equivalent comfort basis for the two HVAC systems. Compressor power was calculated using the measured refrigerant flow rate plus the suction and discharge enthalpy with an estimated mechanical efficiency.

Power Savings Projection

Comparison of the baseline and the TE HVAC system power consumptions allowed the team to estimate the expected power savings with this technology. The methodology used to calculate the expected savings and the proprietary results were used to support the completion of two Phase 2 milestones, the evaluation of initial comfort components and the estimation of the final coefficient of performance for thermoelectric devices. These results indicated that the project should successfully accomplish the stated objectives for energy savings of 30% improvement (current status is 29%) and for coefficient of performance of the TE devices (nearly all initial prototype components exceeded the cooling mode COP target of 1.3 and the heating mode COP target of 2.3).

G3.7.2 Milestone 7 – Evaluate Initial Comfort Components Completed

To complete this milestone, the project team tested the initial set of prototype distributed HVAC components on the Buick Lacrosse in a climatic wind tunnel. For spot cooling, the tunnel ambient condition of 85°F x 55% relative humidity (RH) x 500W/m^2 solar load was the primary development condition for the TE-assisted HVAC System. Typically, steady-state evaluation of the distributed cooling and heating system, including the corresponding passenger comfort, was performed under this tunnel ambient condition. Once the TE-assisted HVAC system met the operational requirements under the standard ambient condition, a higher tunnel ambient condition of 100°F x 40% RH x1000W/m^2 solar load was used as a secondary test condition to assess the system performance under a more severe thermal load. For spot heating, the ambient condition was 0°C with tunnel humidity uncontrolled and with no solar load applied. The proprietary results from these tests were used to guide the team's efforts in Phase 3. The project team's analysis of these test results and overall evaluation of the initial comfort components was completed on November 27, 2012.

G3.7.3 Milestone 8 – Estimate Final Coefficient of Performance for Thermoelectric Components

A key portion of the team's analysis was to evaluate the energy efficiency of this distributed thermoelectric HVAC system. This evaluation had two primary constituents: assessing the initial energy efficiency of the prototype HVAC system in comparison with the production HVAC system on the Buick Lacrosse test vehicle and estimating the final coefficients of performance for the prototype thermoelectric components. The primary energy efficiency assessment of interest is in the area of potential A/C compressor power savings.

Generally speaking, the energy efficiency assessment is based on the steady-state tunnel test data. It is understood that energy saving is available during the transient operations of the vehicle, however, due to the complexity of test protocols and concerns about repeatability, presently only the steady-state energy saving is examined.

The TE system power consumptions are allocated to each passenger in the vehicle. Due to the capability to turn off components by location, unoccupied seats do not consume any power. For example, with the rear seats turned off, all the TE devices, TE cooling fans, and the associated coolant pump are turned off. For the front seats, which share the same coolant pump, power consumption by the pump is divided between the two front seats. It is expected that when there is only the driver in the seat, coolant pump flow rate may be halved to reduce pump power consumption.

The electrical power consumed by each passenger is then combined with the compressor and HVAC blower power to form three different occupancy scenarios: driver only, driver and passenger, and four passengers. There is no effort made to differentiate between one or two rear passengers. Even though the control mechanism may be designed into the vehicle TE control system, due to that the occupancy weighting for the rear passengers are very low as compared with the front passengers, four-passenger occupancy is considered an adequate representation of the power consumption by the rear passengers. The proprietary details of this analysis were used to guide the team's efforts in Phase 3.

In summary, the results of the estimate completed on November 27, 2012, indicate that the project should successfully accomplish the stated objective for A/C energy savings of at least 30% and also achieve the thermoelectric coefficient of performance targets of at least 1.3 in cooling mode and 2.3 in heating mode.

CHAPTER G4:
GM Phase 3 – Advanced Development

The focus of this phase was to develop the final prototype distributed HVAC components while considering production-intent requirements such as noise and packaging. For this phase of the project, GM will continue to utilize Delphi to develop most final prototype HVAC components with Faurecia developing final prototype seats and Marlow Industries developing a final prototype TE-based heater for the Volt. UCB will continue their primary Phase 1 activities in parallel with this phase.

G4.1 Task 14 – Project Management and Planning

The planning and coordination for this phase primarily utilized weekly team meetings. Delays in reaching contractual agreements with key team partners for their support of both Phase 3 and Phase 4 activities resulted in several months delay for the overall project. However, project spending remains on budget, so the delays resulted in a no-cost time extension for the project.

G4.2 Task 15 – Commercialize Design of New Comfort Components

The main activity for this task was to develop the final prototype distributed HVAC components while considering production-intent requirements such as noise and packaging.

G4.2.1 Develop final prototype distributed HVAC components

TED Subassembly Packaging

A major challenge for the project team during Phase 3 was to reduce the blower noise in the thermoelectric device (TED) modules. The objective was to reduce the noise level produced by the final set of prototype distributed HVAC components to create a more production-intent environment for occupants of the demonstration vehicle. The fans in the initial set of prototype components developed during Phase 2 were oversized to support a broad range of airflow values during testing. For Phase 3, the requirements for the final prototypes were reduced to a narrower range of effective airflow values. As Figure G74 demonstrates, the project team undertook extensive investigations to identify and evaluate alternative fans for the final prototype components that both lowered noise levels and required less power. Fan size was also a consideration as the team tried to improve the packaging of the final prototype components and their associated ductwork.

Figure G74: Comparing two fans – new NIDEC fan in purple and old Delta fan in cyan

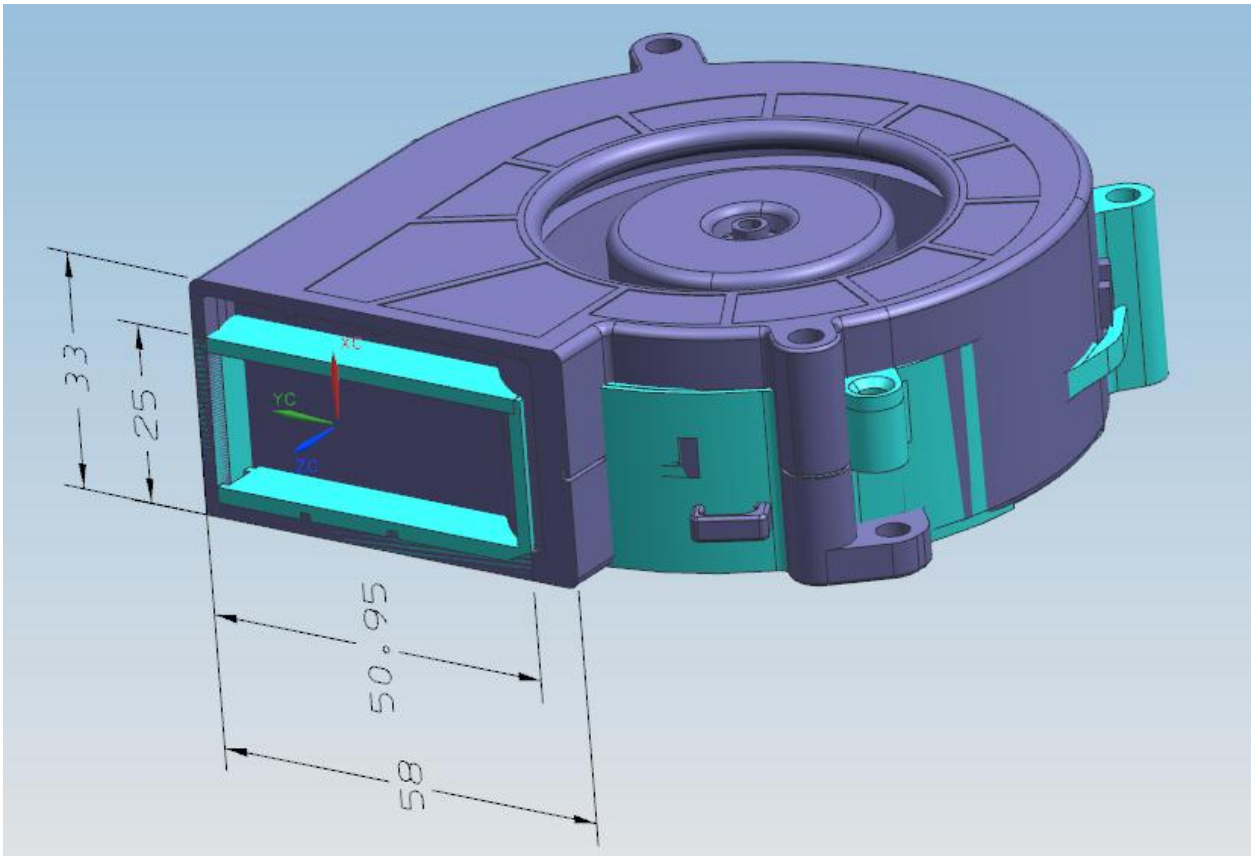

Design of the Plume Seating System

During Phase 2, the team developed, installed, tested, and evaluated two sets of front seats, a conventional seating configuration plus an innovative "plume" system concept that delivered air from near the occupant's neck in an attempt to create a blanket of conditioned air around the front seat occupants. While the initial plume development did not result in power savings for this project, the plume system was designated as an HVAC comfort feature with the potential for future energy savings from further refinement. Based on this potential, the team decided to include the plume system in the Phase 3 front seats, because the plume system feature can be disabled if it detracts from the project's energy savings objective. A revised plume system has been included in the final front seat prototypes for the Buick Lacrosse demonstration vehicle, and this feature will continue to be evaluated for potential improvements in comfort and energy savings. However, the team is confident that it can achieve the project's energy savings objective without using the plume system, so the plume is currently considered an HVAC system comfort feature instead of an energy-saving feature. As shown in Figure G75, air can be diverted from the rear passenger air to feed the plumes for the front seats. A duct switching mechanism featuring an isolator valve has been designed to allow the air to proceed to the rear seats when there are rear occupants or to feed the front plumes when there are no rear seat occupants. The airflow exiting the plumes can be controlled by changing the fan speed.

Figure G75: Isolator valve directing the flow to the front plume system or to the rear vents

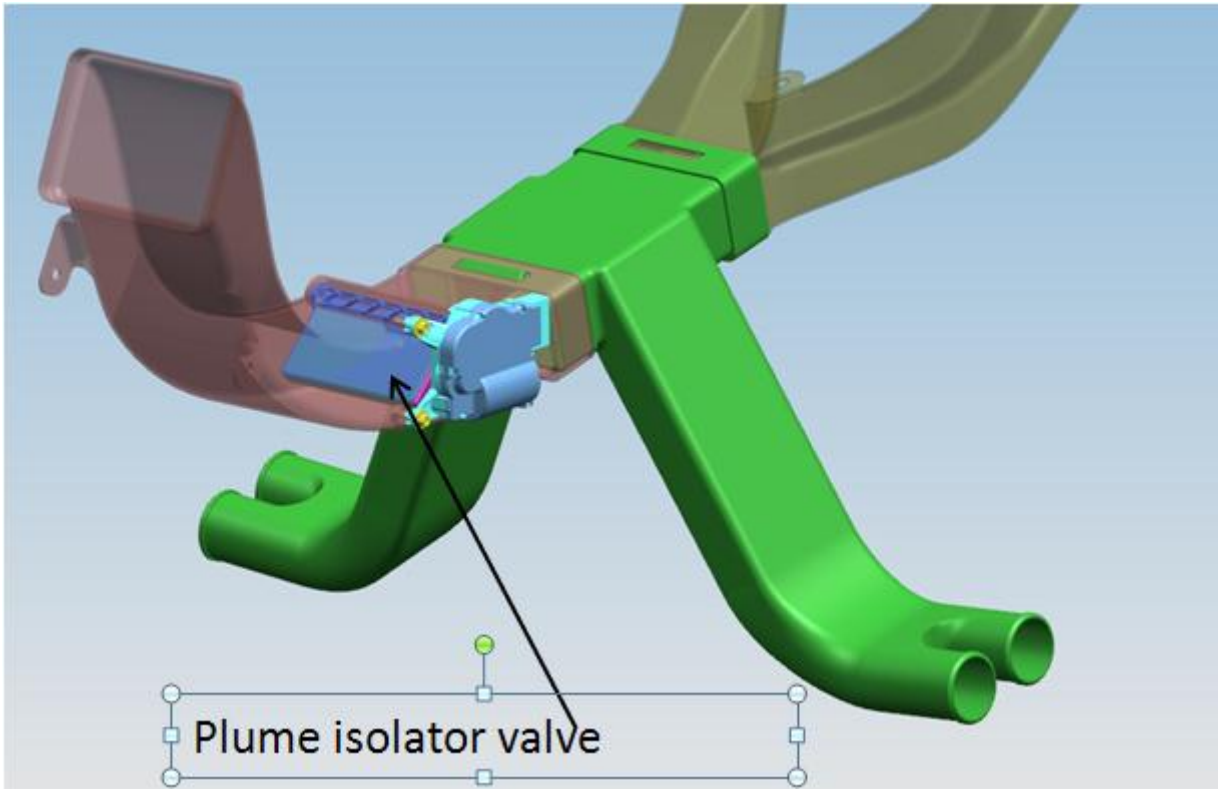

Redesign of Waste Energy Coolant Loop

The coolant system for Phases 3 and 4 has been redesigned to have the system under hood as compared its' previous location in the trunk of the vehicle in Phase 2. The system will rely on a front end heat exchanger to provide cooling to the TED when spot cooling is requested. The system will utilize the same front end heat exchanger evaluated in Phase 2, but all plumbing will be located in the front end of the vehicle. Additionally, to provide a heat source for spot heating requirements, the system has been coupled into the Belt Alternator Starter (BAS) loop. Initial testing showed the loop could provide up to 1 kW of heat over time. Below are some initial test results of the heat provided by the BAS loop.

As seen in Figure G76, the q or heat transfer does not occur until 12-15 minutes where we get about 1kW of heat. However, this is due to the fact that the BAS system's pump does not come on until the alternator pump reaches 65deg C. Therefore, an additional pump was added to the BAS system to allow the TED loop to receive heat all the time. To not affect the loop, a liquid-to-liquid heat exchanger was added with a valve to allow the liquid to flow through this when spot heating is requested. An additional valve is located on the front end heat exchanger to bypass the front end heat exchanger when spot heating is requested, so as not to cool the TED loop.

Figure G76: BAS Heat Transfer

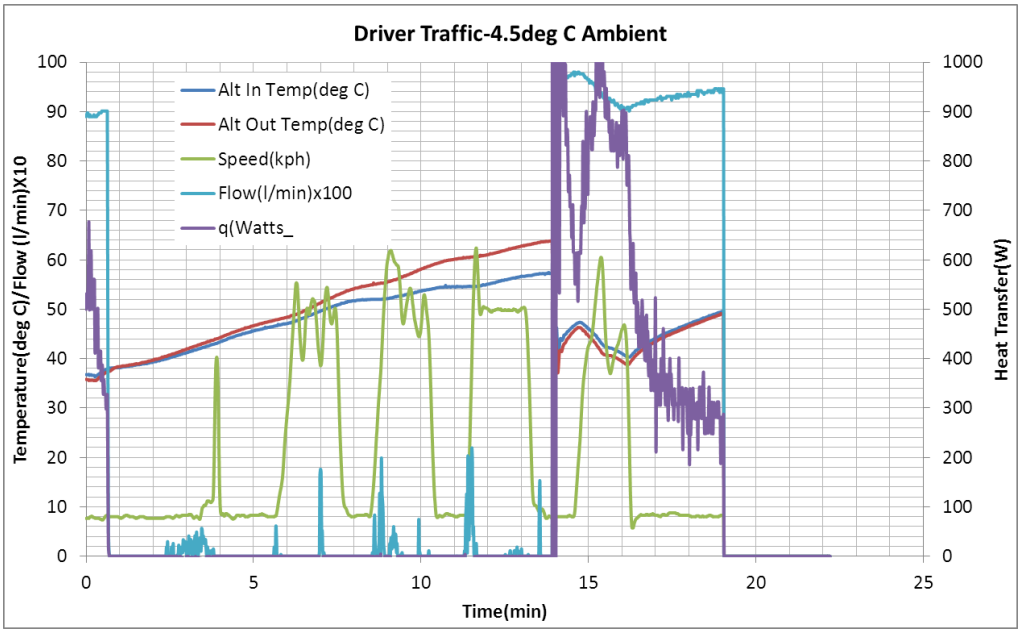

Final Controls Modifications

Due to changes in the intended hardware implementation of the system, the controls and wiring were modified to meet the system needs. Specifications for the Human Machine Interface (HMI), TED locations, addition of plume seats, and coolant system implementations were updated for Phase 3 requirements.

The Human Machine Interface (HMI) designs for the various seating positions were simplified. The control input panels no longer have the option to select offsets to automatic control or direct manual control. The resultant panel offers a hybrid of the two control methods depending on which "level" of control is chosen.

As can be seen from the front panel, there are new controls for controlling the plume seat feature that are unique to the front seats. When enabled, the speed of the plume fan can be varied from its minimum to maximum allowed speeds via the "Plume Speed" knob.

The remaining set of controls is common for each seat location where comfort can be adjusted from "Max Cool" to "Max Warm". The reduction in complexity from the elimination of the Manual and Automatic inputs is reflected in the front seat control state diagram shown in Figure G77: The resultant logic for the rear seat control state is similar except one chart controls the whole rear seat.

Figure G77: Control State Diagram for Front Seats

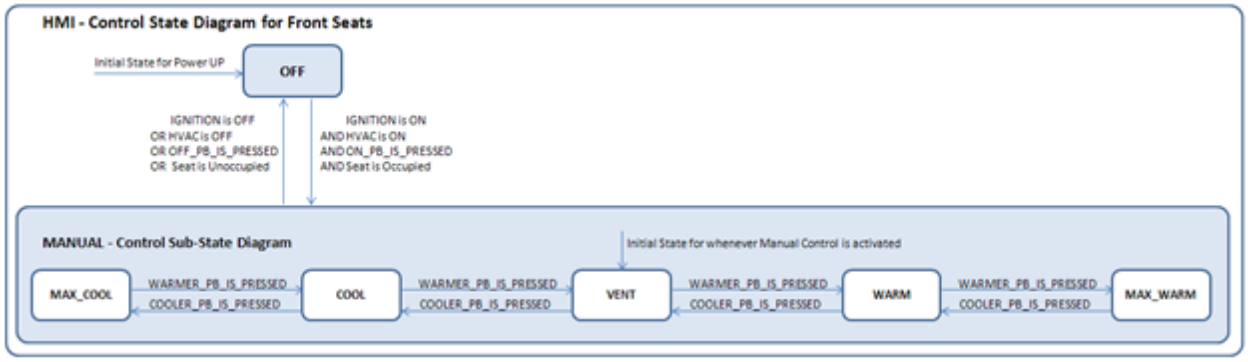

The operation of the front plume seats interacts with the airflow to the rear seats since both have a common airflow source. To insure comfort for the rear passengers a decision was made to place a higher priority on providing rear airflow over the plume seat operation.

The coolant system underwent a drastic reconfiguration that resulted in a simplification of the control logic. The cooling fan for the system was eliminated with the movement of the system's waste heat exchanger being moved to the front of the vehicle. As was described above for the "Redesign of Waste Energy Coolant Loop", the BAS coolant loop was integrated with the TED coolant system.

A good measure of the reduction of complexity of the system is the number of the ECU10 control units used to implement it. For Phase 2, twenty-four units were used. After the changes were made for Phase 3, seven units were removed and two were reconfigured for new functionality.

The previously mentioned changes and redesign of TED packaging led to a significant effort in rewiring the software test bench and vehicle. The movement of the coolant pumps, temperature sensors and coolant control valves to be under hood from the trunk lead to rewiring the whole vehicle coolant system. Changes to the HMI panels forced changes for both the both the software test bench and vehicle. A test panel was developed and built to test the vehicle wiring changes to insure correct operation in preparation to vehicle software debugging.

Flow Meters, TED Pump, and TED Controllers

The vehicle has new TED modules and ducts installed. The liquid system build was completed with flow meters, pumps, valves, heat exchangers in place. Figure G78, Figure G79, and Figure G80 show the build progress.

Figure G78: Buick Lacrosse Trunk with TED Controllers

Figure G79: Adafruit Flow Meters Installation

Figure G80: TED Pump Installation

G4.2.2 Develop final prototype TE-based cabin heater for Volt

Final Design Concept for Plate and Frame Heater System

After testing the beta design prototype, some key issues and potential solutions that could enhance performance of the final prototype heater were quickly identified. Most of the changes would focus on the gasket design, but the changes would also influence other components of the heat exchanger. It was understood that some heat (30% of Qh in some cases) was being transferred from one fluid to another through peripheral parts of the heat exchanger (plates and gaskets) rather than through the TE modules. When there was a negative ΔT across the exchanger, this became problematic as the heat has an alternative path against the desired direction of heat flow. In order to lessen this effect, a smaller gasket design was conceived. Figure G81 shows the original gasket in red and a redesigned, smaller gasket overlaid in black with a plate behind.

Figure G81: Original and Revised Gasket Comparison

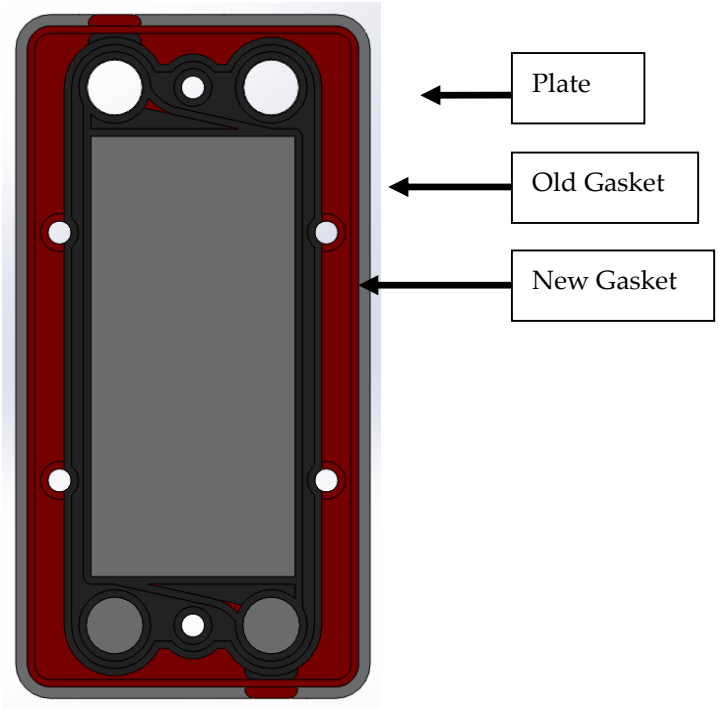

The new gasket maintains a double-sealed design while decreasing total gasket surface area by 49.7% and total gasket weight by 45.9%. The main weight advantage, however, comes not in the gaskets but in the decreased size of the plates: with a smaller gasket, the plates can also shrink accordingly. Using a smaller plate made of 316SS, the overall weight of the unit would be reduced by approximately 18%, a difference of over 3 pounds. The final design is shown in Figure G82 with an optional cover design and electronics interface included on the right.

Figure G82: Final Gamma Prototype Design

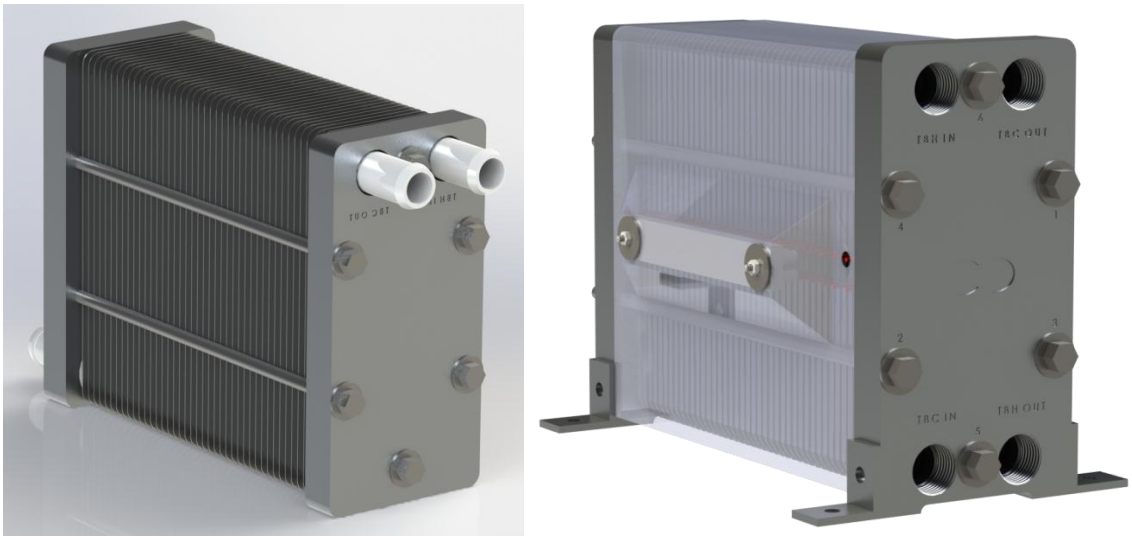

There are several distinct changes to the final gamma prototype design. First, it relocates all four liquid access ports to the front frame. This should allow for the heat exchanger to occupy a smaller volume within the vehicle and simplify the construction process. The ports have also been modified to be ½" NPT pipe thread rather than the previous barbed hose fittings. This allows greater versatility in the design as well as shortens the overall assembly. Second, the gasket and plate designs have been optimized to include as little material as possible while still maintaining a strong static seal. One additional safety feature which is now included is the bent edges of the plates. The plates now wrap around the gasket (see Figure G83), reducing the possibility of gasket movement under high-pressure situations as was previously seen. Third, the materials have also been updated. The frames are now made of 6061 Aluminum rather than 7075 Aluminum to save cost. Additionally, the gaskets are now made of hydrogenated nitrile butadiene rubber (HNBR), which allows the unit to handle liquid temperatures up to 150°C.

Figure G83: Gasket Containment Walls

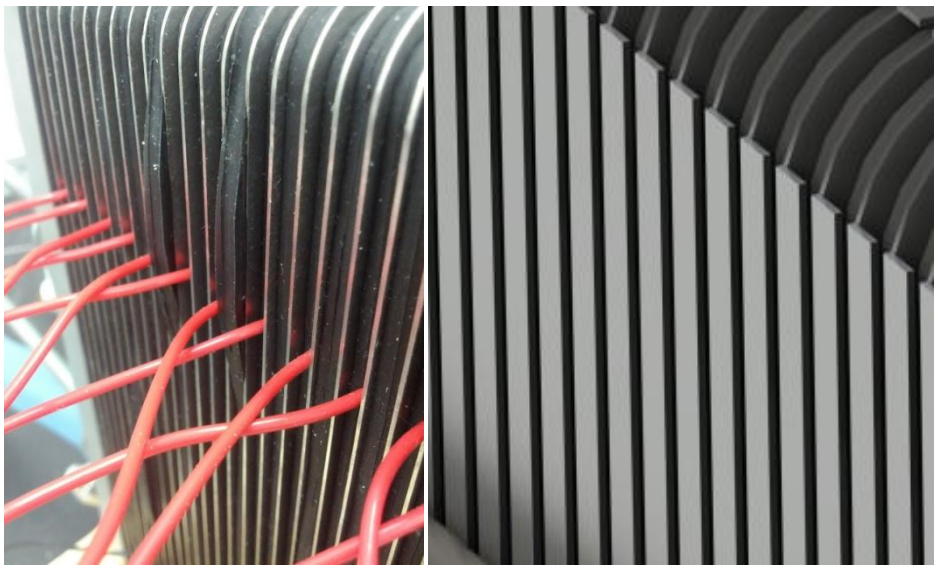

Compared to the Beta prototype, the Gamma prototype will be safer, lighter, more versatile, and capable of handling much higher temperatures.

Limited operating range at 5kW heat load

As was discovered during testing of the beta prototype, the TE-based heater design had limited capability to drive a 5kW heat load, and its COP continues to decrease as it operates for an extended period. To prevent its COP from dropping below that of a resistive heater, the team developed a concept for temporarily connecting the inlet and outlet coolant loops of the TE-based heater. It was determined that by shorting the fluid loops thru the exchanger at the point that COP equals unity, the COP curve would plateau, allowing the thermoelectric heat exchanger to perform similarly to the current resistive heater. To prove such a concept, a simple experiment was carried out in which only one fluid loop was used. That fluid loop was then split between the two exchanger loops before being reunited on the other side and recirculated (see Figure G84).

Figure G84: Shared Liquid Loop Experimental Setup

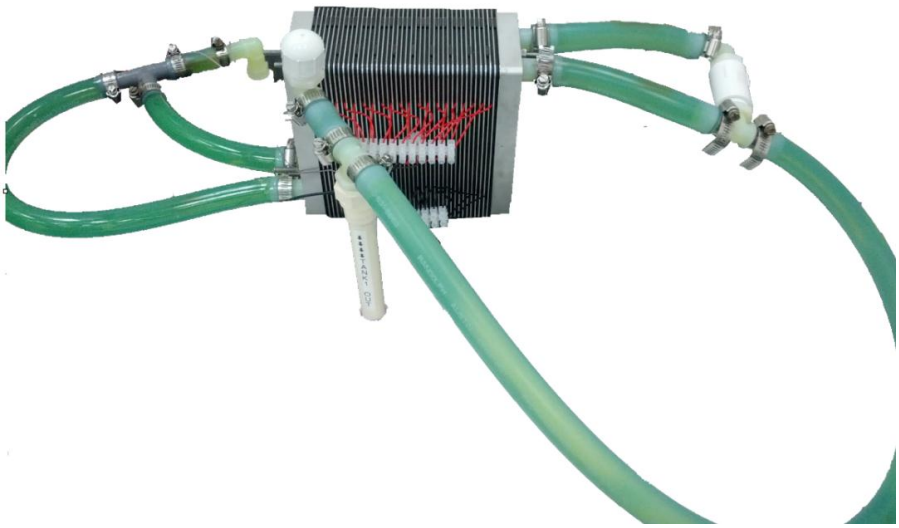

The results from the experiment are shown in Figure G85, indicating that the COP plateaus at 0.9 (there are some thermal losses to ambient) regardless of the inlet liquid temperature. The power to the device decreases with increasing liquid temperature as expected due to the increase in electrical resistivity of the thermoelectric material. The Q_h, thus, also decreases in proportion resulting in a constant COP.

Figure G85: Shared Liquid Loop Results

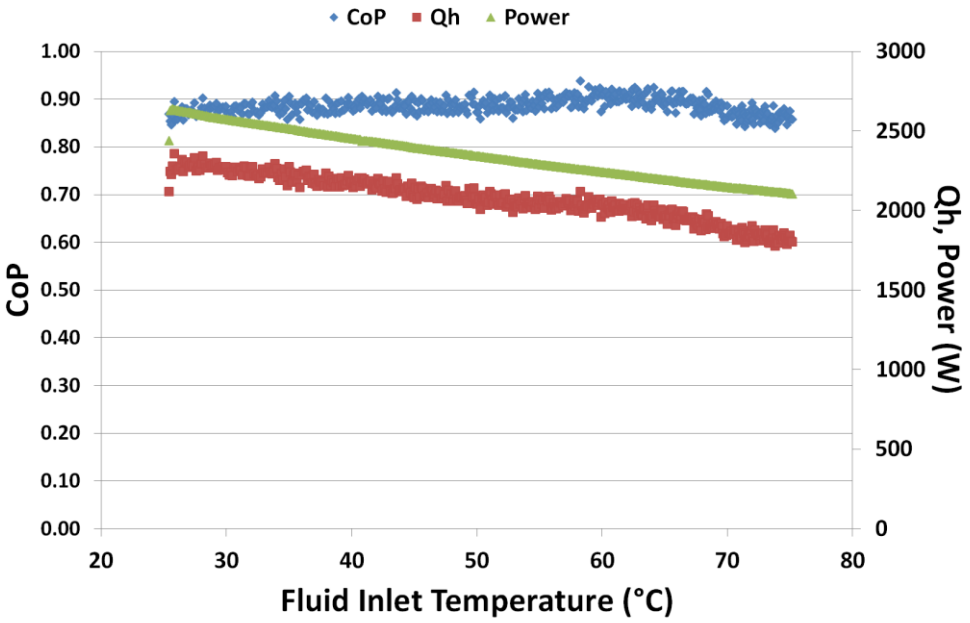

Based on these results, we believe the heat exchanger could be designed in such a way to always perform *at least as well* as a conventional resistive heater. However, to do so would require additional plumbing components capable of redirecting the various liquid loops at the appropriate time based on the temperature difference between the loops.

G4.2.3 TE components in the Chevrolet Volt

Like the Buick Lacrosse vehicle, it was decided by the team that that the contents of the Chevrolet Volt vehicle shall include front chest-face and lap-foot TE cooling and heating. To that end the TED module designs that were implemented and tested in Buick Lacrosse, we adapted and enhanced for the Volt vehicle. Since the Chevrolet Volt is mostly an electric vehicle, with very little engine waste heat available to the cabin, care was taken to optimize the design of TE module assembly geared more towards the heater mode.

Chest-Face TED Module

Figure G86 shows two large TEDs are packaged for the chest-face assembly. The Volt vehicle does not have a sunroof, which significantly simplified the duct routing in the roof liner. Compared to Buick Lacrosse, the total duct length in Volt is little shorter. In addition, the flow path from the fan in the rear to the chest-face nozzles is straight. This will reduce the duct pressure drop measurably, allowing the TED fan to run a lower duty cycle at the desired airflow rate, thus lowering the noise.

The purge valve is designed with slightly longer maximum throw than the previous design. The space in the roof liner allowed this to be packaged. This should enable better circulation in the roof cavity during the initial transients after full solar soak. The actual valve throw for the TE assembly will be calibrated in the vehicle.

The main packaging issue encountered for chest-face TE module is routing the duct and TE underneath the vehicle fame as shown below in Figure G87. The clearance underneath the frame is very small. Putting the TED module underneath the frame helps mounting, as the TEs are quite heavy and facilitates coolant routing from the sides. The downside is potential for parasitic heat conduction /loss through the frame. An insulating layer of felt (1.5mm thick) wrapping the TE and the ducts are designed in to reduce the heat loss/gain to the roof. Fans similar to the ones used in the Lacrosse are used in the Volt design. The nozzles are mounted on a bezel that is separately attached to the duct. This allows flexibility to change the nozzles as desired. CFD modeling work is in progress to verify the airflow and pressure drop estimate.

Figure G86: Chest-Face TED Module

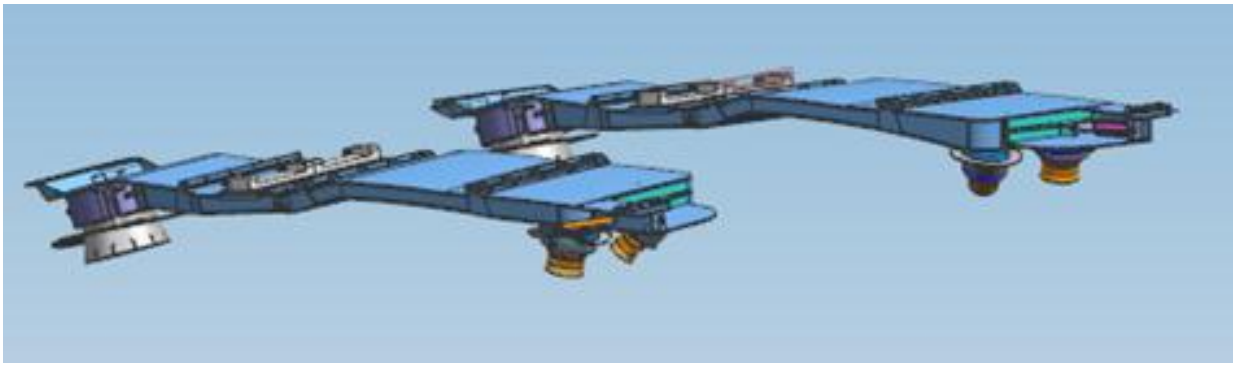

Figure G87: Chest-Face TED Module packaged relative to the frame

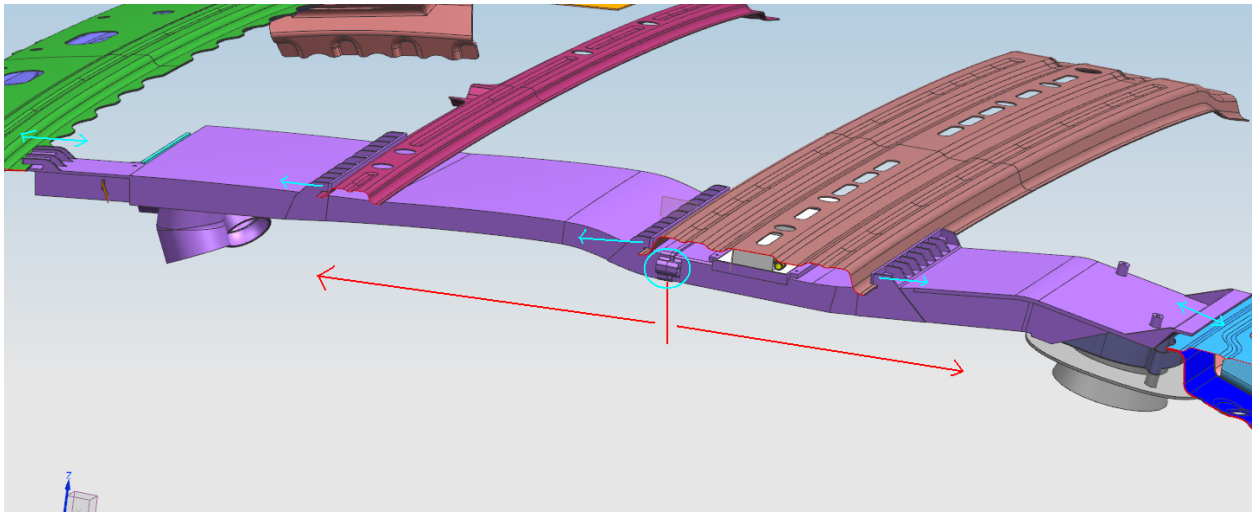

Lap- Foot TED Module

The design for the front lap-foot TE module is similar to Buick Lacrosse. The main difference is the lap-foot module in the Volt will be mechanized with an electrical actuator to switch between lap only and both lap-foot open bi-level configuration. Both the lap-foot modules shall have two large TEDs mounted underneath the foot well. Two new dashboards have been redesigned for Volt to route the ducts from the foot well to the nozzles. Designing a new part for the glove box with all the current mounting constraints proved to be a considerable challenge. Because the Volt is an electrical vehicle with very little parasitic heat from the engine compartment, the foot nozzles have been made wider than the Lacrosse. This should allow more flow to the foot in heating mode to achieve occupant comfort. Figure G88 shows the TE assembly for the driver and passenger side, respectively. Figure G89 shows the airflow path. A medium powered NIDEC fan is planned for airflow.

Figure G88: Driver (Left) and Passenger (Right) front Lap-Foot TE assembly

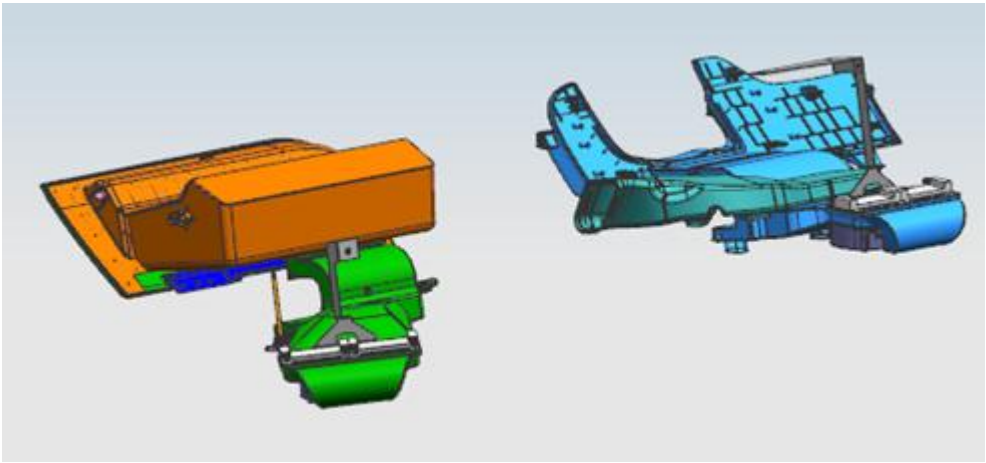

Figure G89: Lap-Foot TE airflow path nozzles in the Instrument Panel

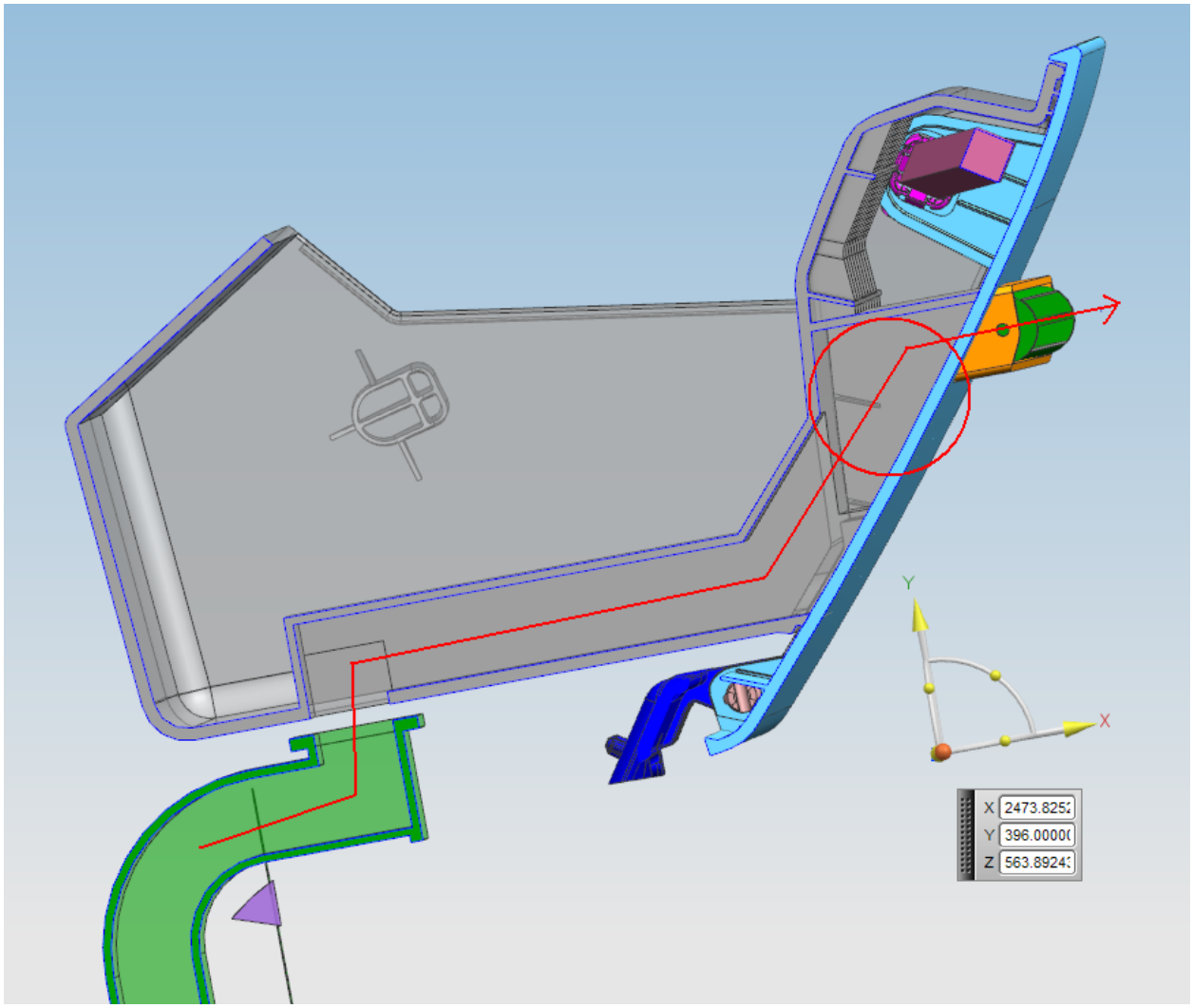

Contact TE driver and front passenger seats

Plume Air Delivery System to the Front Seats

Both front seats are equipped with plume air delivery system. The air supply comes from the conditioned air from the main HVAC source. To effectively manage the air supply, booster fans were selected and fitted into the available space under the IP. Two booster fans are installed under the center IP area to draw the conditioned air from the main source. Figure G90 shows the two booster fans, one for each seat. Flexible ducts are connected to the booster fans and run under the carpet, along the center console of the vehicle. The endpoint of the flexible duct is under the front of the seat for hookup to the plume air intake. Figure G91 shows the flexible duct for the passenger seat. The same connection is for the driver seat. A schematic of the plume air is shown in Figure G92, where air is exiting from both sides of the bolster through vents and openings under the headrest. Figure G93

also shows the plume air delivery in more details. During the cold and warm air delivery, there are differences between the twos for the air coming out of under the headrest. For the cold operation, the cold air is routed toward the two ends of the slot nozzles so the air can come down through the shoulders. For warm air delivery, the nozzles at the two ends are closed and the warm air is exiting through the center opening, which is proved to be more effective during the heating operation.

Figure G90: The two booster fans for seat plume air supply

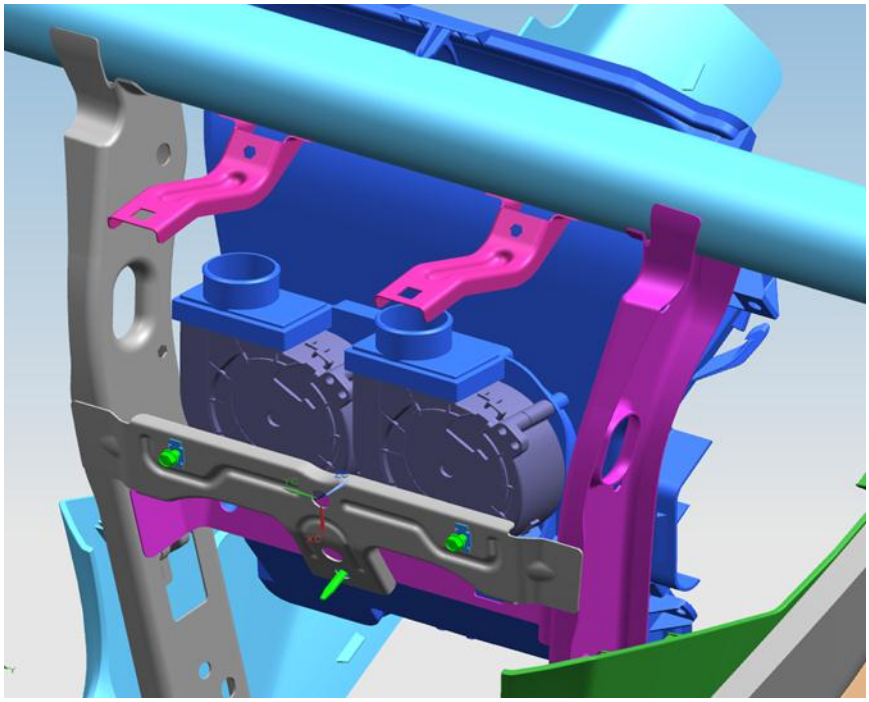

Figure G91: Flexible ducts run under the carpet and along the center console and the endpoint of the duct is under the front of the seats for plume air hookup

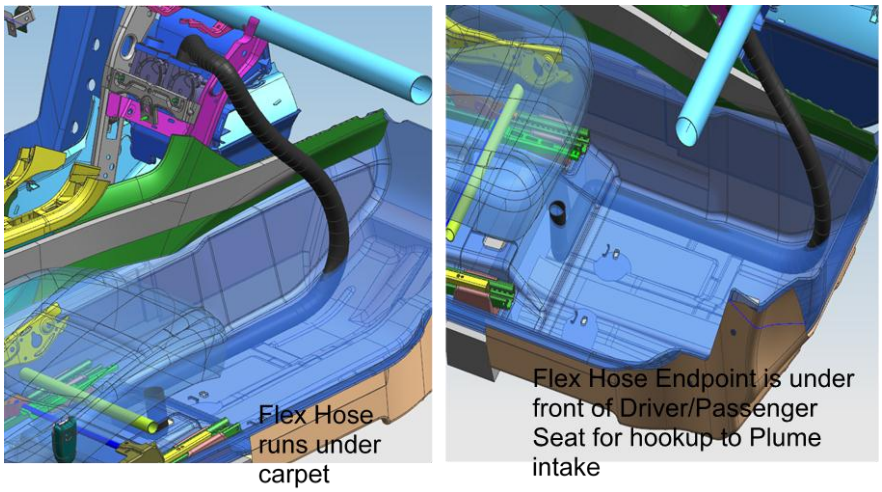

Figure G92: Schematic of plume air system

Figure G93: Plume air delivery showing both cold and warm air directions

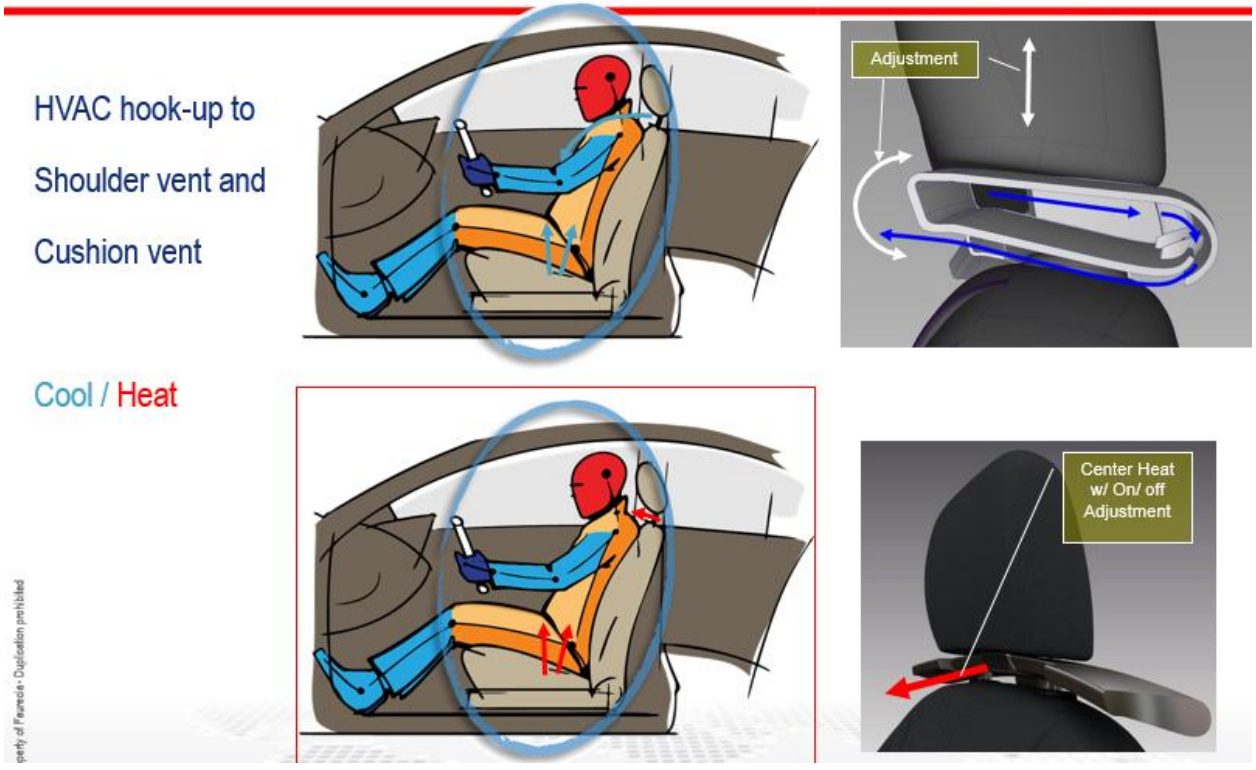

For the Volt demonstration vehicle, a contact-based TE design is used for the seats. This is different from the more conventional ventilation-based TE design. In the ventilation TE design, air is blown across the TE surface (hot or cold) and exchanges heat with the TE before exiting through the vents. In the contact TE design, the TE surface (hot or cold) is in direct contact with the human body to improve the effectiveness of the heat transfer and to speed attainment of the hot/cold sensation and comfort. It is even more important to use contact TE design in seating components since a large portion of human body is in contact with the seating surface and the majority of the contact body surfaces are closer to the core region of human body. The prototype contact TE seat performance was evaluated in a thermal chamber prior to the installation into the Volt. Figure G94 shows GM engineers evaluating the seat performance in the thermal chamber. Figure G95 shows time for "time to sensation" (TTS) and "time to comfort" (TTC). The TTS and TTC were counted from the initial soak condition at 50 C to the time of the 1st sensible cool sensation and the time to feel comfort. It demonstrates the contact TE seat is twice faster to reach both TTS and TTC than the ventilated TE seat and three times quicker to reach TTS than the ventilation seat.

Figure G94: TTS and TTC evaluation in the thermal chamber

Figure G95: Comparison of the TTS and TTC of the contact TE seat to the ventilated TE and vent seats

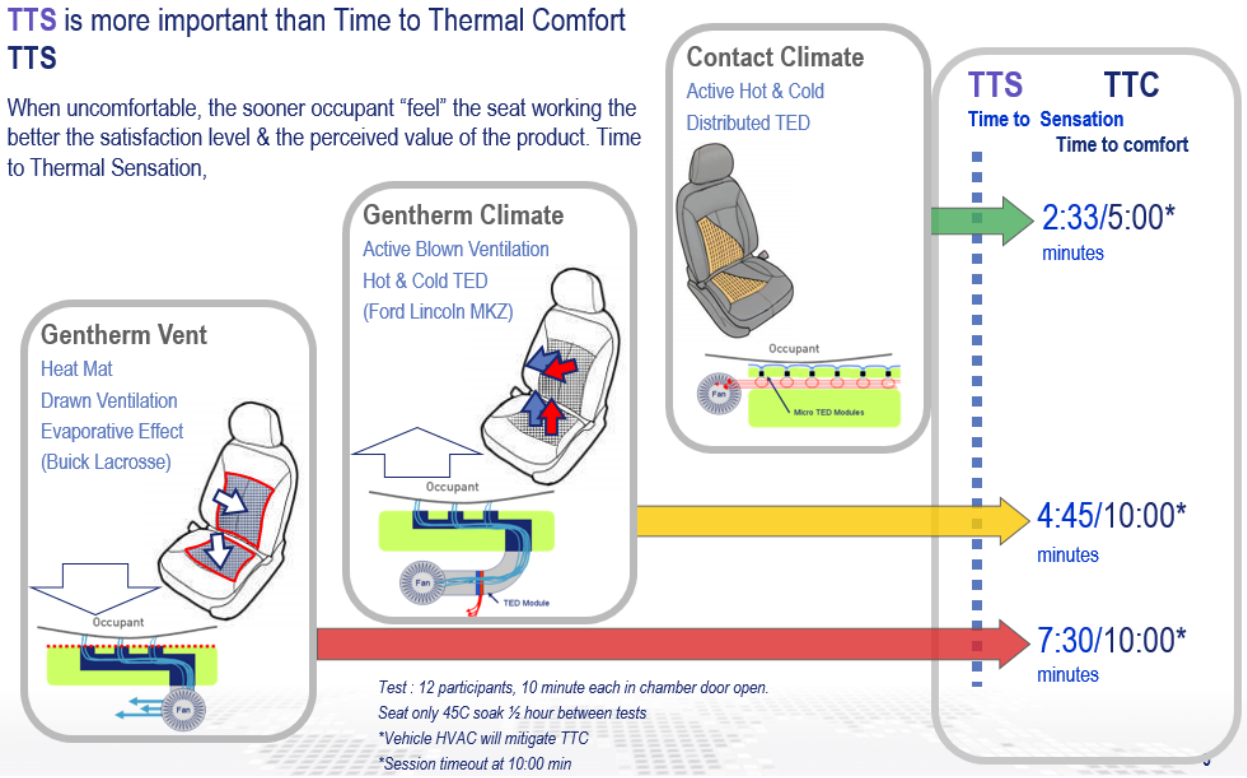

G4.3 Task 16 – Produce Packaging- and Function-Intent Final Components

G4.3.1 Final component assembly in the Buick Lacrosse

The final TE assembly installed in the Buick Lacrosse is shown in Figure G96. Figure G96 (a), (b) and (c) show the lap TE nozzle for the front passenger, Chest-Face nozzle for the driver and TE nozzle off the back of the front seat for the rear seat passengers, respectively. Figure G96 (d) shows the TE control box and data logger in the Buick trunk and Figure G96 (e) reveals the plume air outlet on the inboard side of the driver seat. The TE HMI control panels for the front and rear seats are shown in the Figure G96 (f) and (g) respectively.

Figure G96: Final TE assembly in the Buick Lacrosse vehicle

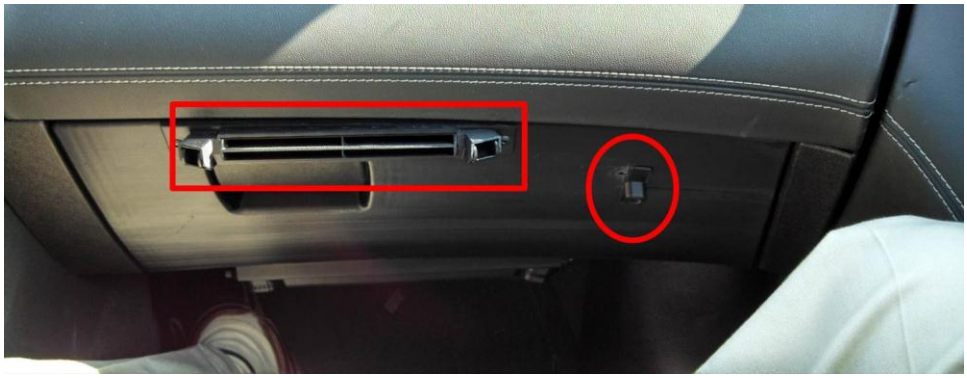

(a) Lap TE slot nozzle on the front passenger side

(b) Chest-Face TE nozzles on the driver side

(c) TE nozzle off the back of the front seat for the rear passenger

Figure G96: Final TE assembly in the Buick Lacrosse vehicle (cont'd)

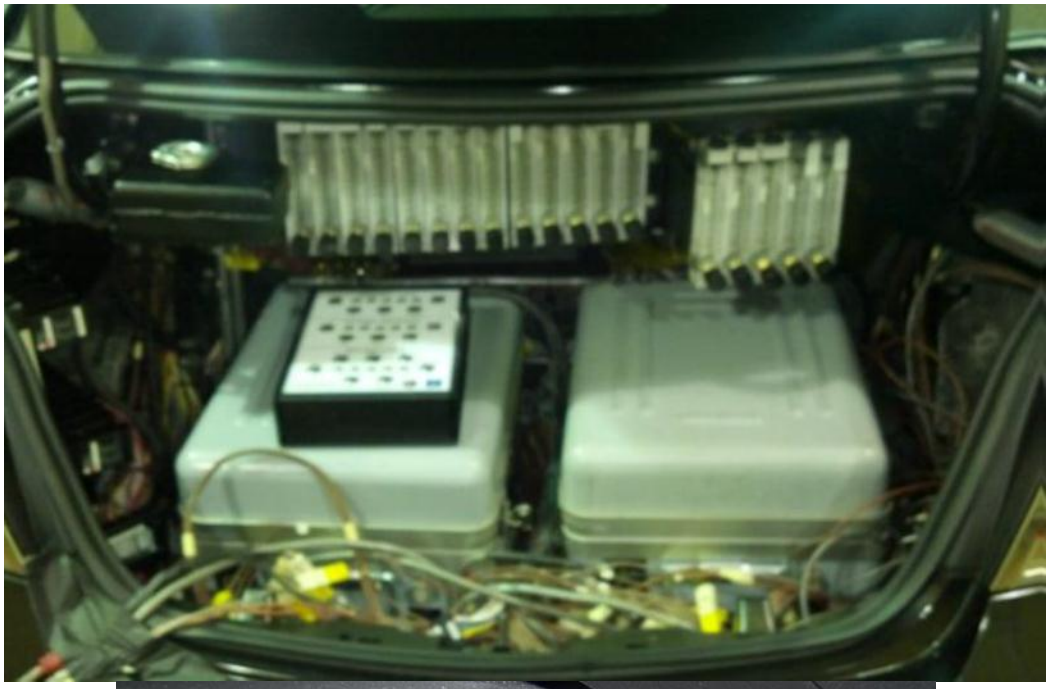

(d) Data logger and TE control in the trunk
(e) Plume air outlet on the inboard side of the driver seat

Figure G96: Final TE assembly in the Buick Lacrosse vehicle (cont'd)

(f) TE HMI control panel for the front passengers
(g) TE HMI control panel for the rear passengers.

G4.3.2 Final component assembly in the Chevrolet Volt

Vehicle Build, Data Logging, Control Hardware, and Software Development

Instrumentation connection to Campbell CR9000X was initiated and completed. More than 100 signals from all the sensors installed in the test vehicle, including thermocouples, pressure sensors, flow meters, current sensors, etc., were connected to the data logger to monitor and record the status of vehicle system operation, including the A/C system and the TE system. Software programming of the data logger was required to acquire data from the sensors and broadcast the data over a CAN bus so that the VehicleSpy software could collate the data from the vehicle CAN bus and Campbell CAN bus for data logging with a uniform time stamp. Figure G97 shows the data logger and TE Controller Unit in the trunk of the Chevrolet Volt. With a great design in consolidating all the wires and cables into three prefabricated boxes, the TE controller and data logger in the trunk of the Chevrolet Volt are very compact and well organized for easy access during debugging and vehicle testing.

Figure G97: TE Controller Unit and CR9000X Data Logger Located in Volt Trunk

Assembled Chest/Face, Lap/Foot TE Nozzles, Contact TE seats and HMI

The final TE HVAC components installed in the Volt are shown in Figure G98. The TE nozzles installed on the roof liner for the chest and face and the nozzles on the lower IP and in the foot well are similar to the ones in the Lacrosse and were carried over to the Volt. Also shown in Figure G98 is the TE control panel on the center console.

Figure G98: TE components installed in the Volt and the TE HMI control panels

(a). Chest-Face nozzle, (b) TE seats, (c) Front passenger lap slot nozzle

Figure G98: TE components installed in the Volt and the TE HMI control panels (cont'd)

(d) TE HMI control for Chest-Face nozzles, (e) TE HMI control for front seats

G4.4 Task 17 – Test and Evaluate Final Comfort Components

Lacrosse Tunnel Test

The objective was to complete the high ambient temperature (70F and higher) spot cooling calibration and possibly further refine lower ambient (70F and lower) TE system calibration. Software development activities continued in the areas of solar driven restart of the compressor and dew point driven restart of the compressor. Software with difference scaling for the solar sensor was implemented and tested. New dew point calibration was further tested to ensure

functionality. Calibration testing was conducted from 70F and stepped up through 85F, 90F, and 100F. Initial testing did not focus on the performance at ambient temperatures of 75F and 80F due to the perceived importance of 70F and 85F. 70F ambient is the last key ambient that the compressor may still be shut down and maintain comfort. An ambient of 85F is recognized as a key design point for the TE HVAC system due to its moderate but high use heating load. 95Fx50%RHx500W is a normal testing point for the TE HVAC system development. 95Fx40%RHx850W was used to simulate SC03 test conditions. 100Fx40%RHx850+W Side Bank Solar is used to simulate high load testing condition. The following conditions were used in the tunnel test.

<u>High Ambient Calibration Testing Conditions:</u>

- 70Fx70%RHx300W, Set Point = 72F
- 85Fx55%RHx500W, Set Point = 72F
- 90Fx50%RHx500W, Set Point = 72F
- 95Fx40%RHx850W, Set Point = 72F
- 100Fx40%RHx850W+SideBank Set Point = 72F

For each of the testing conditions listed above, the TE HVAC operation parameters were initially calibrated and then optimized to provide cooling comfort that matches the comfort provided by the baseline automatic climate control system under the nominal set point of 72F.

Under the high ambient of "100Fx40%RHx850w+SideBank", it was found that TE system capacity was strained in providing spot cooling. Improvement was made to the TE coolant loop by relocating the Low Temperature Radiator for better exposure to the front end airflow in front of the condenser heat exchanger. The TE HVAC system performance was improved for all TE locations due to the better coolant temperature; however, the Chest/Face TE module still struggles due to the high temperature and high solar exposure under the roofline.

Subsequent to the higher ambient calibration tests, additional moderate ambient points were tested and the calibrations refined for TE HVAC system performance improvement. These included the ambient temperature of 75F and 80F that was initially ignored during the higher ambient testing:

- 80Fx60%RHx500w Set Point = 72F
- 75Fx65%RHx400w Set Point = 72F

With the moderate ambient temperatures testing completed, effort was further refocused on the compressor shutdown testing for the mid-ambient conditions:

- 70Fx70%RHx300w (compressor OFF) Set Point = 72F
- 65Fx75%RHx300w (compressor OFF) Set Point = 72F
- 60Fx80%RHx300w (compressor OFF) Set Point = 72F
- 55Fx85%RHx150w (compressor OFF) Set Point = 72F

Low Ambient Spot Heating Confirmation Testing

Spot heating was last developed and validated during the Lake Placid road trip. However, due to the timing of the road trip in late spring (April 29th), the lowest temperature during testing was about 35F. Prior to the Lake Placid road trip, spot heating development in the tunnel was also limited to around 35F because of brine tunnel equipment malfunction. Thus it was beneficial to validate for the lower ambient once the tunnel regained the low temperature capability. The semi-auto Warm button was used to run spot heating under selected ambient temperatures, as is listed below. Two sweeps were made. In the first sweep, as the ambient temperature was reduced through the steps of 50F, 35F, and 15F, the set point on the modified silver box was set to 68F. On the second sweep as the ambient temperature was raised through the steps of 15F, 35F, and 50F, the set point on the modified silver box was at 67F, in order to understand if further cabin cooling was acceptable. Comfort riders were used to evaluate the comfort in the vehicle. In general, it was found that spot heating with silver box at 68F provided comfort that was slightly warm, while at 67F, some people found it slightly cool.

Spot Heating with Modified Silver-box:

- 50Fx90%RHx0w — Set Point = 68F
- 35Fx0w — Set Point = 68F
- 15Fx0w — Set Point = 68F
- 15Fx0w — Set Point = 67F
- 35Fx0w — Set Point = 67F
- 50Fx90%RHx0w — Set Point = 67F

Transient Comfort during Soak and Cool down under High Ambient

Transient comfort rides were conducted to assess the performance of the TE HVAC system under the high ambient condition of 100°Fx40%x1000W/m^2. The vehicle was soaked for 60 minutes to achieve an in-car temperature of 150°F before comfort riders were preconditioned in the tunnel environment for 5 minutes and allowed to enter the car. The standard UC Berkeley comfort rating software was used which was programmed for a ride period of 20 minutes. As soon as the first 20-minute period was completed, the software was reset to initiate a second 20 minute period of survey. Upon the completion of the second 20-minute ride period, the riders exited the car and waited for the car to re-stabilize the in-car thermal conditions. Once the car achieved steady-state condition, the riders were pre-soaked in the tunnel and entered the car for a third ride. The comfort data for all three rides were collected and presented herein as a time history of Thermal Comfort Sensation and Thermal Comfort ratings. Due to the software reset and re-entry into the vehicle, the curves showed some discontinuity for some riders.
For the transient evaluation, *the lower blower curve was consistently chosen for both the baseline system and the TE HVAC system rides*. The intent was to understand whether the standard

blower curve for the TE HVAC system was absolutely necessary as was used during the prior steady-state comfort studies. Due to the lowered airflow for the transient TE HVAC system test, it was expected that there might be a slight deterioration of comfort.

Figure G99 shows the whole body Thermal Sensation ratings for the driver from the baseline ride and the TE HVAC system ride. In general, there was good agreement between the baseline and the TE HVAC system Thermal Sensation ratings. On closer examination, it appears that TE HVAC system achieved slightly faster in-car temperature reduction in the driver's microenvironment than the baseline system. In the last part of the ride after 25 minutes, the baseline system seems to support a slightly lower Thermal Sensation. The difference, however, is not significant.

Figure G99: Transient Thermal Sensation History under High Ambient for Drive

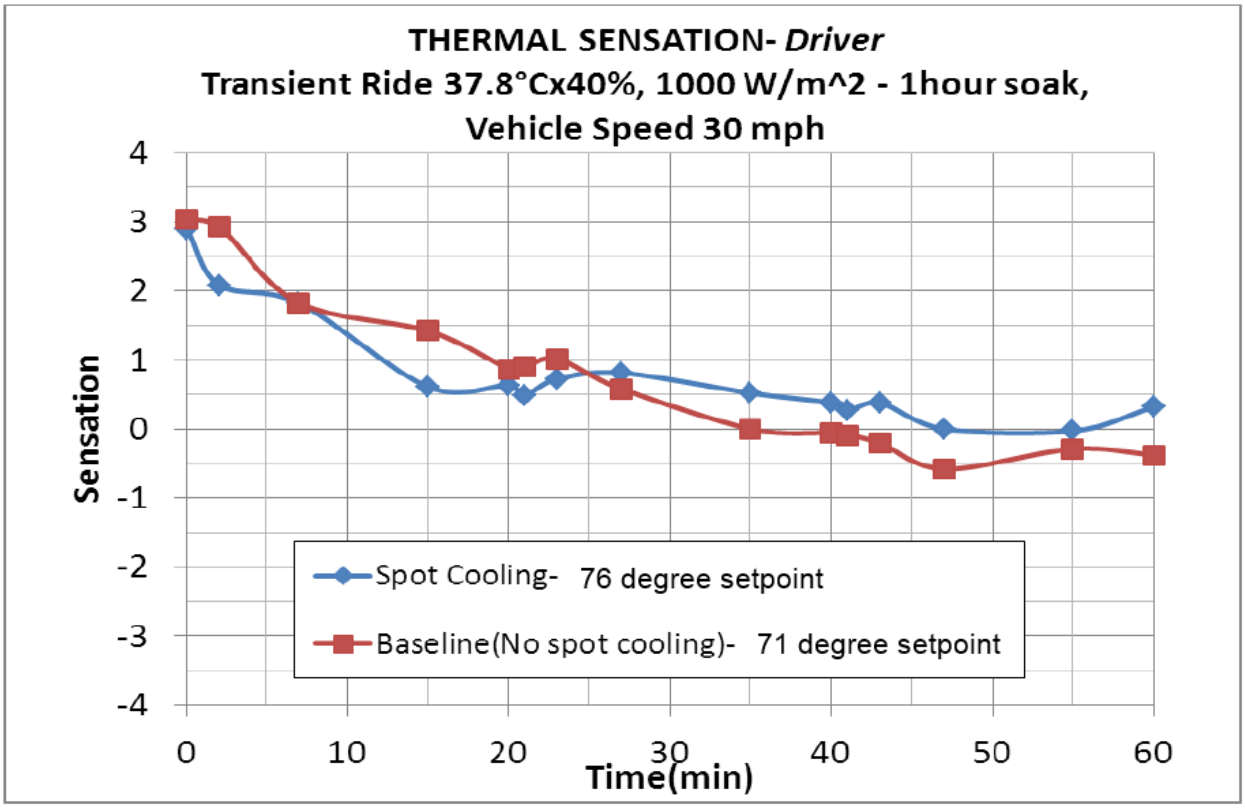

Figure G100 shows the whole body Thermal Comfort ratings for the driver from the same rides. There is confirmation that the TE HVAC system achieved slightly faster Thermal Comfort during the initial transient. However, for the steady-state region, identical Thermal Comfort ratings were recorded. Overall, it is believed that *equivalent* comfort was achieved for the driver with the TE HVAC system.

Figure G100: Transient Thermal Comfort History under High Ambient for Driver

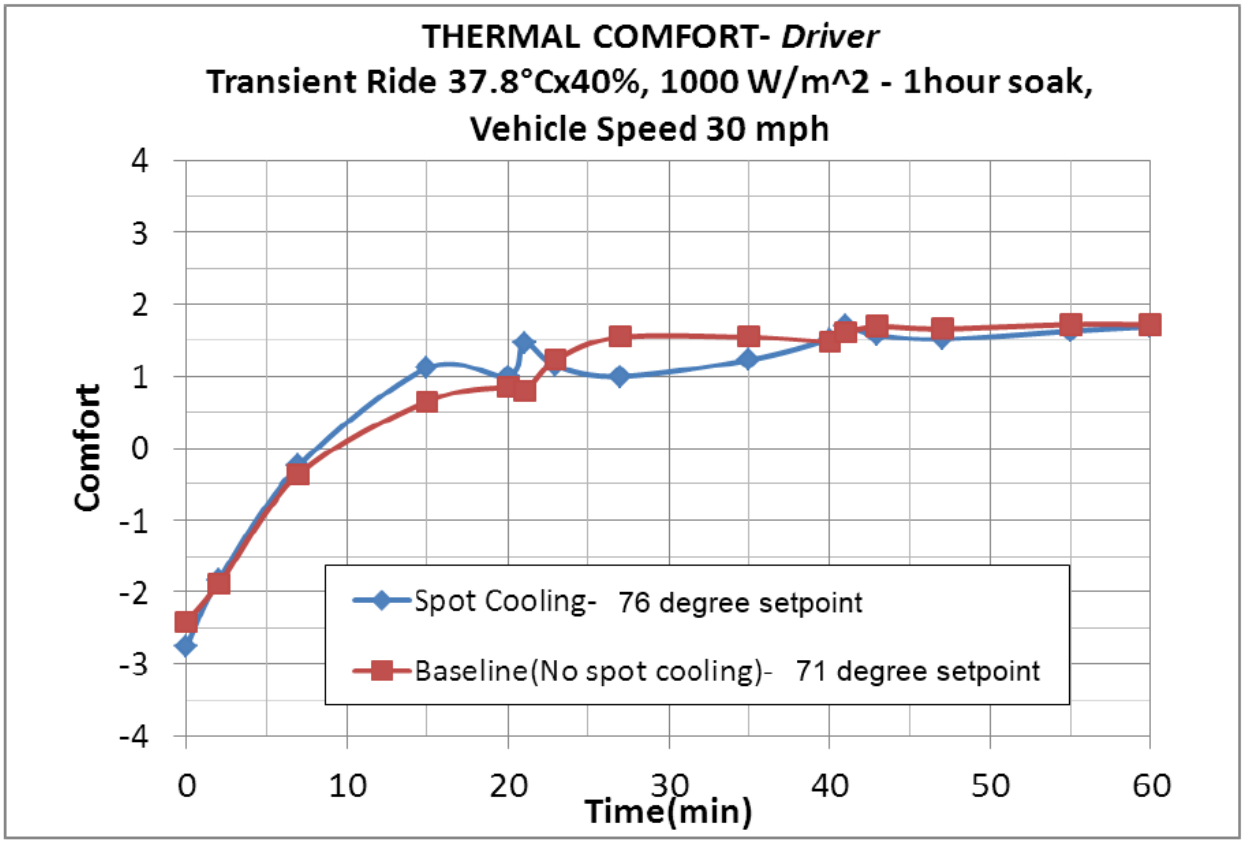

Figure G101 and Figure G102 show the Thermal Sensation and Thermal Comfort ratings for the rear left passenger, who is a 90-percentile rider by height. The Thermal Sensation rating is consistently rated warmer than the baseline, and his Thermal Comfort ratings confirmed the disparity. The rear seat microenvironment formed by the TE seat and the Chest/Face TE module was later recognized to accommodate mid to small statured riders better than tall riders. The face and head area of a tall rider was near the roofline and was more exposed to the radiation from the headliner. Additionally, there was heat radiation from the trunk toward the back neck that was generated by the eAssist battery, causing a taller person to be less comfortable. Under the standard blower curve, both of these issues became mitigated.

Figure G101: Transient Thermal Sensation History under High Ambient for Rear Left Passenger

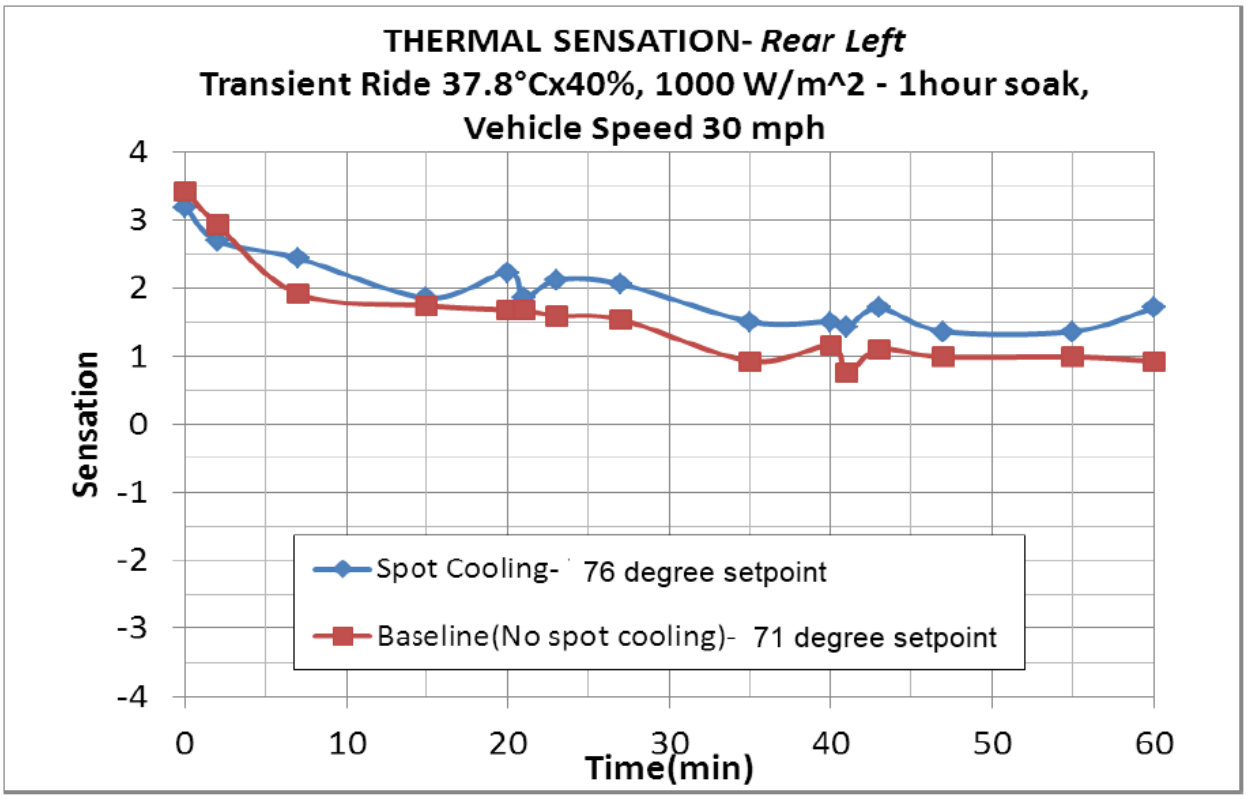

Figure G102: Transient Thermal Comfort History under High Ambient for Rear Right

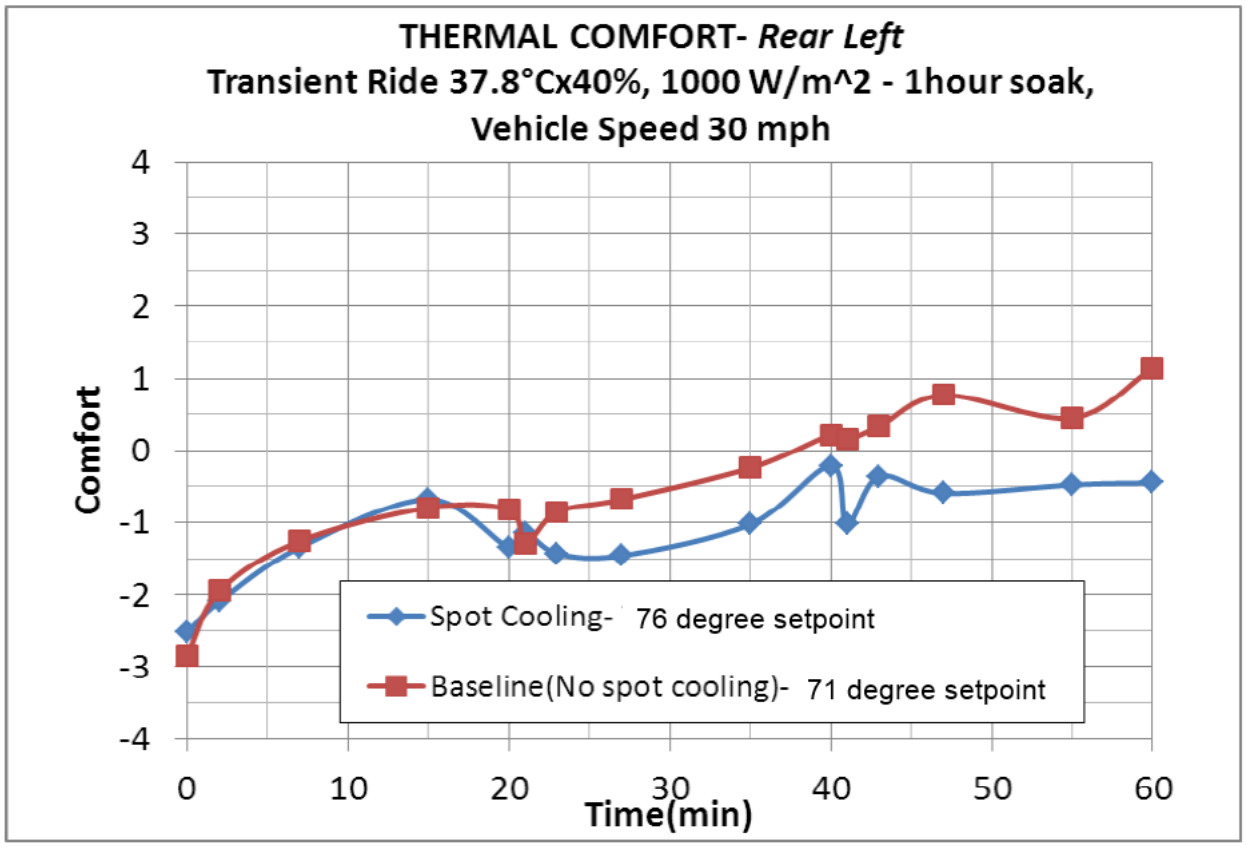

Figure G103 and Figure G104 show ratings for the rear right passenger. The rear right seat was occupied by a shorter person who was less exposed to the heating and radiation from the upper space in the rear cabin. Overall, the rear right passenger perceived equivalent or better comfort than the baseline system. In fact, for the baseline ride, the right rear passenger complained regarding the gradual warming-up of the seat contact surfaces that was subsequently mitigated during the TE HVAC system ride.

Figure G103: Transient Thermal Sensation History under High Ambient for Rear Right Passenger

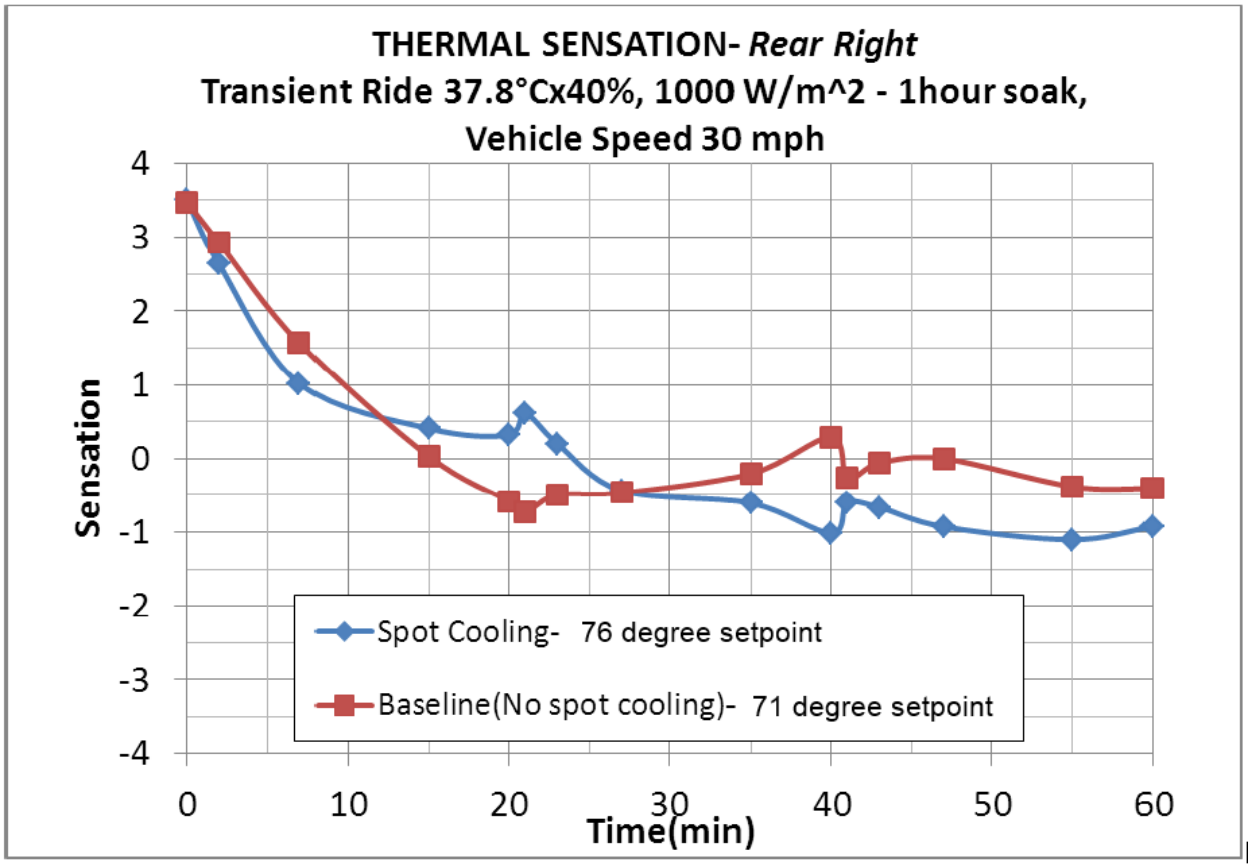

Figure G104: Transient Thermal Comfort History under High Ambient for Rear Right Passenger

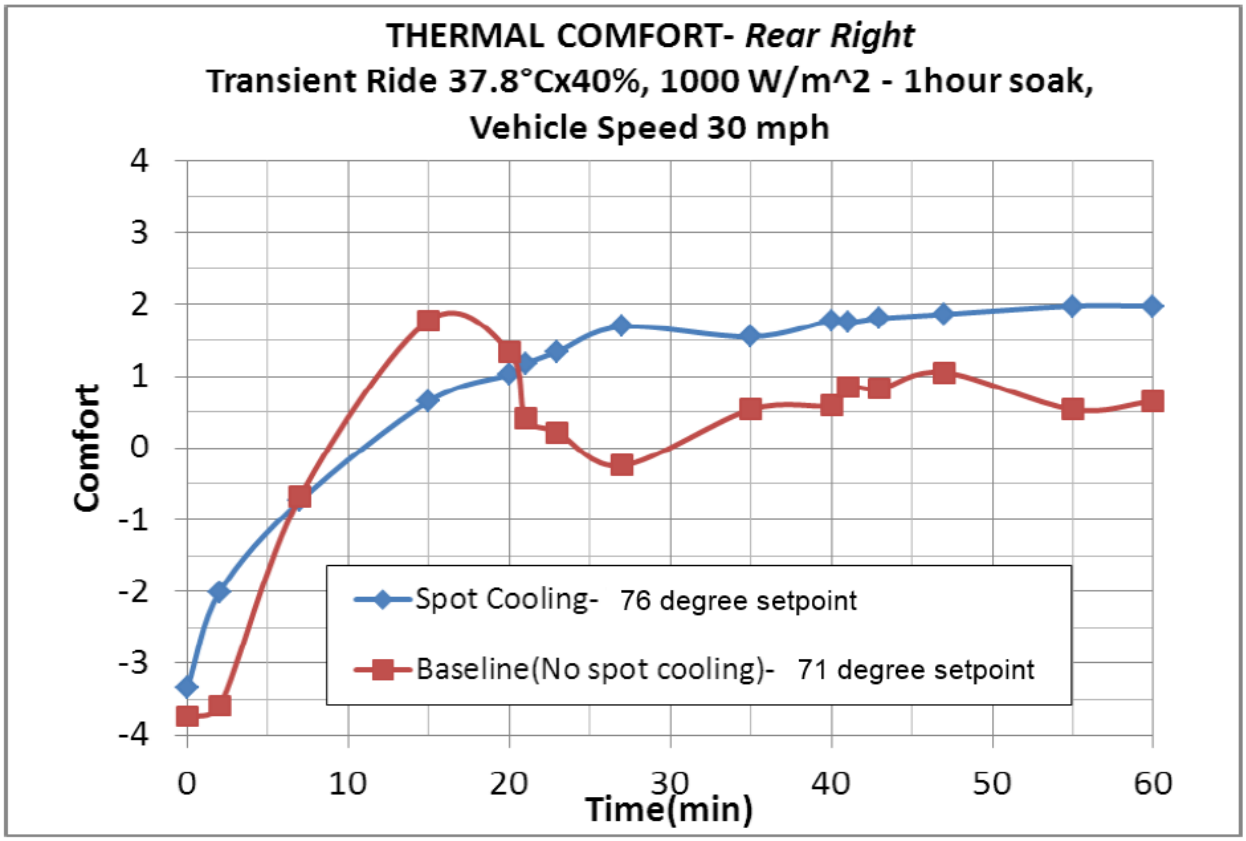

Buick Lacrosse road trip evaluation

Upon the completion of the tunnel tests, Lockport local development trips were taken to expose the TE HVAC system to real world road conditions. This is especially important for response to solar and humidity changes. Due to light spectrum differences, the vehicle solar sensor reading in the tunnel can be significantly different from the real world. Therefore, the calibrations to respond to solar heating by restarting the compressor must be updated and validated through road testing. Similarly, tunnel testing may not be 100% accurate in providing a calibration that can ensure fog free and condensate free operation for the TE HVAC system. Through repeated road trips in the vicinity of Lockport, solar calibration was initially significantly changed but gradually stabilized as more experience was gained. Similarly, calibration for dew point control by restarting the compressor was refreshed through these road trips.

Cold weather road trip:

A joint road trip testing was undertaken to evaluate the performance of the TE-Assisted HVAC system outside the tunnel in real life. The road trip crew of eight engineers from both GM and Delphi were participated. Four vehicles were used in the road trip: the TE-Assist HVAC System development vehicle 2012 Lacrosse; a baseline production Lacrosse of the same model year for comfort comparison; a 2013 Chevrolet Volt targeted for DOE TE HVAC System development and needing mileage for powertrain stabilization; and a pickup truck for road trip

logistics and repair support. The destination was Lake Placid, NY where a colder ambient temperature exposure was still possible in the last weeks of spring due to the higher elevation of Adirondack region. The location was identified after an extensive survey as the nearby areas with lower temperatures. The trip was concluded on May 1st 2013, accomplishing the major objectives of the trip. The ambient temperature range of 35F during early morning hours to 75F in the early afternoon. The performance of the TE-Assisted HVAC system for spot heating was evaluated in sufficient detail. A preliminary spot cooling calibration was devised and tested on the road in the higher ambient temperature conditions. The team was satisfied that the TE HVAC system performed well to provide passenger comfort by spot heating in the cooler ambient and spot cooling in the higher ambient experienced during the road trip. Given the vast amount of work done to arrive at a working TE HVAC system suitable for road testing, the team was quite satisfied. The real life driving experience with the TE system provides a few final adjustments in software control for optimal thermal comfort. Overall, the TE-assisted HVAC system performed well for spot heating. The rear seat TE nozzle design has good performance. Here are a few main comments as a result of the road trip.

1. Need a coolant ramped start. Before the coolant is warmed up to above 25C, the TE system cannot provide 35C plus spot heating air stream temperature. Cold air discharge from the TE system was perceived to be uncomfortable. The TE fan speed needs to be ramped from zero to a full steady-state speed according to the coolant temperature circulating through the TE devices.
2. Semi-Auto TE spot heating or cooling needs functionality change. Warm "Button" (LED location) needs to add cool setting calibrations to provide cooling at high ambient; Cool "Button" (LED location) needs to have warm setting calibrations. Two "buttons" will run on different power curves. The Warm “Button” will have a higher TE power curve (more heating for low ambient, low cooling for high ambient), and the Cool “Button” will have a lower TE power curve (lower heating power for low ambient, and high cooling power for high ambient).
3. Front face nozzles need improvement. Roof mounted nozzles for the front passengers can contact the forehead as the passenger enter and leaves the car. Recommendation is to shorten the nozzles and rubberize the nozzle exterior/edge for protection. The nozzle base may also need to be reinforced.
4. Heating comfort for DOE car is generally good for ambient of 35F~55F.
5. Purge valve logic is activated in low ambient and does not time off. Purge is only for high ambient and during a defined time period after ignition.

Hot weather road trip

The GM-Delphi team conducted a road trip evaluation of the DOE TE HVAC System vehicle (Lacrosse) for spot cooling performance in early September 2013. This trip was intended to cover a higher temperature range than the vehicle was previously exposed to during the Lockport evaluation road trip in mid-August. Additionally, some of the corrective actions taken to address the issues identified during the August trip were to be validated during the

present trip. The road trip was at the Baltimore/Washington DC area. The TE Lacrosse plus a baseline production Lacrosse were driven on the road for performance comparison and evaluation. Between Lockport and Washington, DC, the ambient temperature ranged from 75F to 100F. The DC area temperature was mostly in the mid 90's during day time and as high as 100F on some stretches of highway. The TE system calibration established through tunnel testing and the previous road trip worked well in the high ambient temperature range. Overall, the DC trip team was satisfied with the performance and stability of the TE system in Lacrosse. It was generally recognized that the driver seat in the TE equipped vehicle is more comfortable than the baseline production vehicle. The rear seats passenger also reported better comfort due to the TE rear Chest/Face nozzle airflow. The front passenger seat is at least equally comfortable as the baseline. No calibration change was made during the trip.

Volt initial Tunnel Test

The vehicle and the installed TE spot cooling system were operated for the first time in a realistic operating environment. The objective of the first tunnel week was to ensure that various sub-systems functioned as designed. The first to be debugged and validated was the data logging system. Subsequently the sub-systems related to the operation of the TE modules were validated. In the process, it was found that the overhead TE module fans were too powerful and generated too strong of spot cooling streams. The fans were subsequently replaced with low power fans for better control and comfort. The TE system performance & capacity were tested across a range of ambient conditions from 40 to 95°F. In general, the TE system performed similar to the Buick LaCrosse test vehicle, with the exception that the Volt does not have a rear TE system nor a seat ventilation system. The back seat comfort was compromised in higher ambient conditions.

The second climatic tunnel week was conducted from November 2013. Remaining high was the priority of debugging and validating the vehicle TE spot cooling system. Various minor control issues were discovered and resolved. Subsequently, during the remainder of the week, a functional calibration was established for the TE system. There are at least three modes of Volt climate control operation: Comfort mode, where the priority is to provide excellent passenger comfort in the car; Economy mode, where the priority is to provide acceptable comfort at reduced battery power consumption; and finally, Ventilation where the priority is to maximize driving range with minimal comfort. The powertrain also operates in two modes: Battery Only mode and the engine ON mode.

For spot heating test, the focus was placed on calibrating and testing for the Battery Only mode. Spot heating is most relevant to extending the electrical driving range of Volt. In the Eco mode, the Volt CHCM heater is turned on to supply a low temperature coolant sufficient to allow the TE to deliver the discharge temperature required for spot heating. This was required during the tunnel test for low ambient of about 40~50F.

For spot cooling, elevated in-car temperature was achieved through higher ACC set point and the use of a reduced blower curve. During mid-ambient testing, combination of TE spot cooling and HVAC ventilation only was sufficient to provide comfort.

Some key points from the tunnel testing are:

- Ambient temperatures tested ranged from 40F to 95F.
- Lower blower curve always used (80% of nominal)
- Higher ambient of 75-95F: 75F set point was used to generate elevated in-car temperature for spot cooling, except 73F/74F set point was used for the high ambient of 95F.
- Rear seat is not thermally comfortable at higher ambient
- Mid ambient of 50-73F: ACC Auto Fan Only with set point of 72F from 50-60F ambient and set point of 75F for 65-70F ambient
- Low ambient of 40-50F (TE heating): set point of 70F used with Eco mode
- Coolant ramp was calibrated to 25C; below 25C, no TE heat and no TE fan would be available.

G4.4.1 Milestone 10 – Evaluate Final Comfort Components Completed

The overall evaluation of the final comfort component for Lacrosse was completed on September 16, 2013.

G4.5 Task 18 – Estimate Efficiency Improvements

Annualized energy saving for Lacrosse demonstration vehicle

The estimation of TED and TE HVAC system efficiencies for Lacrosse was completed on Oct. 31, 2013. For the "Calculate Efficiency Improvements of Distributed HVAC System Completed" milestone, the team estimated the annualized and car occupancy weighted savings from the TE-assisted HVAC system over the baseline system. The additional energy used by the prototype HVAC system for TE modules, fans, and the coolant pump was also measured. For the TE–equipped Lacrosse demonstration vehicle, the following HVAC system powers are included.

- TE, TE fan, coolant pump, HVAC blower, compressor power are all included.
- Front-end fan power not included, possibly punishing TE car power use.
- Power consumption is calculated for each seating location.
- Three power consumption scenarios were developed based on vehicle occupancy
    - Driver Only
    - Driver + Front Passenger
    - Fully Occupied

These scenarios were applied to the national distribution of temperatures and then weighted based on average vehicle occupancy estimates to create an annualized estimate of HVAC energy savings. Figure G105 shows the HVAC power consumption curves over ambient temperatures ranging from 4 to 38^{0}C (40 to 100^{0}F) for the baseline and TE vehicles with three

occupancy arrangements by the equivalent comfort ACC setting. The ambient conditions with humidity are 4°Cx90%RH, 10°Cx90%RH, 15°Cx80%RH, 21°Cx70%RH, 27°Cx60%RH, 32°Cx50%RH, 38°Cx40%RH. The occupancy arrangements are shown. The TE-equipped Lacrosse demonstration vehicle clearly shows that over the entire ambient condition sweep it consumes less HVAC energy than the baseline vehicle for all occupancy arrangements.

Figure G105: HVAC energy usage with equivalent thermal comfort for Lacrosse vehicle and for three occupancy scenarios in the TE-equipped vehicle under various ambient conditions

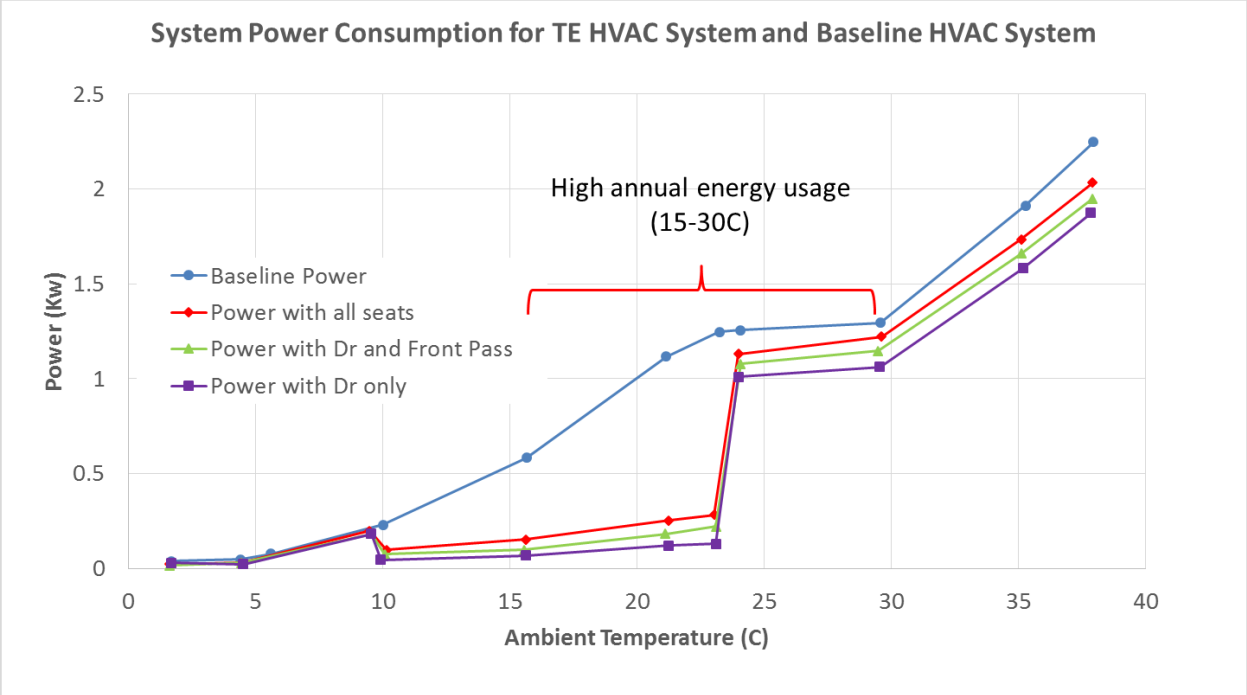

In order to provide an energy savings estimate for all seasons of A/C operation in a single year, the A/C usage data in Figure G106 is used to generate a weighted average of the power use. This weighting was based on the SAE LCCP Ambient-A/C usage. Additional weighting of the power usage data was based on vehicle occupancy. Figure G107 shows the data based on a report submitted by Battelle Memorial Institute for adjusted average vehicle occupancy estimates for national urban freeways. It shows that up to 70% of the time a vehicle was observed to have only one occupant and only 10% of the vehicles travel with 3 or more passengers in the vehicle. For the TE HVAC weighted power usage calculation, the following formula was used:

$$p = \sum_i (\sum_j P_{ij} \ W_a^j) W_o^i$$

where W_a^j represents the ambient weighting (% of occurrence) over a given set of ambient temperatures, W_o^i is the occupancy weightings, and P_{ij} represent the overall system power consumption under a given ambient and occupancy scenario. For ambient temperature between 10 C and 23 C, the compressor is completely shut down and TED alone can maintain

occupant comfort to achieve high energy efficiency except for high solar load and/or high humidity that require compressor to be restarted to ensure comfort and safety. Therefore, the compressor power savings during this ambient temperature needs to be deducted when restarting occurs. Based on one of the analysis by NREL for "Typical Meteorological Year Database V3", 49% Restart Rate for a Climatic Average US City (Topeka, KS, or Philadelphia, PA) is adopted. So in the range of 10C~23C, 51% of compressor shutdown power saving is applied in annualization calculation.

Figure G106: Weighting factors used to calculate annualized energy savings – ambient weighting

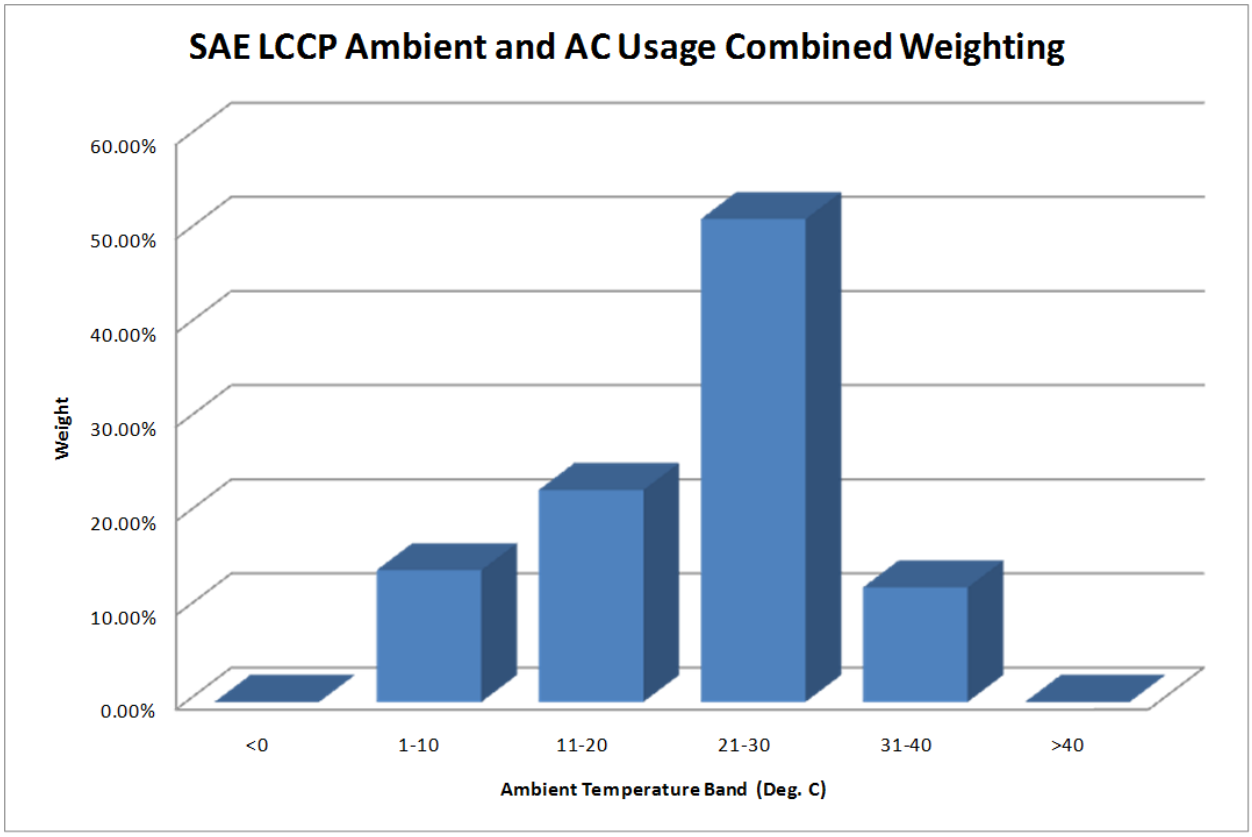

Figure G107: Weighting factors used to calculate annualized energy savings – occupancy weighting

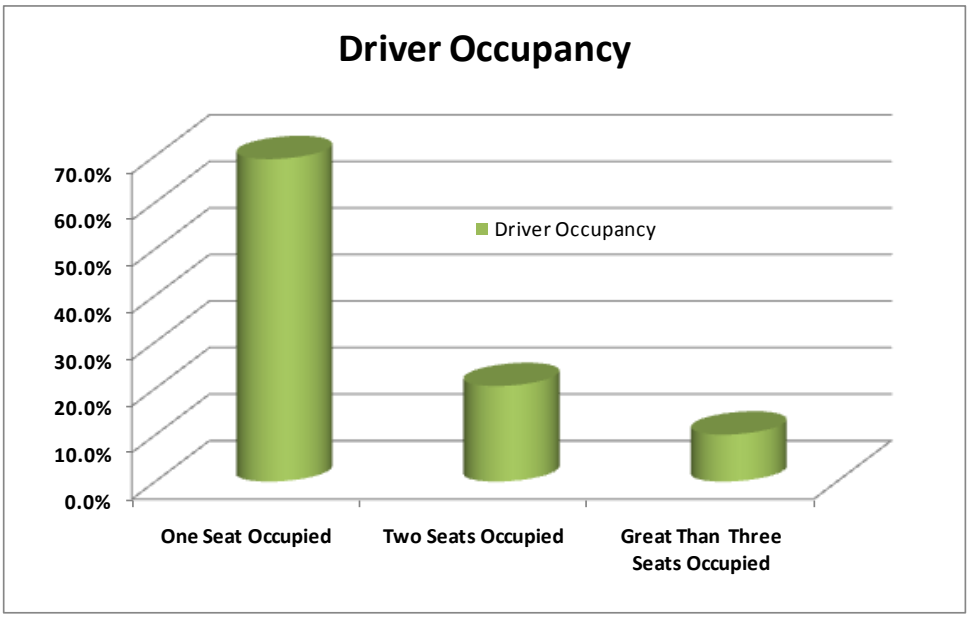

If we ignore synergies between a distributed HVAC system and a hybrid powertrain featuring an engine stop/start function, then the annualized and vehicle occupancy weighted savings for Lacrosse is 30.9%. However, our road tests of the Buick LaCrosse indicated that the engine off time for the hybrid powertrain was extended due to the operation of the distributed HVAC system. In a production vehicle, the engine is shut down when the vehicle is stopped. However, if the temperature within the passenger compartment becomes uncomfortably warm, then the engine is restarted (even though the vehicle is still stopped) in order to operate the air conditioning compressor. In our demonstration vehicle, the distributed HVAC system extends the time that the vehicle occupants are comfortable when the engine is shut down. By extending the engine-stopped duration of the hybrid powertrain, the resulting fuel savings is equivalent to an additional 4% energy savings for the distributed HVAC system.

Coefficient of Performance (COP) of the TE HVAC components for Lacrosse demonstration vehicle

Table G4 shows the Coefficient of Performance (COP) of the prototype TE HVAC components installed in the Buick Lacrosse demonstration vehicle for the cooling and heating operations. For cooling, it clearly shows the COPs > 1.3 except for the seat bottom (with COP = 1.26), and for heating, they all exceeded the required COP of 2.3. Coolant-based waste heat management of the TEDs was essential for meeting the COP requirements. However, coolant-based waste heat management is more complex and costly than simpler (but less efficient) air-based waste heat components. For the minimal TED energy (40 watts per occupant) requirements, which are very modest when compared to the central HVAC system (3000 Watts), the higher COPs of coolant-

based waste heat TEDs do not appear to justify the added cost and complexity for a production application.

Table G4: Coefficient of Performance (COP) for prototype TE HVAC components

	Cooling Requirements			Cooling Actual			
	Airflow	Delta T	COP	Airflow	Delta T	PWM	COP
Chest/Face - 2 Lrg TEDs	13	5	1.3	13	5.1	80%	1.4
Lap/Foot - 1Lgr/1Sm TED's	15	2	1.3	15	5	60%	1.7
Seat-Upper - 1 Lrg TED	4	2	1.3	4	7	60%	1.89
Seat-Lower- 1 Lrg TED	4	2	1.3	4	5.7	60%	1.26
	Heating Requirements			Heating Actual			
	Airflow	Delta T	COP	Airflow	Delta T	PWM	COP
Chest/Face - 2 Lrg TEDs	8	15	2.3	8	15.3	100%	2.5
Lap/Foot - 1 Lrg TED	5	15	2.3	5	14	100%	2.7
Seat-Upper - 1 Lrg TED	5	15	2.3	5	13	100%	2.5
Seat-Lower- 1 Lrg TED	5	15	2.3	5	13.9	100%	2.5

CHAPTER G5:
GM Phase 4 – Engineering Development

The focus of this phase was to integrate the final prototype distributed HVAC components with the production central HVAC system and to optimize the performance of the demonstration vehicles. A final analysis will be made to compare the expected efficiency and fuel economy improvements to the program targets. For this phase of the project, GM will continue to utilize Delphi to integrate most final prototype HVAC components into the demonstration vehicle with Faurecia installing their final prototype seats into the Volt. UCB will support control strategies and tunnel tests while completing their primary Phase 1 activities in parallel with this phase.

G5.1 Task 19 – Project Management and Planning

The planning and coordination for this phase will primarily utilize weekly team meetings. Based on a no-cost time extension, the key deliverables of a Buick Lacrosse demo vehicle will be completed by September 30, 2013, and a Chevrolet Volt demo vehicle by May 30, 2014.

G5.2 Task 20 – Integrate Final Components into Demonstration Vehicles

This activity includes the integration and build of two demonstration vehicles, a Buick Lacrosse and a Chevrolet Volt. This activity also includes the final modifications to the control system in order to deliver a well-integrated solution for distributed heating and cooling.

G5.2.1 Integration and build of mainstream demonstration vehicle (Buick Lacrosse)

The overall evaluation of the final comfort component for Buick Lacrosse was completed on September 16, 2013. See Task 16.

G5.2.2 Integration and build of Chevrolet Volt demonstration vehicle

Unlike the mainstream Buick Lacrosse application, a Chevrolet Volt "mule" vehicle was not built during Phase 2. The assembly TE components for the Volt started at Phase 3 from Delphi installed Chest/Face TE nozzles (in the roof) and Lap/Foot TE nozzles with all required control, TE heat exchangers and data logger retrofitted and improved from the similar ones in Lacrosse. The HMIs for TE operation were also built based on the Lacrosse, not only for the existing Delphi installed TEDs, but also for the later to-be-installed contact TE seats by Faurecia after the Volt was shipped back to GM Warren Tech Center in December 2013. Faurecia installed contact TE seats into the Volt on January 2014. The final integrated Volt demonstration vehicle was then tested at GM's climate wind tunnel for comfort and energy evaluation.

Assembled Chest/Face, Lap/Foot TE Nozzles, Contact TE seats and HMI for the Volt

The final TE HVAC components installed in the Volt are shown in Figure G108. The Chest/Face TE nozzles installed on the roof liner and the Lap/Foot TE nozzles on the lower IP and the foot well area are similar to the ones in the Lacrosse. Also shown in Figure G108 is the TE control panel on the center console. A separate HMI control for the contact TE seats is shown in Figure G108(e).

Figure G108: TE components installed in the Volt and TE HMI control panels

(a) Chest-Face nozzle, (b) TE seats, (c) Front passenger lap slot nozzle

Figure G108: TE components installed in the Volt and TE HMI control panels (cont'd)

(d). TE HMI control for Chest-Face nozzles, (e) TE HMI control for front seats

G5.3 Task 21 – Test and Evaluate Distributed HVAC System in Vehicle

G5.3.1 Test and Evaluate mainstream demonstration vehicle (Buick Lacrosse)

The Buick Lacrosse demonstration vehicle was made available to the California Energy Commission and the US Department of Energy on September 16, 2013. See Task 17 for final test and evaluation of the distributed HVAC system.

G5.3.2 Milestone 12 – Make mainstream demonstration vehicle available to DOE

The Buick Lacrosse demonstration vehicle was made available to the California Energy Commission and the US Department of Energy for their evaluations on September 16, 2013.

G5.3.3 Test and Evaluate Chevrolet Volt demonstration vehicle

Road Test for the Volt

The road tests were conducted in the Southeastern Michigan for 11 days from February 12 to March 14 of 2014. Six human subjects participated during the tests for the ambient temperatures varying between 4F (-15C) and 40F (+4C). Each test started with the vehicle soaking in the open parking space for at least three hours.

There are at least three modes of Volt climate control operation: Comfort mode, where the priority is to provide excellent passenger comfort in the car; Economy mode (Eco mode), where the priority is to provide acceptable comfort at reduced battery power consumption; and finally, Ventilation where the priority is to maximize driving range with minimal comfort. For comfort evaluation for the road test and subsequent tunnel test, the baseline was defined as turning on the main HVAC without TE devices by choosing the comfort mode. The TE Eco mode was turning on all the TE devices and using the Eco mode. The ACC (automatic climate control) control mode was used for both comfort and Eco modes. Figure G109: Transient whole body comfort for the Baseline comfort mode and TE Eco mode shows the transient comfort result for Baseline comfort mode at 74F and TE Eco mode at 72 F. The TE spot heating was very effective in quickly bringing up the whole body thermal comfort index above 0 after 6 minutes, while the baseline took 15 minutes to cross the zero threshold. In general, TE Eco mode at set temperature of 72 F overachieved the baseline comfort. At the end of 60 minutes, the steady-state overall thermal comfort value for the TE Eco mode is 0.7 index higher than the Baseline comfort mode. Figure G110 shows the thermal sensation and thermal comfort at steady state. In the Volt HVAC control system, the Eco mode delivers at 50% of the airflow and the maximum heating power is kept at 50% of the comfort mode to save battery energy. With turning on the TE localized heating devices, the comfort level at steady state is higher than the Baseline, especially for the back, gluteal and the lap, where the TE seat and lap nozzles are very effective in providing the comfort.

Figure G109: Transient whole body comfort for the Baseline comfort mode and TE Eco mode

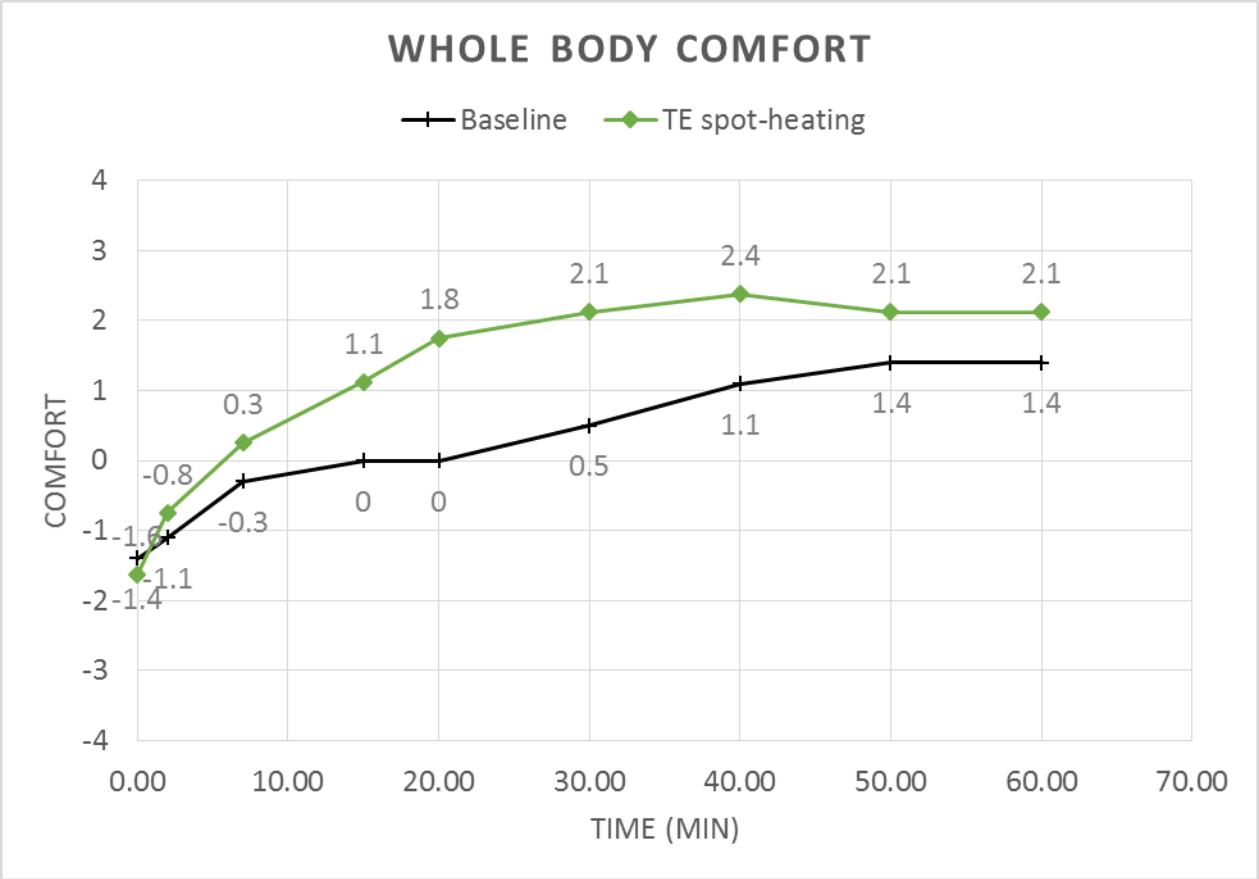

Figure G110: Steady-state whole body sensation and comfort for the Baseline comfort mode (74F) and TE Eco mode (72F)

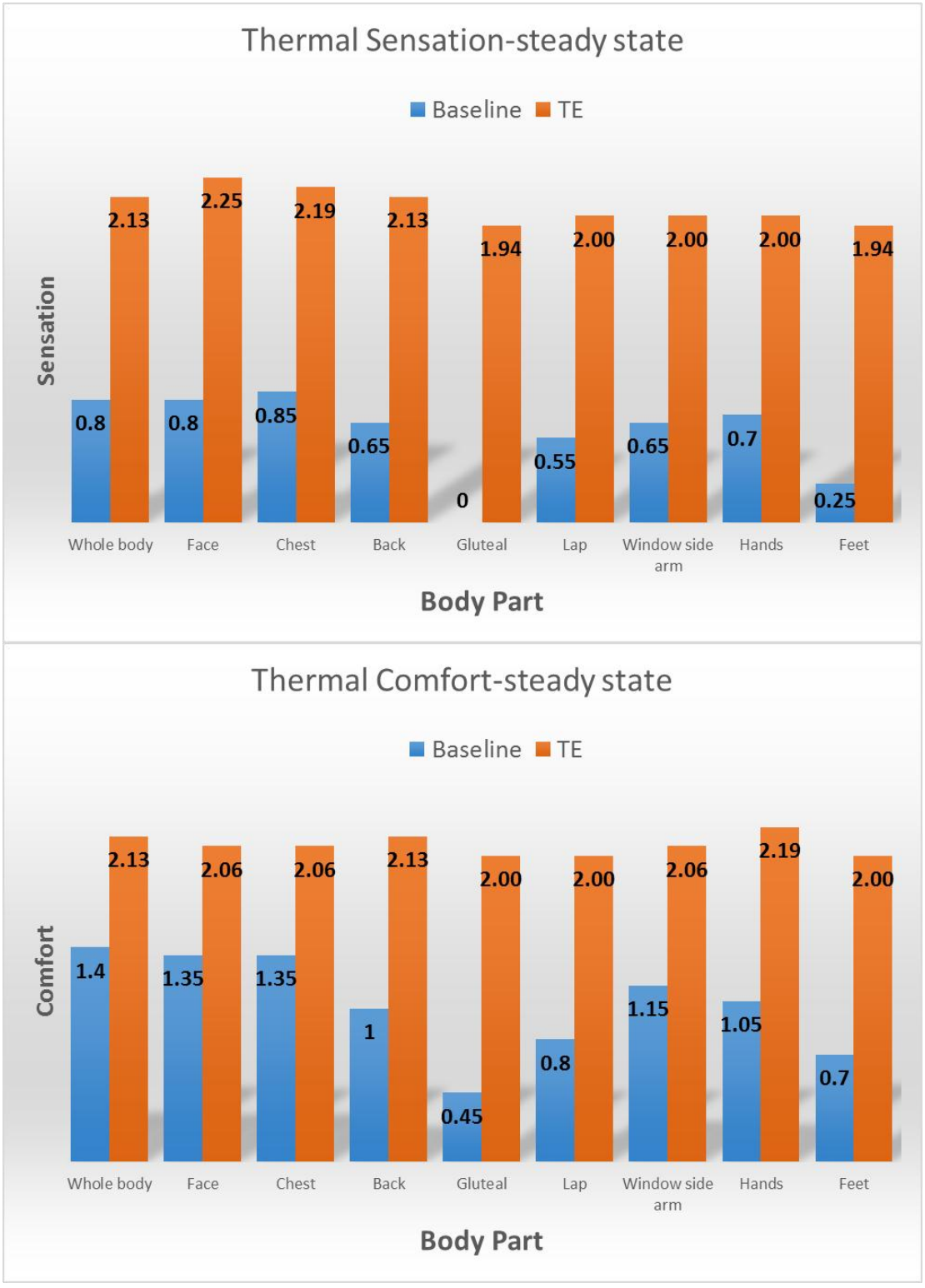

Climate Wind Tunnel Test (CWT) for the Volt

The thermal manikin is an objective evaluation of the thermal comfort by measuring the Equivalent Homogeneous Temperature (EHT) in a well-controlled tunnel environment. The thermal manikin, Monika, provided by the University of California at Berkeley was used in GM's climate wind tunnel to measure the EHT for Baseline and TE modes. Guided by the above-mentioned human subject comfort tests, we were able to experiment several ACC set temperatures for both the Baseline and TE modes to reach an objective EHT. Three ambient conditions were used in the tunnel test throughout the current evaluation. They are -10C x 80% RH, 0C x 80% RH and +10Cx20% RH. The vehicle speed was set at 50 kph. The first tunnel tests were conducted at February 27 and 28 with two complete shifts (16 hours) each day. The second tunnel tests were scheduled at March 31 and April 1 again with two complete shifts each day. The tunnel tests were focused on the "cold" environment for the heating condition and the Volt was operated at EV (Electric Vehicle) mode exclusively for the energy saving evaluation. At the EV mode, the cabin HVAC heating was solely provided by the CHCM (Cabin Heating and Cooling Module) only in the Volt. For the EV mode operation, since there is no engine waste heat, the spot heating provided by the TEDs can be more effective in maintaining equivalent thermal comfort while consuming less CHCM power. The thermal manikin is an objective tool to confirm the subjective road test comfort data and establish a clear equivalent comfort for energy evaluation. Figure G111 shows the Volt in GM's CWT ready for the test.

Figure G111: The Volt in GM's Climate Wind Tunnel and data collection in the control room

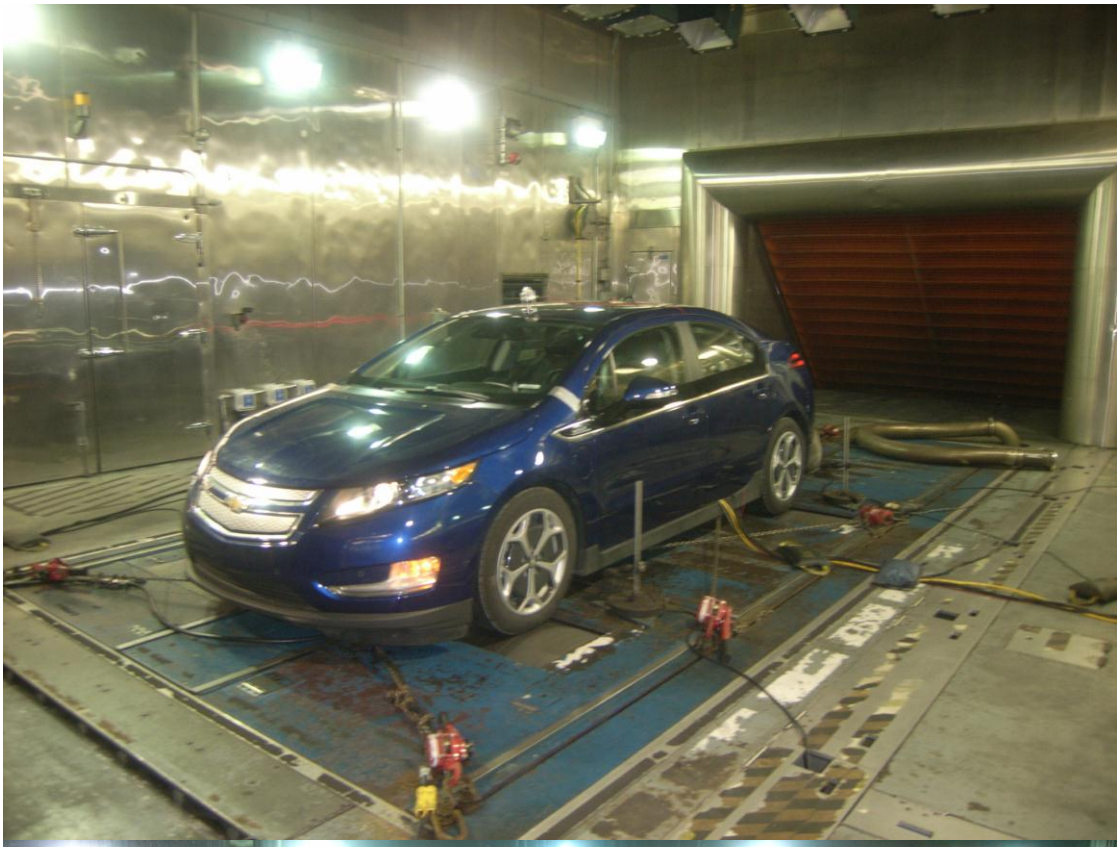

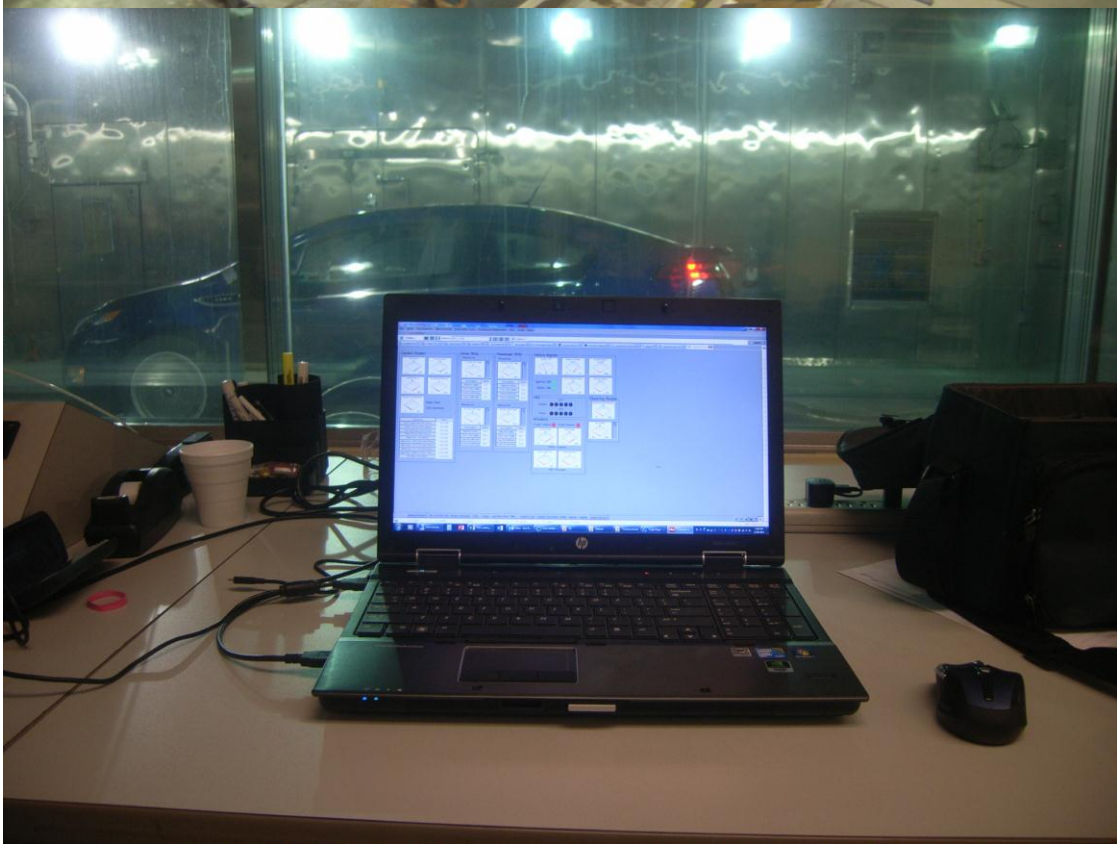

EHT Data from Thermal Manikin Measurement

Figure G112 shows the manikin sits in the front passenger position with the proper winter clothing before tunnel testing. Figure G113 shows the whole body EHT for various set temperatures. The trend of the EHT's dependency on the set temperature and mode of HVAC operation can be clearly identified in Figure G113. It also clearly indicates that 71F TE Eco mode and the 74F comfort mode have the same whole body EHT of about 24C. Furthermore, the local EHTs for 16 body segments for both the 74F Baseline comfort mode and 71F TE Eco mode are shown in Figure G114 where higher EHTs on back, pelvis, and thighs are the contribution from the contact TE seats and lap TE nozzles. The resulting whole body EHT is 24 C for both 74F Baseline with comfort mode and 71F with TE Eco mode.

From the road test, we have shown that the 72F TE Eco mode is more comfort (0.7 index higher) and warmer than the 74F Baseline comfort mode as seen in Figure G110. The manikin's EHT data reconfirmed this, and it is consistent with the subjective road test. So based on the subjective comfort test on the road and the objective thermal manikin data in the tunnel, we have clearly established the equivalent thermal comfort for the Volt demonstration vehicle for the spot heating condition in winter driving. The energy saving calculation for the winter driving will be based on the 74F Baseline comfort mode and the 71F TE Eco mode.

Figure G112: The thermal manikin, Monika, is positioned in the front passenger seat

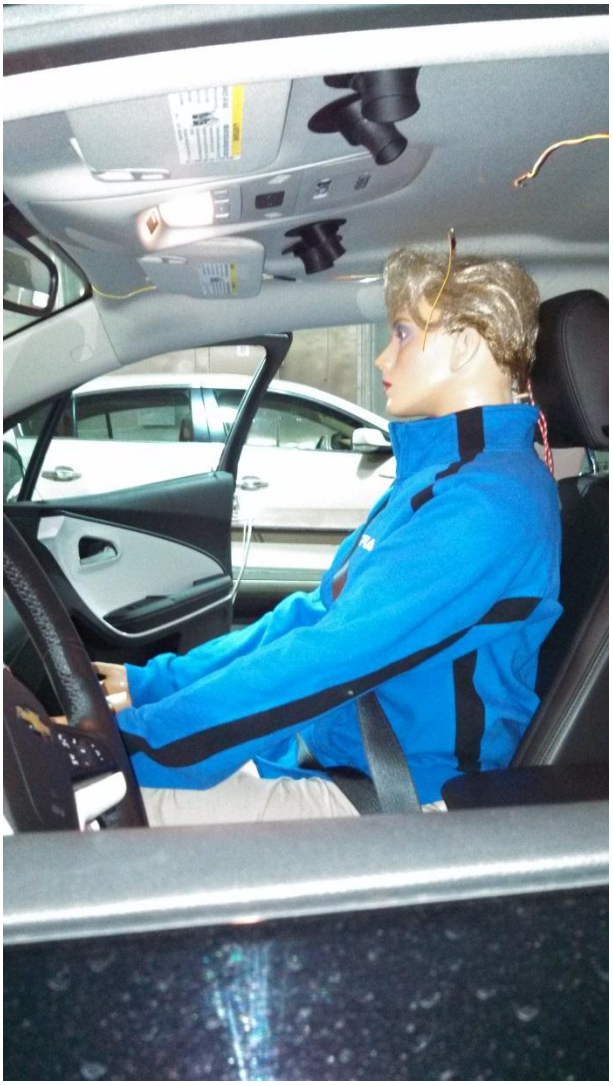

Figure G113: Whole body EHT for various comfort and Eco modes

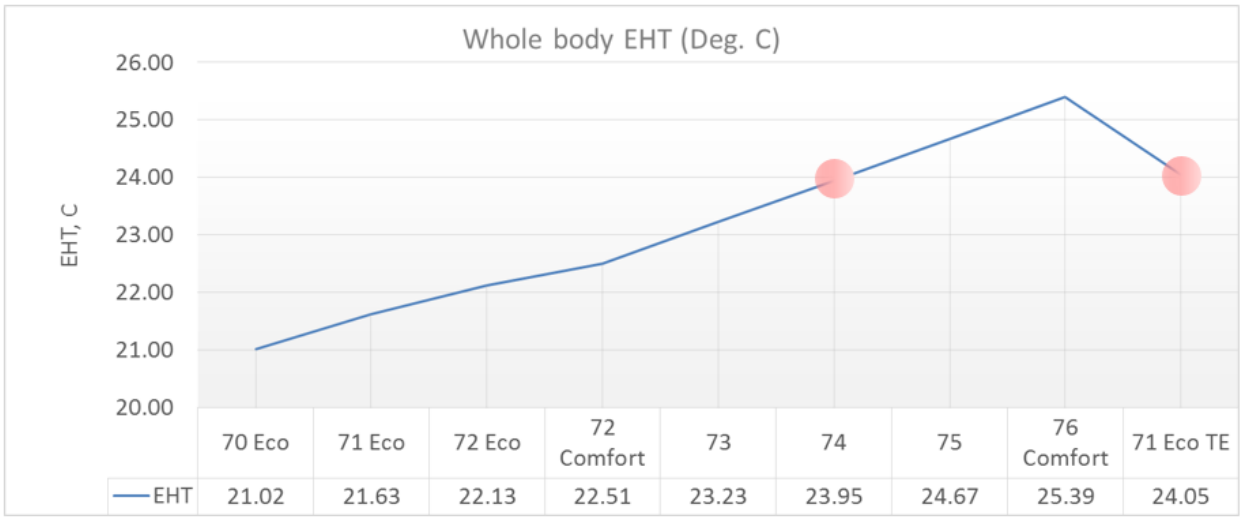

Figure G114: Whole body and local EHTs for the 74F Baseline comfort mode and 71F TE Eco mode

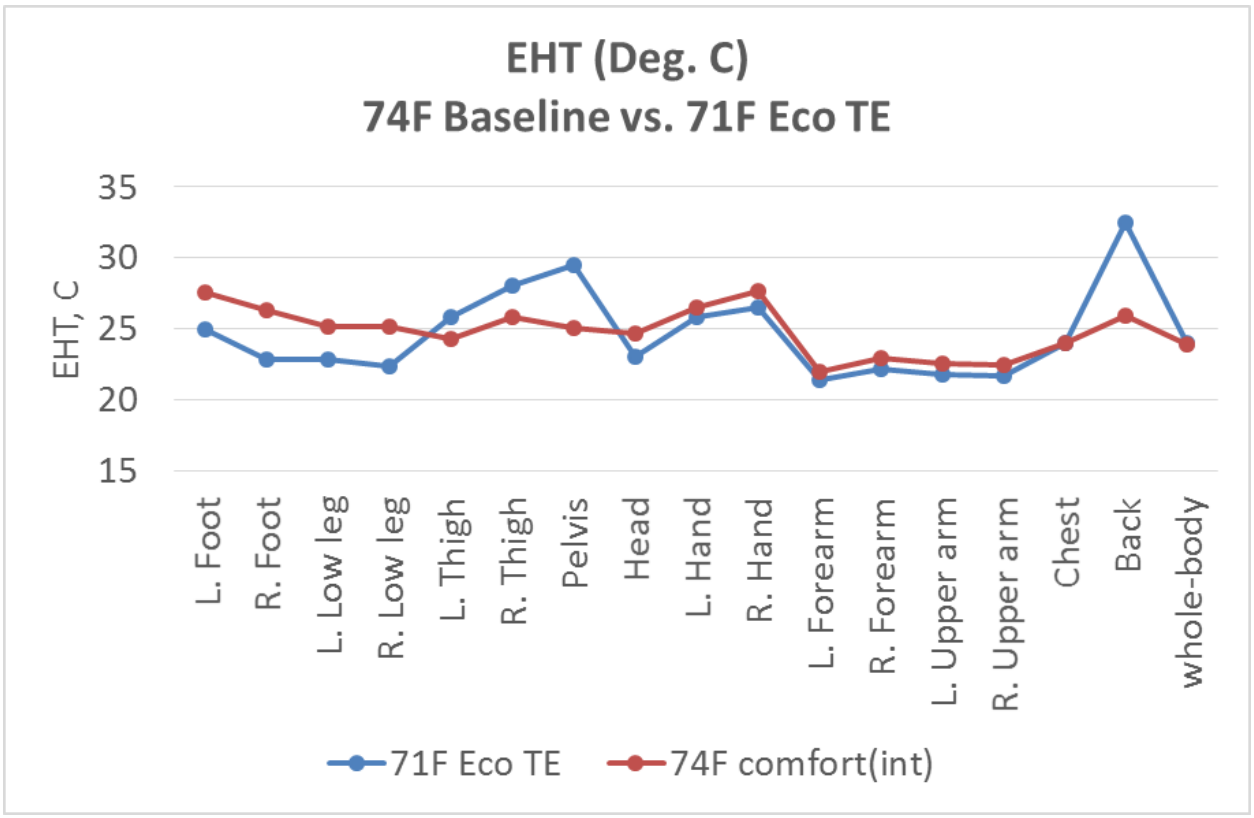

G5.3.4 Milestone 14 – Make Chevrolet Volt demonstration vehicle available to DOE

The Chevrolet Volt is available to the California Energy Commission and the US Department of Energy for their evaluations on May 30, 2014.

G5.4 Task 22 – Calculate Efficiency Improvements of Distributed HVAC System

Energy Saving Analysis for Buick Lacrosse Demonstration Vehicle

The efficiency improvements of the distributed TE HVAC system for the Buick Lacrosse demonstration vehicle has been calculated in Task 18 and achieved 30.9% in annualized energy saving based on ambient temperature and occupancy weighting factors.

Energy Saving Analysis for Volt Demonstration Vehicle

Since the Volt is an Extended Range Electric Vehicle (EREV), it relies on the on-board battery to provide power to heat and cool the cabin in an EV mode. For cooling, AC compressor is used, similar to the Lacrosse operation. For heating, the energy usage is irrelevant to Lacrosse since the engine waste heat is used. However, the Volt, under the pure EV mode, requires a 5 KW electric heater (CHCM) to provide heating power for the cabin air. Therefore for the Volt, in addition to the annualized energy saving for the cooling operation (similar to the one reported for the Lacrosse), a separate annualized energy saving number for the heating will be reported. For the purpose of reporting these two numbers, the temperature ranges for the heating and cooling calculations are defined as:

Heating operation calculation: 10 C and below
Cooling operation calculation: 10 C and above

The tunnel tests for the Volt were focused on the heating mode at three ambient temperatures at -10C, 0C and 10C, respectively to measure the energy usage for 74F baseline with comfort mode and 71F with TE Eco mode. The power consumption was measured in the tunnel for the heating operation. For the Baseline comfort mode, this includes CHCM power and the HVAC blower power. For the TE Eco mode, in addition to the CHCM and blower power, all TE related powers were measured. This includes powers from TE power itself, TE fan, TE coolant pump, CHCM power for the TE coolant, and contact TE seats (and TE seat fan). For the cooling energy calculation, the energy saving reported for the Lacrosse vehicle is used for the Volt with a correction factor of the AC compressor power based on the cabin size and solar load window glass area differences between the two vehicles. This was justified based on the fact that the TEDs used in the Volt demonstration vehicle are identical to the Lacrosse except the front seats where contact TE seats are used in the Volt in contrast to the ventilated TE seat used in the driver seat in Lacrosse. In addition, due to time and budget constraint for the Volt project, it will be more important to focus on the topics not covered in the Lacrosse vehicle.

Based on the tunnel energy data measurement for the heating condition for the ambient temperature below 10 C and the cooling energy calculation above 10 C for the Volt from the Lacrosse's data with proper AC power scaling, the power consumption for is shown in Figure

G115. It includes power consumption for Driver only, Driver and front passenger and all passengers. Similar to the annualized energy saving calculation for the Lacrosse, the same formula was used:

$$p = \sum_i (\sum_j P_{ij} \ W_a^j) W_o^i$$

where W_a^j represents the ambient weighting (% of occurrence) over a given set of ambient temperatures, W_o^i is the occupancy weightings, and P_{ij} represent the overall system power consumption under a given ambient and occupancy scenario. For ambient temperature between 10 C and 23 C, the compressor is completely shut down and all TEDs alone can maintain occupant comfort to achieve high energy efficiency except for high solar load and/or high humidity that require compressor to be restarted to ensure comfort and safety. So the compressor power saving during this ambient temperature needs to be deducted when restarting occurs. Based on one of the analysis by NREL for "Typical Meteorological Year Database V3", 49% Restart Rate for a Climatic Average US City (Topeka, KS, or Philadelphia, PA) is adopted. So in the range of 10C ~ 23C, 51% of compressor shutdown power saving is applied in annualization calculation.

- For annualized cooling energy saving calculation above 10 C, the same weighting distribution for Lacrosse shown in Figs. 2.5 for W_a^j and 2.6 for W_o^i were used. The annualized and vehicle occupancy weighted savings for the Volt in cooling condition is 36.7%.
- For annualized heating energy saving calculation below 10 C, the same occupancy weighting was used. The ambient weighting below 10 C is shown in Figure G116. The method used was a study of the winter months of the US cites of x and y. The annualized and vehicle occupancy weighted savings for the Volt in heating condition is 37.7%.

Figure G115: Volt Power Consumption for Baseline and TE Mode with three Occupancy Configurations

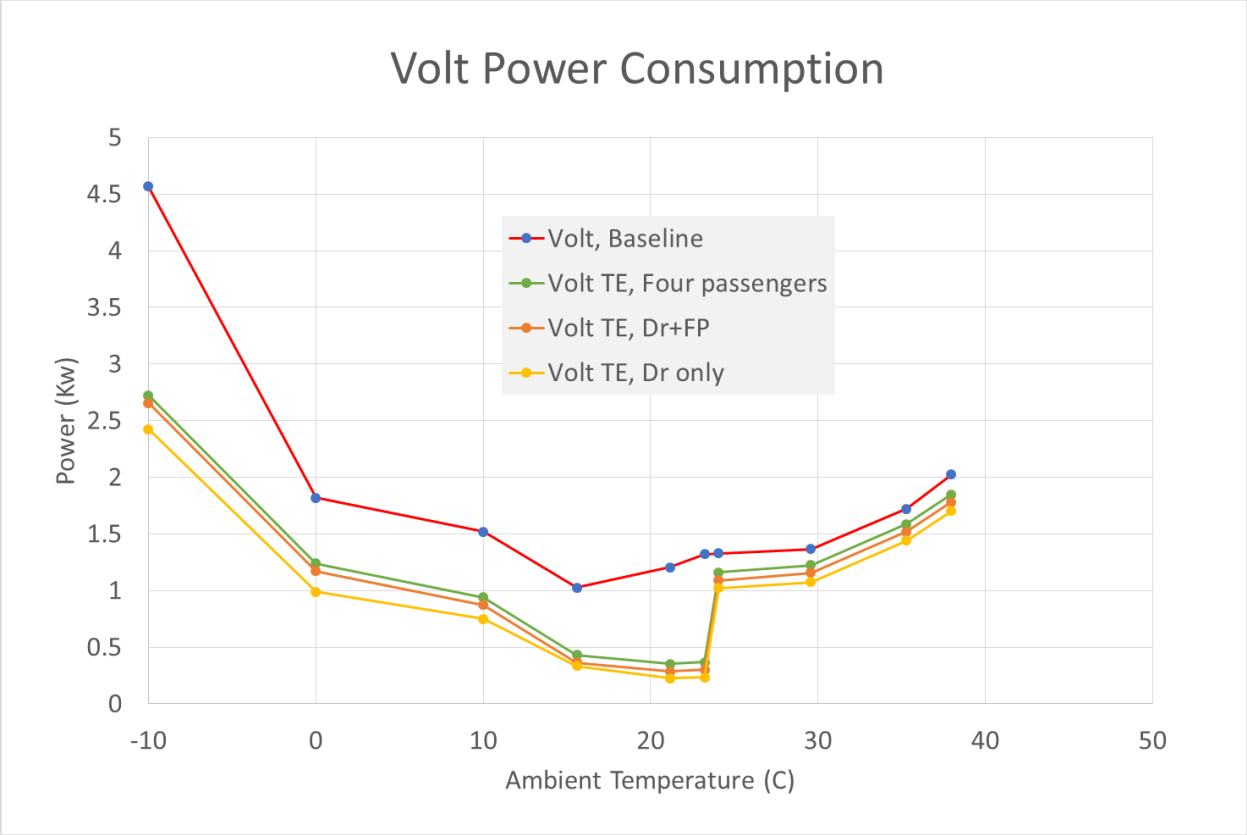

Figure G116: Ambient weighting factors used to calculate annualized heating energy savings

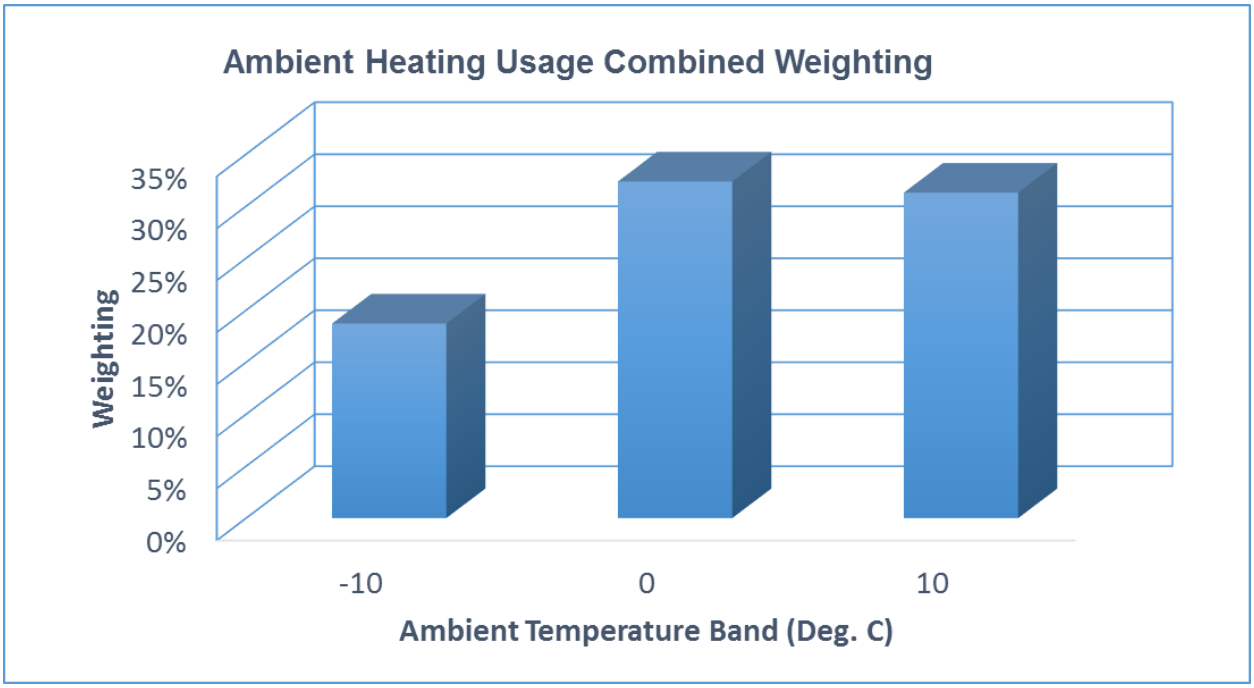

CHAPTER G6:
GM Phase 5 – Thermoelectric Generator Development

The focus of this phase was to develop improvements in the TE materials for thermoelectric generators that could be used to produce electrical power for TE HVAC system loads. For this phase of the project, GM utilized first principle calculations by UNLV to identify underlying mechanisms that guided the research into new TE materials. Oak Ridge National Laboratory advised on potential composition improvements and measured material samples. Marlow Industries developed new module processes to incorporate these optimized TE materials.

G6.1 Task 23 – Develop Thermoelectric Materials / Modules for Waste Heat Recovery

The project team made significant progress under the waste heat recovery objectives of Phase 5. Much of these efforts focused on high-temperature TE materials research, including the evaluation of melt-spun skutterudite materials, low-cost skutterudite TE materials, and defect diamond-like materials. An evaluation of thermal interface materials was also performed.

G6.1.1 Evaluation of Melt Spun Skutterudite Materials

Magnequench delivered several different formulations of n- and p-type skutterudite that were prepared by melt spinning of pre-melted charges. Further for the n-type materials, three different quench rates were investigated (those being slow, fast and very fast that corresponds to the quench wheel's speed). A comparative study was undertaken comparing the thermoelectric properties of materials that were first annealed then consolidated by spark plasma sintering and those that were direct sintered without annealing. For the n-type materials a formulation using dual elemental fillers was chosen for 100 g scale up, for the p-type materials formulations of the type $M_xFe_{4-y}Ni_ySb_{12}$ were selected. Figure G117 below is an SEM micrograph of an as spun skutterudite ribbon showing the contact and free surface.

Figure G117: Back-scattered electron images of as-spun ribbons

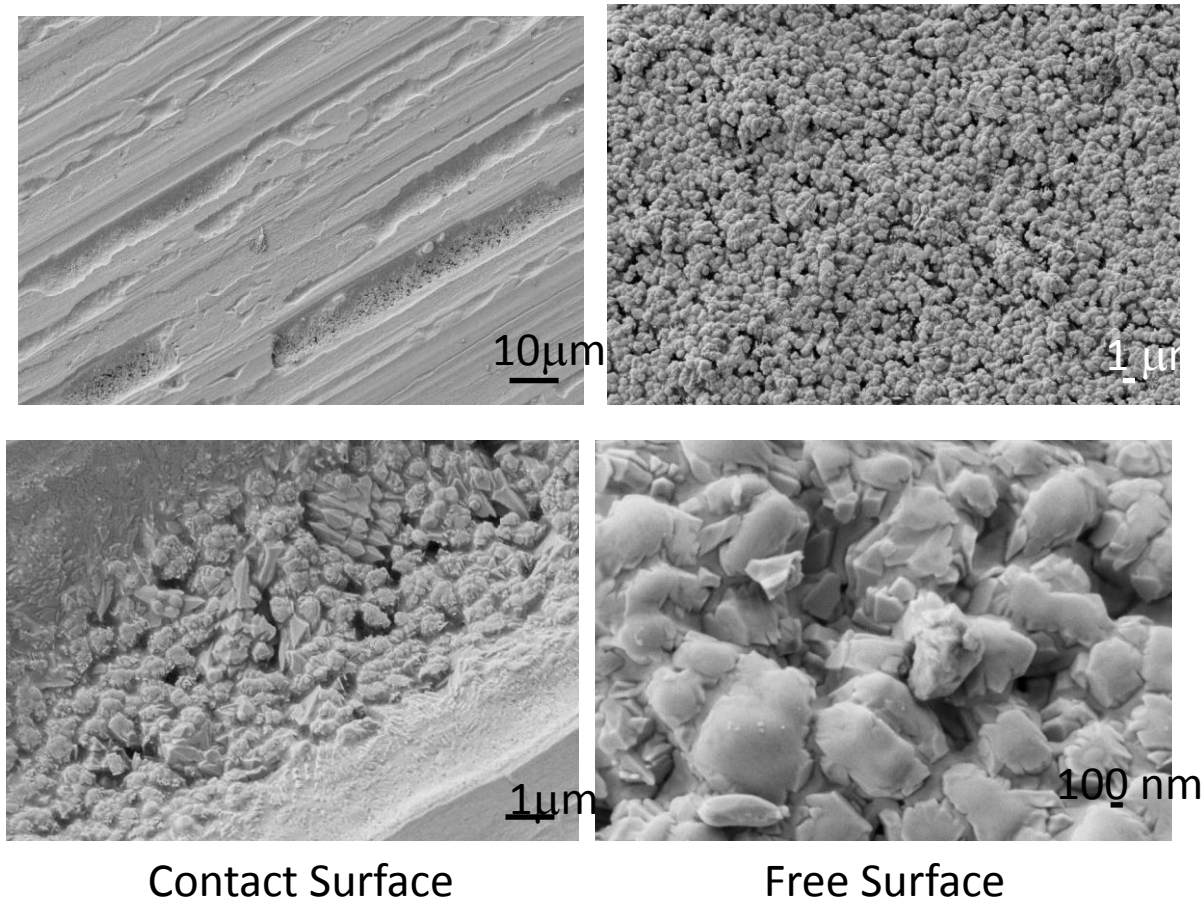

The ribbons pictured in Figure G117 are of the fast quench variety. The images on the left are the contact surface and the gashes observed are due to Ar gas entrainment during quenching. The images on the right are the free surface, which is considerably more textured due to the fact that crystal growth was allowed to take place.

The as-received n-type materials were a complex mixture of binary antimonides and skutterudites. This is a result of the fact that temperatures above the peritectic decomposition are required for processing, however despite this and the rapid quench rates skutterudite phase is still observed in the ribbons by powder x-ray diffraction. Similar multi-phasic materials were observed in the as-received p-type samples with an even wider variety of phases present due the fact that p-type are quinary phases as compared to n-type which are quaternary. We have determined that these materials can be transformed into single-phase materials simply consolidation by spark plasma sintering (SPS). From Powder x-ray diffraction and electron probe microanalysis there is no significant difference in phase purity, composition as far as the extent of homogeneity as it applies to the distribution of fillers from grain to grain. We do however see a significant difference in the grain size distribution between the very fast quench materials and those produced with slower quench rates with the former having a finer grain size. Figure G118 shows the backscattered electron images of polished melt-spun and SPS billets with the EPMA-determined compositions listed in the bottom of the images.

Figure G118: Backscattered electron images of, from left to right, slow quench, fast quench and very fast quench n-type skutterudites

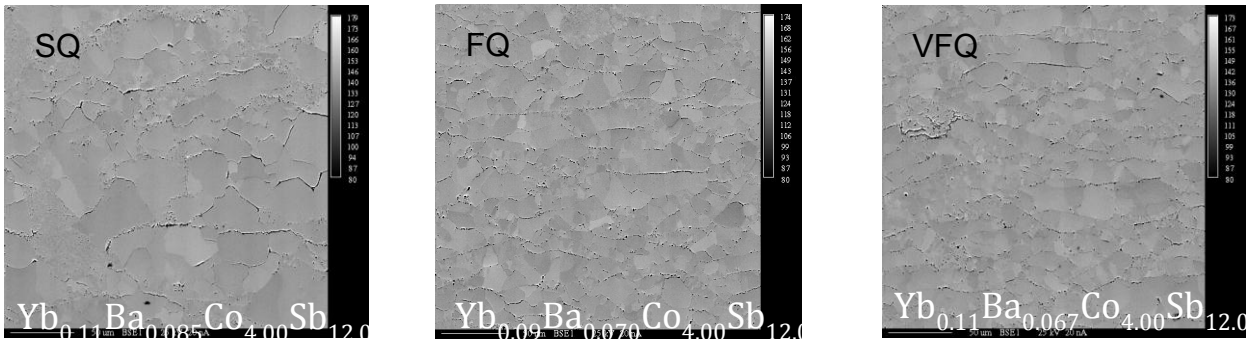

We conclude that melt spinning combined with spark plasma sintering results in materials with properties comparable to those where annealing was performed and so this step can be eliminated, thereby increasing materials throughput and reducing cost and energy inputs for production. This was true of both n- and p-type materials and was independent of quench rate. Further, the direct SPS processing of melt-spun materials is scalable. We have produce 5-gram billets of n- and p- type materials for the purposes of transport property evaluation and 80+ g billets of n- and p-type materials for residual stress analysis and for the fabrication of tensile stress bars. In all cases, the as-spun ribbons can be completely converted to pure phase skutterudites in the matter of 20 min. of processing including the heating ramps.

Figure G119 shows the transport properties of n-type materials, with the three different quench rates. As can be seen all samples have virtually identical thermal and electrical transport properties consistent with their similar compositions. An 80 g billet of fast quench n-type material (3.0 cm in diameter and 1.5 cm in thickness) was delivered to Marlow industries for sectioning into tensile fracture bars. These bars were delivered to Oak Ridge National Laboratory for room and high temperature 3-point bend testing using their test fixture. The results of these tests are presented in Figure G120 below. As can be seen there is a decrease in the characteristic strength as the temperature increases. Fractography was performed to understand the failure modes of the test bars. Comparable p-type fracture strength testing was also performed.

Several n-type fracture test bars were kept for transport, thermal expansion measurements, and resonant ultrasound spectroscopy to determine Young's modulus and Poisson's ratio. The CTE was found to vary from 10 to 14 PPM and the Young's modulus and Poisson's ratio were 139 Gpa and 0.2, respectively at room temperature. These values compare well to those found for n-type materials prepared in the traditional manner. Transport properties from a bar cut from the 80 g billet were also measured to ensure that the properties are retained even when processing at larger batch sizes. Further, the transport properties for the bar cut from the 80 billet were performed along the axis of the billet, while transport properties for 5 g billets are performed perpendicular to the axis. As shown in Figure G121, the transport properties between the 5 g billet and the 80 g billet agree well indicating the quality of material is still high even at larger batch sizes for SPS.

Figure G119: Temperature dependence of the Seebeck coefficient (S), electrical resistivity (ρ), Thermal conductivity (k) and ZT.

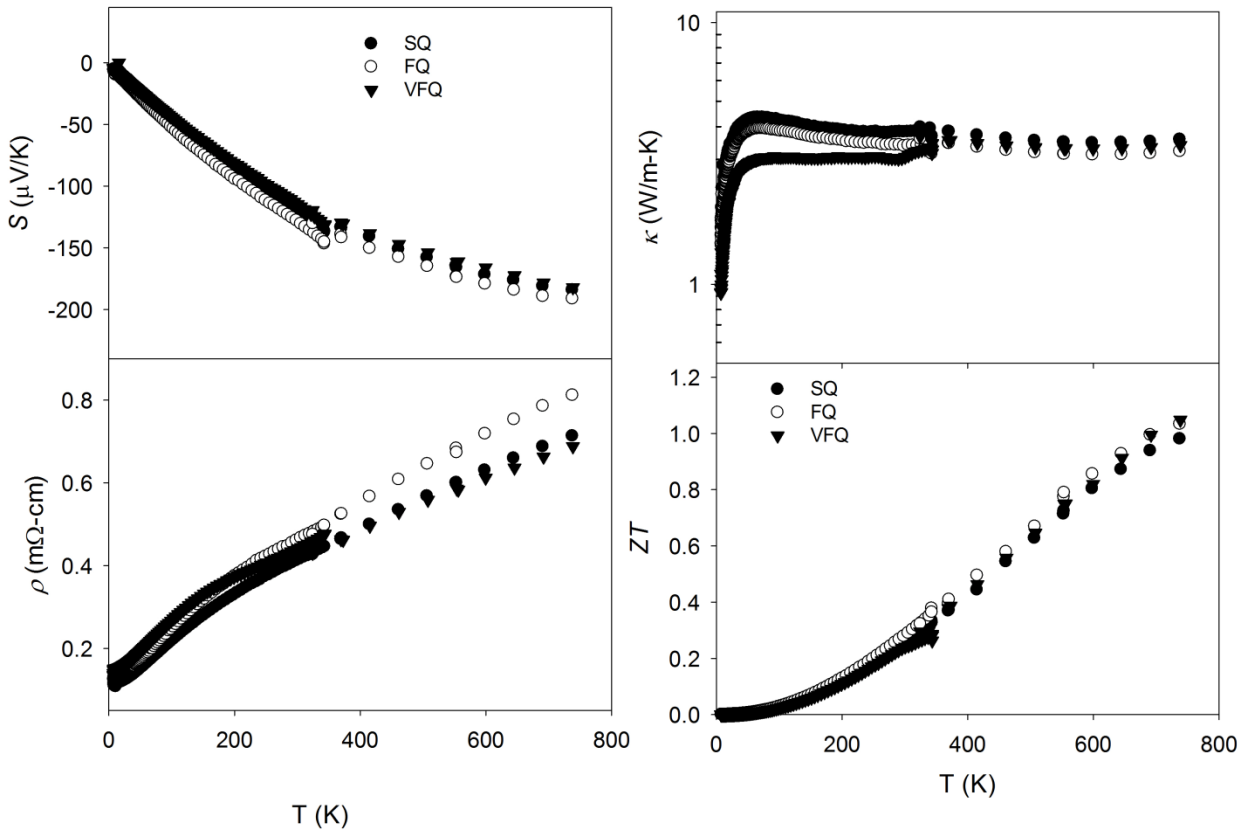

Figure G120: Characteristic tensile strength as a function of temperature for n-type skutterudite materials made by melt spinning and SPS.

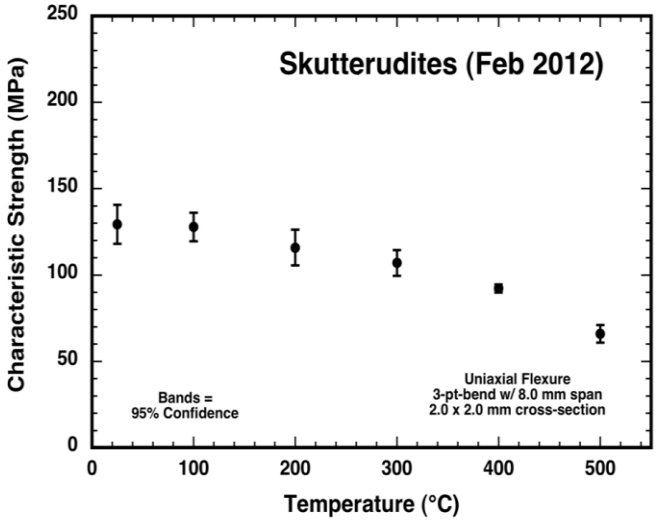

Figure G121: Comparative high temperature transport properties of n-type skutterudite with samples cut from a 5 g and 2 from an 80 g billet.

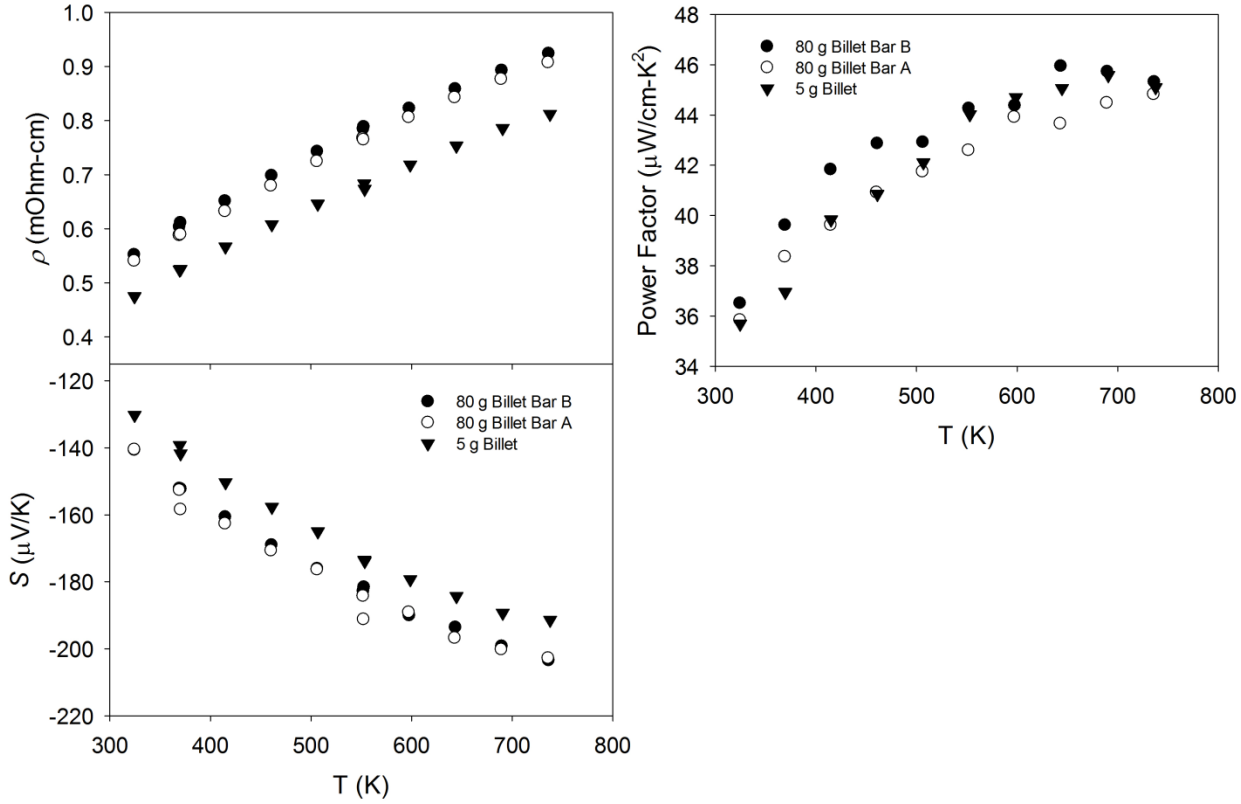

Several formulations of p-type melt spun skutterudite were investigated were the transition metal ratios (Fe and Ni) were altered. In the case for one of the formulations, both slow and fast quench samples were investigated. As was found the for the n-type materials, the fast quench condition led to a finer grain structure but no significant differences were observed in the transport properties. Based on these finding, only fast quench materials were investigated for the later 2 composition. As discussed in the following sections, we have found the best way to affect the carrier concentration is by adjusting the Fe to Ni ratio. Figure G123 shows the transport properties of the three different formulations. High temperature measurements will be performed for the two latter materials. A ZT of ~1 at 750 K was found for $DD_{0.72}Fe_{3.4}Ni_{0.6}Sb_{12}$.

Figure G122: Temperature dependence for three different formulations of p-type skutterudite. As the Fe to Ni ratio is increased, the carrier concentration increases and results in lower ρ.

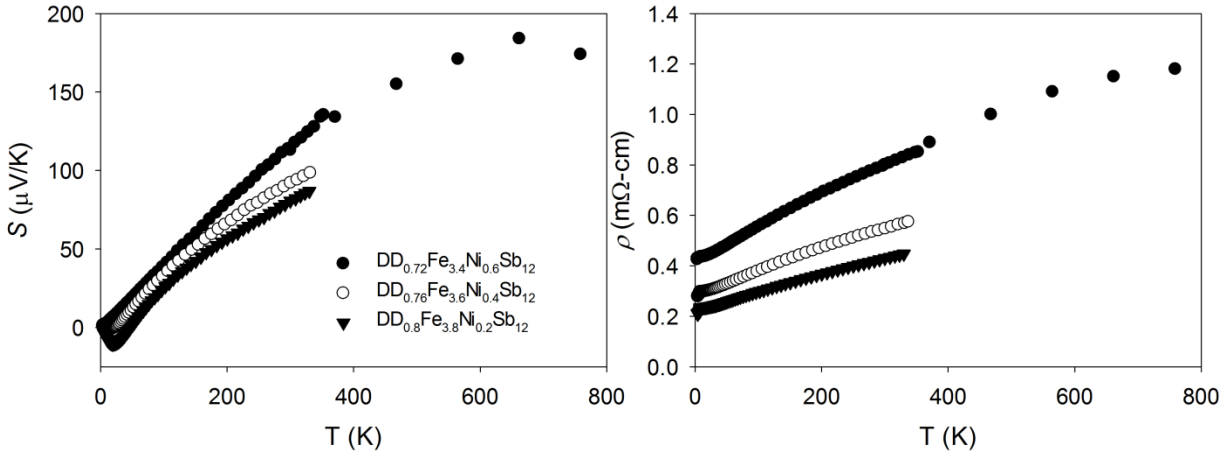

Instrumentation Installation: In the first quarter of 2012, two pieces of new instrumentation were installed at GM R&D that facilitated the rapid screening of high temperature transport properties of both new and developmental thermoelectric materials. A Linseis LSR-3 high temperature Seebeck and Electrical resistivity measurement system was installed in January and an Anter Flashline diffusivity measurement system was installed in March. This instrumentation along with those currently operating at GM R&D will allow for the evaluation of thermopower, electrical resistivity, and thermal conductivity from 3 K to 1000 K.

G6.1.2 Low-Cost p-type Skutterudite Thermoelectric Materials

With the emphasis on the reduction of rare earth materials due to supply concerns, we feel that the current p-type formulations being considered for skutterudites, which are rich in rare earth, are not a long-term sustainable solution for automotive thermoelectric applications. With this in mind, we have begun to explore the thermoelectric properties of $Ca_xFe_{4-y}Ni_ySb_{12}$. These materials were prepared using the traditional melt-quench-anneal technique. Several different formulations were investigated. The first was to hold the Fe and Ni ratio fixed at 3:1 and adjust the filling fraction of Ca resulting in nominal compositions of the type $Ca_xFe_{4-y}Ni_ySb_{12}$ (y is fixed). The second was to fix the nominal composition of Ca and vary the ratio of Fe to Ni resulting in nominal compositions of the type $CaFe_{4-Y}Ni_ySb_{12}$ (Ca content is fixed y varies). From the evaluation of transport measurements, we find that the approach of altering the Fe to Ni ratio is a more effective approach for controlling the carrier concentration as compared to changing the filling fraction. Figure G123 shows the low and high temperature transport properties of $Ca_xFe_{4-y}Ni_ySb_{12}$ (fixed y). The there is little to no variation in the magnitude and temperature dependence of Seebeck coefficient, and, with the exception of one sample, the resistances are quite similar as well. The fact that there is a down turn in the magnitude of S above ~600 K and that there is a significant increase in κ at around the same temperature result in lower ZT above this temperature. Both phenomena are likely associated with the onset of bipolar conduction. There is a peak in the ZT curve at 600 K with a magnitude on the order of 0.55. This is similar to the behavior we observed for Yb-filled p-type materials and indicate that

the Yb and Ca atoms have a similar effect on the band structure of the $Fe_{4-y}Ni_ySb_{12}$ network, which seems to be that of 2+ ions for the balancing of charge.

Figure G123: Thermal transport properties of $Ca_xFe_{4-y}Ni_ySb_{12}$

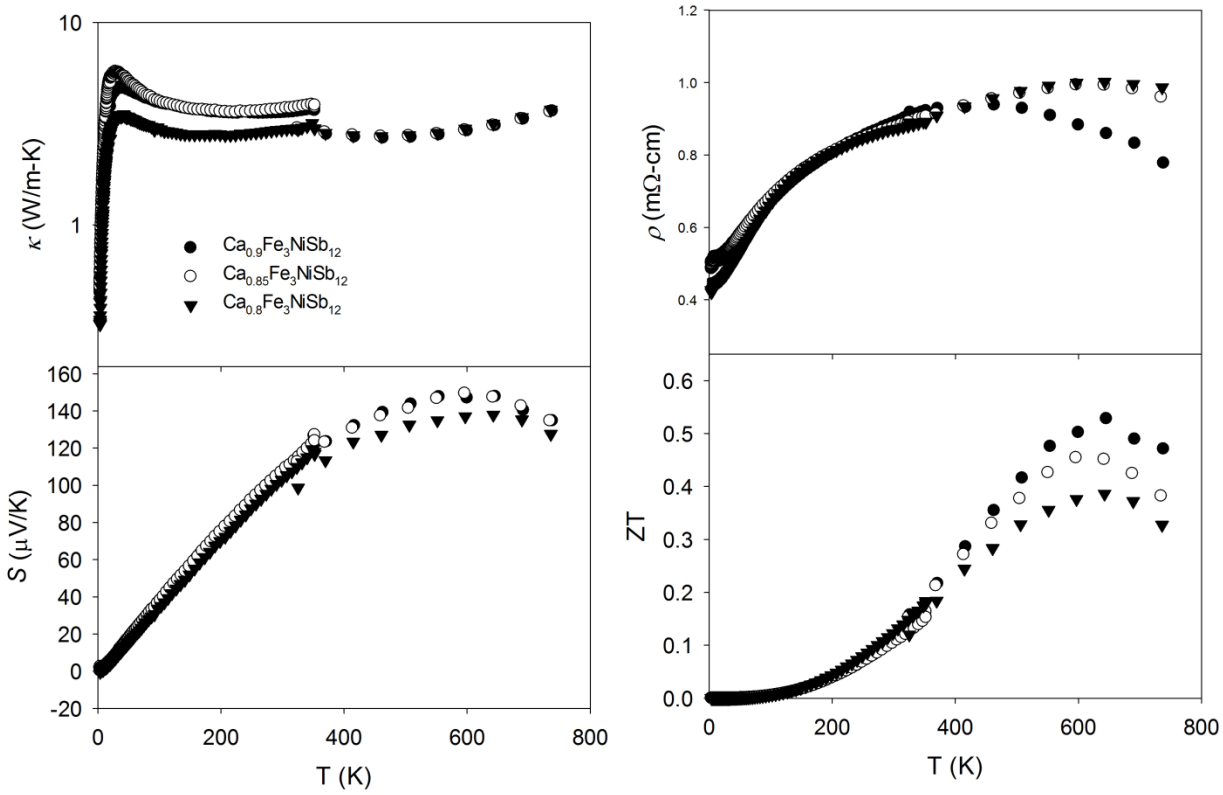

Figure G124 shows the low and high temperature *S* and ρ for the $CaFe_{4-y}Ni_ySb_{12}$ samples. As shown, there is a significant difference in the magnitude and temperature dependence of these parameters for the three samples, which suggests that the hole doping level is increasing with increasing Fe content. Also evident is for the higher Fe ratios the onset of bipolar conduction is suppressed as we would expect for higher hole carrier concentrations, which would tend to cancel out the effects of the minority electron carriers. Power factors approaching 30 $\mu W/cmK^2$ were found for these samples. High temperature thermal conductivity measurements and resultant ZT values of these samples were collected.

Figure G124: Thermoelectric properties of $CaFe_{4-y}Ni_ySb_{12}$

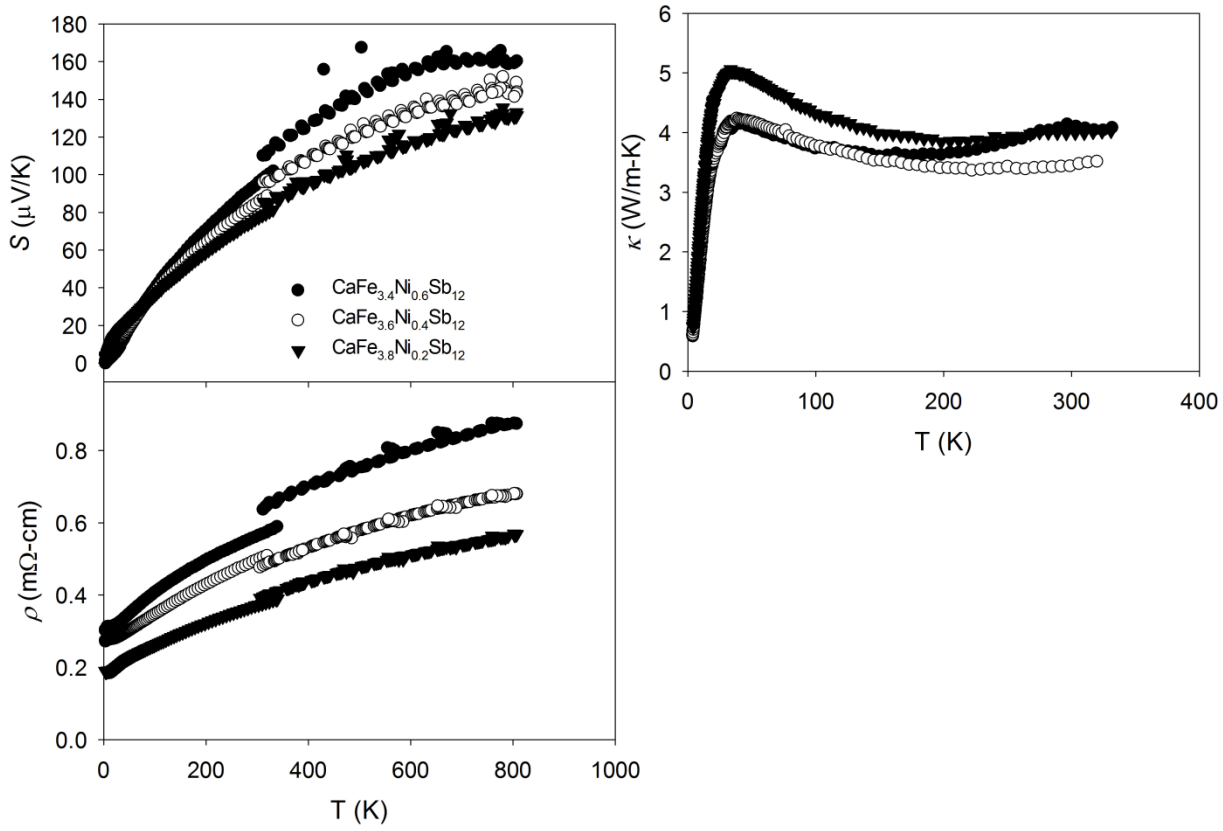

G6.1.3 Defect Diamond-Like Materials

Various zincblende or chalcopyrite compounds with a wide range of transition metal and tri-al ratios may contain structural vacancies, the amount of which increases with the increasing trial content. Although structural vacancies scatter heat-carrying phonons, hence reduce the lattice thermal conductivity, they may also scatter the charge carriers and reduce the electrical conductivity. We have studied $(Cu_2Te)_{1-x}(Ga_2Te_3)_x$ to find out how the overall thermoelectric properties of this material system are affected by the vacancy content. Polycrystalline samples were synthesized by melting, annealing, and hot-pressing. Pure phase materials were obtained for all the compositions. All the samples show *p*-type semiconducting behavior in the temperature dependence of the Seebeck and Hall coefficients. The structural vacancies were found to scatter both phonons and charge carriers. The room temperature charge carrier mobility drops from 91 $cm^2V^{-1}s^{-1}$ 4.6 $cm^2V^{-1}s^{-1}$ depending on vacancy level. The total thermal conductivity decreases significantly as the Ga content increases at low temperatures where the vacancies act as the point defects that dominate the phonon scattering. At high temperatures, the dependence of thermal conductivity on the Ga content is much less significant. The highest ZT ~ 1.4 among the samples in this study was found at 840 K. The temperature dependence of the thermoelectric properties is shown in Figure G125. The thermoelectric properties can be

further tuned by doping. Mn has been found to be an effective dopant. A series of Mn doped samples are being prepared to optimize the thermoelectric properties.

Figure G125: Temperature dependence of the thermal conductivity, resistivity, Seebeck coefficient, and ZT.

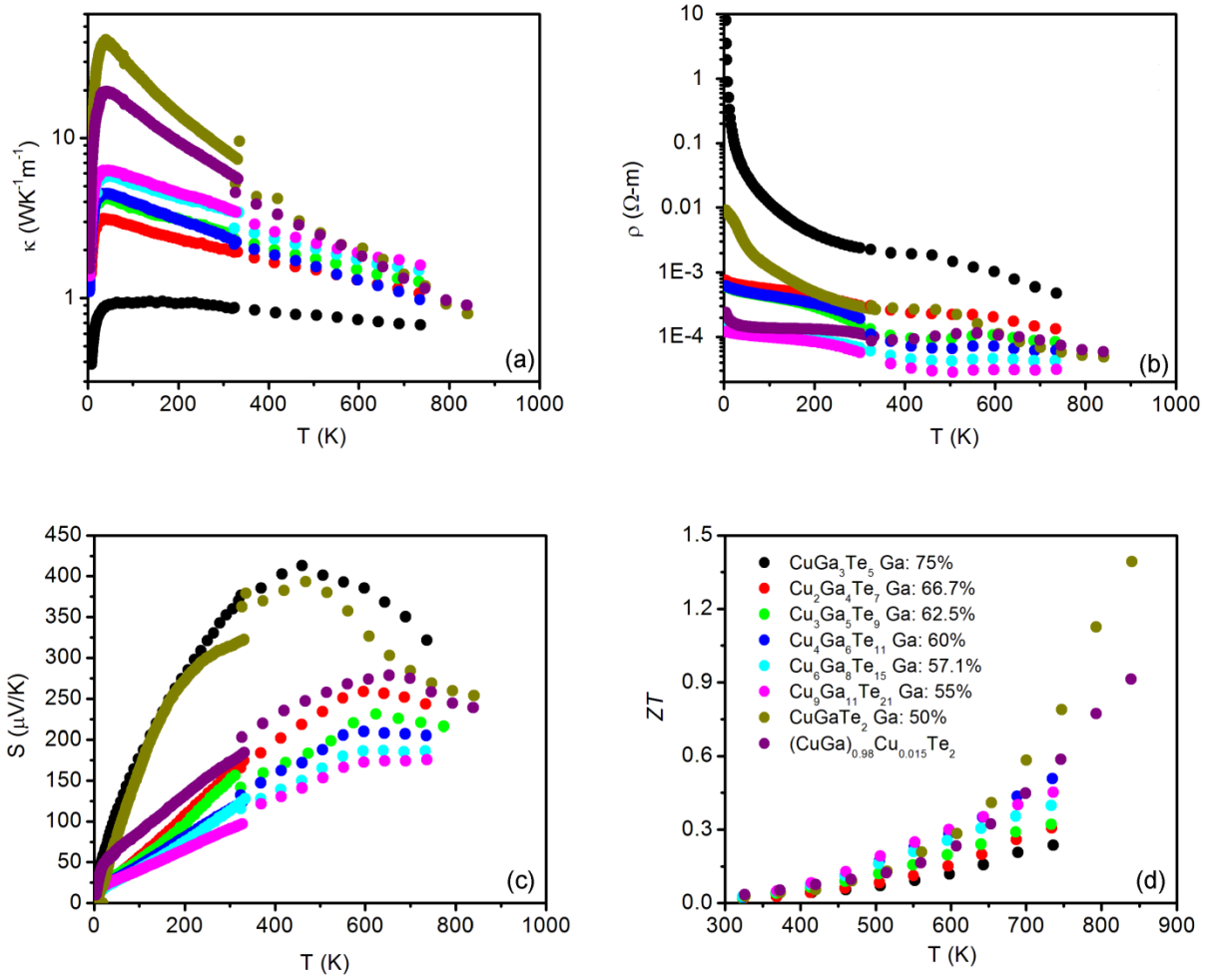

G6.1.4 Evaluation of Thermal Interface Materials

In conjunction with Purdue University, GM R&D has been investigating the effects of carbon nanotube (CNT) based thermal interface materials on the performance of an off-the-shelf Bi_2Te_3 module. Figure G126 shows an SEM micrograph of the carbon nanotube arrays as deposited on a copper foil substrate.

Figure G126: SEM micrograph of CNT arrays deposited on copper foil

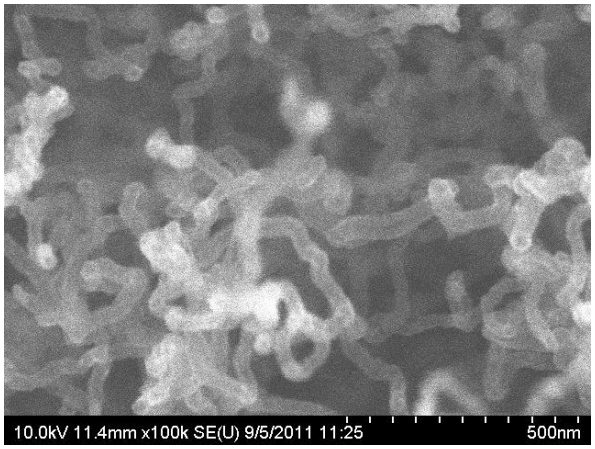

The measurements were performed using an Ulvac PEM module performance test system at GM R&D. The experiment is set up to measure the steady-state electrical power output of a module under a virtually constant thermal gradient. Heat is delivered to the hot side of the module though a Ni bar with a cross sectional area of 4 cm^2 three thermocouples are placed along the length, two to monitor the temperature drop along the length to assess heat flow into the module and one at the bottom of the block near the contact with the module header to transducer the hot side of the thermoelectric module. On the cold side is a symmetrically identical arrangement with a copper block that is cooled to 20°C by a programmable chiller. Thermal contact resistance exists between the hot and cold side block and the module's ceramic header, in addition there is a small but finite thermal resistance associated with the ceramic headers. Under the conditions of steady-state heat flow, both the interface contact resistance and the ceramic header will result in the temperatures of the he TE legs being lower and higher at the hot side and cold side respectively. That is lower (hot side) and higher (cold side) than the temperatures measured by the thermocouples embedded in the hot and cold sinks. This series of thermal resistances is shown schematically in Figure G127.

Figure G127: Thermal equivalent circuit superimposed on an image of Bi_2Te_3 module in the PEM test stand.

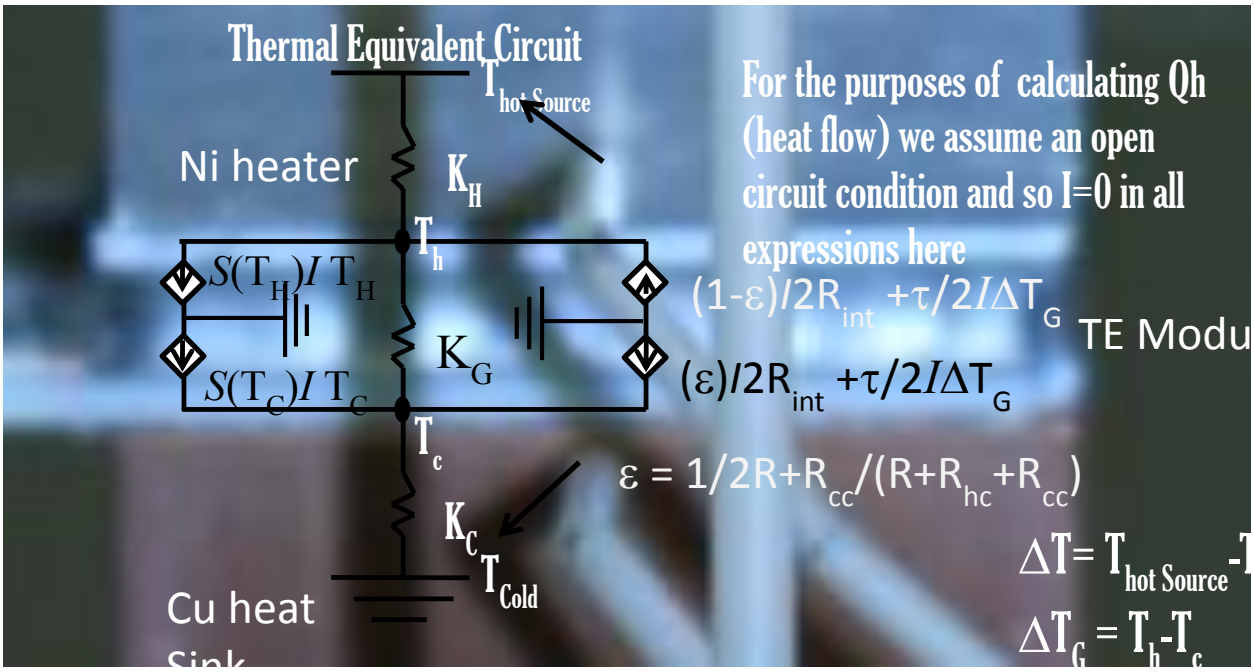

From the last program, we found that thermal interface contact resistance was a major source of parasitic efficiency loss, and was particularly under conditions of high heat flux. To assess the effect of using CNT based arrays as thermal interface materials, a series of experiments were run where the cold side thermal interface material was kept constant with grafoil and the hot side interface materials were altered, varying from no interface materials (bare interface between the Ni heat source and the ceramic header) to grafoil, copper foil, single sided CNT arrays on copper foil with the CNT arrays facing the ceramic header, and a double sided CNT array on copper foil where the CNT arrays were in contact with both the hot source and ceramic header.

Initial findings indicate that there is a gradual increase in the module open-circuit voltage with changing the interface materials from nothing to grafoil to copper to single-sided CNT, and finally, the double-sided CNT array that showed the largest open-circuit voltage. Figure G128 shows this result in a series of I-V curves for the same module and same temperature gradient, but with different interface materials at the hot side. This corresponds to a lower thermal contact resistance between the hot source and the module. Not shown are the results for the bare interface as they are virtually identical to the grafoil interface case. The open-circuit voltage of the module is a sensitive function of the temperature gradient along the length of the legs. Heat flowing through the moudle including the interface between the heater and the ceramic will lead to a temperature drop between the heater and the hot side of the legs. Likewise, thermal contact resistance at the cold side will result in an increase in the cold side tempertaure and depending on the nature of the construction of the module and the thermal contact resistance on the two sides this temperature drop may be symmetric. In any case, the

increase in the open circuite voltage that we observed with a change in the measured delta T is indicative of a larger delta T across the TE materials and corresponds to a decreased thermal contact resistance at the hot side. The larger open-circuit voltage leads to a higher maximum power output and higher effeiciency as shown in Figure G129. The increased efficiency is a result of a higher electrical power output (resulting from the increased Voc) for the same nominal heat flow.

Figure G128: V vs I curve for a module test the Voc (Y intercept of the curve) changes as a function of differing interface materials.

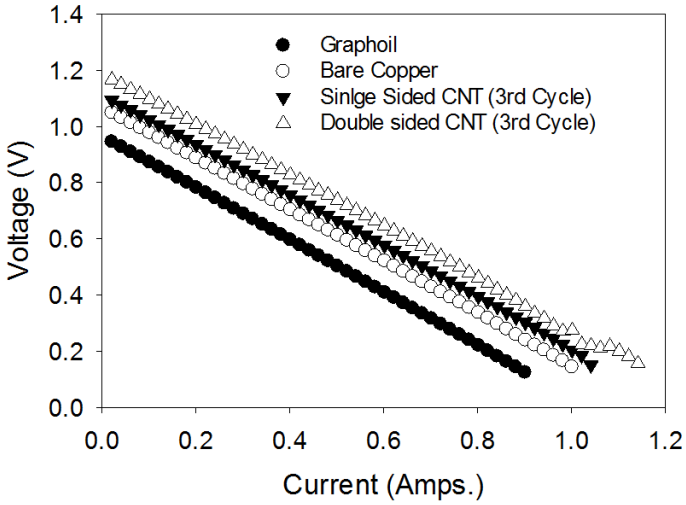

Figure G129: Percent conversion efficiency (P_{out}/Q_H) ($Q_H$is the heat flow).

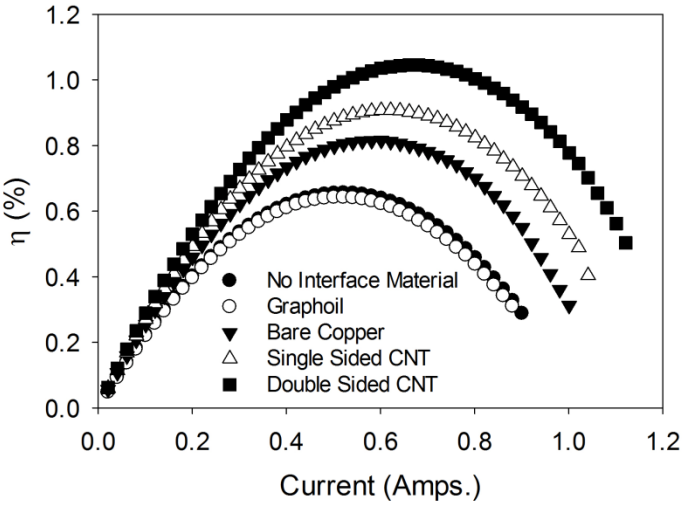

G6.1.5 Diffusion Barrier Evaluation

Thermally arc-sprayed (TAS) diffusion barriers have the potential to provide superior barriers in terms of low cost and performance. During this reporting period, we have continued to focus a substantial effort on the development of these barriers. Based on discussions with TAS experts from Praxair, the manufacturer of our TAS equipment, and observations of the results

achieved using 60T-SS, a greater than 13% Cr TAS wire was evaluated. We sprayed ALCRO, a 23% Cr, Fe-based TAS wire. The adhesion of the ALCRO wire was not satisfactory.

60T-SS was applied to the p-type skutterudite material used in the β-TEG prototype build. ZT as a function temperature was measured on the 40mm^2, β-TEG prototype device. The device underperformed when compared to expected model results. These results will be presented later in our report. The reason for the poor performance was high device ACR. A cross-sectional failure analysis provided evidence of delaminating 60T-SS TAS diffusion barrier from the p-type skutterudite in the second row of elements from the negative lead wire. Figure G130 is an optical image of one of the failed interfaces.

Figure G130: Failed diffusion barrier on p-type skutterudite element from the prototype β-TEG

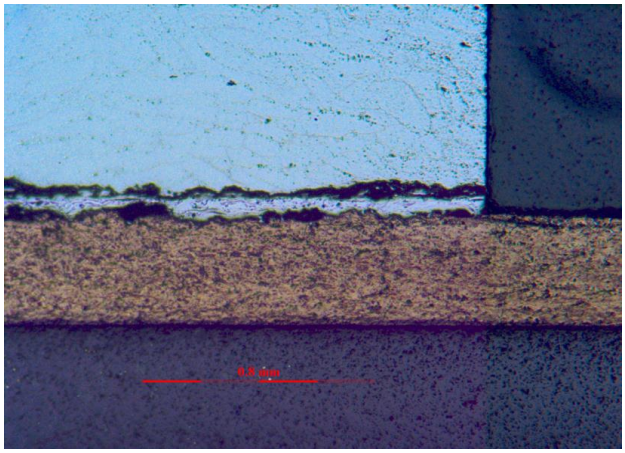

In addition to the observed interface failure in the device, we began to experience unexpected TAS 60T-SS / p-type skutterudite failures. We conducted 23, Fe alloy containing 13% Cr, stainless steel (60T-SS) TAS experiments during this reporting period. After many TAS experiments that concluded with microscopic observations of the TAS / p-type skutterudite interface, we suspect a process change related to the stability of power supply used on the TAS equipment. We will continue to carefully and methodically evaluate eight key processing variables related to the TAS process in order to develop an understanding of the cause for these failures. Table G5 provides a list of 60T-SS experiments conducted with selected processing conditions and a barrier-bond evaluation. A pass (P) or fail (F) in the as-TAS bond state is also included for a quick review of progress.

Table G5: TAS experiment conditions

SAMPLE	PASSES	PSI	FEEDRATE	TRAVERSE RATE	ROTATION SPEED	Pass/Fail	V/A
60T001-N	1.5	25	1.5	152	44	+	
60T002-P	0.5	25	1.35	152	44	+	
60T003-P	1.5	25	1.5			P	
60T006-N	1.5	25	1.5			+	
60T007-P	1.5	25				P	
60T008-P	1.5	25				P	
60T009-P	1.5	25				P	
60T011-N	1.5	25	1.25	152	44	P	
60T013-P	1.5	25	1.5			P/F	
60T014-P*	1.5	25				P	
60T015-P	1.5/2	25	1.3	152			
60T016-P	2	35	1.3	152			
60T018-P*	1.5	25				P	
60T020-P	1.5	25	1.3	154	44	P	
60T021-P	1.5	25	1.25	154	44	P/F	
60T022-N	2/2.5	50	1.25	154	44	P/F	
60T023-N	1.5/2	50	1.25	154	44	F	
60T024-P*	1.5	25	1.25	154	44	P	
60T025-P*	1.5	25	1.25	154	44	P	
60T026-P	1.5	25	1.25	154	44	P	
60T027-P	1.5	25	1.25	154	44	P	
60T028-N	1.5	50	1.25	154	44	P	
60T029-N	1.5	50	1.25	154	44	F	
60T030-N	1.5	50	1.25	154	44	F	
60T031-P	1.5	25	1.6	152	44	F	
60T032-N	1.5	50	1.6	152	44	F	
60T033-N	1	50	1.6	152	44		
	1.5	50	1.25	152	44		
60T034-P1	1.5	25	1.6	152	44	F	
60T034-P2	1.5	25	1.25	152	44	F	
60T034-P3	1	25	1.25	152	44		
60T035-N	1	50	1.6	152	44		
60T036-P	1	25	1.3	152	44		
60T036-P	1	25	1.25	132	44		
60T037-P	1.5	25	1.3	152	44	F	36/130
60T037-P	1	25	1.35	152	44	P	36/130
60T038-P	1	25	1.5	152	44		34/120
60T038-P	1	25	1.7	152	44		34/180
60T039-P	1	25	1.6	152	44		34/180
60T039-P	1.5	25	1.25	152	44		42/100
60T040-P	1.5	25	1.6	152	44		34/180
60T041-P	1	25	1.7	152	44	f	40/200
60T041-P	1	25	2	152	44	f	36/280
60T042-P	2	25	1.25	152	44		42/100

The thermal stability testing started on a Fe alloy containing 13% Cr, stainless steel (60T-SS) has been completed. The results were mixed; the n- and p-type specimens that were heat-treated for 30 days and 60 days showed limited success. Complete evaluation of the Fe-coated skutterudite samples proved to be unsatisfactory. Delaminating occurs when the TAS layer is applied in thicknesses required for a continuous protective barrier.

CHAPTER G7:
GM Conclusions

The major findings from the project plus the GM team's conclusions and recommendations are summarized below.

G7.1 Summary of Major Findings

Energy savings demonstrated on the 2012 Buick eAssist LaCrosse met and exceeded the project targets. The LaCrosse uses a waste engine coolant heating system in the winter. Energy savings were restricted to cooling mode operation. The expected annualized savings in summer usage for the demonstration LaCrosse is 30.9% less energy than the baseline production vehicle. A production Lacrosse has an annualized energy loss due to climate control of 1.86 mpg. Our demonstration vehicle is expected to reduce this loss to 1.30 mpg, a 0.56 mpg improvement.

Energy saving demonstrated in our Buick eAssist LaCrosse was hampered by heat from the optionally equipped large sunroof that reduced the effectiveness of the prototype roof-mounted face and chest localized TEDs. On the warmest days, the face and chest TEDs were not able to drop the air temperature to even the human skin temperature of 33°C. This resulted in no improvement in the occupant breath temperature but did result in improved convective cooling. Experiments with the TEDs turned off, then turned on, showed improved comfort with the TED turned on despite limited temperature performance.

- The demonstration vehicle utilized a TED "blowing" seat for the driver and a lower cost ventilated seat (with "sucking" airflow but no TED) for the passenger. The comfort in the driver seat was often superior to the passenger seat, but both locations proved more comfortable than the baseline vehicle.
- Subjective comfort in the rear seat was significantly improved compared to the baseline vehicle primarily due to the improved climate measures. The proximity of the chest and face cooling TEDs in the front seat back proved to be very effective with improving comfort along with the low cost ventilated seat cushion and backrest.
- The combination of roof, lap, and seat climate measures were shown to improve system efficiency significantly. The TED climate control automatic set point was 24°C while the baseline used an automatic set point of 22°C. The TED system was superior in comfort early in a transient test as a result of the faster TED system response; steady-state comfort was equivalent while saving energy.
- The energy applied to the localized comfort features was about 40 watts per occupant yet was able to save about 36.5% of the 6 kW centralized climate energy.

The Chevrolet Volt heating localized measures included Face, Chest, Lap, Foot, and contact TE seating. Objective comfort data demonstrated equal comfort (EHT) with the baseline Volt at 23°C automatic climate setting compared to the localized setting of 21.5°C ECO mode climate setting.

Subjective transient comfort measured during road tests showed the TED configuration consistently was more comfortable, logging a 0.5 comfort point advantage, during steady operation.

Energy savings demonstrated in the Chevrolet Volt during Electric Vehicle operation met project targets despite several limitations with the demonstration property:

- Winter testing used the hot coolant loop to exchange heat with the cold side of the TEDs. An air-cooled TED cold side heat exchange would save the energy pulled from the hot coolant loop and improve system COP.
- The TED CHCM (coolant heater) was not employed in the demonstration property and the reduced energy of the device was not included in efficiency calculations. The cost and complexity of the TED CHCM was not commercially viable, and the energy gains could not offset the system cost limitation (~$10K per unit if commercialized).
- Winter testing dispelled the notion that the higher winter clothing level would reduce the effectiveness of localized climate control. The comfort rides and objective thermal manikin data shows effective warming using the face, lap, and seat localized measures despite winter clothing.

Annualized Energy reduction values for Electrical Vehicle operation during winter usage were shown to be 37.7% less than the baseline 2013 Chevrolet Volt. The production Chevrolet Volt has a reported 40-mile range in mild climate, but range can be reduced as much as 17 miles in winter usage due in part to climate control energy usage. Our demonstration property is expected to experience less range reduction during the winter, estimated at an 11-mile loss, or a range of 29 miles compared to the production estimate of 23 miles. These six miles in increased range represent a significant improvement.

Annualized Energy reduction values for Electrical Vehicle operation during summer were shown to be 36.6% less than the baseline 2013 Chevrolet Volt.

The Volt demonstration vehicle used many of the same comfort measures demonstrated on the 2012 Buick eAssist LaCrosse. The face, chest, and lap TEDs from the LaCrosse were adapted into the Volt as well. The Volt differed from the LaCrosse in the seat TED; the Volt used a more efficient contact TED fabric whereas the LaCrosse used a TED with an air distribution system for the driver and ventilation only for other seating locations. The peak summer range reduction due to Climate Control energy usage is 15 miles, netting a 25-mile summer range. Our demonstration property is expected to perform 36.6% better in term of range with only 9.5 miles of range reduction. The 30.5-mile peak summer range is a 5.5-mile improvement over the Volt with the baseline climate control system.

G7.2 Conclusions and Recommendations

The GM team has successfully executed the HVAC energy savings project by installing prototype thermoelectric devices (TEDs) that provided distributed and localized climate measures on both an eAssist Buick LaCrosse and a Chevrolet Volt extended-range electric

vehicle. For the Buick LaCrosse, annualized HVAC energy saving of 30.9% was achieved over the baseline vehicle. For the Chevrolet Volt, annualized HVAC energy saving of 36.6% for the summer operation and 37.7% for the winter operation were accomplished. Both vehicles met and exceeded the energy savings target of 30% set for the project. The COPs for the TE components varying between 1.26 to 1.89 (1.56 average value) for cooling and between 2.5 to 2.7 for heating; these values also met the COP targets set for the project to be greater than 1.3 for cooling and 2.3 for heating. While using much less energy, the distributed TED configuration for both vehicles demonstrated that the occupant thermal comfort was not compromised. In fact, subjective transient comfort measured during road tests showed that the TED configuration consistently delivered greater comfort, with a 0.5 comfort point advantage during steady-state operation.

While the GM team was satisfied with the achievements to reach the target set for the project, future study was recommended to make the TE HVAC system more viable for future vehicles.

- To dissipate the TE waste heat in the summer operation and provide heat to the cold side of the TED during winter operation for the electrical vehicle, a liquid heat exchanger was chosen early in the project to conservatively meet the performance targets. The cooling system performed very well for the project and overall thermal comfort level was in general higher than baseline during steady-state operation. To reduce the complexity of the liquid system and to save cost, an air-cooling system might be reconsidered.
- The contact TED system used in the front seats of the Volt is very effective in comfort attainment. Further exploration of such contact TE seats that can provide energy savings while working together with the existing HVAC system while is recommended.

GLOSSARY

Below are the definitions of some acronyms found in this report.

AC or A/C = air conditioning

ACC = automatic climate control; the controls for a vehicle's standard central HVAC system

CAE = computer-aided engineering (tools)

CFD = Computational Fluid Dynamics (Analysis)

COP = coefficient of performance; ratio of the useful output to the amount of energy input

DoE = Design of Experiments

DOE = US Department of Energy

EHT = equivalent homogeneous temperature; a measure used to show equal stratified comfort

EOAT = evaporator out air temperature

OEM = original equipment manufacturer; typically refers to production vehicle features

HVAC = heating, ventilation, and air conditioning (system)

PTC = Positive Temperature Coefficient; a PTC heater provides heat in electrified vehicles

RH = relative humidity

TE = thermoelectric; a material that can convert electricity into a temperature differential

TEC = thermoelectric cooler; standard term for a TE module, but it can also function as a heater

TED = thermoelectric device; a collection of TE modules packaged to provide heating or cooling

TE HVAC system = TE-based system using distributed and localized spot heating and cooling

UCB = University of California at Berkeley, recognized experts in thermal comfort modeling

REFERENCES

Huizenga, C., S. Abbaszadeh, L. Zagreus and E. Arens, 2006. "Air Quality and Thermal Comfort in Office Buildings. Results of a Large Indoor Environmental Quality Survey." *Proceedings, Healthy Buildings 2006*, Vol. III, 393-397, Lisbon, Portugal, June.

de Dear, R.J. (1998) "A global database of thermal comfort field experiments," *ASHRAE Transactions*., V.104(1b), pp.1141-1152. Reprinted in Schiller Brager, G (ed.) (1998) Field Studies of Thermal Comfort and Adaptation - ASHRAE Technical Data Bulletin, V.14(1). pp. 15-26.

Kuno Y (1956), Human perspiration. Charles C. Thomas Publ., Springfield.

Cotter JD, Patterson MJ, Taylor NA (1995), The topography of eccrine sweating in humans during exercise. Eur J Appl Physiol Occup Physiol 71: 549 – 554

Soon Ja Park and Teruko Tamura (1992) ,Distribution of evaporation rate on human body surface. Ann. Physiology Anthropology, 11 (6): 593 – 609.

Caroline J. Smith, George Havenith (2010), Body mapping of sweating patterns in male athletes in mild exercise-induced hyperthermia. European Journal of Applied Physiology.

J. Werner, T. Reents, A contribution to the topography of temperature regulation in man (1980). European Journal of Applied Physiology, 45, 87 – 94.

C. Uher (2010), Journal of Electronic Materials, 39, 2122.

"Improved Vehicle Occupancy Data Collection Methods", Battelle Memorial Institute, April, 1997.

APPENDIX A:
Publications

Meisner, G. P.; "Improving Energy Efficiency by Developing Components for Distributed Cooling and Heating Based on Thermal Comfort Modeling," Vehicle Technologies Program Annual Merit Review Meeting, U.S. Department of Energy, Washington, DC, June 2010.

Meisner, G. P.; "Develop Thermoelectric Technology for Automotive Waste Heat Recovery," Vehicle Technologies Program Annual Merit Review Meeting, U.S. Department of Energy, Washington, DC, June 2010.

Meisner, G. P.; "Thermoelectric Generator Development for Automotive Waste Heat Recovery," 16th Directions in Engine Efficiency & Emissions Research (DEER) Conference, Detroit, MI, September 2010.

Yang, J.; "Advanced Materials for Future Propulsion". 2010 Frontiers of Renewable Energy Sciences & Technologies Conference, Harvard University, Cambridge, MA, September 2010 (Invited).

Shailendra Kaushik, Kuo-Huey Chen, Taeyoung Han, and Bahram Khalighi, "Micro-Cooling/Heating Strategy for Energy Efficient HVAC System", SAE paper #2011-01-0644, 2011.

Shailendra Kaushik, Kuo-Huey Chen, Taeyoung Han, and Bahram Khalighi, "Micro-Cooling/Heating Strategy for Energy Efficient HVAC System", SAE-2011-01-0644, presented at 2011 SAE World Congress, Detroit, MI, April 12, 2011.

Jeffrey Bozeman, Kuo-Huey Chen, and Shailendra Kaushik, "Distributed Climate System Impact on Human Comfort and MAC Efficiency", 11AAR-0029, presented at SAE Alternative Refrigerant and System Efficiency Symposium, Scottsdale, AZ, Sep. 29, 2011.

GM R&D internal report #VDR-282, Shailendra Kaushik, Kuo-Huey Chen, Taeyoung Han, and Bahram Khalighi, "Micro-Cooling/Heating Strategy for Energy Efficient HVAC System", May 17, 2011.

GM R&D internal report #VDR-289, Shailendra Kaushik, Taeyoung Han, and Kuo-Huey Chen, "Development of A Virtual Thermal Manikin to Predict Thermal Comfort in Automobiles", Sep. 20, 2011.

Kaushik S., Han, T and Chen, K-H, "Development of a Virtual Thermal Manikin to Predict Thermal Sensation in Automobiles", SAE 2012-01-0315, April, 2012 SAE World Congress, Detroit, MI.

Chen, K-H, Kaushik, S, Han T, Ghosh, D and Wang, M, "Thermal Comfort Prediction and Validation in a Realistic Vehicle Thermal Environment", SAE 2012-01-0645, April, 2012 SAE World Congress, Detroit, MI.

A. Thompson, J. Sharp, J. Moczygemba, H. Wang, D. Brown, "Implementation and Performance of Skutterudite based Thermoelectric Generators", Presentation, International Conference on Thermoelectrics (Aalborg, Denmark; August 2012).

D. Ghosh, Mingyu Wang, E. Wolfe, K. Chen, S. Kaushik, and T. Han, Energy Efficient HVAC System with Spot Cooling in an Automobile – Design and CFD Analysis, SAE Int. J. Passenger. Cars – Mech. Syst., Vol. 5, pp.885-903, June 2012.

Yi Zhang, Xuezhi Ke, Paul R. C. Kent, Jihui Yang and Changfeng Chen "Anomalous Lattice Dynamics near the Ferroelectric Instability in PbTe,", Physical Review Letters 107, 175503 (2011) [appeared in October 21 issue].

Thermal to Electrical Energy Conversion of Skutterudite-Based Thermoelectric Modules. James R. Salvador, Jung Y. Cho, Zuxin Ye, Gregory P. Meisner, Joshua E. Moczygemba, Alan J. Thompson, Jeffrey W. Sharp, Jan D. König, Ryan Maloney, Travis Thompson, Jeffery Sakamoto, Hsin Wang, Andrew A Wereszczak, and Gregory P. Meisner. Journal of Electronic Materials, DOI: 10.1007/s11664-012-2261-9.

Electrical and thermal properties of Fe substituted double-filled BaxYbyFezCo4−zSb12 skutterudites. Sedat Ballikaya, Neslihan Uzar, Saffettin Yildirim, James R. Salvador. Solid State Chemistry. http://dx.doi.org/10.1016/j.jssc.2012.08.025.